UNIVERSITAT POLITÈCNICA DE CATALUNYA
BARCELONATECH
Escola d'Enginyeria de Barcelona Est

DEGREE THESIS

Mechanical Engineering Degree

FIBER SHIP: CONSTITUTIVE MODELS

Author: Xavier Almendros Carmona
Director: Daniel Di Capua
Co-Director: Rafael Pacheco

Call: 06/2018

Resum

Durant tota la història de la humanitat s'han estudiat els materials i el seu comportament per tal d'entendre les respostes d'aquest a interaccions externes. L'objectiu d'entendre el seu comportament es poder realitzar estructures o objectes amb una funcionalitat.

En els últims cent anys s'han estudiat per a molts materials, i també de manera general, la relació entre la tensió aplicada i la seva deformació com a resposta. Per això aquest treball presenta les principals teories lineals que caracteritzen el comportament de diferents materials, en concret per plaques.

En realitat, els materials no es comporten de manera lineal així que aquest treball també explica una teoria no lineal que es pot implementar juntament amb les primeres explicades amb l'objectiu de donar un caràcter no-lineal al material. En concret, s'estudia la teoria de dany i les diferents maneres en les que evoluciona.

En les últimes dècades, els materials compostos avançats han revolucionat l'enginyeria estructural. La seva bona relació entre rigidesa i pes els fa òptims per a moltes aplicacions d'enginyeria. És per això que és important caracteritzar el seu comportament i la relació entre els seus components. En aquest treball s'expliquen les principals formes en què ens podem trobar els materials compostos i les seves principals utilitats en la indústria. També s'explica una teoria que relaciona el comportament entre la tensió i la deformació per a materials compostos reforçats per fibres llargues.

Finalment, es realitzen diferents simulacions amb l'objectiu de comprovar que les teories estan ben implementades en un programari anomenat Ramseries ® i a la mateixa vegada comprovar que la resposta és l'esperada. En quant a els materials compostos, en aquest treball s'ajusta el comportament del material en la simulació amb el resultat experimental amb l'objectiu de caracteritzar el comportament d'aquest material que serà posteriorment utilitzant en el projecte europeu "Fibership" destinat a desenvolupar les tecnologies necessàries per a la construcció d'un vaixell de gran eslora totalment de materials compostos.

Resumen

Durante toda la historia de la humanidad se han estudiado los materiales y su comportamiento con el fin de entender las respuestas de este a interacciones externas. El objetivo de entender su comportamiento es poder realizar estructuras u objetos con una funcionalidad.

En los últimos cien años se han estudiado para muchos materiales, y también de manera general, la relación entre la tensión aplicada y su deformación como respuesta. Por ello este trabajo presenta las principales teorías lineales que caracterizan el comportamiento de diferentes materiales, en concreto para placas.

En la realidad, los materiales no se comportan de manera lineal así que este trabajo también explica una teoría no lineal que se puede implementar junto a las primeras explicadas con el objetivo de dar un carácter no-lineal a el material. En concreto, se estudia la teoría de daño y sus diferentes tipos de evolución.

En las últimas décadas, los materiales compuestos avanzados han revolucionado la ingeniería estructural. Su buena relación entre rigidez y peso los hace óptimos para muchas aplicaciones ingenieriles. Es por ello que es importante caracterizar su comportamiento y la relación entre sus componentes. En este trabajo se explican las principales formas en las que nos podemos encontrar los materiales compuestos y sus principales utilidades en la industria. También se explica una teoría que relaciona el comportamiento entre la tensión i la deformación para materiales compuestos reforzados por fibras largas.

Por último, se realizan diferentes simulaciones con el objetivo de comprobar que las teorías están bien implementadas en un software llamado *Ramseries* ® y a la misma vez comprobar que la respuesta es la esperada. En el caso de los materiales compuestos, se ajusta el comportamiento del material en simulación con el resultado experimental con el fin de caracterizar el comportamiento del material que será utilizado posteriormente en el proyecto europeo llamado "*Fibership*" destinado a desarrollar las tecnologías para la construcción de buques de gran eslora totalmente de materiales compuestos.

Abstract

Throughout the history of humans, materials and their behaviour have been studied in order to understand their responses to external interactions. The goal of understanding their behavior is to be able to make structures or objects with a function.

In the last hundred years, the relation between the applied tension and its deformation as a response has been studied for many materials, and also general methods. Therefore, this work presents the main linear theories that characterize the behavior of different structures, especially plates.

In reality, the materials do not have a linear behaviour, so this paper also explains a nonlinear theory that can be implemented together with the first ones explained with the aim of giving a non-linear character to the material. In particular, damage theory and its different types of evolution are studied.

In recent decades, advanced composite materials have become a revolution in structural engineering. Their good relation between stiffness and weight makes them optimal for many engineering applications. That is why it is important to characterize its behavior and the relationship between its components. This paper explains the main ways in which we can find composite materials and their main uses in the industry. It also explains a theory that relates the behavior between tension and deformation for composite materials reinforced by long fibers.

Finally, different simulations are launched in order to verify that the theories are well implemented in a software called Ramseries ® and at the same time verify that the response is the expected one. With respect to composite materials, this work fits the behaviour of the simulation with the experimental result with the objective of characterizing the behaviour of the material that afterward will be used in the European project called "*Fibership"* destined to develop the technologies to construct a ship made totally from composite materials.

Acknowledgments

I would like to express my grateful acknowledgement to my supervisor, Rafael Pacheco, who helped me in this project. Without his help and knowledge this work would never have been possible.

Also, I would like to express my deep gratitude to my director, Daniel Di Capua. He created my passion for finite element method and constitutive equations. Moreover, he gave me the opportunity to do this project.

Thanks to CIMNE for the license in the computational software *Ramseries®*

Thanks to BLLVGS and Tahnee for all that moments they supported me. Thanks to my father for the philosophy he taught me. Thanks to my mother, for her daily support and love.

Índex

1. Motivation

In the history of humanity, humans have used materials since the first moment with a lot of different objectives. I think that in the way we understand better the materials and the behaviour under mechanical loads, we will improve our capacity to use these materials.

Nowadays, a new type of material is winning importance inside the industrial markets: Composite materials. Composite materials are the future when we talk of the industry. So, physical and mathematical models are needed to describe the behavuior of composite materials

In order to improve and optimize the design of structural parts made of composite materials, the industry requires engineering tools capable to solve and simulate the behaviour of these materials, specific in the nonlinear region. This is the reason why it is necessary to create new theories that can predict this behaviour when we implement in a typical FEM code. Keeping in mind that the computational cost cannot be elevated. One example of these type of theories is the Serial Parallel Rule of Mixtures theory that describes the behaviour of composite materials reinforced with fibers.

2. Objective

The aim of this work is to explain the most important structural constitutive equations applied in shells. Also, a simulation is going to be launched with different models in *Ramseries* in order to verify that they are well implemented in the software and validate that the behaviour of the structure is the expected.

The structural constitutive equation that is going to be studied is the relationship between stress and strains. There are different models to set when we want to study the behaviour of a shell. We can consider that his behaviour is linear or not. Also, if we want to study as a 3-D body or make some assumptions to simplify the calculus and do a 2D simulation. It depends on the results accuracy you need.

Moreover, a differentiation between homogeneous materials and heterogeneous materials and see which constitutive equations uses each one. In addition, an explanation of the different types of composite and their use in the industry is going to be done.

Also, the present work focus on the importance of understanding the physics you want to simulate when a non-linear simulation is set. It is very important to reduce the costs of the project.

Finally, the objective of this work is to validate and collaborate in the adaptation of the finite element code in *Ramseries* for the simulations required in the European project called "*Fibreship*" destined to the construction of large ships totally of compounds materials.

2.1. Range

The range of this work is to understand the different types of simulations you can do when you are studying the behaviour of a shell and which one is the best depending on the accuracy we need or the type of problem we have.

Moreover, this work wants to notice the importance of adaptative mesh for non-linear simulation.

For last, the purpose is to obtain an approximation of an experimental composite case in *Ramseries* with the composite theory implemented.

3. Constitutive models

In physics, a constitutive model is a relation between two physical quantities that is specific to a material and approximates the response of that material to an external perturbation, usually fields or forces. They are combined with other equations governing physical laws to solve physical problems.

For example, in fluid mechanics the flow of a fluid in a pipe, the response of a crystal to an electric field, or in structural analysis, the connection between applied stresses to strains.

In this job, we are going to focus on structural analysis in shells.

4. Homogeneous Materials

A material of uniform composition throughout that cannot be mechanically separated into different materials.

There are different, even infinite, constitutive models that define the behaviour between the strain and stress. It depends of the type of problem or the way we solve them. Problems can be very different, only in structural mechanics the are a lot of different problem types. For example: 1D solid, 2D solid, 3D solid, plate, shell, membrane, cable, beam.

4.1. Elastic tridimensional solids (3-D)

As it can be seen in [9] there are a lot of structures that have geometrical, mechanical or loading features which make impossible to use simple models with simplifications, as we will see later. The only solution available is to use a full three-dimensional analysis based on general 3D elasticity theory.

The three-dimensional analysis of a solid with a *Finite Element Method* does not introduce a lot of conceptual problems. Although, the computation of a three-dimensional problem need more computational power and take more time to obtain the results than, for example, a two-dimension problem. This is because we are adding a space dimension, so all the tensors will be bigger and will appear new variables.

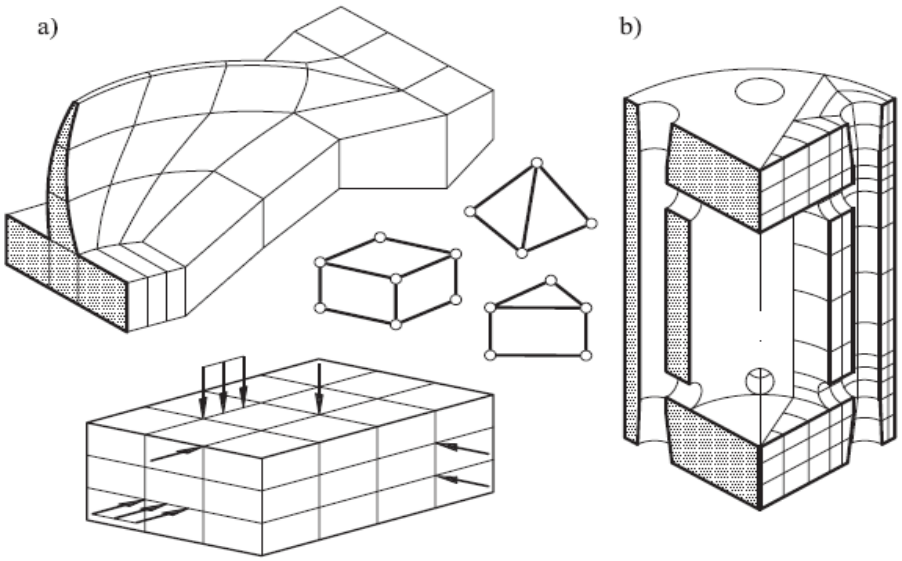

Figure 4.1.1 Structure which require a 3D analysys

Source: Oñate, E. (2009). Structural Analysis with the Finite Element Method. Eugenio Oñate. Structural Analysis with the Finite Element Method. Solids.

The next figure describes the different types of interactions that three dimensional solid have.

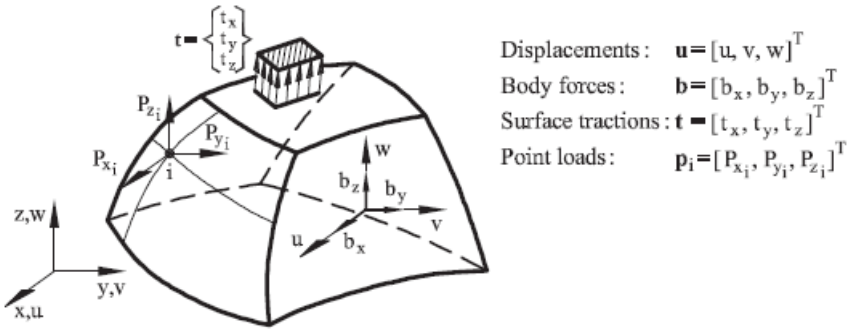

Figure 4.1.2 3D solid. Displacements and loads.
Source: Oñate, E. (2009). Structural Analysis with the Finite Element Method. Eugenio Oñate. Structural Analysis with the Finite Element Method. Solids

According to [9] there are different types of load applied in a 3D solid:

- Body force: Describes a load in the entire volume. The units are N/m^3 (SI).
- Surface force: Represents a load in the surface. The units are N/m^2(SI).
- Point or Punctual load: Represents a load in a point of the volume. Depending on the dimensions of our problem we can say which loads will be point or surface. The units are N/m (SI).

4.1.1. Stress field:

$$\sigma = [\sigma_x, \sigma_y, \sigma_z, \tau_{xy}, \tau_{xz}, \tau_{yz}]^T$$

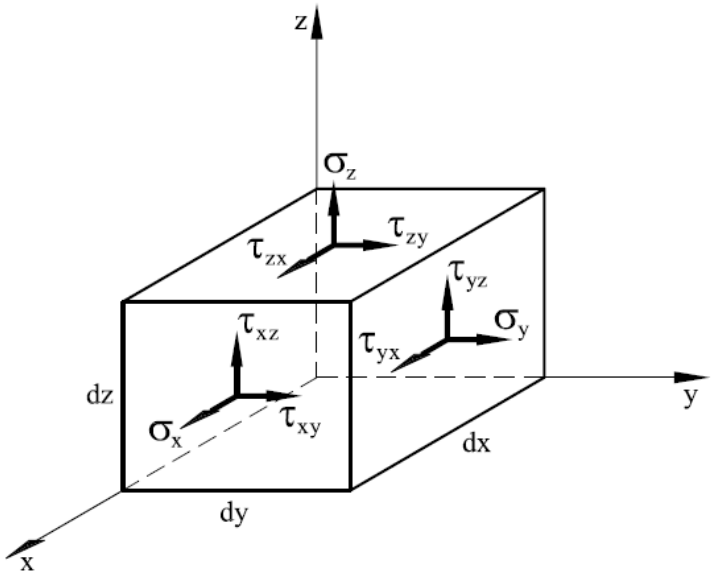

Figure 4.1.1.1 Sign criterion for the stress in a 3D solid

Source: Oñate, E. (2009). Structural Analysis with the Finite Element Method. Eugenio Oñate. Structural Analysis with the Finite Element Method. Solids

In fact, the tensor has 9 (3x3) components but, as it can be seen in the figure, some components have symmetry so a simplification can be done and turn it into a vector.

4.1.2. Strain and displacement field

$$\varepsilon = [\varepsilon_x, \varepsilon_y, \varepsilon_z, \gamma_{xy}, \lambda_{xz}, \gamma_{yz}]^T$$

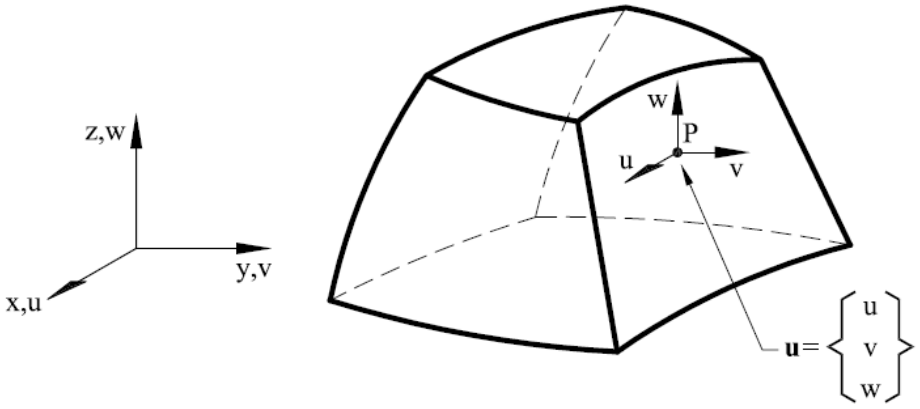

Figure 4.1.2.1 Sign criterion for displacement in a 3D solid
Source: Oñate, E. (2009). Structural Analysis with the Finite Element Method. Eugenio Oñate. Structural Analysis with the Finite Element Method. Solids.

The strain field is defined by the standard six strain components of three-dimensional elasticity.

$$\varepsilon_x = \frac{\partial u}{\partial x} \qquad \varepsilon_y = \frac{\partial v}{\partial y} \qquad \varepsilon_z = \frac{\partial w}{\partial z}$$

$$\gamma_{xy} = \frac{\partial u}{\partial y} + \frac{\partial v}{\partial x} \qquad \gamma_{xz} = \frac{\partial u}{\partial z} + \frac{\partial w}{\partial x} \qquad \gamma_{yz} = \frac{\partial v}{\partial z} + \frac{\partial w}{\partial y}$$

4.1.3. Constitutive equation

In the most general case of the theory of the anisotropy elasticity it is necessary a constitutive matrix with 21 independent coefficients. Orthotropic materials with principal orthotropy directions are 1,2,3; the constitutive equation is written as:

$$\varepsilon_1 = \frac{1}{E_1}\sigma_1 - \frac{v_{21}}{E_2}\sigma_2 - \frac{v_{31}}{E_3}\sigma_3 \quad , \quad \varepsilon_2 = \frac{1}{E_2}\sigma_2 - \frac{v_{12}}{E_1}\sigma_1 - \frac{v_{32}}{E_3}\sigma_3$$

$$\varepsilon_3 = \frac{1}{E_3}\sigma_3 - \frac{v_{13}}{E_1}\sigma_1 - \frac{v_{23}}{E_2}\sigma_2 \quad , \quad \gamma_{12} = \frac{\tau_{12}}{G_{12}} \quad ; \quad \gamma_{23} = \frac{\tau_{23}}{G_{23}} \quad ; \quad \gamma_{13} = \frac{\tau_{13}}{G_{13}}$$

The number of material parameters reduces further to five for an orthotropic material in the plane 1-2 and isotropic in the plane 2-3. This situation is very typical for fiber-reinforced composite materials.

One usual case used in practice is isotropy elasticity where the independent coefficients of constitutive equation is reduced to 2: Young Modulus and Poisson coefficient.

The constitutive equation can be written (having in account the initial stress and strain) as:

$$\sigma = D\ (\varepsilon - \varepsilon_0) + \sigma_0$$

Where the constitutive matrix is:

$$\mathbf{D} = \frac{\mathrm{E}(1-\nu)}{(1+\nu)(1-2\nu)} \begin{bmatrix} 1 & \frac{\nu}{1-\nu} & \frac{\nu}{1-\nu} & 0 & 0 & 0 \\ & 1 & \frac{\nu}{1-\nu} & 0 & 0 & 0 \\ & & 1 & 0 & 0 & 0 \\ & & & \frac{1-2\nu}{2(1-\nu)} & 0 & 0 \\ & \text{Simetrica} & & & \frac{1-2\nu}{2(1-\nu)} & 0 \\ & & & & & \frac{1-2\nu}{2(1-\nu)} \end{bmatrix}$$

Also, the variables involved in FEM three-dimensional are a little bit different than in other dimensions. The aspect about the difference between the FEM code in function of the dimension can be studied in [9].

4.2. Bidimensional solids (2-D)

There are different structures which satisfy the assumptions of two-dimensional elasticity. These assumptions are:

-Plane stress

-Plane strain.

In the following figure different examples of plane stress and plane strain are explained.

Plane stress problems

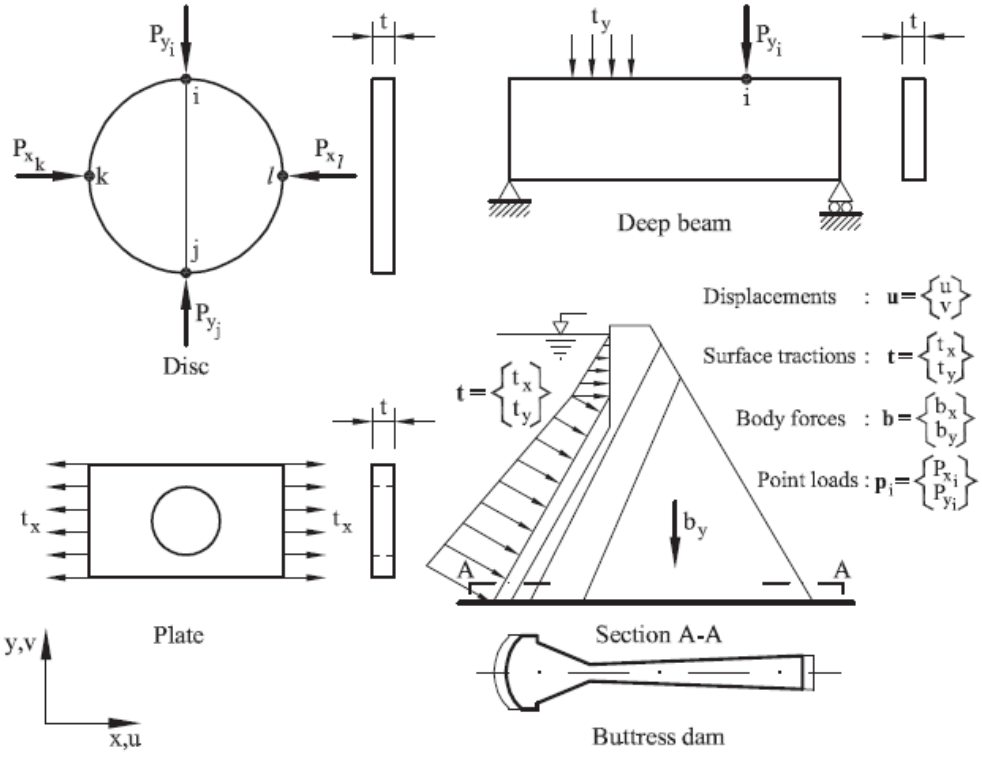

Figure 4.2.1 Examples of plan stress problems. Displacement field and loads acting on the middle plane section
Source: Oñate, E. (2009). Structural Analysis with the Finite Element Method. Eugenio Oñate. Structural Analysis with the Finite Element Method. Solids

A prismatic structure is under plane stress if one of its dimensions (thickness) is much smaller than the other two dimensions and all the loads are contained in the middle plane of the structure.

Plane strain problems

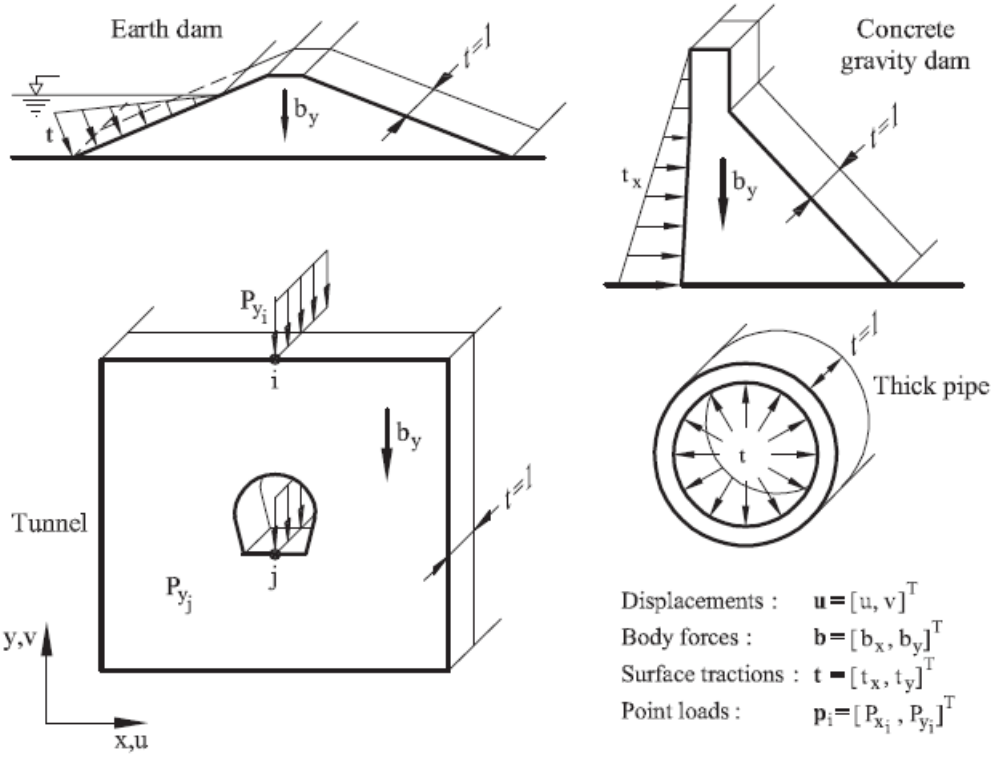

Figure 4.2.2 Examples of plane strain problems. Displacement field and loads acting on a transverse section
Source: Oñate, E. (2009). Structural Analysis with the Finite Element Method. Eugenio Oñate. Structural Analysis with the Finite Element Method. Solids

A prismatic structure is under plain strain if one of its dimensions(length) is larger than the other two dimensions and all the loads are uniformly distributed along its length and they act orthogonally to de longitudinal axis.

4.2.1. Displacement field

The geometrical and load characteristics of the structure in a plain strain or plain stress allow us to establish the hypothesis that all the sections perpendicular to the prismatic axis z deform in their plane in an identical way.

The deformation field of the section Is perfectly defined if the displacement is known in the directions of the axis x and y. The vector of a point can be defined as:

$$\boldsymbol{u}(x,y) = \begin{bmatrix} u(x,y) \\ v(x,y) \end{bmatrix}$$

4.2.2. Strain field

From the displacement field it is easy to obtain the strain field using the general elasticity theory:

$$\varepsilon = [\varepsilon_x, \varepsilon_y, \gamma_{xy}]$$

Where:

$$\varepsilon_x = \frac{\partial u}{\partial x}\, \varepsilon_y = \frac{\partial v}{\partial y}\, \nu_{xy} = \frac{\partial u}{\partial y} + \frac{\partial v}{\partial x}$$

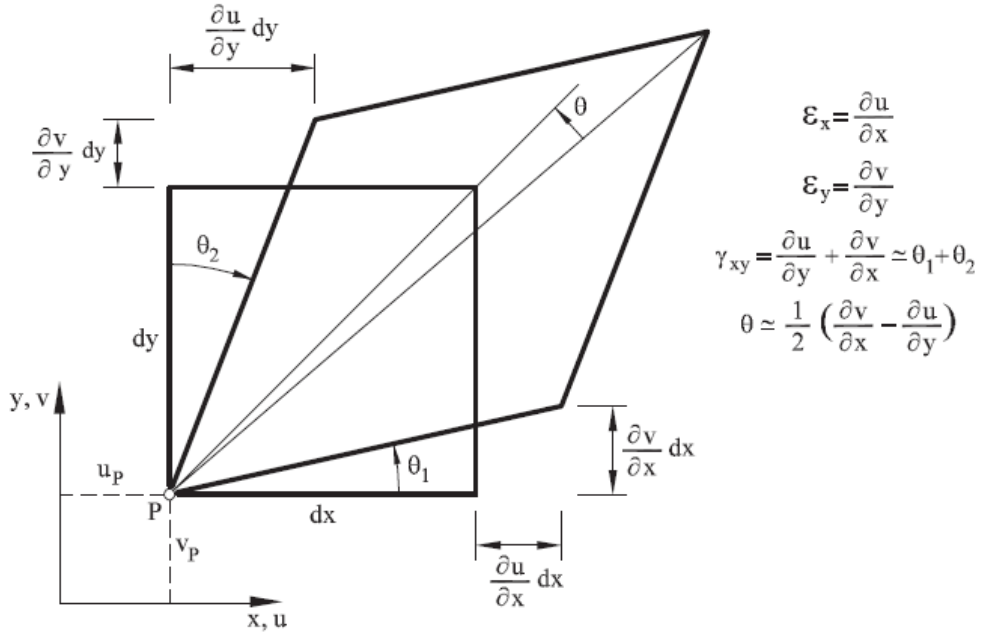

Figure 4.2.2.1 Deformation of an infinitesimal 2D domain and definition of strains

Source: Oñate, E. (2009). Structural Analysis with the Finite Element Method. Eugenio Oñate. Structural Analysis with the Finite Element Method. Solids

4.2.3. Stress field.

It follows that the tangential stresses are zero. On the other hand, for the same reasons explained in the previous section for the deformation ε_z, the stress σ_z does not work. The stress vector is:

$$\sigma = [\sigma_x, \sigma_y, \tau_{xy}]$$

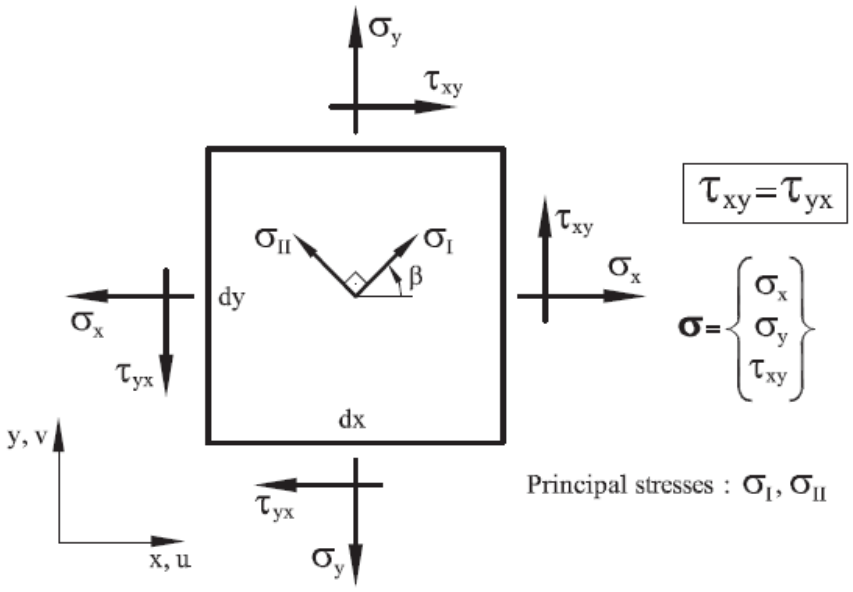

Figure 4.2.3.1 Definition of stresses and principal stresses in 2D solids

Source: Oñate, E. (2009). Structural Analysis with the Finite Element Method. Eugenio Oñate. Structural Analysis with the Finite Element Method. Solids

4.2.4. Constitutive equation

The relationship between stress and strain can be deduced from the general tridimensional elasticity theory, with the hypothesis said before ($\sigma_z = 0$ for plain stress and $\varepsilon_z = 0$ for plain strain) the following matrix relation can be obtained:

$$\boldsymbol{\sigma} = \boldsymbol{D}\,\boldsymbol{\varepsilon}$$

Where D is the elastic constants matrix or constitutive matrix:

$$D = \begin{bmatrix} d_{11} & d_{12} & 0 \\ d_{21} & d_{22} & 0 \\ 0 & 0 & d_{33} \end{bmatrix}$$

From the Maxwell-Betti we know that D is always symmetric.

For isotropic elasticity, according to [9] we obtain:

Plane stress	**Plane strain**
$d_{11} = d_{22} = \frac{E}{1-\nu^2}$	$d_{11} = d_{22} = \frac{E(1-\nu)}{(1+\nu)(1-2\nu)}$
$d_{12} = d_{21} = \nu \cdot d_{11}$	$d_{12} = d_{21} = d_{11} \cdot \frac{\nu}{1-\nu}$
$d_{33} = \frac{E}{2(1+\nu)} = G$	$d_{33} = \frac{E}{2(1+\nu)} = G$

Table 4.2.4.1 Constitutive matrix elements

Where E is the elastic modulus, ν is Poisson modulus and G the shear modulus.

4.3. Thick slender plates

4.3.1. Kirchhoff theory

A plate is defined by [10] as a flat solid with one dimension much smaller than its others dimensions. The reference plane is $(z = 0)$ and it is assumed that this plane is equidistant from the upper and lower faces of the plate.

Thickness/average side ratio: ${}^{t}/_{L} \leq 0.05$. For other cases, we have to apply other theories.

A plate with homogeneous isotropic material carries lateral loads by bending, like a straight beam.
Assumptions:

- In the point belonging to the middle plane $(z = 0)$ $u = v = 0$
- The points along a normal to the middle plane have the same vertical displacement. The thickness does not chance during deformation.
- Normal stress σ_z is negligible.
- A straight line normal to the undeformed middle plane remains straight and normal to the deformed middle plane. Because this, we can calculate the angle deformed with the derivate.

4.3.1.1. Displacement field

It is deduced:

$$u(x, y, z) = -z\theta_x(x, y)$$

$$v(x, y, z) = -z\theta_y(x, y)$$

$$w(x, y, z) = w(x, y)$$

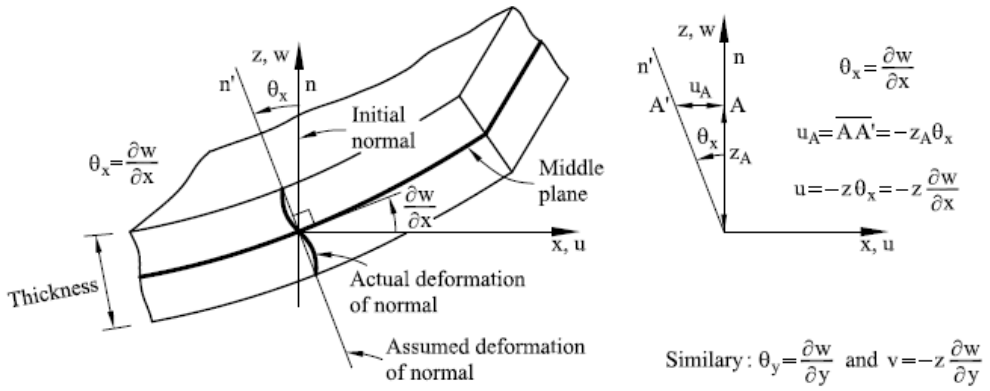

Figure 4.3.1.1 Deformation of the normal vector and in-plane displacement field in a thin plate
Source: Oñate, E. (2009). Structural Analysis with the Finite Element Method. Eugenio Oñate. Structural Analysis with the Finite Element Method. Shells and Plates

w is the vertical displacement of the points on the middle plane and the rotations θ_x and θ_y coincide with the angles followed by the normal vectors contained in the planes xz and yz respectively.

$$\mathrm{u} = \left[w, \theta_x, \theta_y\right]^T$$

u is the displacement vector of a point on the middle of the plate.

$$\theta_y = \frac{\partial w}{\partial y} \qquad \theta_x = \frac{\partial w}{\partial x}$$

This derive from the 3D elasticity theory.

4.3.1.2. Strain:

From the 3-D elasticity theory it is deduced in [10]:

$$\varepsilon_x = \frac{\partial u}{\partial x} = -z\frac{\partial^2 w}{\partial x^2}$$
$$\varepsilon_y = \frac{\partial v}{\partial y} = -z\frac{\partial^2 w}{\partial y^2}$$
$$\varepsilon_z = 0$$
$$\gamma_{xy} = \frac{\partial u}{\partial y} + \frac{\partial v}{\partial x} = -2x\frac{\partial^2 w}{\partial x \partial y}$$
$$\gamma_{xz} = \frac{\partial w}{\partial x} + \frac{\partial u}{\partial x} = \frac{\partial w}{\partial x} - \frac{\partial w}{\partial x} = 0$$

$$\gamma_{yz} = \frac{\partial w}{\partial y} + \frac{\partial v}{\partial z} = \frac{\partial w}{\partial y} - \frac{\partial w}{\partial y} = 0$$

$$\varepsilon = [\varepsilon_x, \varepsilon_y, \gamma_{xy}]^T = \left[-z\frac{\partial^2 w}{\partial x^2}, -z\frac{\partial^2 w}{\partial y^2}, -2z\frac{\partial^2 w}{\partial x \partial y}\right] = S\hat{\varepsilon}_b$$

where

$$S = -z\begin{bmatrix}1 & 0 & 0\\ 0 & 1 & 0\\ 0 & 0 & 1\end{bmatrix} = -z\mathrm{I}_3\,,\ \hat{\varepsilon}_b = \left[\frac{\partial^2 w}{\partial x^2}, \frac{\partial^2 w}{\partial y^2}, 2\frac{\partial^2 w}{\partial x \partial y}\right]^T$$

The $\hat{\varepsilon}_b$ is the generalized strain vector or curvature vector. Index b is because. Matrix ***S*** transforms this vector into strain at any point across the thickness.

4.3.1.3. Stress

The stresses are the same as in 2-D bidimensional solid.

$$\sigma = [\sigma_x, \sigma_y, \tau_{xy}]^T$$

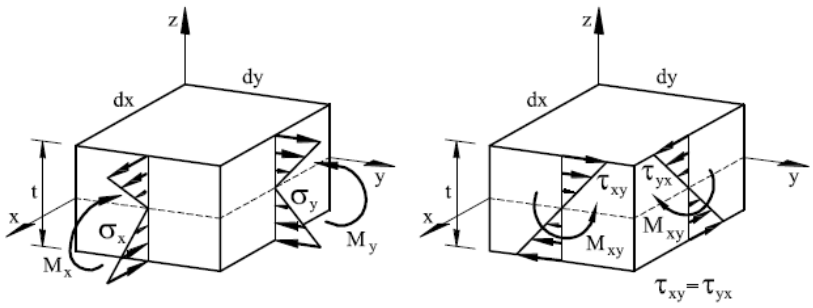

Figure 4.3.1.3 Sign convention for stresses and bending moments

Source: Oñate, E. (2009). Structural Analysis with the Finite Element Method. Eugenio Oñate. Structural Analysis with the Finite Element Method. Shells and Plates

4.3.1.4. Constitutive relationship

The constitutive relationship between stress and strains in the generalized form is the next:

$$\boldsymbol{\sigma} = \boldsymbol{D}\,\boldsymbol{\varepsilon}$$

Where **D** is the constitutive matrix obtained from the general expression of 3D elasticity by introducing the plane stress assumption ($\sigma_z = 0$) and also $\sigma_{xz} = \gamma_{yz} = 0$.
The result is exactly the same as in bidimensional elasticity in plane stress.
For isotropic material the result is:

$$D = \frac{E}{1-v^2}\begin{bmatrix} 1 & v & 0 \\ v & 1 & 0 \\ 0 & 0 & \dfrac{1-v}{2} \end{bmatrix}$$

4.3.2. Reissner-Mindlin Theory

As it is said before, Kirchhoff plate elements are restricted to thin plate situations and also his C^1 continuity requirement poses severe difficulties for deriving. These problems can be overcome by using the plate theory made by Reissner and Mindlin.

This theory assumes that the normal to the plate do not remain orthogonal to the mid-plane after deformation, thus allowing for transverse shear deformation effects. This allows to use C^0 continuous element.
Reissner-Mindlin plate theory is very adequate for studying composite materials because shear deformation effects are important.

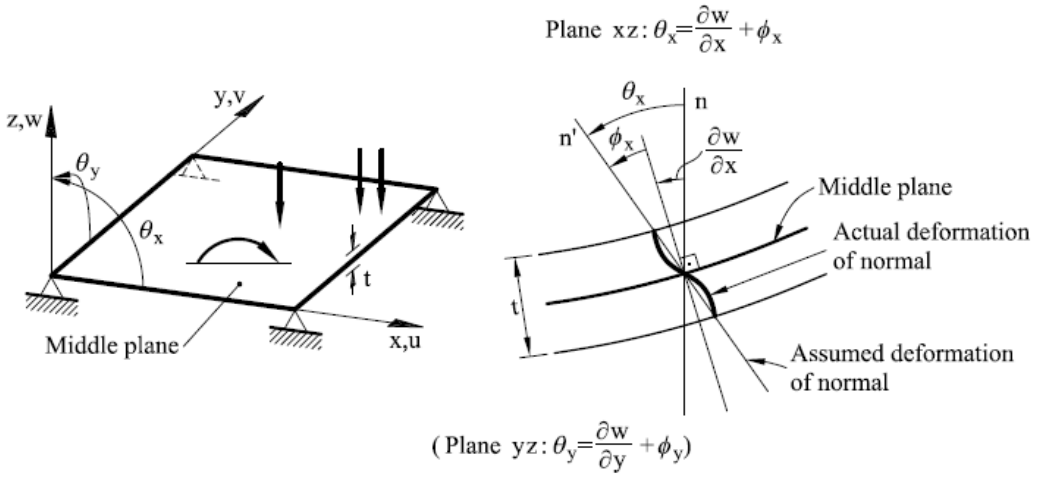

Figure 4.3.2.1 Sign convention for the displacements and the rotations of the normal.
Source Oñate, E. (2009). Structural Analysis with the Finite Element Method. Eugenio Oñate. Structural Analysis with the Finite Element Method. Shells and Plates

The Reissner-Mindlin theory has the same first tree assumptions of Kirchhoff plate theory but the fourth is different:

- A straight line normal to the undeformed middle plane remains straight but not necessarily orthogonal to the middle plane after deformation.

4.3.2.1. Displacement field

In [10] it is only analyzed the middle plane of the plate.

$$u(x,y,z) = -z\theta_x(x,y)$$

$$v(x,y,z) = -z\theta_y(x,y)$$

$$w(x,y,z) = w(x,y)$$

The displacement vector is:

$$\mathrm{u} = \left[w, \theta_x, \theta_y\right]^T$$

Assumption 4 that it is explained before, allows to express the rotations of the plane in:

$$\theta_x = \frac{\partial w}{\partial x} + \phi_x$$
$$\theta_y = \frac{\partial w}{\partial y} + \phi_y$$

As it can be seen the rotation of the planes is obtained as the sum of two terms. The first one is the adequate slope of the middle plane and the second one is an additional rotation ϕ resulting from the assumption 4. The lack of orthogonally make necessary to add a rotation therm.

Consequently, the rotations θx and θy cannot be computed in terms of the deflection only and, therefore, are treated as independent variables. This is a substantial difference between Reissner–Mindlin and Kirchhoff plate theories.

4.3.2.2. Strain and stress fields

$$\varepsilon_x = \frac{\partial u}{\partial x} = -z\frac{\partial \theta_x}{\partial x}$$
$$\varepsilon_y = \frac{\partial v}{\partial y} = -z\frac{\partial \theta_y}{\partial y}$$

$$\varepsilon_z = 0$$

$$\gamma_{xy} = \frac{\partial u}{\partial y} + \frac{\partial v}{\partial x} = -z\left(\frac{\partial \theta_x}{\partial y} + \frac{\partial \theta_y}{\partial x}\right)$$
$$\gamma_{xz} = \frac{\partial u}{\partial z} + \frac{\partial w}{\partial x} = -\theta_x + \frac{\partial w}{\partial x} = -\phi_x$$
$$\gamma_{yz} = \frac{\partial v}{\partial z} + \frac{\partial w}{\partial y} = -\theta_y + \frac{\partial w}{\partial y} = -\phi_y$$

The non-orthogonality of the normal vector induces non-zero transverse shear strains which coincide with the rotations. These strains are independent of the coordinate z.

$$\varepsilon = \begin{bmatrix} \varepsilon_x \\ \varepsilon_y \\ \gamma_{xy} \\ \cdots \\ \gamma_{xz} \\ \gamma_{yz} \end{bmatrix} = \begin{bmatrix} -z\dfrac{\partial \theta_x}{\partial x} \\ -z\dfrac{\partial \theta_y}{\partial y} \\ -z\left(\dfrac{\partial \theta_x}{\partial y} + \dfrac{\partial \theta_y}{\partial x}\right) \\ \cdots \\ -\theta_x + \dfrac{\partial w}{\partial x} \\ -\theta_y + \dfrac{\partial w}{\partial y} \end{bmatrix} = \begin{bmatrix} \varepsilon_b \\ \cdots \\ \varepsilon_s \end{bmatrix}$$

Where the vector $\varepsilon_b \; and \; \varepsilon_s$ contain the bending and the transverse shear strains, respectively. The strain vector of can be expressed as:

$$\varepsilon = S\hat{\varepsilon}$$

Where: $$\hat{\varepsilon} = \begin{bmatrix} \hat{\varepsilon}_b \\ \hat{\varepsilon}_s \end{bmatrix}$$

$$\boldsymbol{S} = \begin{bmatrix} -z & 0 & 0 & 0 & 0 \\ 0 & -z & 0 & 0 & 0 \\ 0 & 0 & -z & 0 & 0 \\ 0 & 0 & 0 & 1 & 0 \\ 0 & 0 & 0 & 0 & 1 \end{bmatrix}$$

The stress vector is:

$$\sigma = \begin{bmatrix} \sigma_x \\ \sigma_y \\ \tau_{xy} \\ \cdots \\ \tau_{xz} \\ \tau_{yz} \end{bmatrix} = \begin{bmatrix} \sigma_b \\ \cdots \\ \sigma_s \end{bmatrix}$$

4.3.2.3. Stress-strain relationship

These relationships are for a homogeneous material under isothermal conditions. Axial effects appear for composite laminated materials.

Starting from the constitutive equation of 3D elasticity and also using the plane stress assumption the relationship for an orthotropic material that satisfy the condition of plane anisotropy can be found:

$$\sigma = \begin{bmatrix} \sigma_b \\ \sigma_s \end{bmatrix} = \begin{bmatrix} D_b & \cdot & 0 \\ \cdots & \cdots & \cdots \\ 0 & \cdot & D_s \end{bmatrix} \cdot \begin{bmatrix} \varepsilon_b \\ \varepsilon_s \end{bmatrix}$$

where

$$D_b = \frac{1}{1 - v_{xy}v_{yz}} \begin{bmatrix} E_x & v_{yx}E_x & 0 \\ v_{xy}E_x & E_y & 0 \\ 0 & 0 & (1 - v_{xy}v_{yx})G_{xy} \end{bmatrix}$$

$$D_s = \begin{bmatrix} G_{xz} & \\ & G_{yz} \end{bmatrix}$$

4.4. Damage theory

The damage mechanics is an expression usually used for models that his principle characteristic is the loss of stiffness, I mean, the loss of the constitutive secant model. Basically, they present an irreversible degradation of the material.

Damage models are very attractive because from a computational view they are really easy to use in big dimensions problems. This theory is applicable in any of the fourth before explained.

From these models you can make different complex models for more specific materials.

4.4.1. Infinitesimal deformation damage model

Suppose a 1-dimension problem where a traction force which his stress is σ, that works in a section s. Because of the damage, it is only considered the non-damaged region. Meaning that, according to [12], it will have an effective stress $\bar{\sigma}$ applied in an effective area $\bar{s}$.

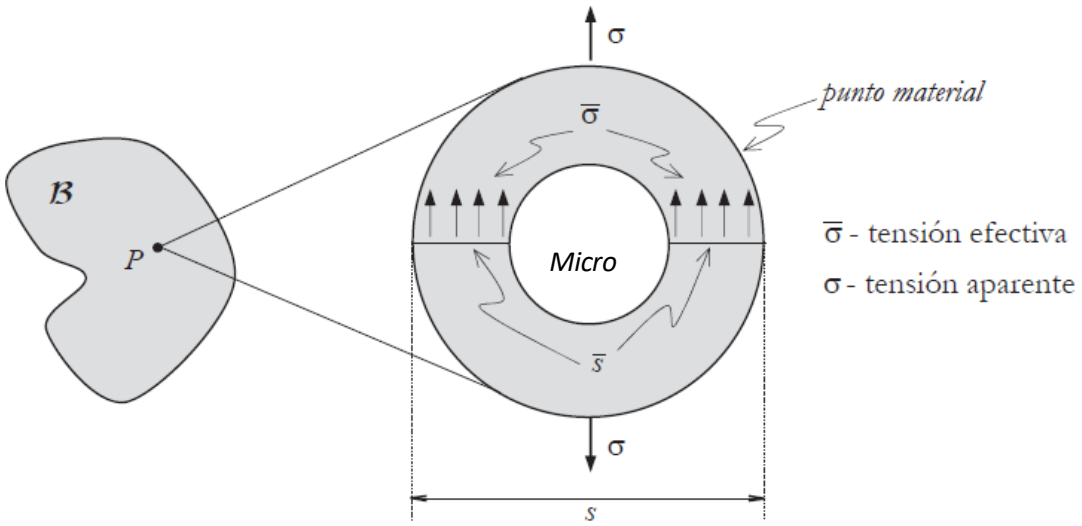

Figure 4.4.1.1 Body under a traction load.
Source: Chaves. Mecánica del medio continuo: Modelos constitutivos. Editor: C.I.M.N.E ISBN 978-8496736689

Applying second Newton's Law, supposing that the body is not under acceleration, the next relationship is obtained.

$$\sum F = 0$$

$$\bar{\sigma}\,\bar{s} = \sigma\, s$$

$$\sigma = \frac{\bar{s}}{s}\bar{\sigma} = \left(\frac{\bar{s} - s}{s} + 1\right)\bar{\sigma} = \left(1 - \frac{s - \bar{s}}{s}\right)\bar{\sigma}$$

where $s - \bar{s}$ is the damaged section, now s_d. Finally, it is obtained:

$$\sigma = \left(1 - \frac{s_d}{s}\right)\bar{\sigma}$$

The relation $\frac{s_d}{s}$ represents the quantity of original section that is damaged. For extreme cases is:

No damaged section	$s_d = 0 \rightarrow \frac{s_d}{s} = 0 \rightarrow \bar{\sigma} = \sigma$
Totally damaged section	$s_d = s \rightarrow \frac{s_d}{s} = 1 \rightarrow \bar{\sigma} = 0$

As it can be seen in the previous table, if the section is totally damaged, it cannot support any stress.

The no dimensional relationship $\frac{s_d}{s}$ represents the damage variable designate d.

The equation can be rewritten as:

$$\sigma = (1 - d)\bar{\sigma}$$

Where the d domain is:

$$0 \leq d \geq 1$$

4.4.1.1. Constitutive equation for 1D

As it is said before, is a 1-dimensional study so the constative relationship will also be with one dimension.

$$\bar{\sigma} = E\ \varepsilon$$

It is used $\bar{\sigma}$ instead of σ because the first one is the real stress.

Using the damage relationship:

$$\sigma = (1 - d)E\varepsilon$$

The damage suffered by a material is no reversible so damage process is permanent. The mathematical representation is:

$$\dot{d} \geq 0$$

It means that the function d is always increasing.

Also, the constitutive equation as:

$$\sigma = E_{dg}\varepsilon$$

where

$$E_{dg} = (1-d)E$$

In general, the materials have an elastic limit that split the elastic zone (reversible process) from the inelastic zone (irreversible process). In strain field we represent that limit by ε_0. Then:

$$d = 0 \quad if \quad \varepsilon < \varepsilon_0$$

In the elastic zone we can guarantee:

- $s_d = 0 \rightarrow d = 0$
- $\varepsilon < \varepsilon_0$ where ε_0 depends from the material.

To summarize, the fundamental characteristics of the 1-dimensional damage model:

$$\sigma = (1-d)E\varepsilon \quad if \quad 0 \leq d \leq 1$$

$$d = 0 \;\; (\sigma = E\varepsilon) \quad if \quad \varepsilon < \varepsilon_0$$

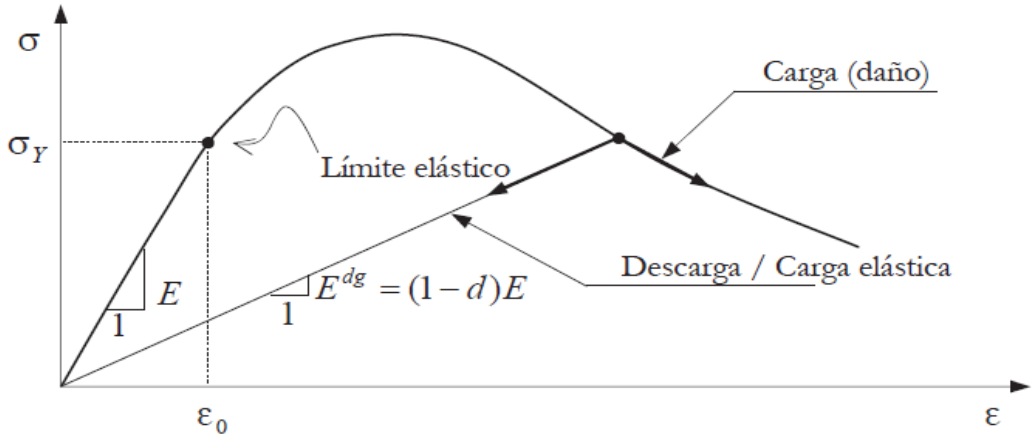

Figure 4.4.1.1.1 Strain-Stress field

Source: Chaves. Mecánica del medio continuo: Modelos constitutivos. Editor: C.I.M.N.E ISBN 978-8496736689

4.4.2. 3-dimensional isotropic damage model

The basis of all damage models consists, as it is seen before in 1 dimensional problem and in [12], in defining a transformation from the real space to the effective space.

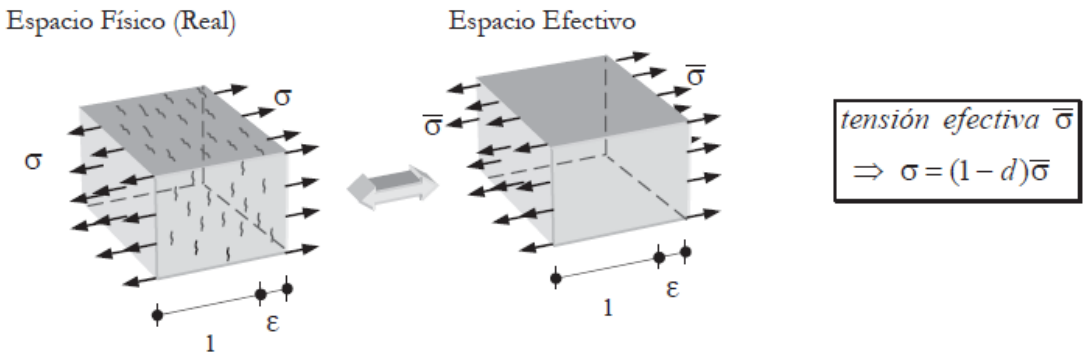

Figure 4.4.2.1 Real space and effective space

Source: Chaves. Mecánica del medio continuo: Modelos constitutivos. Editor: C.I.M.N.E ISBN 978-8496736689

4.4.2.1. Free energy of Helmholtz

It is considered a function of free energy of Helmholtz $\Psi = \Psi(F, T, \alpha)$ where F is gradient of strain, T is temperature and α are group of intern variables. If also it is considered an isothermal problem and the intern variable associated to this problem is d.

Also, the Helmholtz energy can be expressed in function of the Green-Lagrange strain tensor($\boldsymbol{E}$). In the case of small strains, the Green Lagrange tensor is the same as strain tensor($\boldsymbol{\varepsilon}$).

$$Free\ energy\ of\ Helmholtz \qquad \Psi = U - T \cdot S$$

As it is said before, the heat energy sent out by the thermal environment is 0 so:

$$\Psi = U$$

where U is the internal energy.

The internal energy is:

$$U_e = Q + W = W = \frac{1}{2}\varepsilon : \mathbb{C}_e : \varepsilon$$

where

- $Q = 0$. Because isothermal process.

- $W = \frac{1}{2}\varepsilon : \sigma = \frac{1}{2}\varepsilon : \mathbb{C}_e : \varepsilon$

Finally, it is obtained:

$$\Psi_e = \frac{1}{2}\varepsilon : \mathbb{C}_e : \varepsilon$$

And also,

$$\Psi = (1-d)\frac{1}{2}\varepsilon : \mathbb{C}_e : \varepsilon$$

4.4.2.2. Energy dissipation

Damage model has thermodynamic consistence so it has to accomplish entropy inequality. One way to express this inequality is by the Clausius-Planck form, where the intern dissipation is:

$$\mathcal{D}_{int} = \sigma : D - \left[\eta T + \dot{\Psi}\right] \geq 0 \qquad where\ units\ are\ \left[\frac{J}{m^3 s}\right]$$

$$D \rightarrow Strain\ tensor\ of\ Green\ Lagrange$$

When the process is isothermal ($\dot{T} = 0$) as it is said and in little strains system ($D \approx \dot{\varepsilon}$) the last equation, according to [12], can be expressed as:

$$\mathcal{D}_{int} = \sigma : \dot{\varepsilon} - \dot{\Psi} \geq 0$$

where

$$\dot{\Psi}(\varepsilon, d) = \frac{\partial \Psi}{\partial \varepsilon} : \dot{\varepsilon} + \frac{\partial \Psi}{\partial d}\dot{d}$$

Combining the two lasts expression:

$$\mathcal{D}_{int} = \sigma : \dot{\varepsilon} - \frac{\partial \Psi}{\partial \varepsilon} : \dot{\varepsilon} - \frac{\partial \Psi}{\partial d}\dot{d} \geq 0$$

From this expression, the *constitutive law of stress is obtained (Obtained by supposing different types of thermodynamics process):*

$$\sigma = \frac{\partial \Psi}{\partial \varepsilon}$$

Taking into account the previous consideration:

$$\mathcal{D}_{int} = \left[\sigma - \frac{\partial \Psi}{\partial \varepsilon}\right] : \dot{\varepsilon} - \frac{\partial \Psi}{\partial d}\dot{d} = -\frac{\partial \Psi}{\partial d}\dot{d} \geq 0$$

The derivate of $\Psi(\Psi = (1 - \mathrm{d})\Psi_e$) is $\frac{\partial \Psi}{\partial d} = -\Psi_e$ so:

$$\mathcal{D}_{int} = \Psi_e \dot{d} \geq 0$$

Because $\Psi_e \geq 0$ by definition, $\dot{d}$ also has to be positive to satisfy the last inequality.

To sum up:

$$\sigma = \frac{\partial \Psi}{\partial \varepsilon} \quad ; \quad \dot{d} \geq 0$$

Also, it is obtained this relationship doing the previous derivate:

$$\sigma = \frac{\partial \Psi(\varepsilon, \mathrm{d})}{\partial \varepsilon} = (1 - d)\mathbb{C}_e : \varepsilon \qquad Constitutive\ law\ of\ isotropic\ damage$$

Analyzing the previous constitutive law, it can be observed:

- Damage variable is a number without a direction so the degradation of the material is isotropic.
- Once the strains are known and the intern variable of damage d you immediately know the stress.
- The last constitutive law can be written by the sum of two terms, one elastic and one inelastic.

$$\sigma = (1 - d)\mathbb{C}_e : \varepsilon = \mathbb{C}_e : \varepsilon - d\mathbb{C}_e : \varepsilon = \sigma_e - \sigma_i$$

a) <u>Secant Constitutive Tensor</u>

The constitutive tensor for the isotropic damage model is:

$$\mathbb{C}_d = (1 - d)\mathbb{C}_e$$

In the following figure it is observed a uniaxial example where a material is loaded since a point P, next is unloaded where the pendent is: $(1 - d)\mathbb{C}_e$

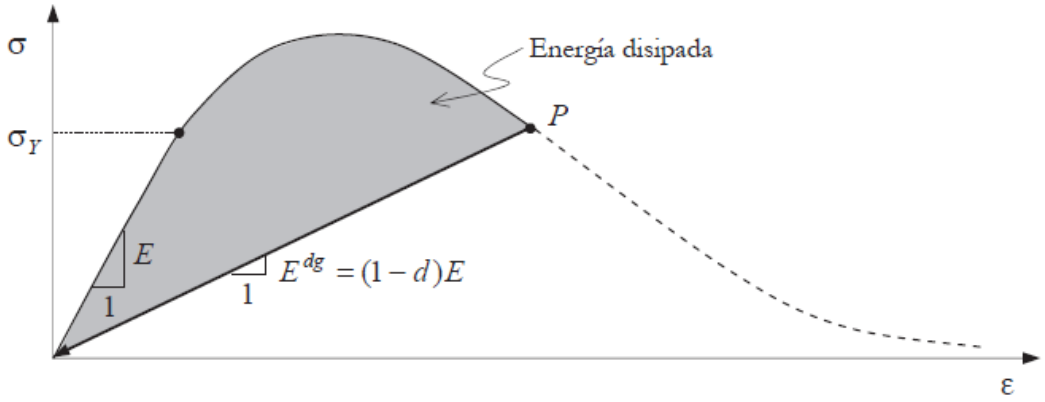

Figure 4.4.2.2.1 Stress-Strain curve
Source: Chaves. Mecánica del medio continuo: Modelos constitutivos. Editor: C.I.M.N.E ISBN 978-8496736689

4.4.2.3. Damage model ingredients

As it is said in [12] the constitutive damage model is totally defined if we know the parameter d in each instant time t.

Also, it is important to define the next elements of the constitutive equation:

- The norm of stress tensor
- Damage surface. The damage surface defines the limit of the elastic behaviour.
- Damage rule. Says when the material is in an elastic process or damage process.
- A group of laws for the evolution of intern variables.

Norm of stress tensor

The norm is a distance measure, also a number. It is defined one possible norm in stress field and one in strain field.

$$\tau_\sigma = \|\sigma\|_{\mathbb{C}^{-1}} = \sqrt{\sigma : \mathbb{C}_e : \sigma}$$

$$\tau_\varepsilon = \|\varepsilon\|_{\mathbb{C}^e} = \sqrt{\varepsilon : \mathbb{C}_e : \varepsilon} = \sqrt{2\Psi_e}$$

The relationship between the norms are:

$$\tau_\sigma = (1-d)\tau_\varepsilon$$

where τ_ε and τ_σ are surface equation that characterize the stress state in a point.

Damage rule

Following we define the damage criteria in stress and strain fields:

$$\Im(\tau_\sigma - q(r)) \leq 0$$

$$\mathcal{g}(\tau_\varepsilon - r) \leq 0$$

where *r* is an intern variable of damage and q is the variable of *softening* or *hardening* in function of *r*. Every material in the initial state has and initial valor of r_0, this valor defines the yield point.

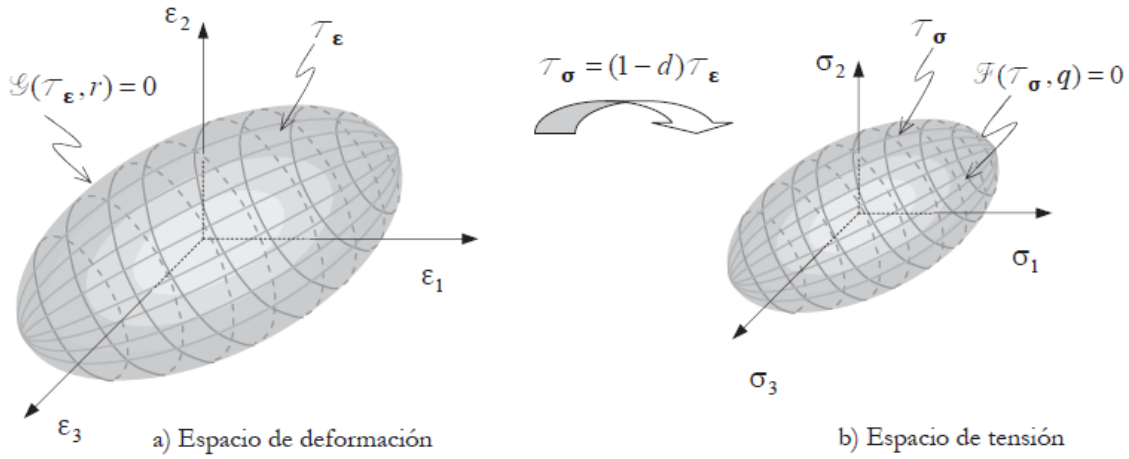

Figure 4.4.2.3.1 Stress field and strain field in the principal strain

Source: Chaves. Mecánica del medio continuo: Modelos constitutivos. Editor: C.I.M.N.E ISBN 978-8496736689

The damage rule requires that the current tensional or strain state must be or on the surface or inside the surface. When the tensional state is inside of the surface of damage, the material is in the elastic regime. It can be in charge or discharge.

$$q(r) = (1 - d)r$$

Evolution of intern variable r

In the model explained before there are three different types of variables:

- Free variable (ε)
- Intern variable (r)
- Dependent variables $(\Psi(\varepsilon, \mathrm{r}), \sigma(\varepsilon, \mathrm{d}), \mathrm{d}(\mathrm{r}))$

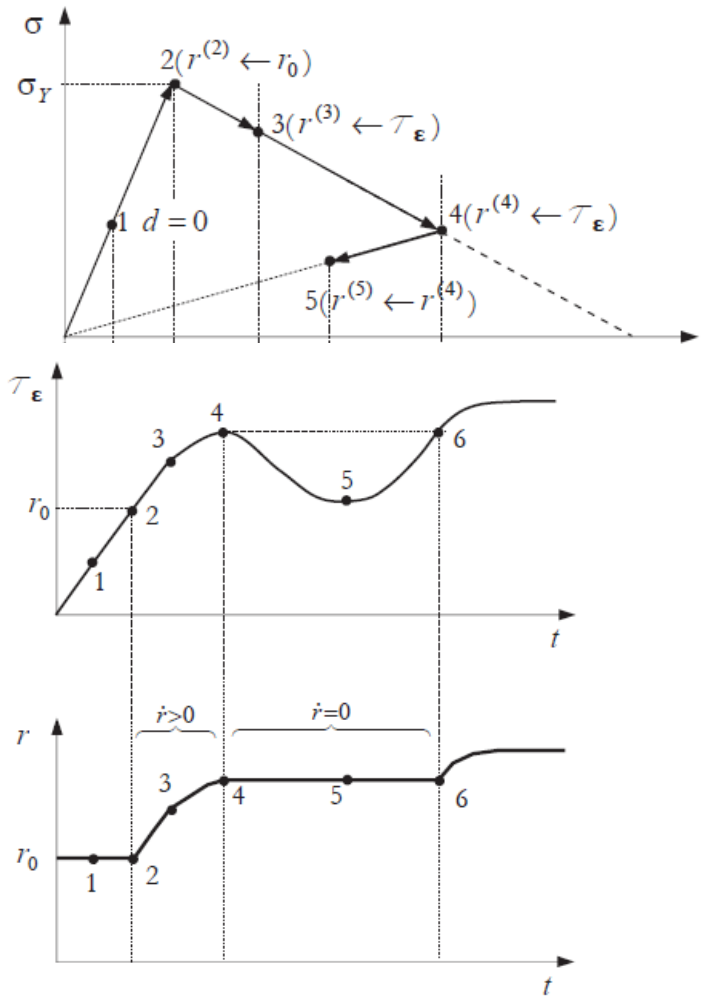

As it is observed in the previous graphics, the variation of the variable r is always increasing so:

$$\dot{r} \geq 0$$

As it can be seen in [12], the free energy of Helmholtz is $\partial\Psi(\varepsilon, \mathrm{d}(\mathrm{r}))$ where now the damage variable is a function of the intern variable r. So, we have:

$$\Psi(\varepsilon, \mathrm{d}(\mathrm{r})) = [1 - \mathrm{d}(\mathrm{r})]\, \Psi^{e}(\varepsilon)$$

$$\dot{\Psi}(\varepsilon, \mathrm{d}(\mathrm{r})) = \frac{\partial \Psi}{\partial \varepsilon} : \dot{\varepsilon} + \frac{\partial \Psi}{\partial d} \frac{\partial \mathrm{d}(\mathrm{r})}{\partial r} \frac{\partial \mathrm{r}}{\partial t} = \frac{\partial \Psi}{\partial \varepsilon} : \dot{\epsilon} - \Psi_{e} \frac{\partial d(r)}{\partial r} \dot{r}$$

where $\frac{\partial \Psi}{\partial d} = -\Psi_{e}$

Using the previous expression now the energy dissipation in terms of damage and elastic energy is:

$$\mathcal{D}_{int} = \sigma : \dot{\varepsilon} - \dot{\Psi}(\varepsilon, r) = \underbrace{\left[\sigma - \frac{\partial \Psi}{\partial \varepsilon}\right]}_{0} : \dot{\varepsilon} + \Psi_e \frac{\partial d(r)}{\partial r}\dot{r} \geq 0$$

So,

$$\dot{d} = \frac{\partial d(r)}{\partial r}\dot{r} = \mathcal{H}(\tau_\varepsilon, d)\dot{r}$$

where $\mathcal{H}$ is the softening /hardening module.

Damage variable

The parameter q is the softening/hardening parameter of stress. Is a function of r.

$$q(r) = (1-d)r \quad \rightarrow \quad d(r) = 1 - \frac{q(r)}{r}$$

The limits of the previous variables are:

$$0 \leq d \leq 1 \qquad r \in [r_0, \infty]$$

The relationship between q and r can approach a lineal law or exponential law.

$$d(r) = 1 - \frac{q(r)}{r}$$

$$\dot{d} = \frac{\partial d(r)}{\partial r}\dot{r} = \frac{\partial}{\partial r}\left[1 - \frac{q(r)}{r}\right]\dot{r} = \left[\frac{q(r) - \frac{\partial d(r)}{\partial r}}{r^2}\right]\dot{r} \quad \rightarrow\rightarrow \dot{d} = \left[\frac{q(r) - \mathcal{H}^d(r)}{r^2}\right]\dot{r}$$

Defining another parameter $\mathcal{H}^d(r) = \frac{\partial d(r)}{\partial r}$, as the softening/hardening parameter

4.4.3. Softening/Hardening

$\frac{\partial d(r)}{\partial r}$ this expression defines the softening/hardening parameter so:

$$\dot{q} = \mathcal{H}^d(r)\,\dot{r} \quad r \in [r_0(d=0), \infty(d=1)] \qquad q \in [r_0, a] \;\; q_0 = r_0 = \frac{\sigma_y}{\sqrt{E}}$$

There are three different types of values that the softening/hardening parameter can obtain:

$$Damage\ with\ hardening \rightarrow \mathcal{H}^d(r) > 0$$

$$Perfect\ damage \rightarrow \mathcal{H}^d(r) = 0$$

$$Damage\ with\ softening \rightarrow \mathcal{H}^d(r) < 0$$

4.4.4. Laws

4.4.4.1. Lineal Law

It is supposed that q has a lineal variation with r. So, we have:

$$q(r) = \begin{cases} r_0 & r \leq 0 \\ r_0 + \mathcal{H}^d(r - r_0) \nless 0 & r > r_0 \end{cases}$$

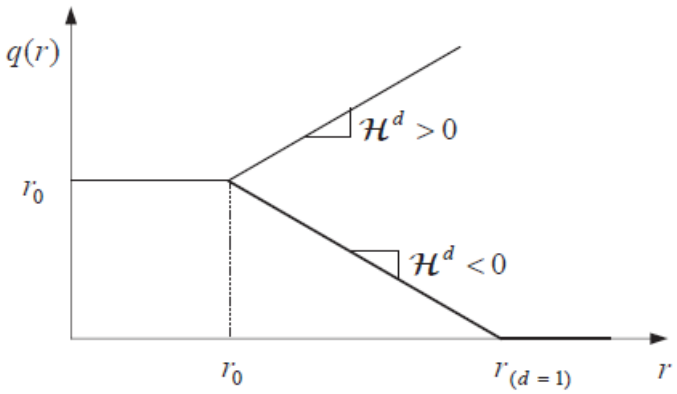

Figure 4.4.4.1.1. Lineal Softening Hardening.
Source Chaves. Mecánica del medio continuo: Modelos constitutivos. Editor: C.I.M.N.E ISBN 978-8496736689

The plot starts at (r_0, r_0) because inside this range the material has an elastic behaviour.

From the valor of H, we can predict the asymptotic valor of d by solving the next limit:

$$d = \lim_{r\to\infty} 1 - \frac{q(r)}{r} = 1 - \frac{r_0 + \mathcal{H}^d(r - r_0)}{r} = H\hat{o}ptial = 1 - \mathcal{H}^d$$

4.4.4.2. Exponential Law

This law is described, according to [12], by the following function:

$$q(r) = q_\infty - (q_\infty - r_0)e^{A\left(1-\frac{r}{r_0}\right)}$$

$$\frac{\partial q(r)}{\partial r} = A\frac{(q_\infty - r_0)}{r_0}e^{A\left(1-\frac{r}{r_0}\right)}$$

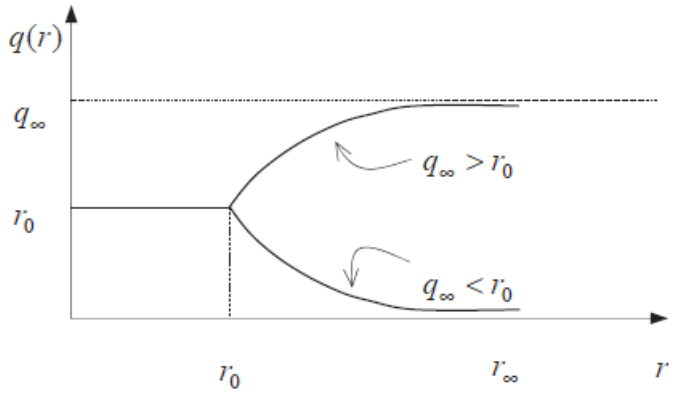

Figure 4.4.4.2.1. Exponential Softening Hardening
Source Chaves. Mecánica del medio continuo: Modelos constitutivos. Editor: C.I.M.N.E ISBN 978-8496736689

In the figure it can be observed that if $q_\infty > r_0$ it has hardening and if not, it has softening. Before, the softening/hardening response it is explained with this variable: $\frac{\partial q(r)}{\partial r}$ .Note that in the previous equation, this variable has a lineal term and an exponential term. As it is known, exponentials are always positive so, if the lineal term is positive the response will be hardening if not, softening.

The lineal term has 3 parts:

- A : Always positive
- r_0: Always positive
- $(q_\infty - r_0)$: Depend on this, the response will be hardening or softening.

With the objective of understanding better the equation behavior, have been realized to observe the influence of the variables in the relationship between $q(r)$ and r.

The variable A from the equation depends on the fracture energy. In the next plot the influence of A it is observed. As it is said before, the term A has relationship with fracture energy so if the influence of A is known, also the influence of the fracture energy in the model.

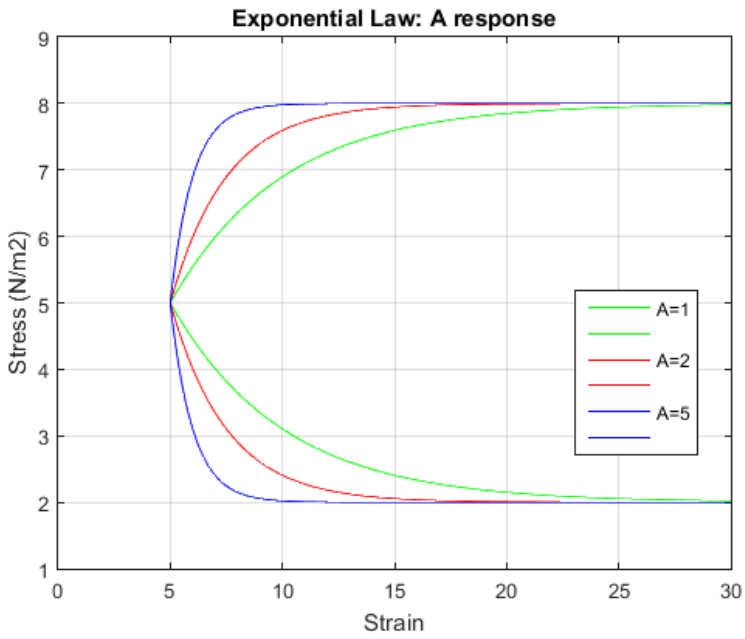

Figure 4.4.4.2.2 Response variation for different values of "A"

As it can be observed in the previous figure, in the way the value of A increases the angle between the derivate of the function and the horizontal axis increase.

Another important plot to see is the variation, or rather, the incrementation of the variable d in function of Hardening or Softening.

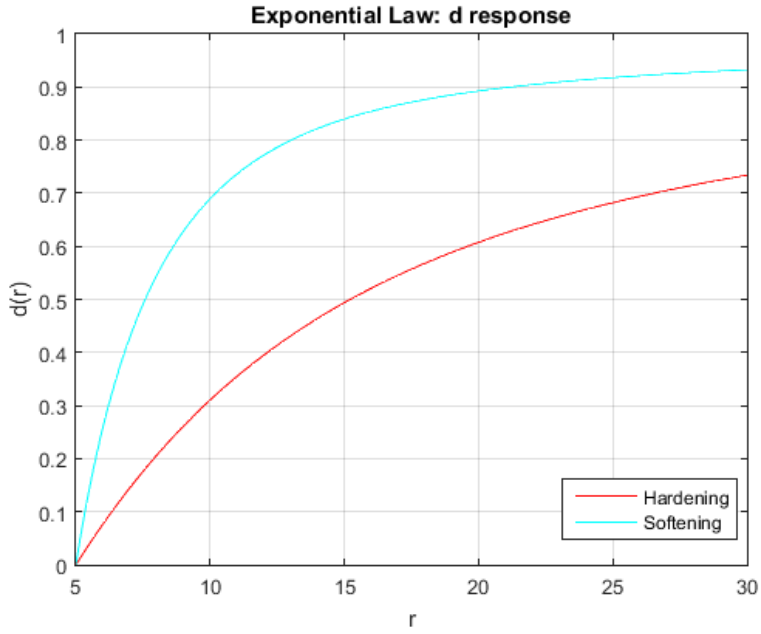

Figure 4.4.4.2.3 Evolution of damage variable "d" for softening and hardening

As it can be seen, the damage increases faster when it's Softening.

In the next plot two zones can be differentiated in two different color. The red zone represents de fracture energy of our damaged material.

One of the conditions is that the blue zone has to be smaller than the fracture's energy area.

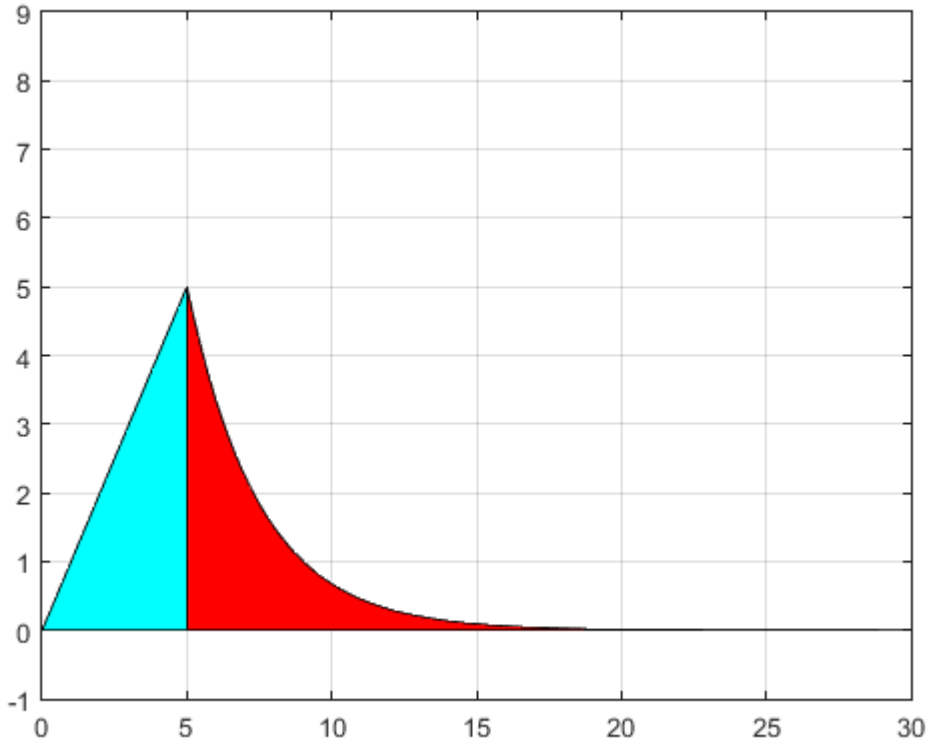

Figure 4.4.4.2.4 Fracture energy and minimum condition

The labels of the plot are not important because the behaviour will be the same in $\sigma_{/\varepsilon}$ and $q(r)_{/r}$.

4.4.5. Constitutive tangent tensor of isotropic damage

By definition, the relationship between $\dot{\sigma}$ and $\dot{\varepsilon}$ give use the constitutive tangent damage tensor $\mathbb{C}^{\tan\_d}$ i.e $\dot{\sigma} = \mathbb{C}^{\tan\_d}\dot{\varepsilon}$. Taking in account the previous considerations we obtain:

$$\dot{\sigma}(\varepsilon, d) = \frac{\partial \sigma}{\partial \varepsilon} : \dot{\varepsilon} + \frac{\partial \sigma}{\partial d} : \dot{d} = (1-d)\mathbb{C}_e : \dot{\varepsilon} - \bar{\sigma} \otimes \dot{d}$$

There are different types of cases:

1. Process with elastic charge or discharge
   $\dot{d} = 0$, so, the previous equation is: $\dot{\sigma} = (1-d)\mathbb{C}_e : \dot{\varepsilon}$. In this case the constitutive tangent tensor is the same as the secant constitutive tensor.

$$\mathbb{C}^{\tan\_d} = \mathbb{C}^{\sec\_d} = (1-d)\mathbb{C}_e$$

2. Charge process with damage
   $\tau_\varepsilon = r \rightarrow \dot{\tau_\varepsilon} = \dot{r}$ and the differential of d:

$$\dot{d} = \frac{\partial \mathrm{d(r)}}{\partial r}\frac{\partial \mathrm{r}}{\partial t} = \frac{\partial d}{\partial \tau_\varepsilon}\dot{\tau_\varepsilon}$$

   $\dot{\tau_\varepsilon}$from the norm defined:

$$\dot{\tau_\varepsilon} = \frac{1}{\tau_\varepsilon}\bar{\sigma} : \dot{\varepsilon}$$

   So:

$$\dot{\sigma} = (1-d)\mathbb{C}_e : \dot{\varepsilon} - \bar{\sigma}\otimes\dot{d} = \left[(1-d)\mathbb{C}_e - \frac{\partial}{\partial \tau_\varepsilon}\frac{1}{\tau_\varepsilon}\bar{\sigma}\otimes\bar{\sigma}\right] : \dot{\varepsilon}$$

   This is the definition of the constitutive tangent tensor

$$\mathbb{C}^{\tan\_d} = \left[(1-d)\mathbb{C}_e - \frac{\partial}{\partial \tau_\varepsilon}\frac{1}{\tau_\varepsilon}\bar{\sigma}\otimes\bar{\sigma}\right]$$

   In charge process, it is known that $\tau_\varepsilon = r(at\ least)$:

$$\mathbb{C}^{\tan_d} = (1-d)\mathbb{C}_e - \left(\frac{q(r) - \mathcal{H}^d(r)}{r^3}\right)(\mathbb{C}_e : \varepsilon \otimes \varepsilon : \mathbb{C}_e)$$

   The general expression for the damage constitutive tensor is:

$$\mathbb{C}^{\tan_d} = \begin{cases} \mathbb{C}_e & elastic\ with\ d = 0 \\ (1-d)\mathbb{C}_e - \mathcal{K}(\mathbb{C}_e : \varepsilon \otimes \varepsilon : \mathbb{C}_e) & charge/\underbrace{discharge}_{\dot{r}=0 \rightarrow\ \mathcal{K}=0 \rightarrow\ \mathbb{C}^{\tan_d}} \end{cases} = \mathbb{C}^{\sec_d}$$

   where

$$\mathcal{K} = \frac{q(r) - \mathcal{H}^d(r)}{r^3}$$

4.4.6. The Norms

The different norms are going to be defined in order to use the one that represents better the material studied. These norms together with the damage criterion (lineal or exponential), play a very important role to define the bounders of the damage surface.
Depending on the material that is intended to be represented, there will be a need to define different standards to simulate the real behavior of the material. For example, a simple model for concrete, if the failure process due to traction is the only process wanted to simulate, this model is not able to capture the failure due to compression.

Models used in the isotropic damage process are going to be studied:

4.4.6.1. Model I

This model represents one approximation of the behavior of that materials that have more or less the same stiffness for traction and compression.
The norm of this model is:

$$\tau_\sigma{}^I = \sqrt{\sigma : \mathbb{C}_e{}^{-1} : \sigma} = (1-d)\sqrt{\overline{\sigma : \varepsilon}}$$

$$\tau_\varepsilon{}^I = \sqrt{\varepsilon : \mathbb{C}_e : \varepsilon} = \sqrt{2\Psi_e}$$

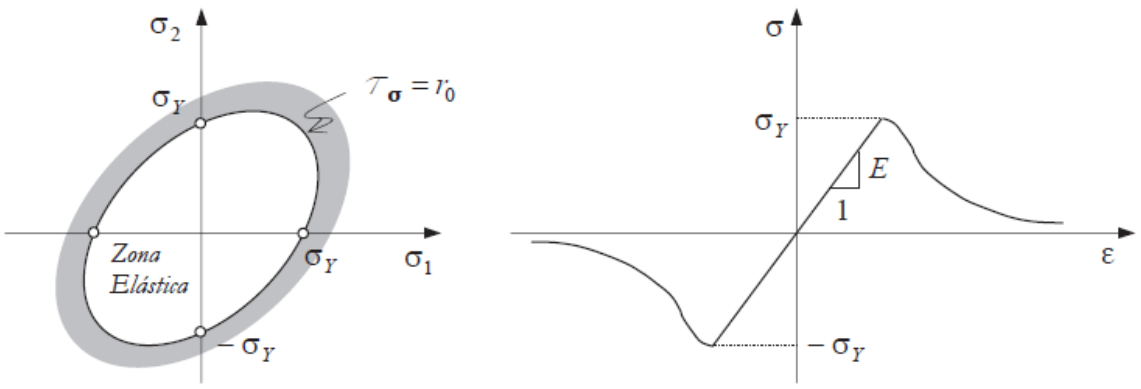

Figure 4.4.6.1.1-D damage surface and 1-D damage line for model 1
Source: Chaves. Mecánica del medio continuo: Modelos constitutivos. Editor: C.I.M.N.E ISBN 978-8496736689

4.4.6.2. Model II Only Traction

This type of model is applied on those materials that have a big stiffness in compression so the material only will suffer in traction. Also, is used when is known that will not be big compression stress.

Using Macauley parenthesis we can obtain:

$$\langle\sigma\rangle = \frac{\sigma + |\sigma|}{2}$$

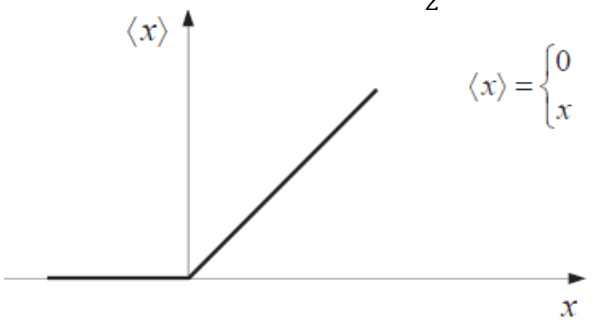

$$\langle x\rangle = \begin{cases} 0 & si \quad x < 0 \\ x & si \quad x \geq 0 \end{cases}$$

In the principal stress state, we can represent the stress tensor by his principal values and principal vectors. Using the Macauley parenthesis:

$$\langle\sigma\rangle = \sum_{a=1}^{3} \langle\sigma_a\rangle\, \hat{n}^{(a)} \otimes \hat{n}^{(a)}$$

The strain model for only traction is (replacing the previous equation in model I):

$$\tau_\varepsilon{}^{II} = \sqrt{\langle\bar{\sigma}\rangle : \mathbb{C}_e{}^{-1} : \bar{\sigma}} = \frac{1}{(1-d)} \sqrt{\langle\sigma\rangle : \mathbb{C}_e{}^{-1} : \sigma}$$

Taking into account the relationship between the strain and stress norm we conclude:

$$\tau_\sigma{}^{II} = \sqrt{\langle\sigma\rangle : \mathbb{C}_e{}^{-1} : \sigma}$$

In the next figure we can see the representation in plane case:

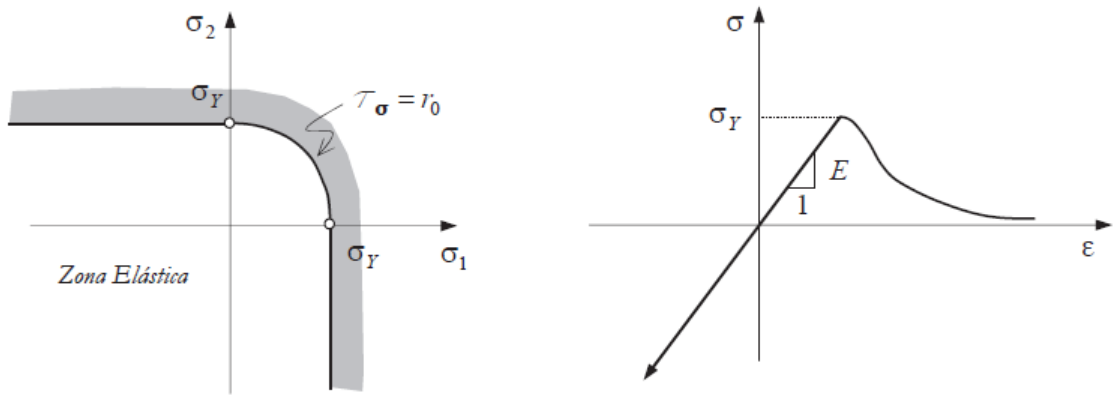

Figure 4.4.6.2.1 Damage surface in 2-D and uniaxial damage curve 1-D for model 2
Source: Chaves. Mecánica del medio continuo: Modelos constitutivos. Editor: C.I.M.N.E ISBN 978-8496736689

4.4.6.3. Model III: Non-symmetric damage

This last model is very useful to simulate those materials that his stiffness in compression is different than in traction. One example of this type of materials is concrete.

The norm used by this model is:

$$\tau_\sigma{}^{III} = \theta + \frac{1-\theta}{n}\sqrt{\sigma : \mathbb{C}_e{}^{-1} : \sigma}$$

Where the parameter θ depends of the stress state σ:

$$\theta = \frac{\sum_{i=1}^{3}\langle\sigma_i\rangle}{\sum_{i=1}^{3}|\sigma_i|}$$

The parameter n defines the relationship between the yield limit in compression and the yield limit in traction:

$$n = \frac{\sigma_Y^c}{\sigma_Y^t}$$

For example, concrete has a $n = 10$

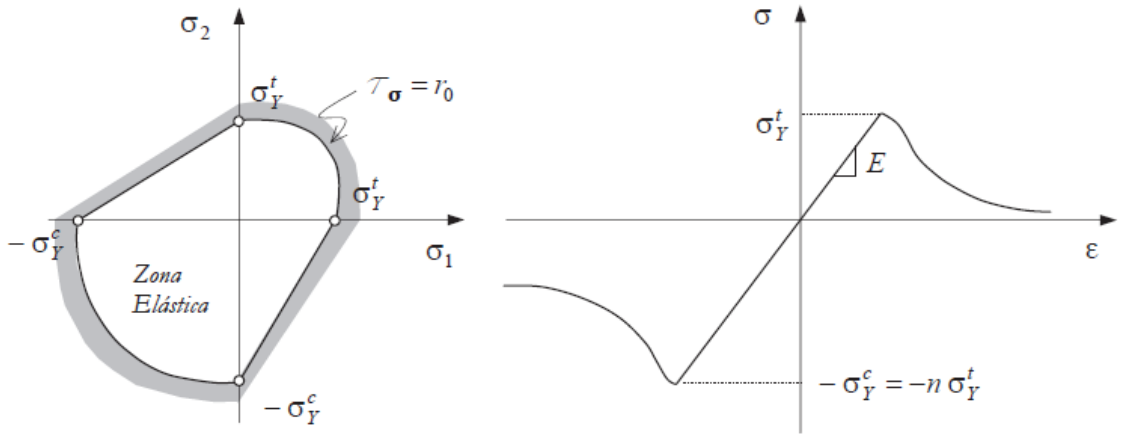

Figure 4.4.6.3.1 Damage surface 2-D and damage curve 1-D for model 3

Source: Chaves. Mecánica del medio continuo: Modelos constitutivos. Editor: C.I.M.N.E ISBN 978-8496736689

To sum up, damage norms define when the material starts to damage and the exponential and lineal law define how is the evolution.

5. Heterogeneous Materials

5.1. Definition

Composites materials can be defined as those materials formed by combining two or more constituents by a chemistry or not union. The reinforcing constituent is embedded in a matrix to form the composite. These materials have better properties than the individual components.

It is important to say that the materials of the composite must not dissolve neither fusion. The materials can be identified by physics ways, meaning that the composite is heterogenic. This is the reason why normally they also have anisotropic properties (the properties are different in each direction).

They are very important for automation industry because of their mechanical resistance and their low density.

According to [13] two phases can be identified:

- Matrix: Continuous phase. Is the responsible for the consistency of the final material. The function of the matrix is to bond the fibers together and to transfer loads between them.
- Fiber: Discontinuous phase. Is the responsible for stiffness of the composite.

The final properties of the composite will be definite by following:

- Fiber properties
- Matrix properties
- Geometry and fiber orientation
- Relation between amount of fiber and amount of matrix.

Mostly composite materials have high stiffness and low density, this is why humans use it along their history. Composite materials allow us to create light structures with high resistance.

5.2. Composite materials characteristics

Low density: Composite materials present a good stiffness by unit of weight. This is possible because of the together work made by fiber and matrix. Both with low density.

High stiffness: Composite materials have a high stiffness, as we said before. It is possible to make the same structures like metals but lighter. In function of the reinforcement and the matrix determinate mechanical properties can be obtained to accomplish a specific requirement.

Shape flexibility: Because of reinforcement is easier to work than other materials, it is easy to make a lot of different geometries.

High dielectric resistance: Composites are insulating materials.

Corrosion resistance: This property depends of the type of matrix used. There are different types of matrix that can resist a corrosive environment. Because of this property, the maintenance of this materials is cheaper than others.

Fatigue: Composite materials have a good behaviour when repeated loads are applied. Because of their amorphous internal structure is difficult that they can suffer the same behaviour than, for example, metals. However, laminate composites can suffer delamination when cyclic loads are applied.

5.3. Classification of composite materials

Composite materials can be classified in different ways. There are two types of classification: Depending on the matrix and depending on the fiber.

5.3.1.1. Metal matrix(MMC)

Metal-matrix composites are either in use or prototyping for the space shuttle, commercial airliners, electronic substrates, bicycles, automobiles, golf clubs, and a variety of other applications. While the vast majority are aluminium matrix composites, a growing number of applications require the matrix properties of superalloys, titanium, copper, magnesium, or iron.

The main properties of these materials are high stiffness and low weight.
Superalloy composites reinforced with tungsten alloy fibers are being developed for components in jet turbine engines that operate temperatures above 1000 °C.
There are two big families:

- Shear and fatigue applications
- Structural applications: Usually used in automotive industry.

Sometimes there are another material coating the exterior walls preventing reactions that can damage the behaviour of our material.

The functions of the metal matrix are the followings:

- Protect the fibers or particles from the out weather.
- Provide a good union between the elements. It unites the fibers but with a gap that not permit the transmission of cracks
- Distribute the loads
- It is important that the matrix doesn't have a big Young modulus.
- In function of the porpoise of the material, maybe also it is important a good thermal resistance(strength)

The most important MMC systems are:

- Aluminum matrix
    - Continuous fibers: boron, silicon carbide, alumina, graphite
    - Discontinuous fibers: alumina, alumina-silica
    - Whiskers: silicon carbide
    - Particulates: silicon carbide, boron carbide
- Magnesium matrix
    - Continuous fibers: graphite, alumina
    - Whiskers: silicon carbide
    - Particulates: silicon carbide, boron carbide
- Titanium matrix
    - Continuous fibers: silicon carbide, coated boron
    - Particulates: titanium carbide
- Copper matrix
    - Continuous fibers: graphite, silicon carbide
    - Wires: niobium-titanium, niobium-tin
    - Particulates: silicon carbide, boron carbide, titanium carbide.
- Superalloy matrices
    - Wires: tungsten

5.3.1.2. Ceramic matrix (CMC)

The motivation to develop ceramic matrix composites was to overcome problems associated with conventional ceramics like alumina, silicon carbide, etc. They fracture easily under mechanical or thermo-mechanical loads.

Composite with a ceramic matrix have better resistance and tenacity than common ceramics. Especially when they work in low range temperature.
General properties:

- High strength-to-weight ratio
- Corrosion resistance
- Greater fatigue life than common ceramics
- Low electrical conductivity
- Anisotropic
- Easy processing

The advanced ceramics developed during the last three decades were initially found with the objective to have some favourable properties in order to use it in high temperature structural parts in industrial process and in heat conversion devices.

The reinforced fibers usually used with this type of matrix are silicon carbide and aluminium oxide. The most common particle reinforcement is also silicon carbide

5.3.1.3. Polymeric matrix (PMC)

Polymeric matrix composites are materials with good mechanical properties and corrosion resistance. Some of the advantages with polymeric matrix composites include their lightweight, high stiffness and their high strength along the direction of the reinforcement.

Inside this category, it is important to focus on thermostable and thermoplastics. In particular, thermostable are usually used on naval structures.

Some drawbacks of polymeric matrix are his environmental degradation and internal stresses because thermal effects.

5.3.2. Classification in function of type of reinforcement

5.3.2.1. Particle reinforcement (reinforced)

Particulate composites offer several advantages. They provide reinforcement to the matrix material thereby strengthening the material. The combination of reinforcement and matrix can provide for very specific material properties. For example, the inclusion of conductive reinforcements in a plastic can produce plastics that are somewhat conductive. Particulate composites can often use more traditional manufacturing methods such as injection moulding which reduces cost.
The reinforcement is better in order we have homogenization and little particles.

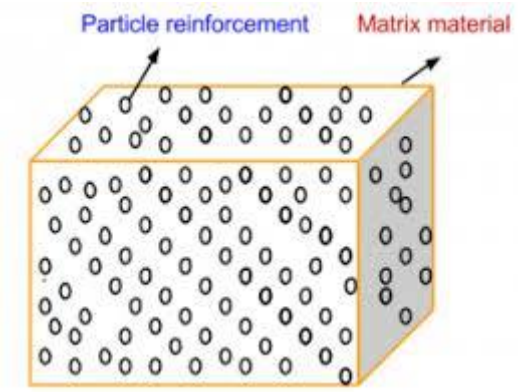

Figure 5.3.2.1. Schematic representation of particle reinforcement

Usually particles occupy the 15-40% of the volume.

In most of the composites reinforced, particle phase has more strength and resistance than matrix phase. Particles have two functions:

- Restrict movement
- Support loads transferred by matrix

It can be differentiated in two groups:

- Dispersion. The diameters of the particles are between 10 to 250nm and these are dispersed homogeny in the matrix. The interaction will be at atomic level. The particles restrict the movement of cracks, this produce an effect of hardening in the composite. An example of this type of reinforcement is black fumes. Black fume are micro spherical particles ($20 - 50\ nm$) produced in the incomplete combustion of natural gas or other petroleum derivates. The addition of this material is very cheaper and it increase the tenacity and stiffness of the material. The car pneumatics are made of 15-30% of this material.

- Big particles. It is considered as big because the interaction between the particles and the matrix are macroscopic (continuous mechanics can be applied). The particles restrict the movement of the matrix and support most of the loads. The typical particle size is $1 - 50\ \mu m$. An example of this type of composite is concrete.

The geometry of particles can be different but it is important that all of them has the same dimension in all directions so the material will have the same properties in all directions. There will not be a direction with more fragility. Unless this is the objective.

Industry applications

The most common particulate composite materials are reinforced plastics which are used in a variety of industries.

- **Automotive**

Glass reinforced plastics are used in many automotive applications including body panels bumpers and intake manifolds. Brakes are made of particulate composite composed of carbon or ceramics particulates.

- **Consumer Products**

Many of the plastic components we use in daily life are reinforced in some way. Appliances, toys, electrical products, computer housings, cell phone casings, office furniture, helmets, etc. are made from particulate reinforced plastics.

5.3.2.2. Fiber reinforcement

Fiber reinforced composites are the most important composite for technological use. The objective is to achieve materials with high stiffness and high fatigue resistance, either in high temperatures mixed with low density. It can be obtained using light materials in fiber and matrix. Keeping in mind the mechanical properties you want to give to the final composite.

There are different factors you have to take in account:

- Fiber length
- Fiber diameter
- Orientation
- Concentration
- Fiber properties
- Matrix properties
- Interaction matrix-fiber

Fiber geometry

There are a lot of ways to place the fibers inside the matrix but we are going to explain the most common ways to place it.

- Aligned

  The properties of aligned fiber-reinforced composite materials are highly anisotropic. The longitudinal ensile strength will be high but the transverse tensile strength maybe will be less than the matrix tensile strength.

  Inside this group it can be differentiated two groups:

  - Continuous

    The fibers are longer than a critical length. Critical length is the minimum length necessary to transmit all the load from the matrix to the fibers. Fiber length greater than 15 times de critical length are considered optimal. Continuous fibers give the most effective strengthening for fiber composites.

- Discontinious

  The fibers are shorter than the critical length. They can approach 50-90% of the tensiles strength of continuous fibers and they are cheaper, faster and easier to fabricate into complicated shapes.

Here it can be observed schematic representation of aligned fibers and continuous.

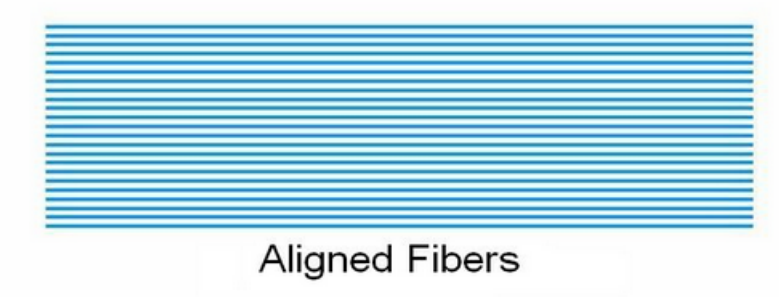

Figure 5.3.2.2.1 Schematic representation of aligned reinforcement

- Random

  It is also called discrete fibers. The strength will not be as high as with aligned fibers, however, the advantage is the material will be more isotropic and cheaper.

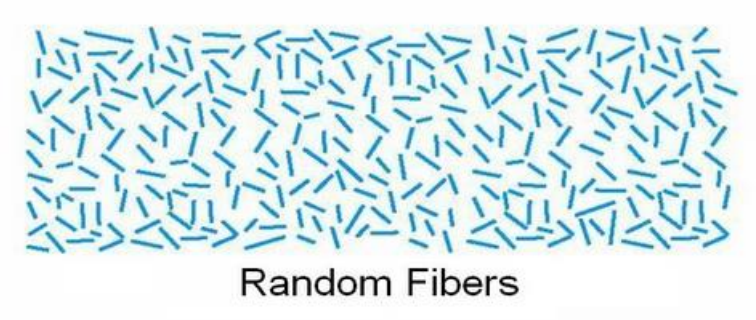

Figure 5.3.2.2.2. Schematic representation of random reinforcement

- Woven

  The fibers are woven into a fabric which is layered with the matrix material to make a laminated structure

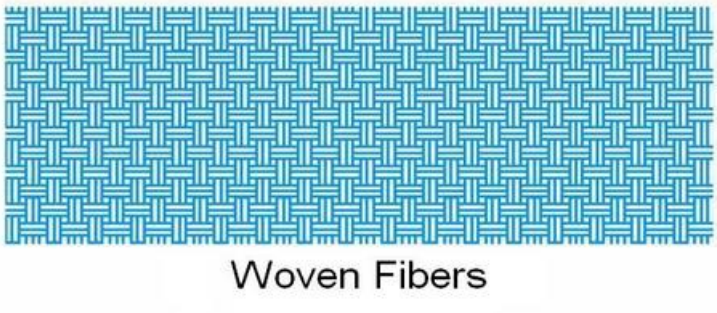

Figure 5.3.2.2.3. Schematich representation of particle reinforcement

Fiber section

The fiber cross shape have a big influence in the behaviour of the composite.

Some common examples of the cross-sectional areas of reinforcing fibers are the followings:

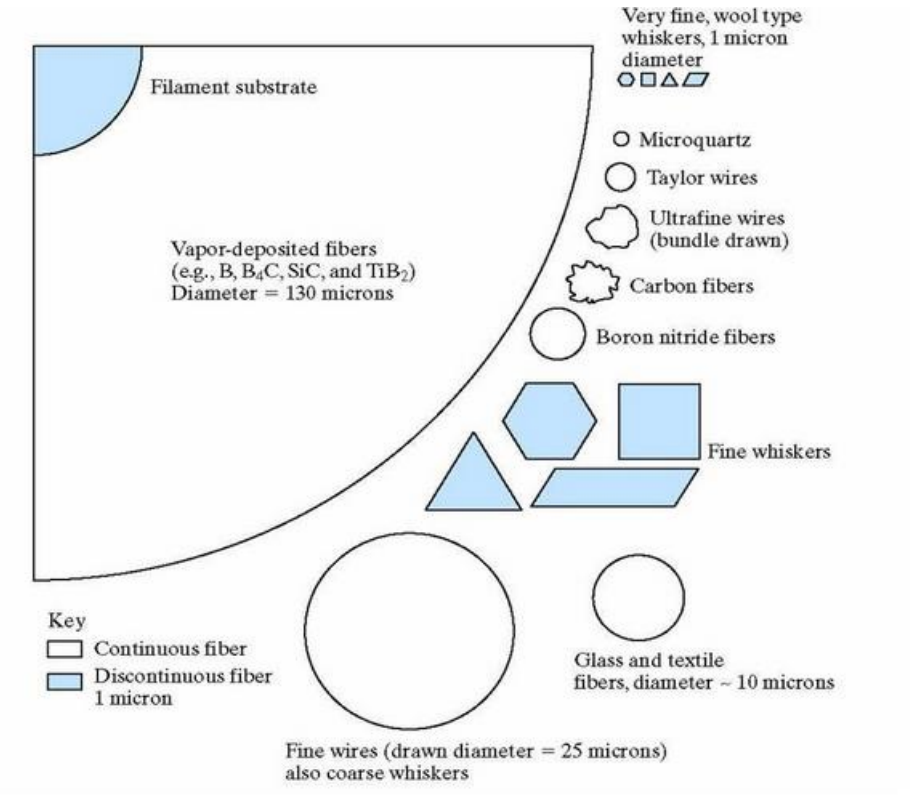

Figure 5.3.2.2.3. Schematic representation of different types of section for fiber reinforcement

General categories based on cross section can be differentiated:

- Whiskers.
  - Very small diameter ($1\mu m$).
  - Strong because they are flaw free (because of it dimension).
  - Expensive.
  - Difficult to place in a matrix.
  - C, SiN, Al_2O_3, SiC.
- Fibers.
  - Small diameter ($10\mu m$).
  - Can be plycristalline or amorphous.
- Wires.
  - Small diameter ($10\mu m$).
  - Made from metals such as steel, Mo, W.

Industry applications

Automotive

The automotive industry has adopted composites slowly due to their higher costs. Particulate reinforced plastics have been used for some time but fiber reinforced composites have only really been used in high end sports cars but are starting to make their way into traditional vehicles. Race cars have used carbon fiber materials for many years.

Aerospace

Carbon fiber composites are now quite common in commercial and military aviation. The Boeing 787 and Airbus A350 XWB have roughly 50% of their structure from composite materials. Carbon fiber materials are also common in helicopter systems, rocket motors, satellite systems, and turbine engines.

Naval

Fiberglass has been the common material for recreational boats and yachts for many years. These are not traditional laminated composites, rather the glass fibers are oriented randomly giving the structure more uniform material properties. Being fairly cheap, glass fiber can be used in large structures; whereas carbon fiber would be too expensive.

Sport

Golf clubs and tennis rackets have used carbon fiber for many years as it provides light weight and high stiffness.

5.4. Micro/Meso/Macro Scale

In the mechanics of composite materials can be taken into consideration different lengths of scale. Some models are built under the point of view of only one of these scales, others use more than one. However, in many cases, it is necessary take into account different behavior that happen on different scales. Normally they are considered the next three scales:

Micro-scale: This is the scale that is at the level of heterogeneity (inclusions, fibers, etc.) in which each constituent material is homogeneous and the interaction between them is analyzed taking into account their strain and stress fields.

This scale provides useful data to simulate effects such as fiber-matrix delamination, damage, plasticity, fatigue, etc. by models homogeneous for simple materials.

Meso-scale: Some models must deal with groups of fibers or shells (in compounds reinforced with long fibers). This level of intermediate scale is usually called meso-scale. Different computational models of elements finites work with these scales to consider a group of fibers.

Macro-scale: This is the scale of the complete structure or component mechanical that is under study.

The scale length involved in the different scale levels normally has big variations. For this reason, the work of mesh a macrostructure with micro-details is hardly feasible. To solve this problem, the concept of equivalent homogeneity has been applied, developing different homogenization techniques to obtain models constituents that can work properly at the macroscopic level.

The concept of equivalent homogeneity

Although the properties and behavior of a material depend strongly from its micro-scale, most engineering problems must be solved at macro-scale level. The macroscopic properties of a material can be obtained experimentally. However, it is also of interest relate the global behavior with the micro behavior obtained at the micro-structural level, and that will lead to improve the knowledge of the material, being able to reduce the experimental costs.

The composite materials are highly heterogeneous at the micro-structural level, but the fact of solving a macro-problem taking into account the amount of information related to the micro-structure, ends up being a task practically impossible. The most common way to overcome this

difficulty is to consider an equivalent homogeneous material. It is considered that this material has the average properties of the heterogeneous material, so we can avoid the complex intern structure.

The development of methods that allow to obtain the average properties is one of the historical themes of the mechanics of composite materials.

5.5. Constitutive models for composite materials

Several homogenization techniques have been developed to obtain a good constitutive model for his using at the macroscopic level. They have been made lot of analytical and numerical studies of the behavior of composite materials. In both points of view, micro-mechanical and macro-mechanical.

In this section, the main models for composite materials are classified according to their scale: macro, micro or multi-scale (using more than one scale).

5.5.1. Macro-mechanical methods

These methods formulate the behavior of the composite material as that of a simple homogeneous material. They can consider the anisotropy of the material in the point of view of the global form. For example, orthotropic plasticity models have been formulated, to simulate non-linear behavior, based on the yield criterion of Hill.

Other authors make use of micro-mechanics to establish yield criterions for the matrix with a restriction in the direction of the embedded reinforcement. The final result is a homogeneous macromodel for compounds that considers anisotropic plasticity restricted by the fiber, such as the "Vanishing" model

5.5.1.1. Hill plasticty model

Hill proposed in 1948 an orthotropic fluency criterion to explain the anisotropic plasticity in metals. Hill's yield surface is often used together with the associated flow rule and adequate hardening laws.

Different authors have applied Hill's criteria in elasto-plastics analysis of fiber-reinforced composite materials, despite the fact that this criterion considers that the material never fails under hydrostatic pressures and ignores the Bauschinger effect (does not take into account kinematic hardening).

Note that micromechanical and experimental considerations indicate that it is not always possible to define a global creep surface for the entire laminate. It is also important to note that mathematical expressions equivalent to Hill's fluency surface are often used to predict failure in compounds at the level of the laminate, even if they describe a physical phenomenon other than plastic failure. These are known as the Tsai-Hill criteria and normally is implemented in several finite elements commercial codes as for example: ABAQUS, ANSYS, NASTRAN. This criterion can be used to predict the elastic limit, but it is not adequate once you are upper elastic limit.

5.5.1.2. Model "Vanishing fiber diameter"

In 1982, Dvorak & Bahei-El-Din proposed a series of relationships simple constituents, based on micromechanics, to model the non-linear behavior of composite materials in which an elastic-plastic matrix is reinforced with elastic fibers, continuous and aligned. Under any axial load, the fibers will only contribute in their direction because there is no interaction between the components in the others directions. For this reason, the model is known as a model with fiber invisible diameter (VFD, Vanishing Fiber Diameter).

The main drawback of this model is its tendency to underestimate the transversal rigidity and shear stress. Also, the VFD model is not suitable for thermal analysis. Thus, in case of having thermal loads, an additional theorical work is necessary.

It is also necessary to make modifications to the model in order to have in count plastically extendable fibers or perfectly plastic matrices. The implementation of the VFD model in a finite element code is described in Bahei-El-Din.

5.5.2. Micro-mechanical methods

These methods determine the constitutive relationships by making a series of hypotheses about the fields of stress and strains at the micro-scale level. They solve analytically the elastic problem.

The initial methods used in micro-mechanical are the average fields methods (MFM), these include the theory of mixtures, Eshelby models and self-consistent methods. Another approach to solution of the problem through micro mechanical models is the method of cells (MOC) and their derivatives.

5.5.2.1. Mean field models

The average field models (MFM) assume that the average values of stresses and strains are representative of the behavior of each phase. It is also assumed that the average of stresses and strains in the phases are related to stresses and strains of each compound (effective) through certain functions of mechanical called "concentration tensors". These functions depend on the form (particles, short fibers or long fibers), the spatial distribution and the fraction volumetric of the reinforcement.

b) Theory of Mixtures

The first applications of the MFM to calculate the elastic constants of composite materials was made by Voigt and Reuss [32], which assumed that the fields of stresses and deformations are, respectively, constants in each of the phases. Voigt and Reuss developed simple formulations called **mixing rule (ROM, Rule of Mixtures)**, and reverse mix rule (iROM, inverse Rule of Mixtures). The global properties are calculated as the average of the properties of each of the constituents, weighted by their volumetric fraction but they result independent of the geometry of the phase or its spatial distribution.

This approach takes into account a single micro-structural feature: the volumetric fraction of each of the phases; then, it is only used when we want to obtain an estimate of linear characteristics of the material (for example, the elastic modulus).

However, the ROM is the starting point for many other methods until you can model the non-linear behavior that many composite materials show due to plastic deformations and creep of the matrix.

In 1960, Truesdell and Toupin proposed the classical theory of mixtures (CMT, classical mixing theory) for the first time based on ROM. The CMT allows the simulation of non-linear behaviour of the material, under a hypothesis of iso-deformation (all the components that coexist in the same

point of the material are under the same field of strains. This hypothesis is a limitation to accurately reproduce the behaviour of material compounds, because are usually found between the state of iso-strain (pure parallel) and iso-stress (pure series). Several authors have tried to solve this problem from different approaches but, unfortunately, these models are not as general as one would wish to correctly represent the behaviour of fiber-reinforced materials.

c) Eshelby models

Eshelby developed in 1956 a method to calculate concentration tensors for an ellipsoidal inclusion embedded in an infinite matrix. However, in most cases, the volumetric fraction of the reinforcement is comparable to that of the matrix and, therefore, the interaction of the elastic fields between neighboring inclusions should be taken into account.

d) Self-consistent models

A similar approximation is the self-consistent method, initially proposed by Kröner to study crystalline plasticity. This model assumes that each reinforcement inclusion is embedded in a continuous material whose effective properties correspond to those of the compound. This model was developed later by several authors, such as, Hashin (1962), Hashin and Shtrikman (1963), Budiansky (1965), Hill (1965), Christensen and Lo (1979), Hashin (1983).

The model of Christensen and Lo is a generalized version of the self-consistent method, in which the reinforcement is immersed in a matrix that, in turn, is embedded in a continuous material whose effective properties are those of compound. Analytical expressions have been derived for elastic constants of composite materials reinforced with continuous fibers and with spherical particles.

5.5.2.2. Cell method

Aboudi developed a micromechanical approach to the problem that is known as the cell method (MOC, Method of Cells). This considers a periodic distribution of fibers to model the thermomechanical behaviour of compounds with unidirectional fibers. Aboudi considers a square unit cell that in turn is divided into 4 sub-cells, three of them with a matrix behaviour and the fourth with fiber characteristics.

The standard MOC employs a linear expansion of the displacements in each one of the sub-cells, the faces of which have continuity in the tractions and the strains average. These equilibrium equations, together with the constitutive models of the constituents allow us to obtain the expansion coefficient. The macro response, transversally isotropic, of the compound is obtained through a process of averaging, in which the elastic modulus is obtained using analytical formulas

The generalized method of cells (GMC) is an extension of the standard method that allows the unit cell to be split into a greater number of sub-cells, which will allow us to simulate complex microstructures.

Non-linear behavior can be taken into account by combining the MOC with an appropriate constitutive model for the matrix. The relative simplicity of model, compared to other approaches based on the unit cell, does also suitable for handling the lower scales of multi-scale models.

5.5.3. Methods of homogenization (or multi-scale)

The homogenization methods are also known as micro-macro models since they obtain the behavior of heterogeneous material to macro-scale level solving a problem on a double scale. Some models they even use multiple scales despite their high computational cost. Many of approaches based on homogenization make a global assumption of periodicity in the microstructure, considering that the entire macro-structure it consists of spatially repeated unitary cells.

A mathematical approach is the theory of asymptotic homogenization. This method considers an asymptotic expansion of the fields of strians and stresses to approximate their respective macroscopic distribution. The relation between the micro and the macro scale is made using variational principles.

The asymptotic homogenization provides an effective estimation of the global properties, as well as values of local stresses and strains. However, it is usually restricted to very simple microstructures and simple materials.

Another common technique used in homogenization is the unit cell method. The effective properties of the material are determined by solving a series of macroscopic constitutive relationships that use the results of a detailed model of a single RVE (representative volume element) usually using the finite element method. Unitary cell methods can easily work with complex microstructures.

But, because they use the behavior of a single RVE subject to a certain history of charges to formulate the macroscopic constitutive equations, their use is restricted to small deformations and simple material behaviors. If we use this formulation in problems with bigger deformations, errors will appear.

One example of this method is the **SPROM** because uses different scale models to solve the problem.

5.6. Serial-Parallel Rule of Mixtures Theory

In order to improve and optimize the design of structural parts made of composite materials, the industry requires new technology tools capable to reproduce the behaviour of composite materials, even in the nonlinear region. Therefore, it is important to find numerical models that could take into account the morphology and structure of the material. Having in account the computational cost.

The numerical model we are talking about is ***Serial Parallel Rule of Mixtures.*** This formulation aims to combine the behaviour of simple materials with the objective of obtaining the mechanical response of the composite material, it can be seen in [13].

The algorithm of this theory is developed to be implemented easy as a constitutive model in a FEM code.

The numerical results compared with experiments show the capability of the proposed model to describe the non-linear behaviour of fibre-reinforced laminates to multiaxial loading, either static or cyclical.

5.6.1. Notation and definition.

Considering a biphasic fiber composite, one representative volume element (RVE) with transversally isotropic symmetry is going to be studied. The differentiation is set between fiber and matrix (f, m).

The reference place of our material will be noted by $\Omega \subset \mathbb{R}^3$. The RVE can be decomposed as the union of two non-overlapping component materials: $\Omega = {}^{f}\Omega \cup {}^{m}\Omega$. The volume fraction is denoted by ${}^{f}k$ ${}^{m}k.$; ${}^{f}k + {}^{m}k = 1$.

According to [13], the standard definition of the volumetric average of the strain and stress field for each respective subdomain is:

$$\bar{\varepsilon} = \frac{\int_\Omega \varepsilon \, dV}{\int_\Omega dV} \qquad \overline{{}^{f}\varepsilon} = \frac{\int_{{}^{f}\Omega} \varepsilon \, dV}{\int_{{}^{f}\Omega} dV} \qquad \overline{{}^{m}\varepsilon} = \frac{\int_{{}^{m}\Omega} \varepsilon \, dV}{\int_{{}^{m}\Omega} dV}$$

$$\bar{\sigma} = \frac{\int_\Omega \sigma \, dV}{\int_\Omega dV} \qquad \overline{{}^{f}\sigma} = \frac{\int_{{}^{f}\Omega} \sigma \, dV}{\int_{{}^{f}\Omega} dV} \qquad \overline{{}^{m}\varepsilon} = \frac{\int_{{}^{m}\Omega} \sigma \, dV}{\int_{{}^{m}\Omega} dV}$$

The relationship between average tensors of our composite is given by the following equation (ROM):

$$\bar{\varepsilon} = {}^{f}k \cdot \bar{\varepsilon} + {}^{m}k \cdot \bar{\varepsilon}$$

$$\bar{\sigma} = {}^{f}k \cdot \bar{\sigma} + {}^{m}k \cdot \bar{\sigma}$$

With a strain driven formulation where the free variable of the problem is strain state. We consider the actual state of the matrix in a point x in ${}^{m}\Omega$ totally defined with the strain in that point $\overline{{}^{m}\varepsilon}\,(x)$ and a finite set of internal variables.

$${}^{m}S = \boldsymbol{Sym} \; x \; {}^{m}I = \{({}^{m}\varepsilon, {}^{m}\beta) | {}^{m}\varepsilon \in \boldsymbol{Sym}, {}^{m}\beta \in {}^{m}I$$

The stress is the independent variable. We define the following differential equation that defines the evolution of the stress and the internal variables.

$${}^{i}\dot{\sigma} = {}^{i}g\,({}^{i}\varepsilon, {}^{i}\beta, {}^{i}\dot{\varepsilon}), \quad i = f, m..$$

$${}^{i}\dot{\beta} = {}^{i}h\,({}^{i}\varepsilon, {}^{i}\beta, {}^{i}\dot{\varepsilon}), \quad i = f, m..$$

These are the constitutive laws for each material.

5.6.2. Equivalent homogeneity

Composite materials, at micro structural level, are very heterogeneous. But if we have to solve a macro-structural problem, it will be practically impossible. The most common form to solve this problem is considering the material homogeneous but with the average properties of the heterogeneous material. Avoiding the internal complex of the material.

5.6.3. SPROM THEORY

The aim of this theory is to model the behaviour of nonlinear material of sheel reinforced with long fibre unidirectional.

5.6.3.1. Directions

An orthogonal reference frame is used to set the material local basis. This model considers a principal direction where the materials behaviour is parallel. In the rest directions, the behaviour is in series.

The direction of the unidirectional fibre will be defined as the direction with parallel behaviour, noted as e_1 . The others orthogonal directions, e_2, e_3 will define the serial behaviour.

It is defined the projector second order tensor N_p:

$$N_p = e_1 \otimes e_1$$

With this tensor you can obtain the parallel projector to fiber direction of a generic vector.

$$v_p = N_p \cdot v$$

Now, the forth order tensor $\mathbb{P}_p$ can be defined as:

$$\mathbb{P}_p = N_p \otimes N_p$$

The forth order projector tensor is easily obtained with his complementary:

$$\mathbb{P}_s = \mathbb{I} - \mathbb{P}_p$$

The function of this tensors is to split the strain and stress field in his serial and parallel parts.

Consequently, it may be defined the following split strain and strass fields for the composite:

$$\varepsilon_p = \mathbb{P}_p : \varepsilon \quad ; \quad \varepsilon_s = \mathbb{P}_s : \varepsilon$$

$$\sigma_p = \mathbb{P}_p : \sigma \quad ; \quad \sigma_s = \mathbb{P}_s : \sigma$$

Since parallel and serial components are complementary, also we have that:

$$\varepsilon = \varepsilon_s + \varepsilon_p$$

$$\sigma = \sigma_s + \sigma_p$$

5.6.3.2. Closure equations for basic serial-parallel model

The distinctive feature of long fiber composites is the well-known strongly anisotropic mechanical behaviour.

The assumptions take are not sufficient for the total definition of the material model. It is needed an additional equation that specify somehow the interaction between the component phases.

It is important that the closure equations for a problem of unidirectional LFC possess the following properties:

1. It should retain the axial constraint of the phases and maintain the transverse isotropy whenever component materials exhibit this property.

2. It should provide a great tangent stiffness, which should be equal to the initial elastic one when no-inelastic phenomena have occurred.

3. It should retain a character of simplicity since the convenience of an approximate model, like the one proposed, relies the possibility of avoid complex calculus.

Furthermore, the constitutive model has to be independent of the specific models of components phases, it will be assumed that the closure equations does not depend on the internal variables ${}^{f}\beta; {}^{m}\beta$. It implies that the closure equation has to account only for the morphological properties of the material.

$$f_i\left({}^{f}\bar{\varepsilon}{}^{m}\bar{\varepsilon}\,{}^{f}\sigma{}^{m}\sigma\right) = 0, \qquad i = 1, \dots, 6.$$

The ***Basic serial parallel*** model is based on the next closure equations, according to [13]:

$${}^{\mathrm{m}}\varepsilon_P = {}^{\mathrm{f}}\varepsilon_P$$

$${}^{\mathrm{m}}\sigma_S = {}^{\mathrm{f}}\sigma_S$$

These are the equations that specify the behavior between components.

To sum up, the BSP ROM model (***Basic serial parallel rule of mixtures)*** is set up by the following differential equations:

$${}^{i}\dot{\sigma} = {}^{i}g\,({}^{i}\varepsilon,\ {}^{i}\beta,\ {}^{i}\dot{\varepsilon}), \quad i = f, m..$$

$${}^{i}\dot{\beta} = {}^{i}h\,({}^{i}\varepsilon,\ {}^{i}\beta,\ {}^{i}\dot{\varepsilon}), \quad i = f, m..$$

$$\bar{\varepsilon} = {}^{f}k \cdot \bar{\varepsilon} + {}^{m}k \cdot \bar{\varepsilon}$$

$$\bar{\sigma} = {}^{f}k \cdot \bar{\sigma} + {}^{m}k \cdot \bar{\sigma}$$

$${}^{m}\bar{\varepsilon}_p = {}^{f}\bar{\varepsilon}_p$$

$${}^{m}\bar{\sigma}_S = {}^{f}\bar{\sigma}_S$$

5.6.4. Algorithm for the resolution of the BSPROM model.

The state variables that define the problem are ${}^{m}\varepsilon,\ {}^{f}\varepsilon, \varepsilon, {}^{m}\beta,\ {}^{f}\beta$.

The equations governing the problem are:

1. Constitutive law of each material.
   $${}^{i}\dot{\sigma} = {}^{i}g\,({}^{i}\varepsilon,\ {}^{i}\beta,\ {}^{i}\dot{\varepsilon}), \quad i = f, m..$$
   $${}^{i}\dot{\beta} = {}^{i}h\,({}^{i}\varepsilon,\ {}^{i}\beta,\ {}^{i}\dot{\varepsilon}), \quad i = f, m..$$

2. The equation relating the states of stress and stiff of the component with the material.
   $$\bar{\varepsilon} = {}^{f}k \cdot \bar{\varepsilon} + {}^{m}k \cdot \bar{\varepsilon}$$
   $$\bar{\sigma} = {}^{f}k \cdot \bar{\sigma} + {}^{m}k \cdot \bar{\sigma}$$

3. Closure equation that define the compatibility between the components.
   $${}^{m}\bar{\varepsilon}_p = {}^{f}\bar{\varepsilon}_p$$
   $${}^{m}\bar{\sigma}_S = {}^{f}\bar{\sigma}_S$$

This algorithm is considered “strain driven” (the strain is the free variable).

Given the state variables at time “t”:

$$[{}^{m}\varepsilon], \left[{}^{f}\varepsilon\right], [{}^{m}\beta], \left[{}^{f}\beta\right], [\varepsilon]$$

And the deformation at time $t + \Delta t$

$$[\varepsilon]^{t+\Delta t}$$

It is needed to find the state of the composite at time $t + \Delta t$, defined by the following group of variables:

$$[{}^{m}\varepsilon], \left[{}^{f}\varepsilon\right], [{}^{m}\beta], \left[{}^{f}\beta\right], [\sigma], \left[{}^{f}\sigma\right], [{}^{m}\sigma]$$

The following chart shows us the know and the unknow variables of the problem.

Known variables	Free variables: ${}^{t+\Delta t}[\varepsilon]$ Intern variables: ${}^{t}[{}^{m}\varepsilon]$, ${}^{t}\left[{}^{f}\varepsilon\right]$, ${}^{t}[{}^{m}\beta]$, ${}^{t}\left[{}^{f}\beta\right]$
Unknown variables (All in time $\boldsymbol{t+\Delta t}$)	Independent variables: $[\sigma]$, $\left[{}^{f}\sigma\right]$, $[{}^{m}\sigma]$ Actualized intern variables: $[{}^{m}\varepsilon]$, $\left[{}^{f}\varepsilon\right]$, $[{}^{m}\beta]$, $\left[{}^{f}\beta\right]$

The variables $[{}^{m}\beta]$, $\left[{}^{f}\beta\right]$ group all the intern variables that defines the state of the components materials. For example, the intern variables of damage and plasticity.

For solve our non-lineal equation problem we will use an iterative method called: ***Newton-Raphson.***

When applying the serial/parallel mixing theory, it is possible to use any constitutive equation to describe the structural behavior of the composite material. The constitutive equations used can be different for each component (i.e. elastic law to describe the fiber behavior and a damage formulation to describe the matrix behavior.

$$ {}^{m}\sigma = {}^{m}\mathbb{C} : {}^{m}\varepsilon $$

$$ {}^{f}\sigma = {}^{f}\mathbb{C} : {}^{f}\varepsilon $$

Where $\mathbb{C}$ is the constitutive tensor.

The algorithm will use the following decomposition of the tangent operators. The equations can be rewritten to consider the serial and parallel separation of the strain and stress tensors.

$$ \begin{bmatrix} {}^{i}\sigma_P \\ {}^{i}\sigma_S \end{bmatrix} = \begin{bmatrix} {}^{i}\mathbb{C}_{PP} & {}^{i}\mathbb{C}_{PS} \\ {}^{i}\mathbb{C}_{SP} & {}^{i}\mathbb{C}_{SS} \end{bmatrix} : \begin{bmatrix} {}^{i}\varepsilon_P \\ {}^{i}\varepsilon_S \end{bmatrix} $$

$$ \mathbb{C} = \begin{bmatrix} \dfrac{\partial\, {}^{c}\sigma_P}{\partial\, {}^{c}\varepsilon_P} & \dfrac{\partial\, {}^{c}\sigma_P}{\partial\, {}^{c}\varepsilon_S} \\ \dfrac{\partial\, {}^{c}\sigma_S}{\partial\, {}^{c}\varepsilon_P} & \dfrac{\partial\, {}^{c}\sigma_S}{\partial\, {}^{c}\varepsilon_S} \end{bmatrix} $$

Where:

$$^{i}\mathbb{C}_{PP} = \mathbb{P}_P : {}^{c}\mathbb{C} : \mathbb{P}_P$$

$$^{i}\mathbb{C}_{PS} = \mathbb{P}_P : {}^{c}\mathbb{C} : \mathbb{P}_S$$

$$^{i}\mathbb{C}_{SP} = \mathbb{P}_S : {}^{c}\mathbb{C} : \mathbb{P}_P$$

$$^{i}\mathbb{C}_{SS} = \mathbb{P}_S : {}^{c}\mathbb{C} : \mathbb{P}_S$$

In order to understand the complex algorithm of the SPMODEL

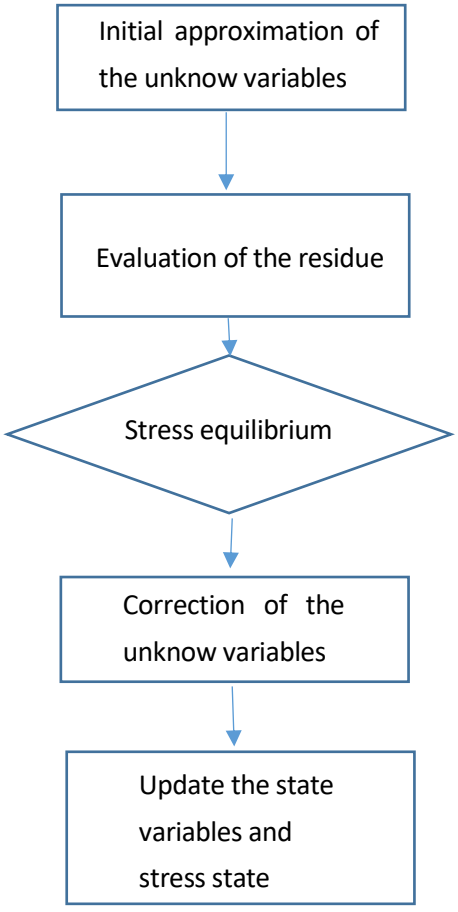

SPROM extended algorithm

The next algorithm is applied in each gauss point. A gaussian quadrature rule is a numerical method used to solve exact integration of polynomial equation of degree $2n - 1$ or less. Is the same as any other quadrature integration but if we apply this integration in a gauss point the exact value is obtained. This, is very important for solving the elements in the finite element method because in the gauss points we obtain a higher order approximation than in other point of the element.

The next schematic figures represent the gauss points for the most important elements in 2D elasticity.

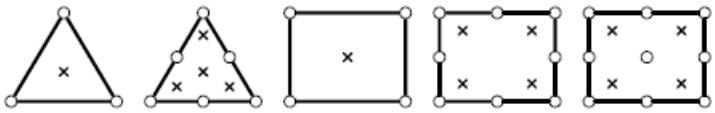

As It is said, the next algorithm is applied for each gauss element, in each element and for each layer in order to obtain the global convergence.

First of all, it is important to know which variables we know at the initial of the algorithm.

Initial variables	$[\varepsilon]^{n+1}$	$[\varepsilon]^{n}$	${}^{\mathrm{m}}\varepsilon_S^n$

where n is the number of the step.

When the algorithm starts, the initial value of ${}^{\mathrm{m}}\varepsilon_S^n$ is 0.

Now, all the equations of the BSPROM model are going to be used to obtain the unknow variables, then check if the obtained variables accomplish the requirements of the closure equations.

1. $\varepsilon_p^n = \mathbb{P}_P : [\varepsilon]^n$

2. ${}^{\mathrm{f}}\varepsilon_p^n = {}^{\mathrm{m}}\varepsilon_p^n = \varepsilon_p^n$

These variables can be obtained by applying the first condition of the SPROM: ${}^{\mathrm{m}}\bar{\varepsilon}_p = {}^{\mathrm{f}}\bar{\varepsilon}_p = \varepsilon_p^n$

3. ${}^{\mathrm{m}}\varepsilon^n = {}^{\mathrm{m}}\varepsilon_s^n + {}^{\mathrm{m}}\varepsilon_p^n$

   - ${}^{\mathrm{m}}\varepsilon_s^n$ This variable is known from the beginning
   - ${}^{\mathrm{m}}\varepsilon_p^n$ obtained in 1.

4. $\varepsilon_s^n = \mathbb{P}_S : \varepsilon^n$
5. ${}^{\mathrm{f}}\varepsilon_s^n = \frac{k_m}{k_f}\,{}^{\mathrm{m}}\varepsilon_s^n - \frac{1}{k_f}\,\varepsilon_s^n$
6. ${}^{\mathrm{f}}\varepsilon^n = {}^{\mathrm{f}}\varepsilon_s^n + {}^{\mathrm{f}}\varepsilon_p^n$

   - ${}^{\mathrm{f}}\varepsilon_s^n$ obtained from 5.
   - ${}^{\mathrm{f}}\varepsilon_p^n$ obtained from 1.

Now we know the next varibales:

Known variables	Initial variables	${}^{\mathrm{m}}\varepsilon^n$	${}^{\mathrm{m}}\varepsilon_p^n$	${}^{f}\varepsilon^n$	${}^{f}\varepsilon_s^n$	${}^{f}\varepsilon_p^n$	ε_p^n	ε_s^n

Once all the strain is known, the stress field is obtained by using the constitutive equation of each material.

$${}^{m}\mathbb{C}\,({}^{m}\varepsilon)\,;\,{}^{f}\mathbb{C}\,\left({}^{f}\varepsilon\right)$$

With this tensor, the constitutive tensor can be obtained of the composite:

$$\mathbb{C}^n\left({}^{m}\varepsilon,\,{}^{f}\varepsilon\right) = \begin{bmatrix} {}^{i}\mathbb{C}_{PP} & {}^{i}\mathbb{C}_{PS} \\ {}^{i}\mathbb{C}_{SP} & {}^{i}\mathbb{C}_{SS} \end{bmatrix}$$

$$\mathbb{C}_{PP} = \left(k^f\,{\mathbb{C}_{PP}}^f + k^m{\mathbb{C}^m}_{PP}\right) + k^f k^m\left({\mathbb{C}_{PS}}^f - {\mathbb{C}_{PS}}^m\right) : \mathbb{A} : \left({\mathbb{C}_{SP}}^m - {\mathbb{C}_{SP}}^f\right)$$

$$\mathbb{C}_{PS} = \left(k^f\,{\mathbb{C}_{PS}}^f : \mathbb{A} : {\mathbb{C}_{SS}}^m + \; k^m{\mathbb{C}_{PS}}^m : \mathbb{A} : {\mathbb{C}_{SS}}^f\right)$$

$$\mathbb{C}_{SP} = \left(k^m\,{\mathbb{C}_{SS}}^f : \mathbb{A} : {\mathbb{C}_{SP}}^m + \; k^f{\mathbb{C}_{SS}}^m : \mathbb{A} : {\mathbb{C}_{SP}}^f\right)$$

$$\mathbb{C}_{SS} = \frac{1}{2}\left({\mathbb{C}_{SS}}^m : \mathbb{A} : {\mathbb{C}_{SS}}^f + \; {\mathbb{C}_{SS}}^f : \mathbb{A} : {\mathbb{C}_{SS}}^m\right)$$

Where $\mathbb{A} = (k^m \mathbb{C}_{SS}{}^f + k^f \mathbb{C}_{SS}{}^m)^{-1}$

Then, we can calculate the stress of the composite:

$$\sigma^n = \mathbb{C}^n : \varepsilon^n$$

This result cannot be validated yet because the second condition of the SPROM is unaccomplished.
Second closure condition: ${}^{\mathrm{m}}\overline{\sigma}_S = {}^{\mathrm{f}}\overline{\sigma}_S$

By applying the constitutive equation of each material, it is obtained:

${}^{\mathrm{m}}\overline{\sigma}_S = {}^{\mathrm{m}}\overline{\sigma} : \mathbb{P}_s = ({}^m\mathbb{C} : {}^m\varepsilon) : \mathbb{P}_s$

${}^{\mathrm{f}}\overline{\sigma}_S = {}^{\mathrm{f}}\overline{\sigma} : \mathbb{P}_s = ({}^f\mathbb{C} : {}^f\varepsilon) : \mathbb{P}_s$

Now, the next step is to calculate the second condition of the SPMODEL.

${}^{\mathrm{m}}\overline{\sigma}_S - {}^{\mathrm{f}}\overline{\sigma}_S = 0$

There are two possibilities (as it can be seen in the algorithm sequence drowned before).

1. ${}^{\mathrm{m}}\overline{\sigma}_S - {}^{\mathrm{f}}\overline{\sigma}_S = 0$

   Once the convergence of the constitutive model has been obtained, all the variables of the model must be updated.

   Where n is the last step of the algorithm and t is time.

Strain field	Intern variables	Stress field
${}^{\mathrm{m}}\varepsilon_s^{t+\Delta t} = {}^{\mathrm{m}}\varepsilon_s^n$	${}^{\mathrm{m}}\beta_s^{t+\Delta t} = {}^{\mathrm{m}}\beta_s^n$	${}^{\mathrm{m}}\sigma_s^{t+\Delta t} = {}^{\mathrm{m}}\sigma_s^n$
${}^{\mathrm{f}}\varepsilon_s^{t+\Delta t} = {}^{\mathrm{f}}\varepsilon_s^n$	${}^{\mathrm{f}}\beta_s^{t+\Delta t} = {}^{\mathrm{f}}\beta_s^n$	${}^{\mathrm{f}}\sigma_s^{t+\Delta t} = {}^{\mathrm{f}}\sigma_s^n$

   Now the variables have been updated, finally the algorithm can pass to the next gauss point. If there is no more gauss point, the algorithm pass to the next element and for last if there is no more element, the algorithm pass to the next layer.

2. ${}^{\mathrm{m}}\overline{\sigma}_S - {}^{\mathrm{f}}\overline{\sigma}_S \neq 0$

   In this case, the variable ${}^{\mathrm{m}}\varepsilon_s^n$ has to be updated.

$$^{\mathrm{m}}\varepsilon_s^{n+1} = {}^{\mathrm{m}}\varepsilon_s^{n} - \mathbb{J}^{-1}{:}\,\Delta \quad \bar{\sigma}_S^n$$

Where

$$\mathbb{J} = \frac{\partial \Delta \quad \bar{\sigma}_S^n}{\partial\, ^{\mathrm{m}}\varepsilon_s} = {}^{m}\mathbb{C}_{SS} + \frac{k_m}{k_f}\, {}^{f}\mathbb{C}_{SS}$$

$^{\mathrm{m}}\varepsilon_s^{n+1}$ with this variable we can repeat the process going back to 1.

Finally, if the step 5 is done the algorithm can go to the last step:

All the states of the composite have to be updated. They are used to update the variables to calculate the final state of the composite

$$\overline{^{t+\Delta t}\sigma} = {}^{f}k \cdot \bar{\sigma} + {}^{m}k \cdot \bar{\sigma}$$

6. Simulations

6.1. Lineal cases

The aim of this inform is to find the best element type for modelling shell structures in Ramseries. The different types of element implemented in Ramseries that are going to be studied are:

- Linear DKT triangle
- Linear drilling rotation triangle
- Linear six node triangle
- Linear quadrilateral

In particular, this part aims to demonstrate the goodness of the drilling-rotation triangular element versus both, the classical triangular DKT and the quadrilateral elements.

6.1.1. Scrodelis-Lo roof

It is only analysed one quadrant of the roof because his symmetry and only self-weight load condition is applied. For the validation is studied the vertical downward deflection at the point B (Figure 6.1.1.1).

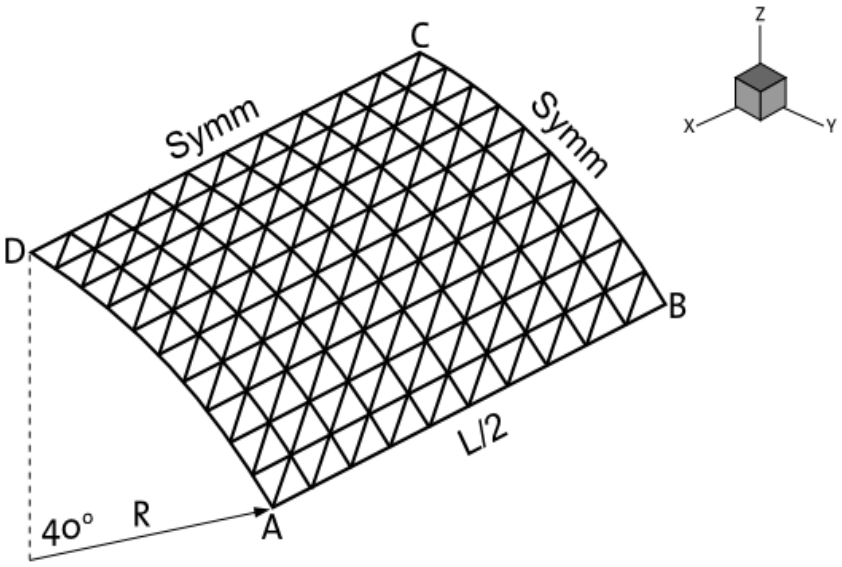

Figure 6.1.1.1. Schematic representation of the geometrical model uset to analyse the Scordelis-Lo roof problem.

6.1.1.1. Geometrical characteristics

Roof radius	R=25m
Roof length	L=50m
Shell thickness	t=0.25m
Young modulus	E=4.32e8 Pa
Poisson coefficient	v=0
Self Weight	W=90N/m^2

6.1.2. Vertical downward deflection

The exact value of deflection used to compare our results is 0.3024m, as stated in (1).

N of nodes	24	77	273	1025	3969
DKT Triangle	0.2493	0.26639	0.28932	0.29743	0.29964
Drill Rotation Triangle	0.3236	0.3059	0.3018	0.3010	0.3008
6 nodes	0.31251	0.30189	0.30315	0.30337	0.30347
Linear Quadrilateral	0.28751	0.29699	0.30156	0.30252	0.30289

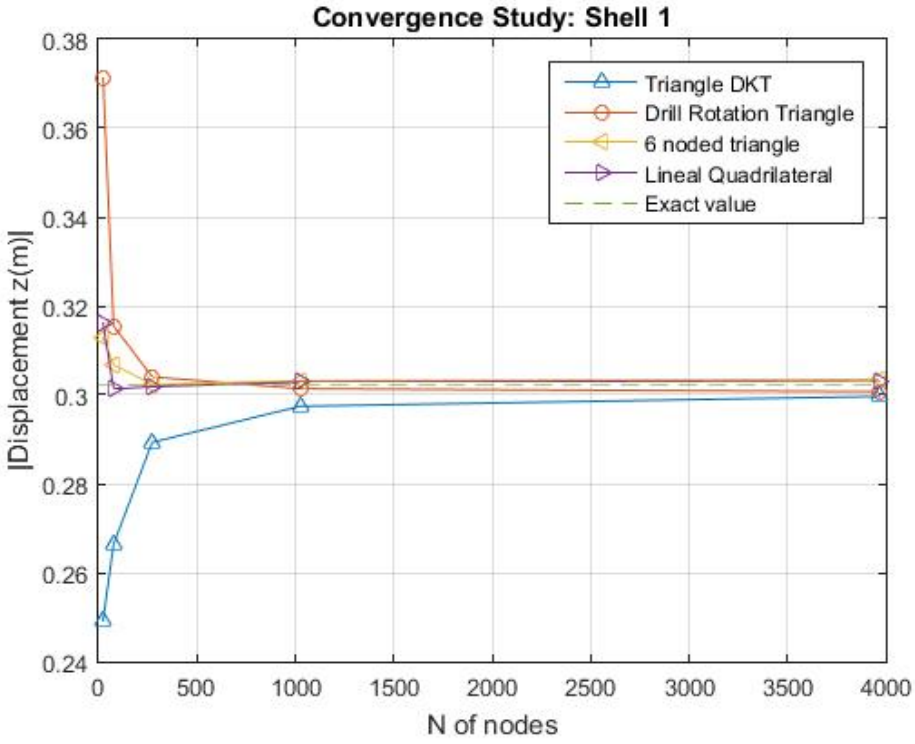

Figure 6.1.2.1 Convergence study for Scrodelis Lo-roof benchmark

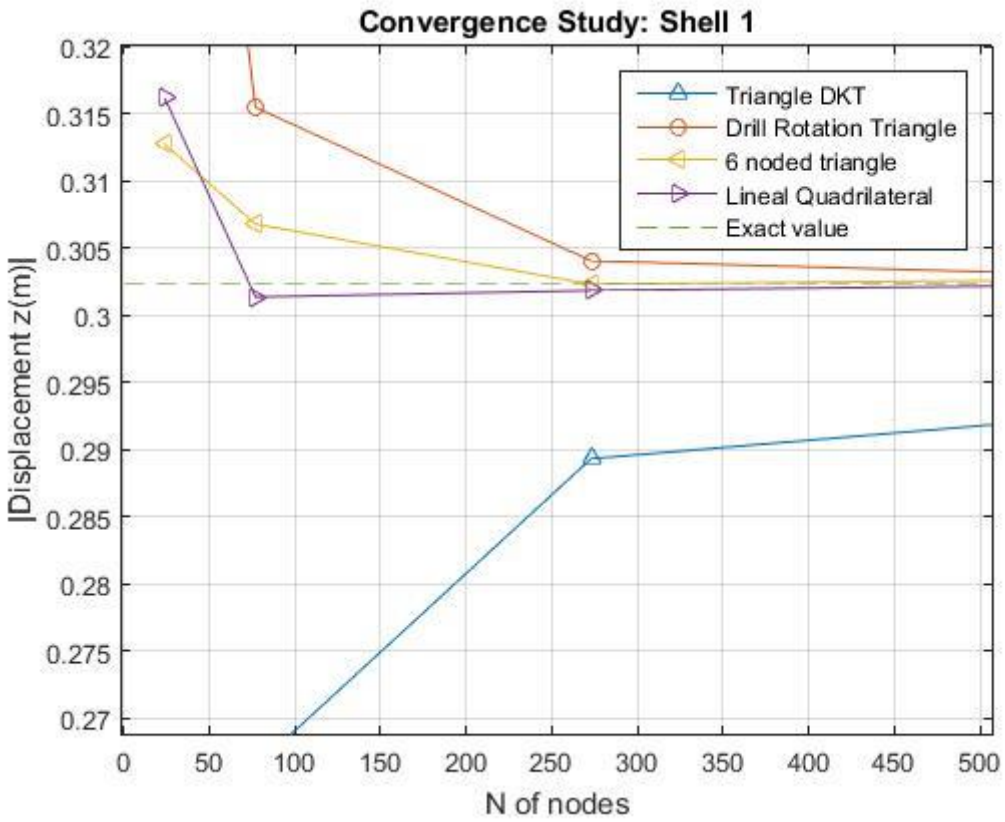

Figure 6.1.2.2 Convergence study ampliated Scrodelis-Lo roof

It can be observed that the Lineal Quadrilateral has a faster convergence than drill-rotation triangle. Also, it is seen that 6 nodded element has a very good convergence and almost the better final approximation.

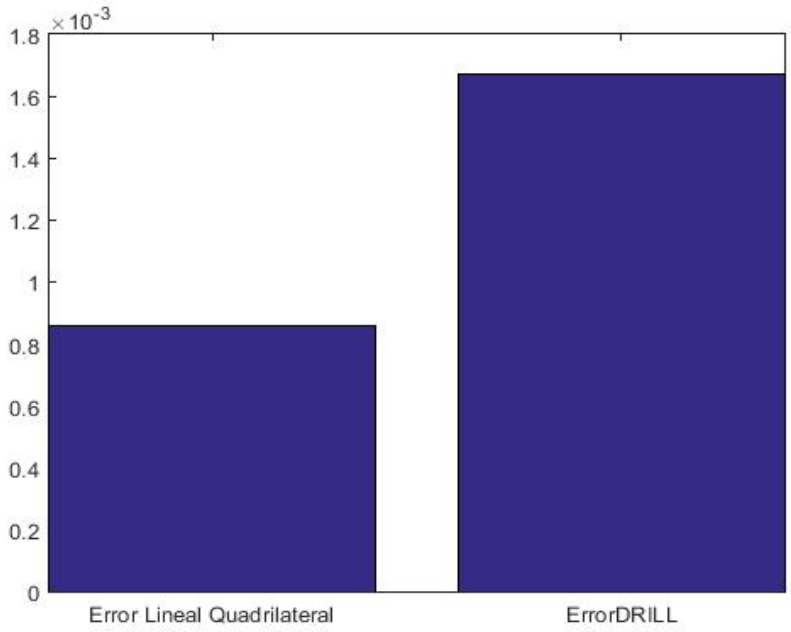

Figure 6.1.2.3 Error between element types Ramseries

This simple bar plot shows how the difference between de best approximation of these two different element types is, Lineal Quadrilateral and Drill rotation triangle, and the exact value is smaller with Lineal Quadrilateral.

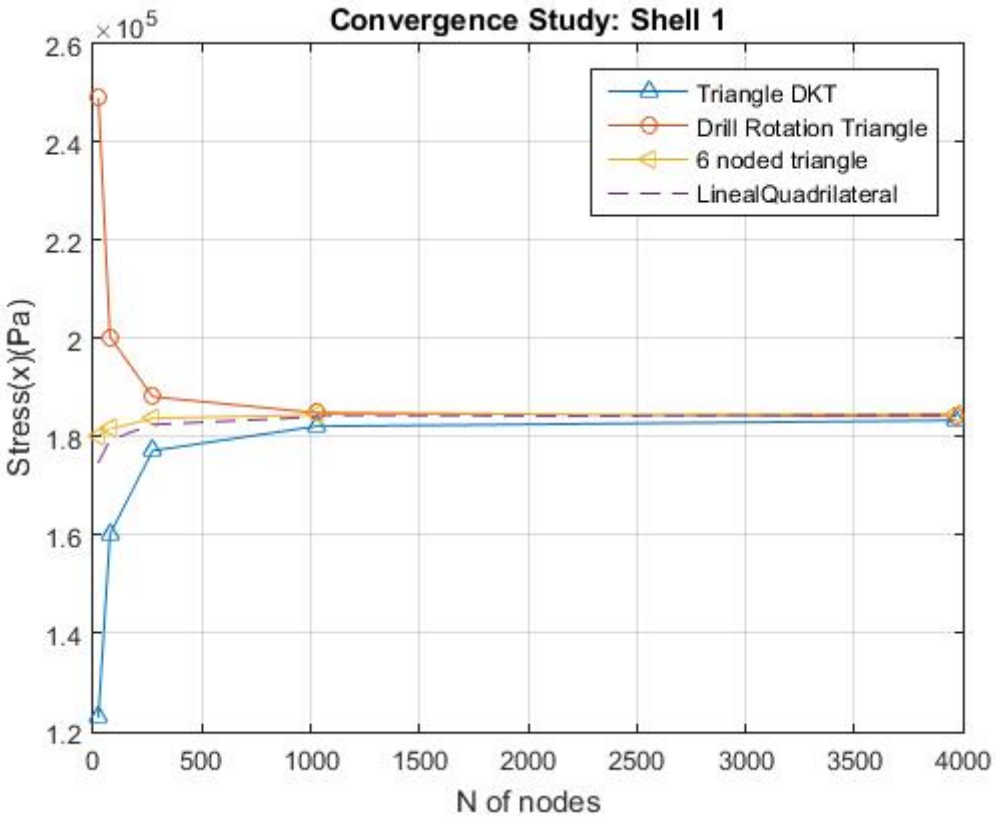

Figure 6.1.2.4 Convergence study stress Scrodellis-Lo roof

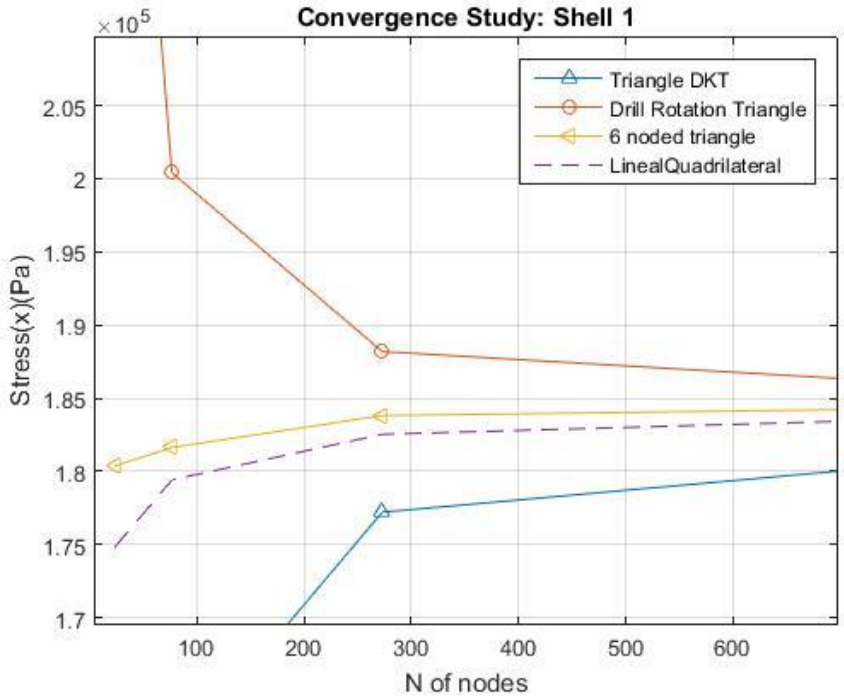

Figure 6.1.2.5 Convergence study stress ampliated Scrodellis-Lo roof

Also, if the stress in x-component is faster with *drill rotation triangle* than with the *DKT element.* Although the final approximation for *DKT element* is good.

6.1.3. Cook's problem model

In this verification test a benchmark test proposed by Cook it is going to be studied. It consists on a clamped trapezoidal under shear. The characteristics and geometrics of this problem are showed below.

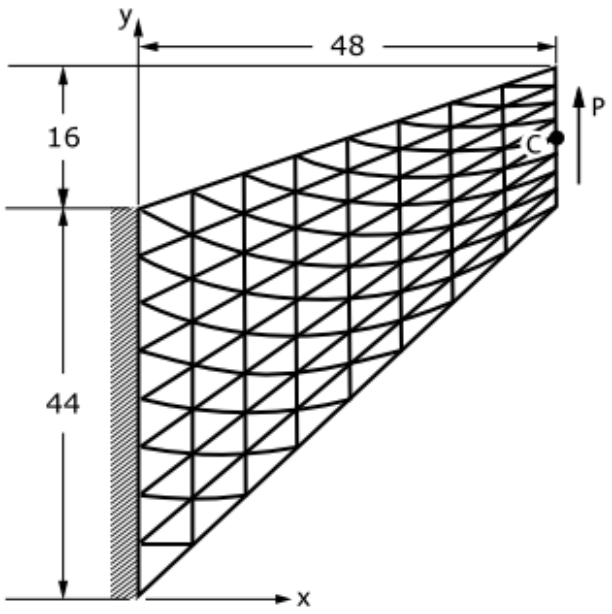

Figure 6.1.3.1 Geometrical description of Cook's problem.

- $P = 0.0625\ N/m$

Shell thickness	t = 1.0 m
Young modulus	E = 1.0 Pa
Poisson coefficient	v=0.3333

It doesn't exist an exact analytical solution so the result of the 64x64 mesh is going to be used to compare the results obtained by Ramseries elements types. The extrapolation of the OPT results yields a theoretical value for the vertical displacement for the mid-point of the loaded face u_{yc} = 23.956 m.

N of nodes	**40**	**135**	**493**	**1881**
DKT Triangle	13.93	19.59	22.57	23.67
DRILL	22.7	23.37	23.7	23.87
6 nodes	23.7	23.89	23.94	23.95
Linear Quadrilateral	20.89	23.03	23.68	23.89

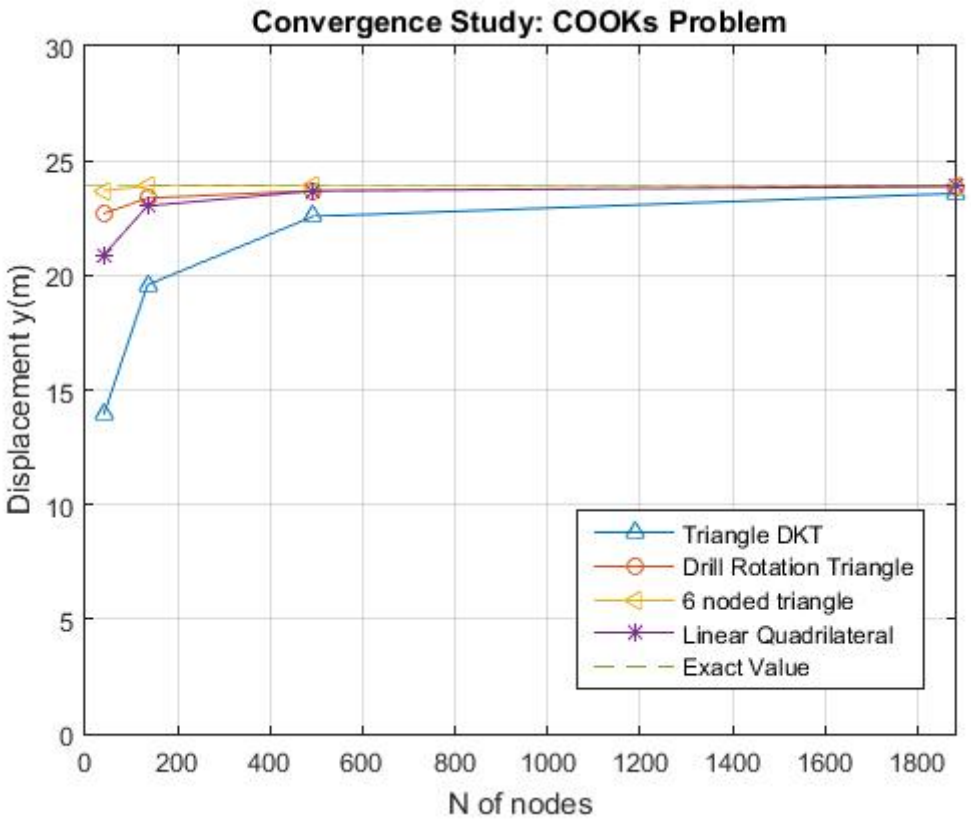

Figure 6.1.3.2*:* Convergence study Cook's Problem

As it can be observed, in this example the 6-node element has the best approximation of the solution and also is the fastest. Comparing *Drill rotation element* with *Linear quadrilateral* it is concluded that *drill rotation* is a little bit faster but *Linear quadrilateral* has a better approximation of the solution. Finally, the *DKT* element has a good approximation of the solution but you can notice in the plot that the convergence is slower than the others.

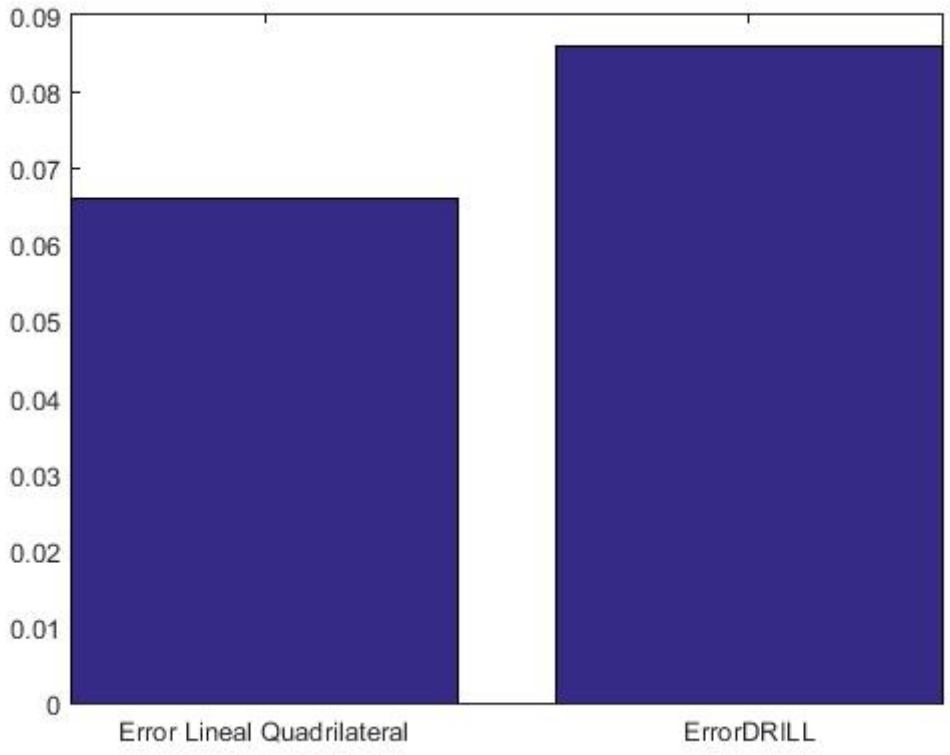

Figure 6.1.3.3 Error between element types Ramseries

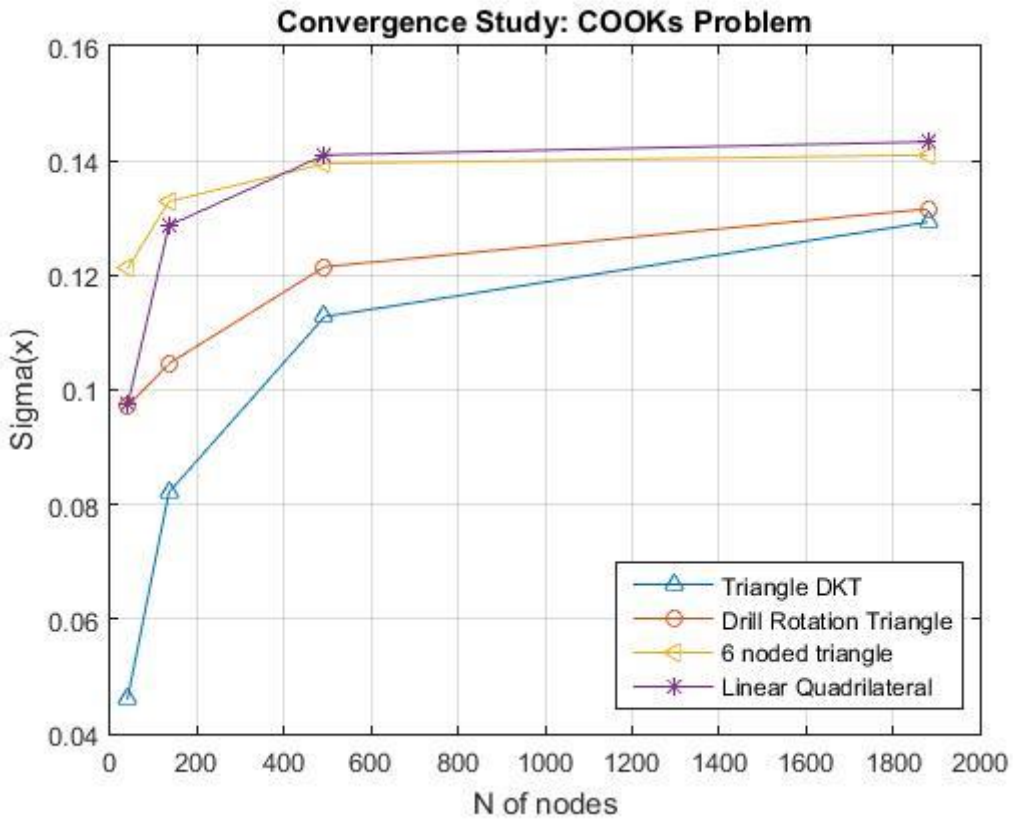

Figure 6.1.3.4

6.1.4. Cantilever beam under punctual load

This verification model is based on analysis of a clamped thick cantilever beam under a point load with its free end. For the exact solution of our problem we use the next formula:

$$\delta_{max} = \frac{PL^3}{3EI} + \frac{PL}{GA_r}$$

where P=900N is the applied punctual load, L=10 m is the length of the beam, E=2.0e8 Pa is the Young's modulus, $I = bh^3/12$ being b=0.1 m and h=1.0 m the thickness and height respectively of the beam. G is the shear modulus $G = E(1+\nu)/2$ (being $\nu = 0.2$) and $A_r = 5/6 \cdot b \cdot h$.

The geometrical characteristics of this problem are showed in the next representation:

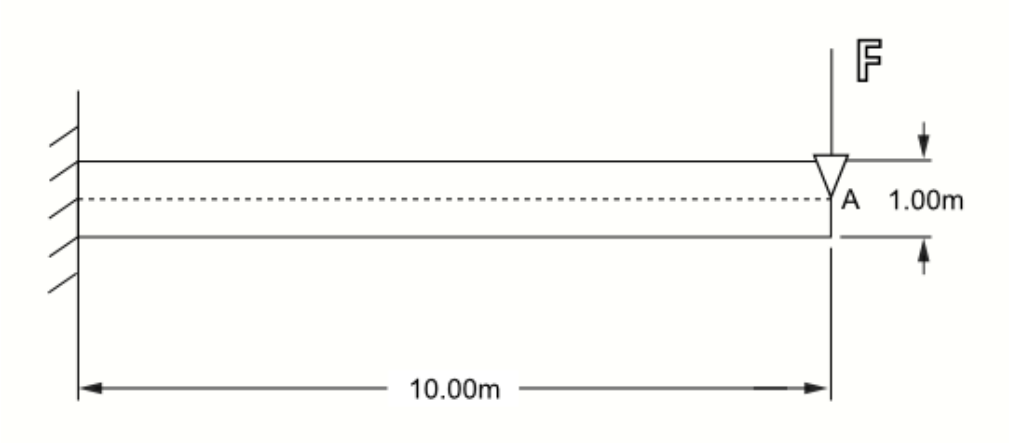

Figure 6.1.4.1: Geometrical model cantilever beam

Using the formula for the maximum deflection we obtain:

$$\delta_{max} = 0.181\ m$$

This value is going to be used to compare the results with Ramseries elements types.

N of nodes	63	205	729	2737
DKT Triangle	0.094755	0.14383	0.16542	0.1719
DRILL	0.19663	0.18147	0.17712	0.17349
6 nodes	0.17402	0.17415	0.17418	0.17419
Linear Quadrilateral	0.067	0.1275	0.1638	0.1730

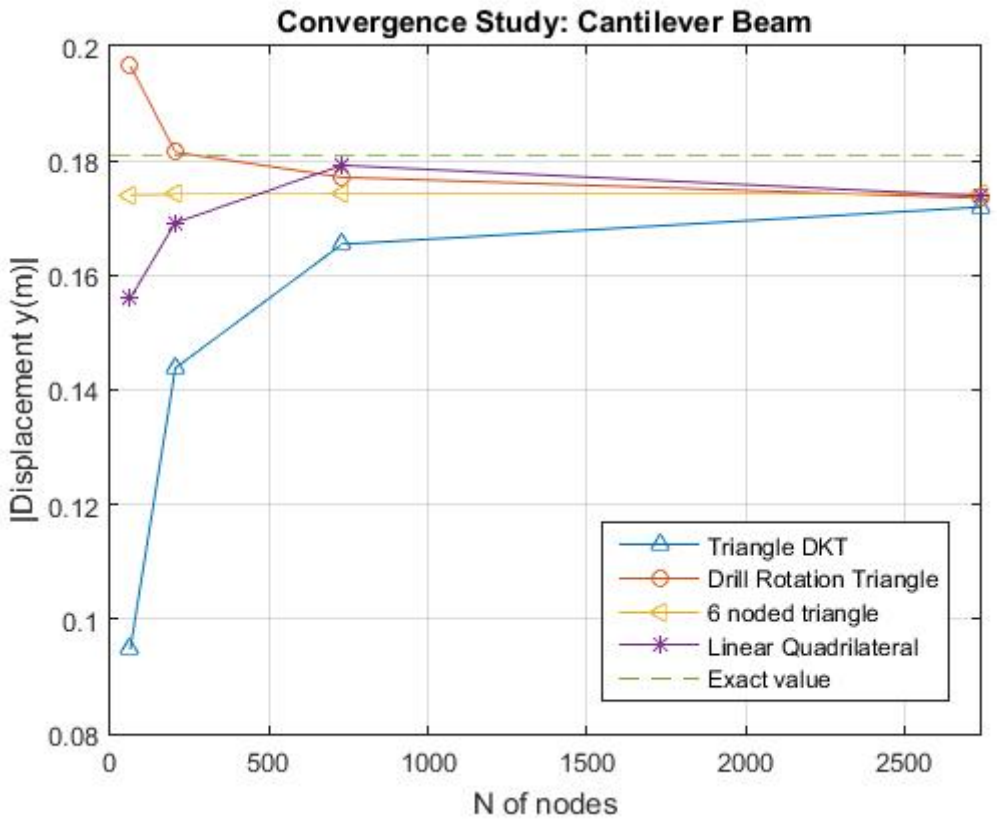

Figure 6.1.4.2: Convergence study Cantilever beam

As it can be observed in the plot, the convergence of drill rotation triangle is faster than Linear Quadrilateral, and also the final approximation is better in *drill rotation triangle.* The *6nodded element* has more or less the same convergence as *drill rotation triangle. Finally, the DKT element is, like in the other examples, the slowest convergence and the worst approximation of all of them.*

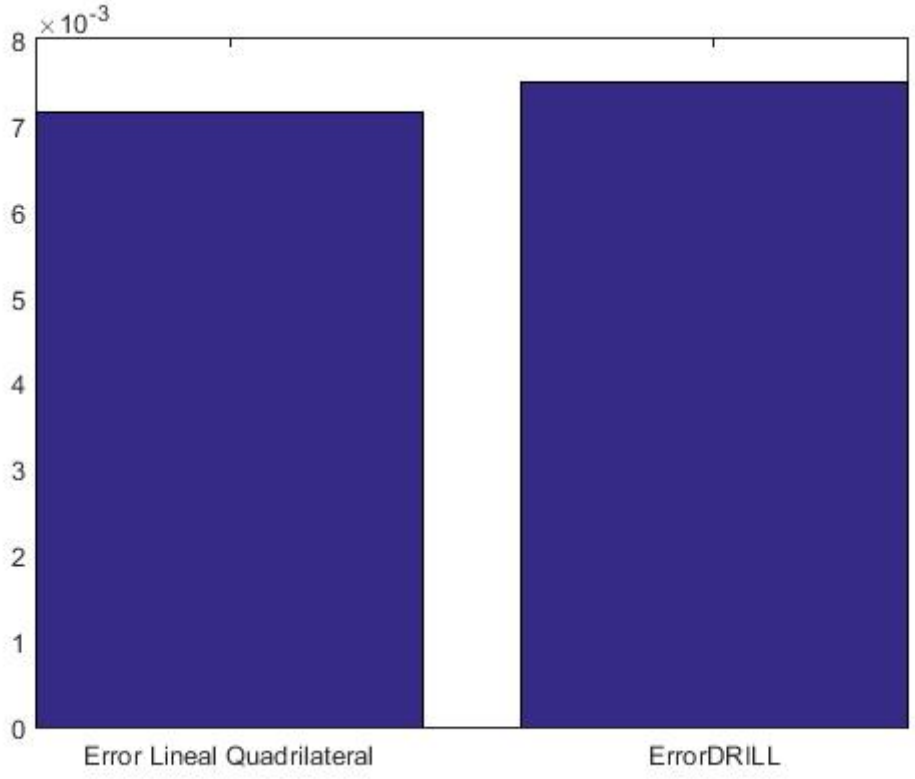

Figure 6.1.4.3: Error between element types Ramseries

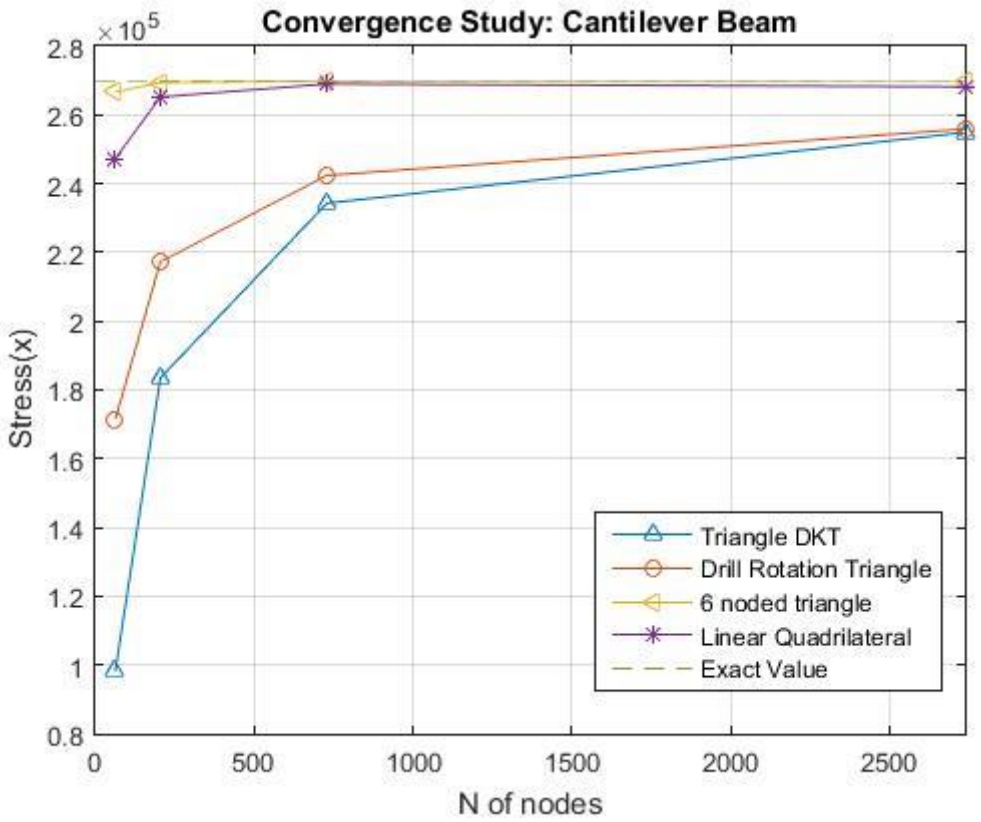

Figure 6.1.4.4: Convergence study Stress Cantilever Beam

As it can be observed the best element is 6 *node triangles,* it has the best approximation and also the fastest convergence. Focusing on *Drill rotation triangle* and *Linear Quadrilateral* it is concluded that the second is faster and also the final approximation is better in *Linear Quadrilateral* for the same number of nodes.

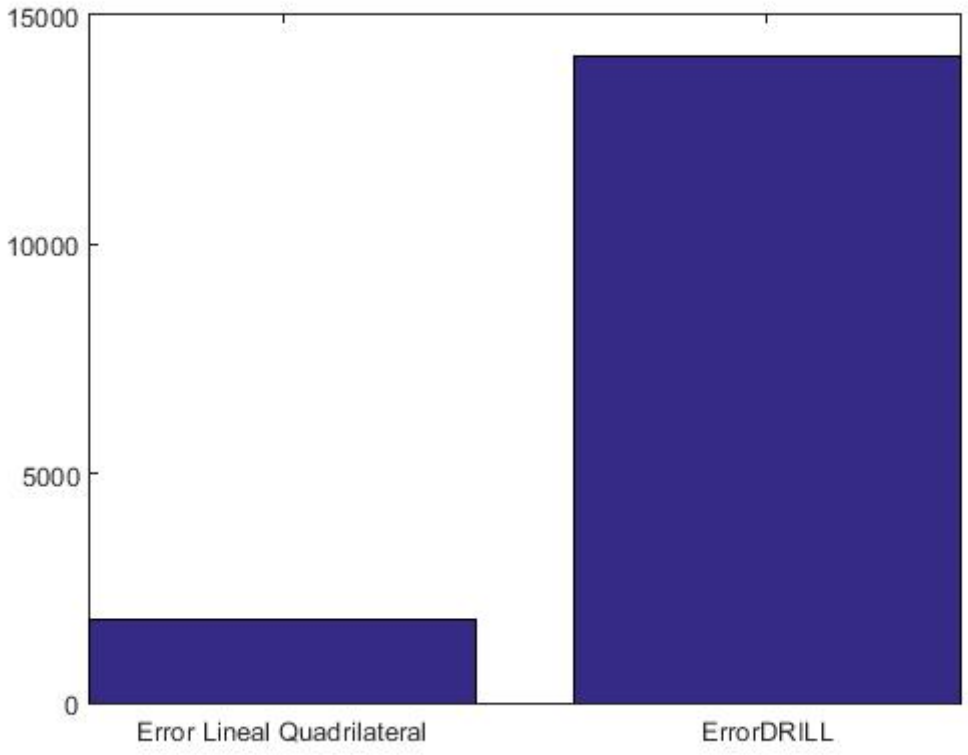

Figure 6.1.4.5: Error between element types Ramseries

6.1.5. Thin plate under axial load

For this verification it is used the next model, when $P = 10MN/m$.

The geometrical characteristics are represented in the next schematic model:

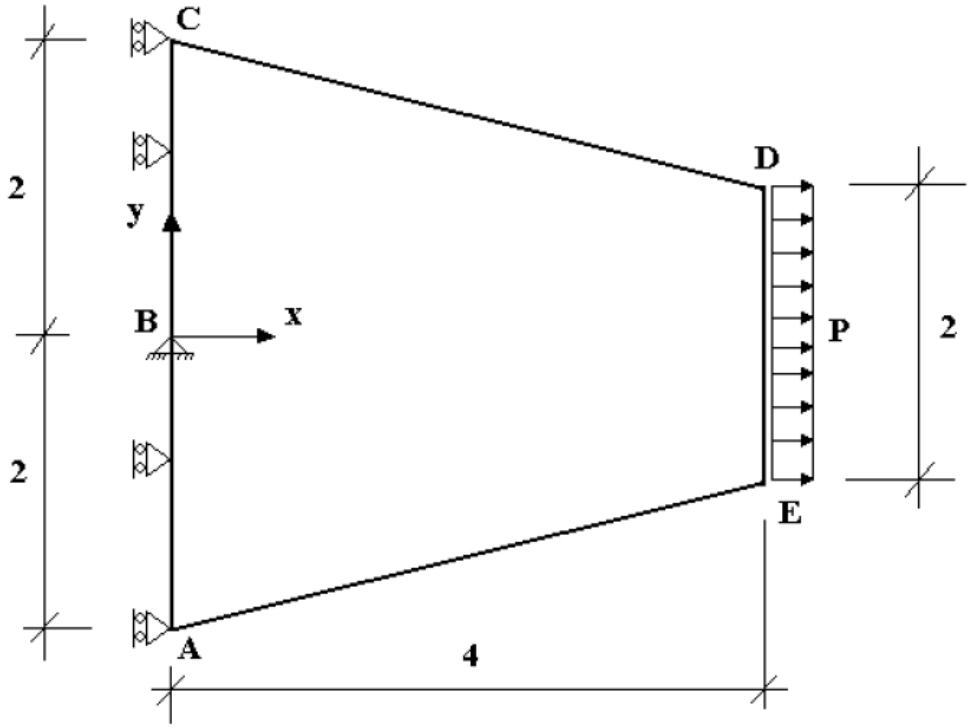

Figure 6.1.5.1 Schematic representation Thin plate under axial load

The exacts value of the x-displacement at the middle point of the loaded face and the stress at the point B are:

- $u = 0.001441\ m$
- $\sigma = 61.3\ MPa$

Comparing these results with the solution that is obtained when refining the mesh with *Ramseries* element types.

Nodes	**25**	**81**	**289**	**1089**	**4225**

TriangDKT	0.0014136	0.0014297	0.001435	0.0014411	0.0014418
Drill	0.001485	0.001448	0.001441	0.001442	0.0014422
6 noded	0.0014406	0.0014423	0.001442	0.001442	0.001442
Lineal Quadrilateral	0.0014281	0.0014377	0.00144	0.001447	0.001447

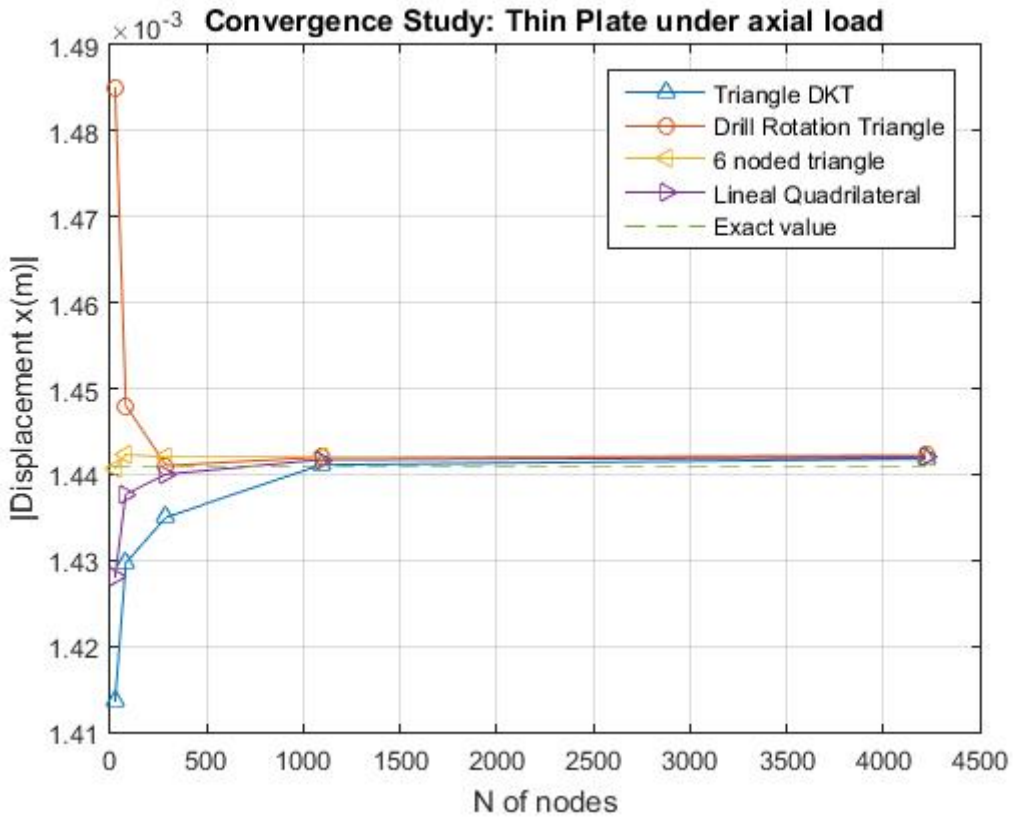

Figure 6.1.5.2: Convergence study Thin plate under axial load

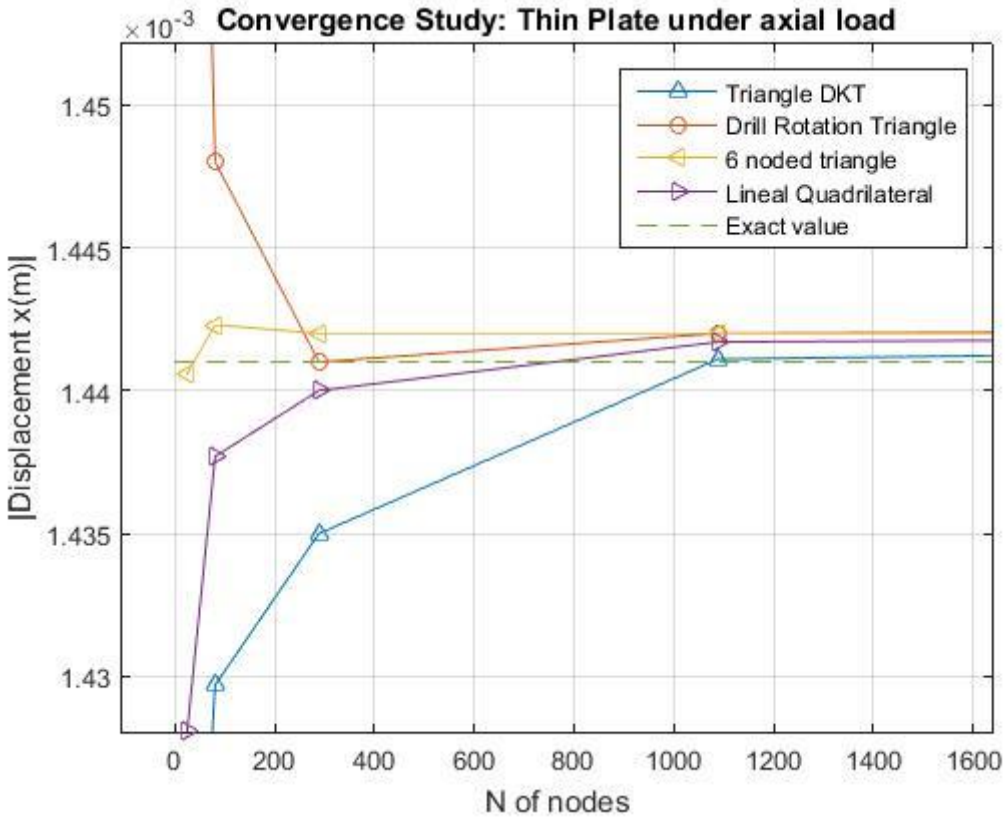

Figure 6.1.5.3: Convergence study Thin plate under axial load

It is shown that *drill rotation* has a better convergence than *Linear quadrilateral* but finally the approximation is better when we use Lineal Quadrilateral. DKT element is the slowest element but it converges to a good final approximation

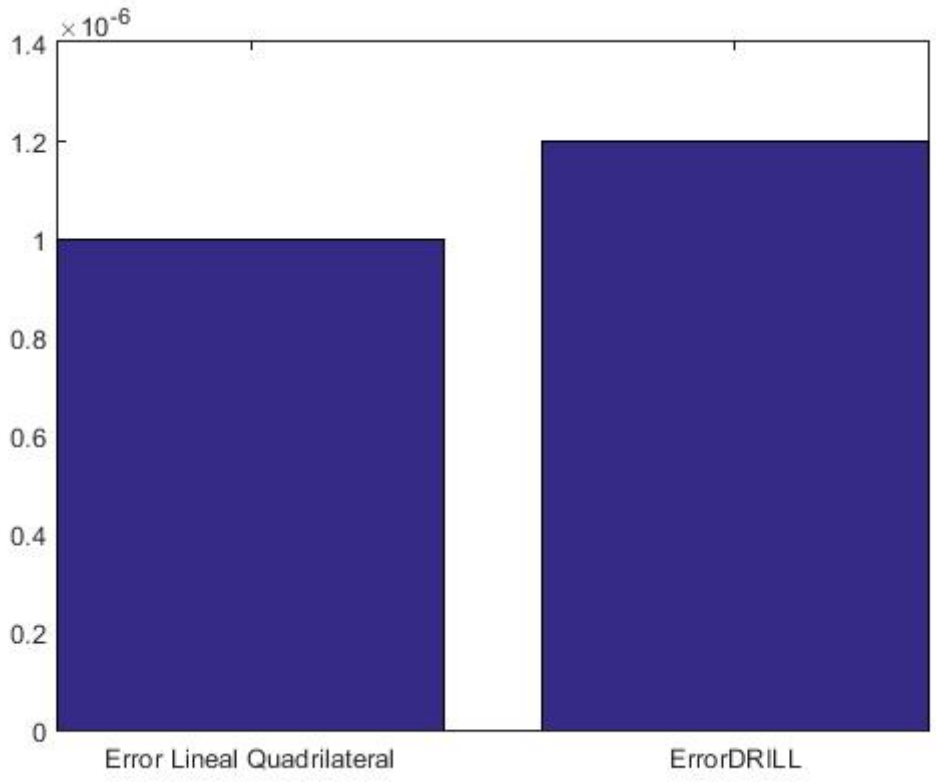

Figure 6.1.5.4: Error between element types Ramseries

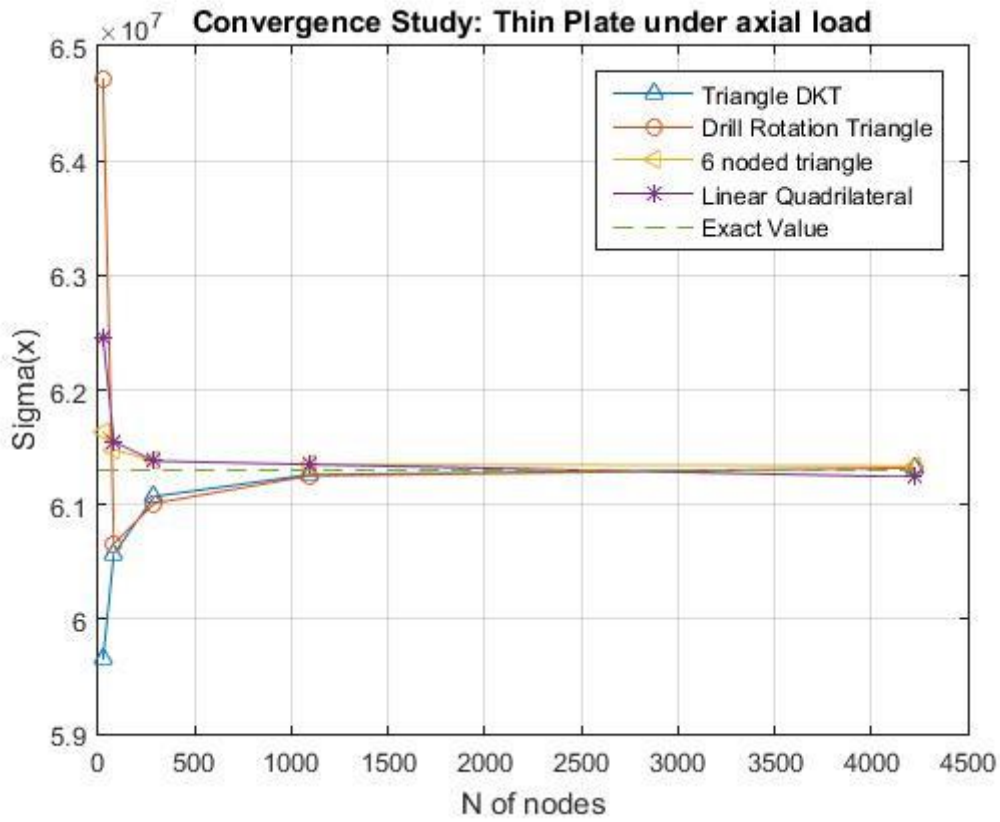

Figure 6.1.5.5: Convergence study stress Thin plate under axial load

In the previous figure it is shown that *Linear Quadrilateral* is fast. But when we see the approximation we observe that *drill rotation triangle* has less error. *DKT element* and *Drill rotation triangle* have more or less the same convergence, a little bit better *DKT* than *Drill rotation triangle.*

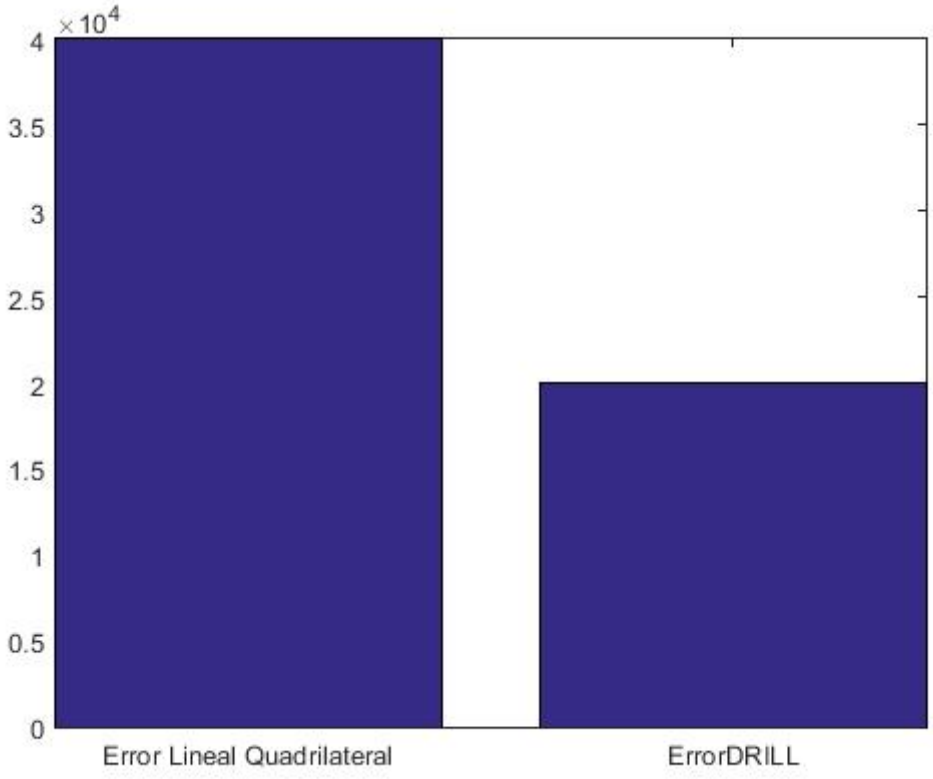

Figure 6.1.5.6: Error between element types Ramseries

6.1.6. Thin plate under dead weight

For this last verification model, the same thin plate will be used but now, only under his weight. The schematic model and dimensions are represented below.

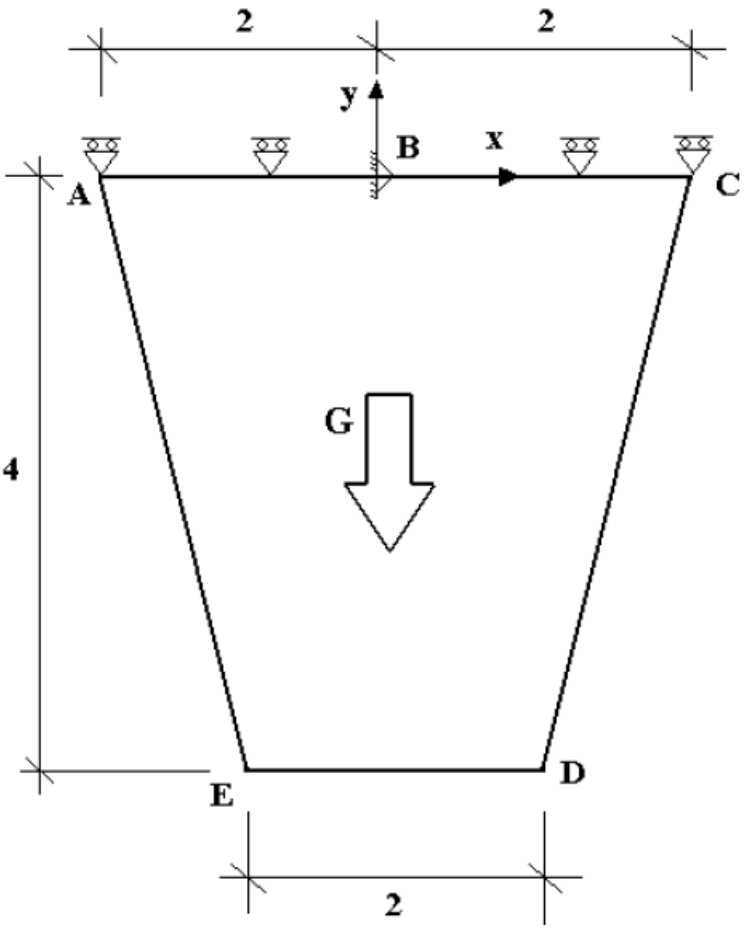

Figure 6.1.6.1 Thin plate under dead weight 1

The exacts values of y-displacement and stress at point B are:

- $v = 2.26e - 6\ m$
- $\sigma\ = 0.247\,\frac{MN}{m^2}$

These values will be used to compare with the solution obtained refining the mesh with different elements types of Ramseries.

Nodes	25	81	289	1089	4225
TriangDKT	2.25e-6	2.257e-6	2.258e-6	2.259e-6	2.26e-6
DRILL	2.437e-6	2.292e-6	2.266e-6	2.261e-6	2.26e-6
6 noded	2.257e-6	2.259e-6	2.26e-6	2.26e-6	2.26e-6
Lineal Quadrilateral	2.266e-6	2.26e-6	2.26e-6	2.26e-6	2.26e-6

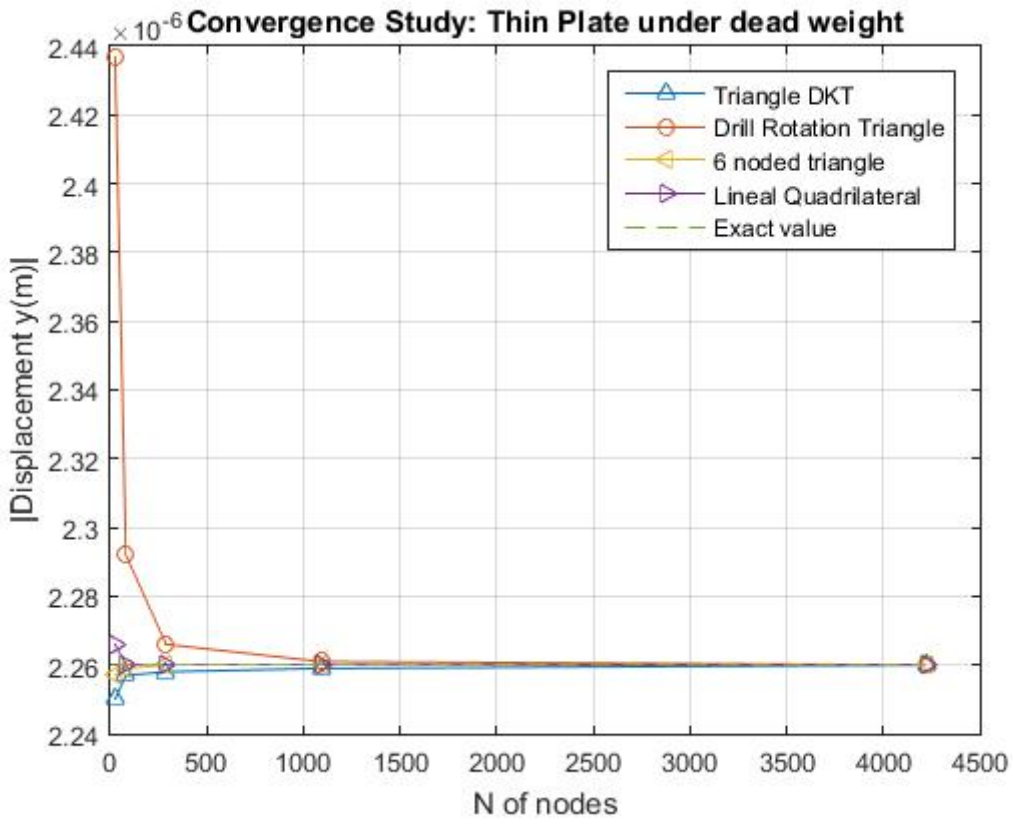

Figure 6.1.6.2 Convergence study Thin plate under dead weight

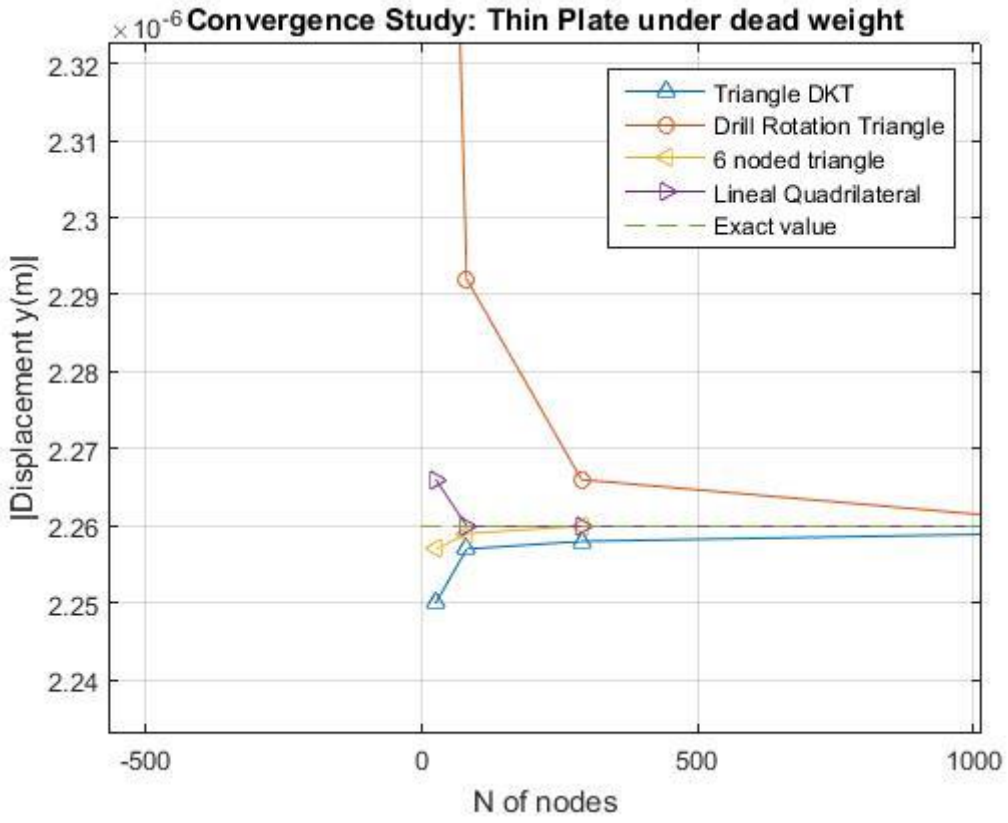

Figure 6.1.6.3: Convergence study ampliated Thin plate under dead weight

Linear Quadrilateral has the fast convergence followed by *6 nodded elements*. *DKT elements* also have a good approximation. The final value for 4225 nodes is the same in *Linear Quadrilateral* and *Drill rotation triangle.* All the elements have the same final solution, but, as I said before, the *Linear Quadrilateral* is the best in this study.

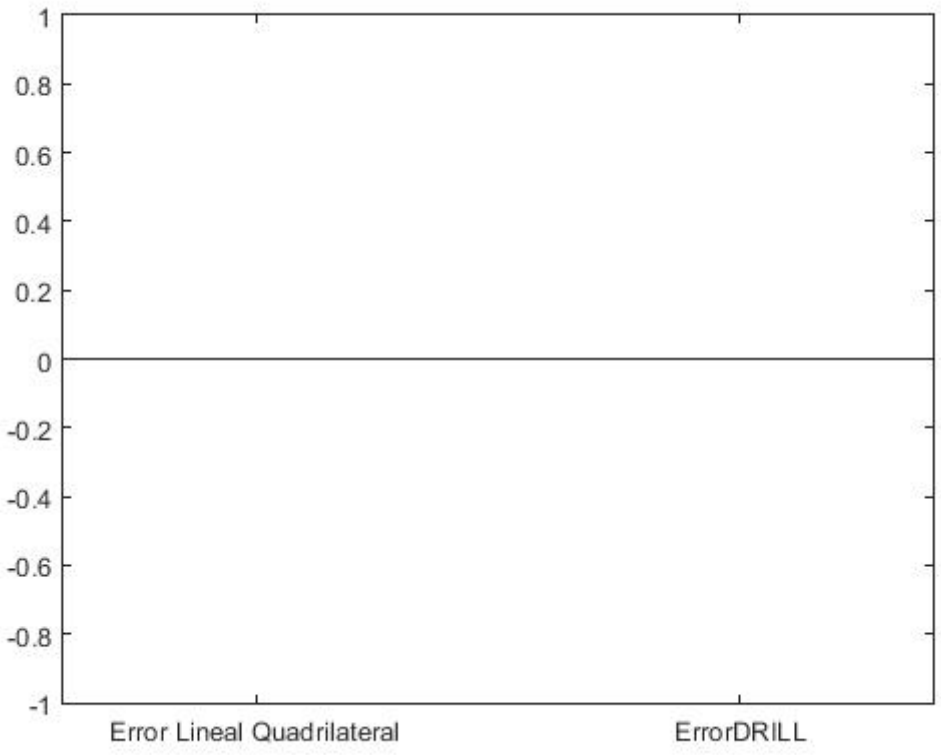

Figure 6.1.6.4: Error between element types Ramseries

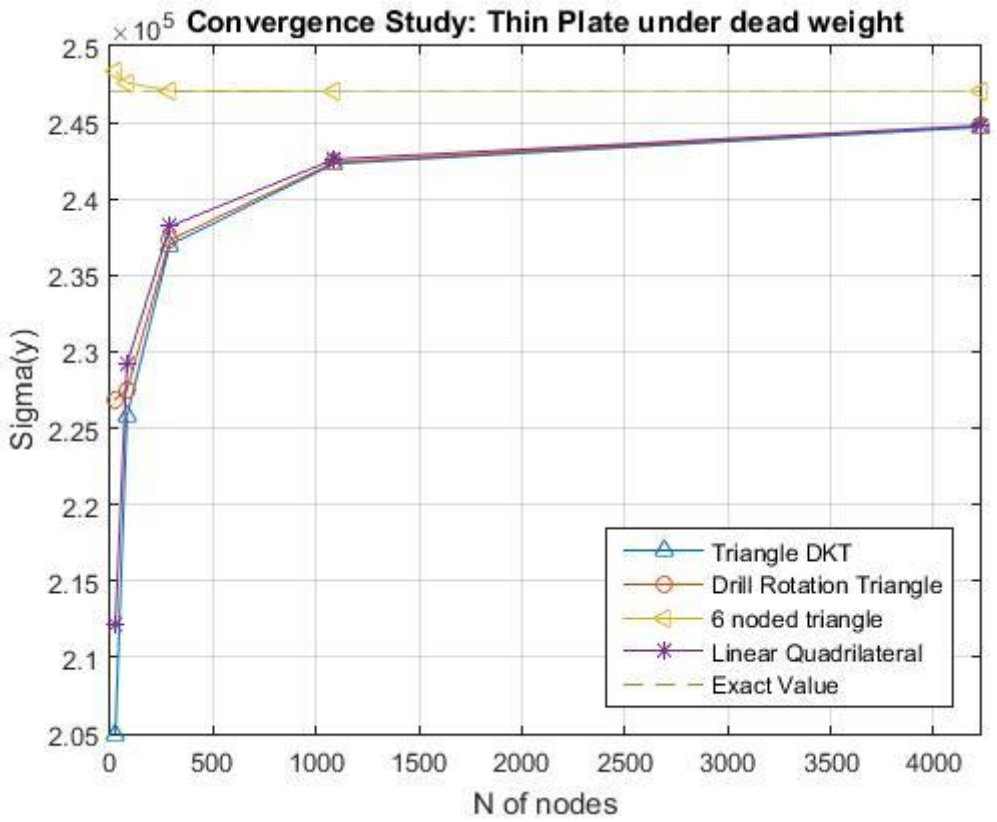

Figure 6.1.6.5 Convergence study stress Thin plate under dead weight

In stress study, happens the same as displacement. *Linear Quadrilateral* has a fast convergence than *drill rotation triangle* but the final value is the same for both of them.

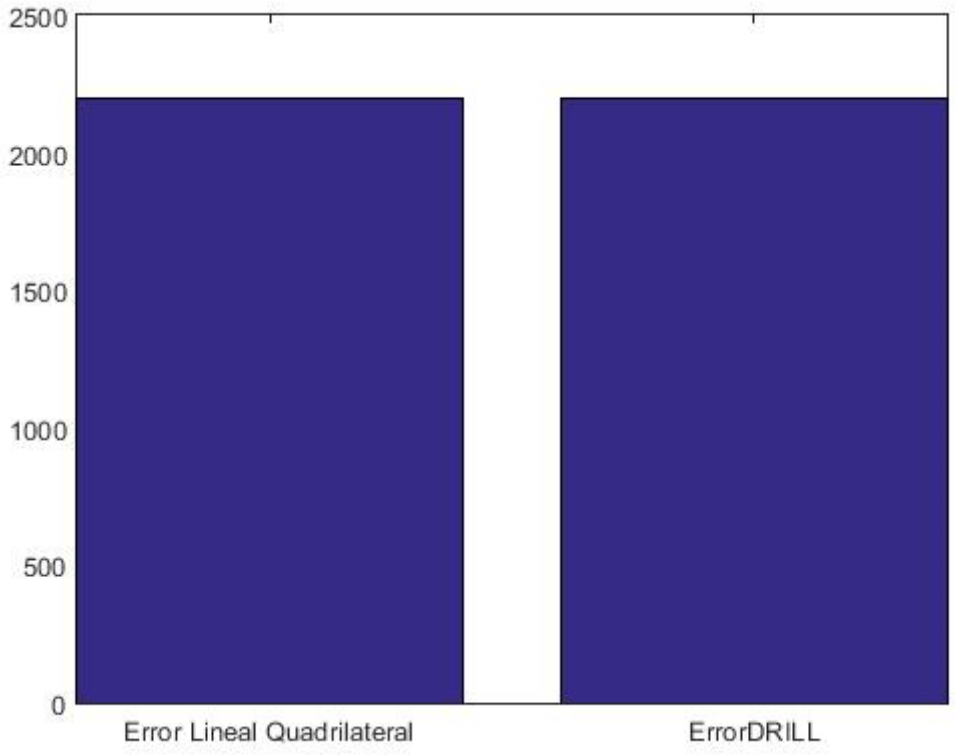

Figure 6.1.6.6: Error between element types Ramseries

6.2. Damage cases

6.2.1. Verification

In order to check the good implementation of the different types of damage models, one model is going to be launched with different damage type.

In verification cases, it is not necessary a complex model because the objective is to know if the model response is mathematically correct or not. Because of this, the simplest geometry is going to be performed. A single element.

Any load is going to be applied to the element because when applying a horizontal load in a triangular element, vertical displacement appears. And that's not correct. Because of this, the final displacement of the nodes is going to be defined. The result will be the same, but with this method, it is sure that displacement will be the wanted. It is going to be a displacement of 0.5m

The constrains are applied in the same way as loads, to fix one node, put his final displacement 0.

Because of the different types of norms, also it is important a model that can verify the compression behaviour. So, the displacement will be in the opposite direction. All the other parts of the model are identical as in traction. Then, if we apply, for example, the norm 1, we have to calculate the variables in the two models and put it together to observe if the behaviour is the expected for norm one.

The representation of the models in the simplest way is with a line 2-D element.

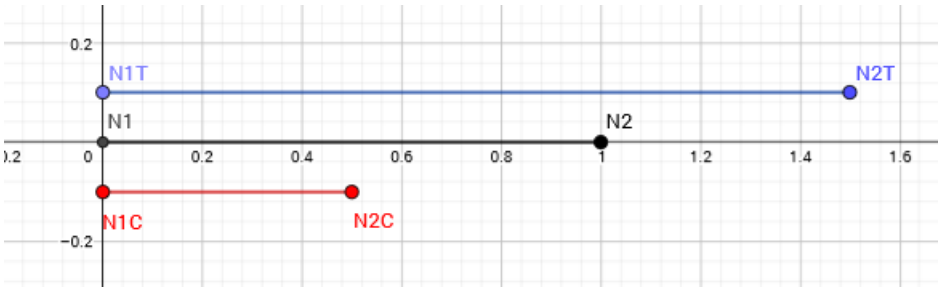

Figure 6.2.1.1 Schematic representation of the displacement in Compression-Traction

The characteristics of the material are the next:

Young's modulus	40 MPa
G (Shear modulus)	0.384615 MPa
Poisson modulus	0.3
Specific weight	1 N/m^3

Table 6.1.1.1 Properties of the material

Moreover, the simulations are going to launch with different elements types in order to check the response with all of them.

- DKT

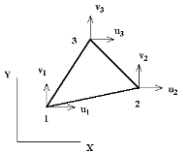

- DKT + Drill Rotation

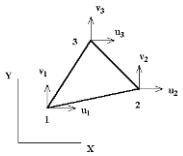

+ Rotations

- Quadrilateral

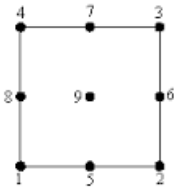

- Tetrahedral

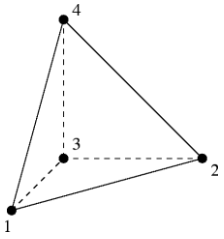

- Hexahedral

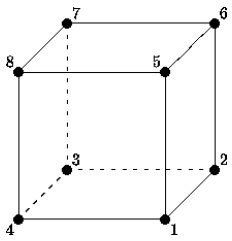

6.2.1.1. Exponential law

a) <u>Norm 1</u>

<u>Softening:</u>

Element	%	Increments	σ_y	H	G_f	σ_{sat}	n
CLL	0.01	500	1.43	0	0.08	0	1
DKT+DR	0.01	500	1.43	0	0.1	0	1
DKT	0.01	500	1.43	0	0.1	0	1
Hexahedra	0.01	500	1.43	0	0.1	0	1
Tetrahedra	0.01	500	1.43	0	0.1	0	1

Table 1 Properties of a Traction-Compression with Softening

Hardening:

Element	%	Increments	σ_y	H	G_f	σ_{sat}	n
CLL	0.01	500	1.43	0	0.08	2.86	1
DKT+DR	0.01	500	1.43	0	0.1	2.86	1
DKT	0.01	500	1.43	0	0.1	2.86	1
Hexahedra	0.01	500	1.43	0	0.1	2.86	1
Tetrahedra	0.01	500	1.43	0	0.1	2.86	1

Table 2 Properties of a Traction-Compression with Hardening

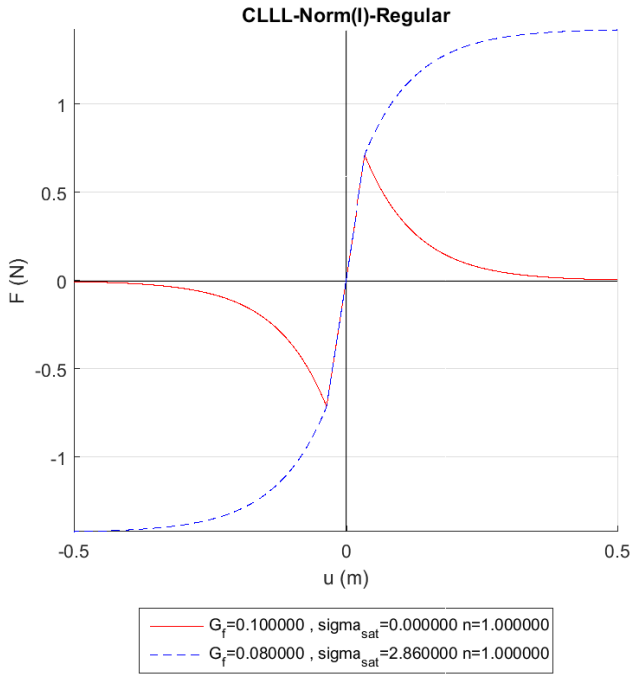

Figure 6.2.1.1.1 Force-displacement plot of Traction-Compression with Hardening-Softening

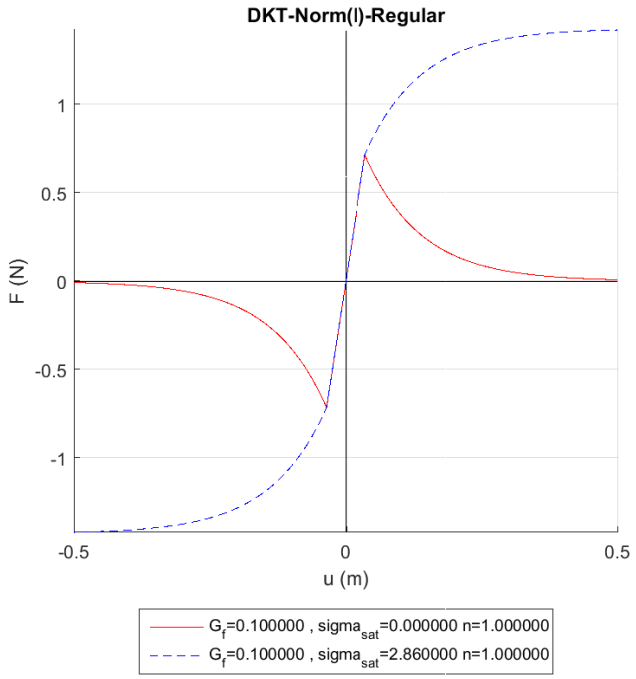

Figure 6.2.1.1.2 Force-displacement plot of Traction-Compression with Hardening-Softening

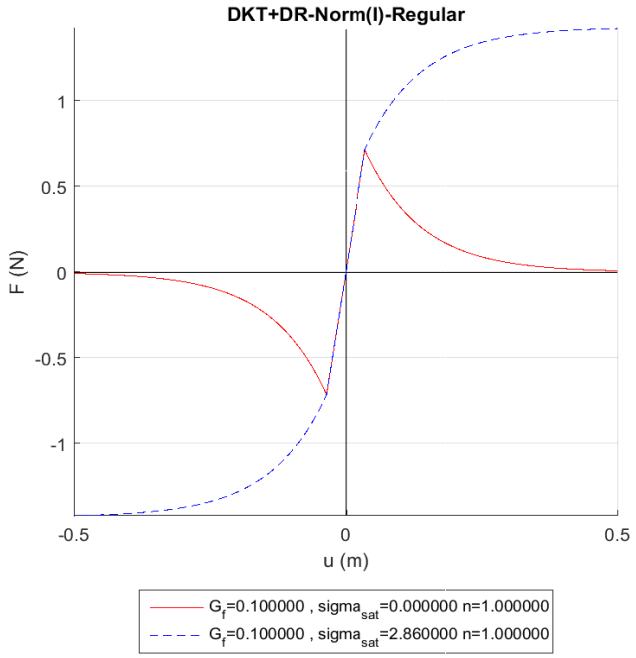

Figure 6.2.1.1.3 Force-displacement plot of Traction-Compression with Hardening-Softening

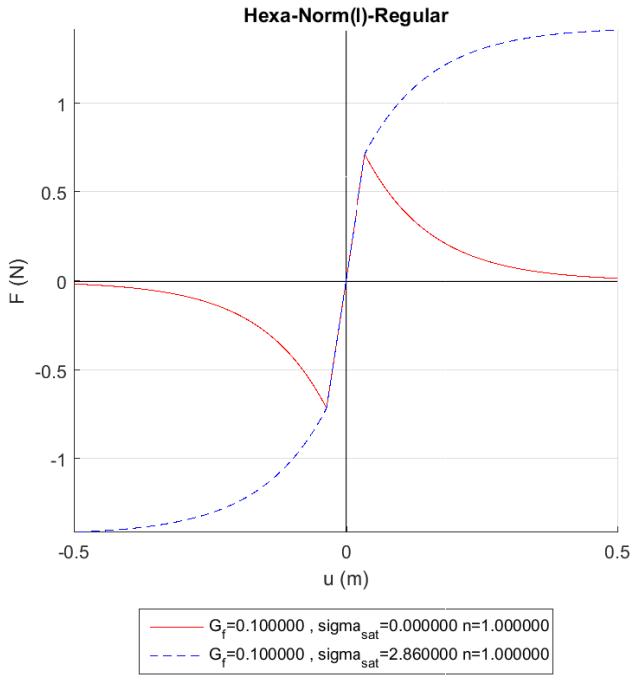

Figure 6.2.1.1.4 Force-displacement plot of Traction-Compression with Hardening-Softening

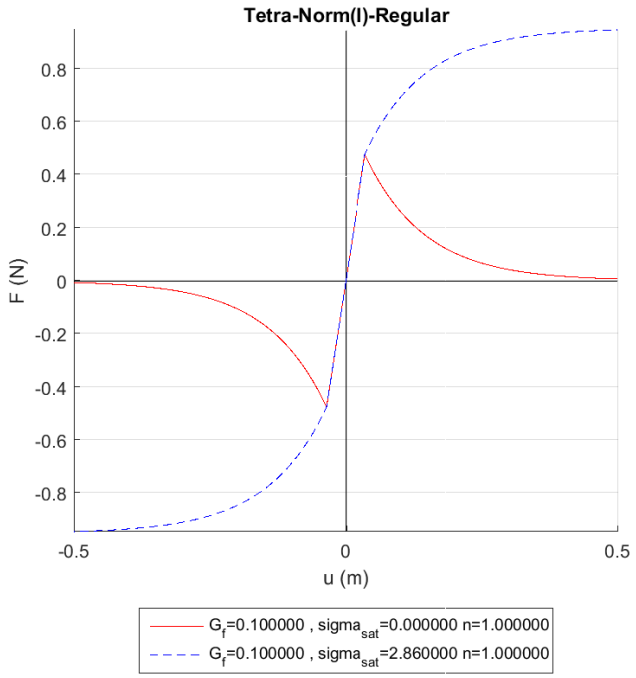

Figure 6.2.1.1.5 Force-displacement plot of Traction-Compression with Hardening-Softening

b) Norm 2

Softening:

Element	%	Increments	σ_y	H	G_f	σ_{sat}	n
CLL	0.01	500	1.43	0	0.08	0	1
DKT+DR	0.01	500	1.43	0	0.1	0	1
DKT	0.01	500	1.43	0	0.1	0	1
Hexahedra	0.01	500	1.43	0	0.1	0	1
Tetrahedra	0.01	500	1.43	0	0.1	0	1

Table 3 Properties for a Traction-Compression with Softening

Hardering:

Element	%	Increments	σ_y	H	G_f	σ_{sat}	n
CLL	0.01	500	1.43	0	0.08	2.86	1
DKT+DR	0.01	500	1.43	0	0.1	2.86	1
DKT	0.01	500	1.43	0	0.1	2.86	1
Hexahedra	0.01	500	1.43	0	0.1	2.86	1
Tetrahedra	0.01	500	1.43	0	0.1	2.86	1

Table 4 Properties for a Traction-Compression with Hardening

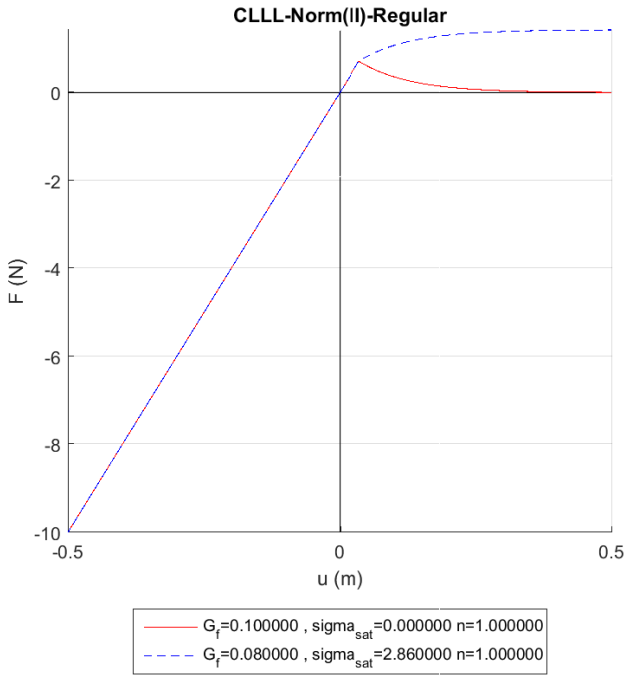

Figure 6.2.1.1.6 Force-displacement plot of Traction-Compression with Hardening-Softening

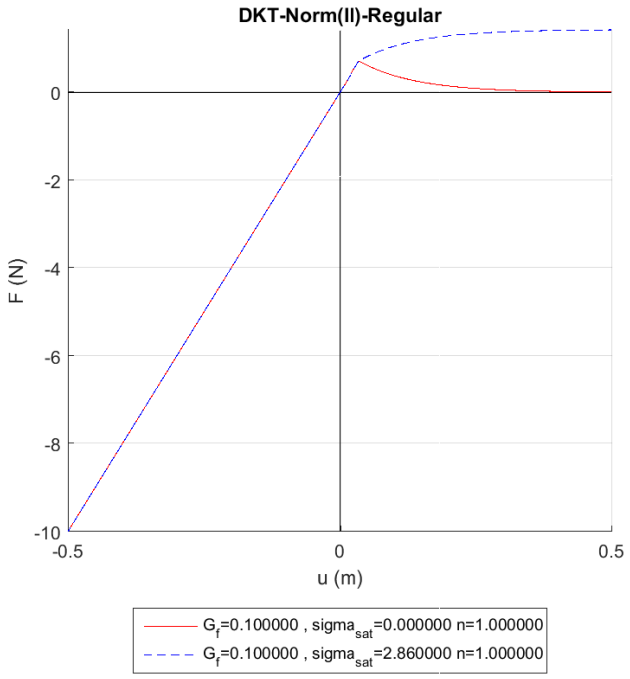

Figure 6.2.1.1.7 Force-displacement plot of Traction-Compression with Hardening-Softening

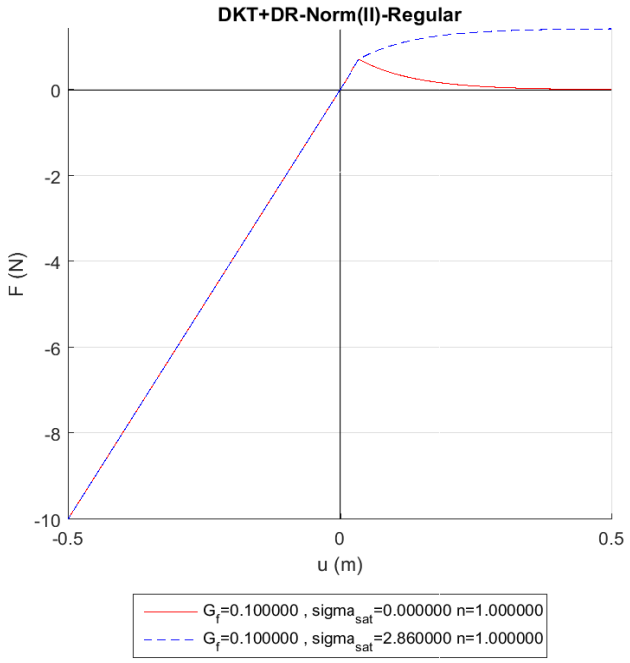

Figure 6.2.1.1.8 Force-displacement plot of Traction-Compression with Hardening-Softening

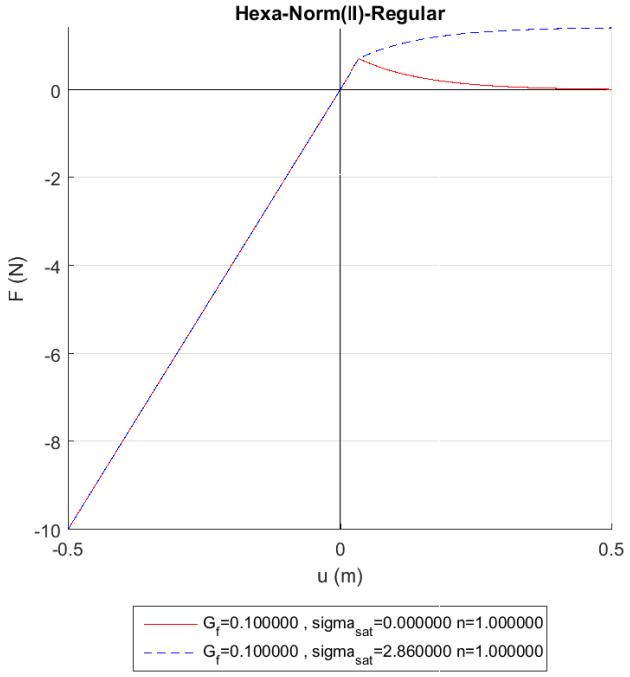

Figure 6.2.1.1.9 Force-displacement plot of Traction-Compression with Hardening-Softening

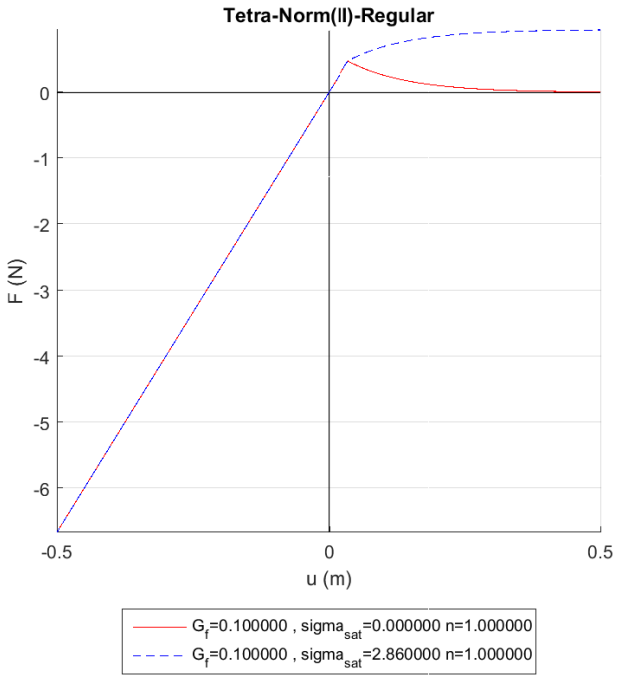

Figure 6.2.1.1.10 Force-displacement plot of Traction-Compression with Hardening-Softening

c) Norm 3

Softening:

Element	%	Increments	σ_y	H	G_f	σ_{sat}	n
CLL	0.01	500	1.43	0	0.08	0	3
DKT+DR	0.01	500	1.43	0	0.1	0	3
DKT	0.01	500	1.43	0	0.1	0	3
Hexahedra	0.01	500	1.43	0	0.1	0	3
Tetrahedra	0.01	500	1.43	0	0.1	0	3

Table 5 Properties for a Traction-Compression with Softening

Hardering:

Element	%	Increments	σ_y	H	G_f	σ_{sat}	n
CLL	0.01	500	1.43	0	0.08	2.86	3
DKT+DR	0.01	500	1.43	0	0.1	2.86	3
DKT	0.01	500	1.43	0	0.1	2.86	3
Hexahedra	0.01	500	1.43	0	0.1	2.86	3
Tetrahedra	0.01	500	1.43	0	0.1	2.86	3

Table 6 Properties for a Traction-Compression with Hardening

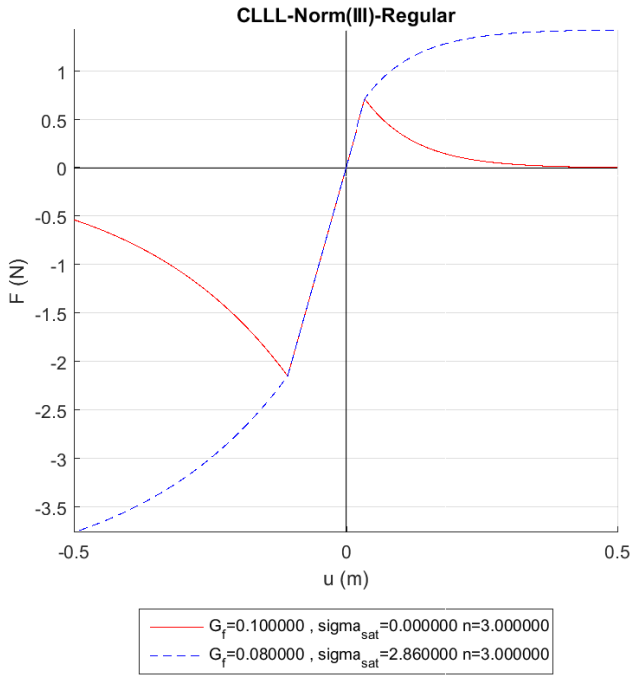

Figure 6.2.1.1.11 Force-displacement plot of Traction-Compression with Hardening-Softening

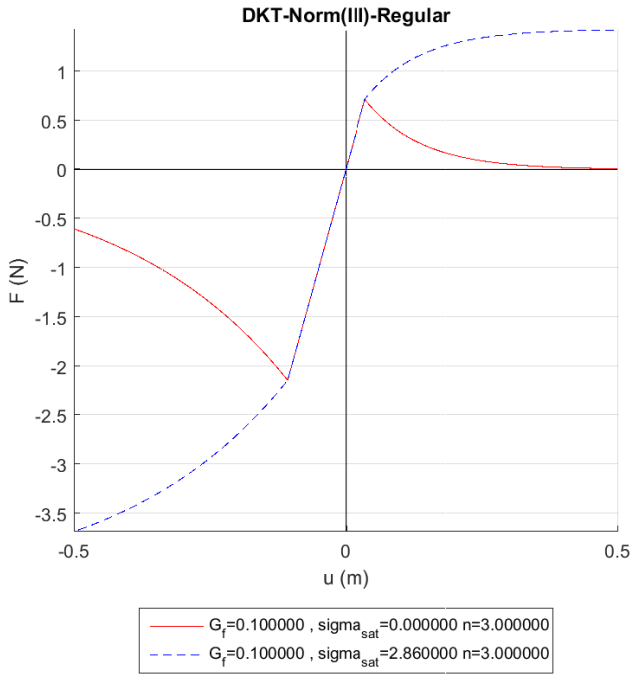

Figure 6.2.1.1.12 Force-displacement plot of Traction-Compression with Hardening-Softening

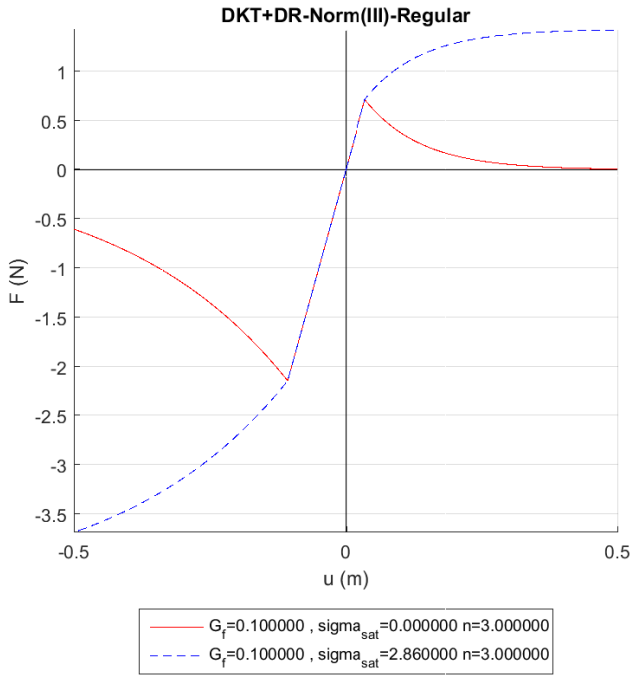

Figure 6.2.1.1.13 Force-displacement plot of Traction-Compression with Hardening-Softening

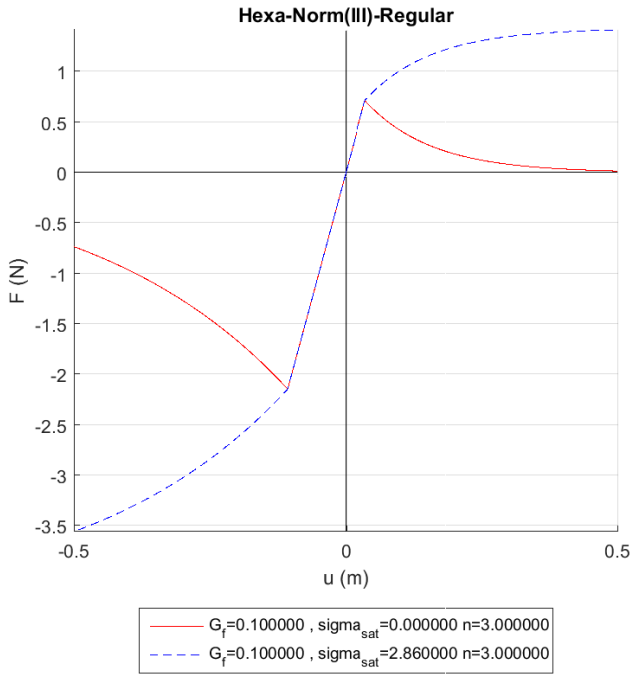

Figure 6.2.1.1.14 Force-displacement plot of Traction-Compression with Hardening-Softening

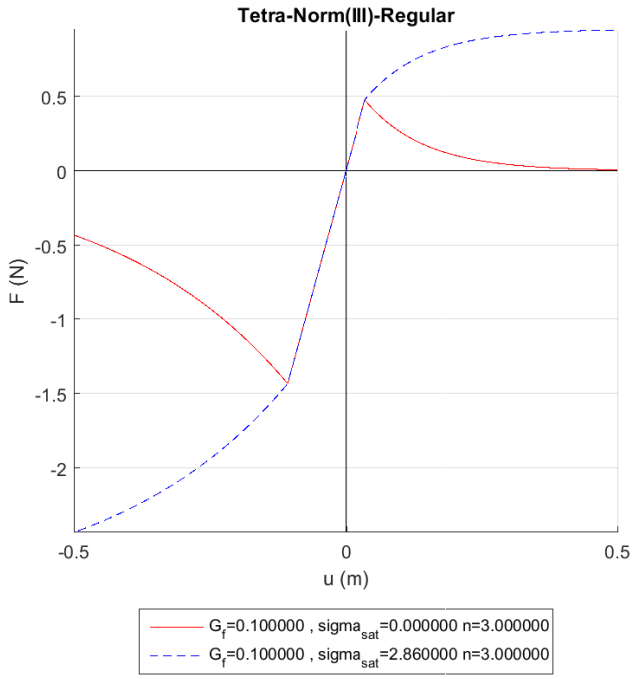

Figure 6.2.1.1.15 Force-displacement plot of Traction-Compression with Hardening-Softening

Comments

The previous checked behaviour is the exponential law. As it can be seen, when the plasticity begins, the behaviour of the element is exponential.

There are three different norms to validly. The norm one, as it is said in theory, have symmetric behaviour as you can see in the figures 6.2.1.1.1 to Figure 6.2.1.1.5

The norm two have different response in traction and in compression. The compression behaviour is linear and the traction exponential as in Norm 1

Finally, the norm three have a non-symmetrical behaviour but the traction and compression behaviour have a relationship between it, as it is explained in theory, in this case, this relationship is 3.

Moreover, comparing the different response between hardening and softening. As it can be seen in the plots by observing the softening is concluded that all figures tend to 0. This is the expected behaviour. Otherwise, hardening also tends to the expected value. To check this value the comparison has to be in the same field. We have to pass the saturation stress into force field in order to compare it.

Between elements, there is no a suitable difference only in *Quadrilateral* where the energy fracture is 20% less. Studying only one element is difficult to see differences but it is probably that if a finer mesh is made, all the elements tend to the same value of stress and strain.

6.2.1.2. Lineal Law

a) Norm 1

Softening:

Element	%	Increments	σ_y	H	G_f	σ_{sat}	n
CLL	0.01	500	1.43	-0.1	0	0	1
DKT+DR	0.01	500	1.43	-0.1	0	0	1
DKT	0.01	500	1.43	-0.1	0	0	1
Hexahedra	0.01	500	1.43	-0.1	0	0	1
Tetrahedra	0.01	500	1.43	-0.1	0	0	1

Table 7 Properties for a Traction-Compression with Softening

Hardening:

Element	%	Increments	σ_y	H	G_f	σ_{sat}	n
CLL	0.01	500	1.43	0.1	0	0	1
DKT+DR	0.01	500	1.43	0.1	0	0	1
DKT	0.01	500	1.43	0.1	0	0	1
Hexahedra	0.01	500	1.43	0.1	0	0	1
Tetrahedra	0.01	500	1.43	0.1	0	0	1

Table 8 Properties for a Traction-Compression with Hardening

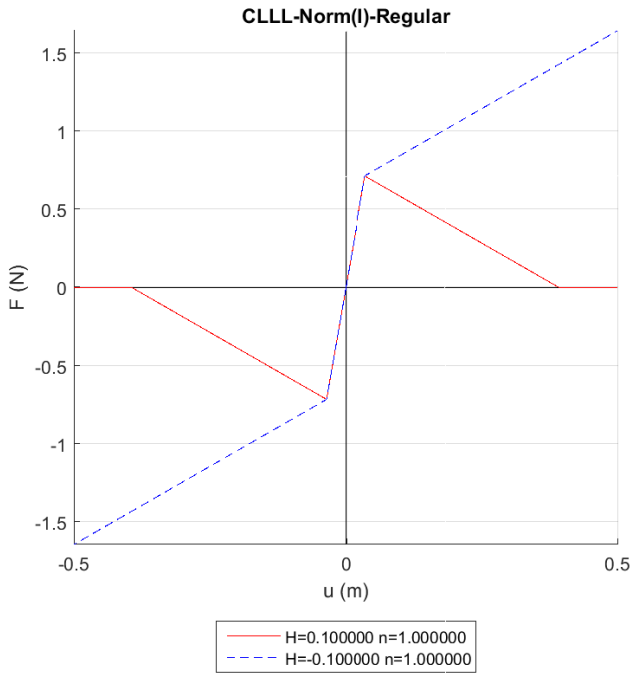

Figure 6.2.1.2.1 Force-displacement plot of Traction-Compression with Hardening-Softening

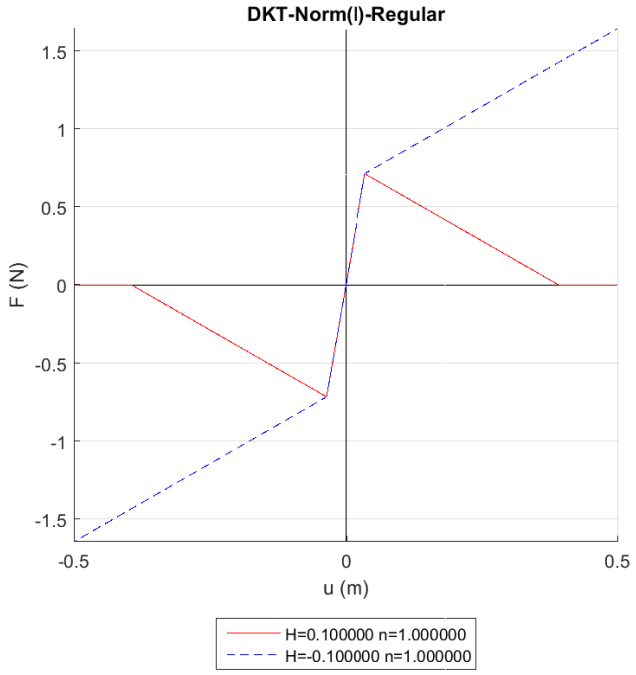

Figure 6.2.1.2.2 Force-displacement plot of Traction-Compression with Hardening-Softening

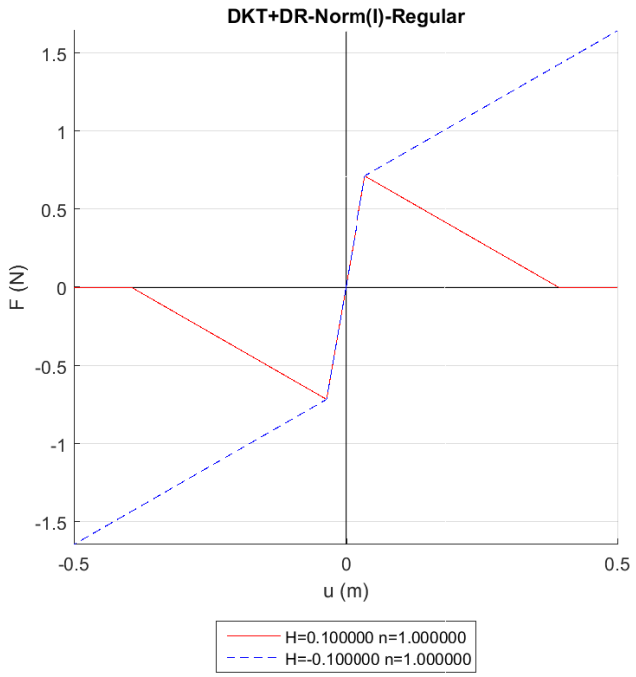

Figure 6.2.1.2.3 Force-displacement plot of Traction-Compression with Hardening-Softening

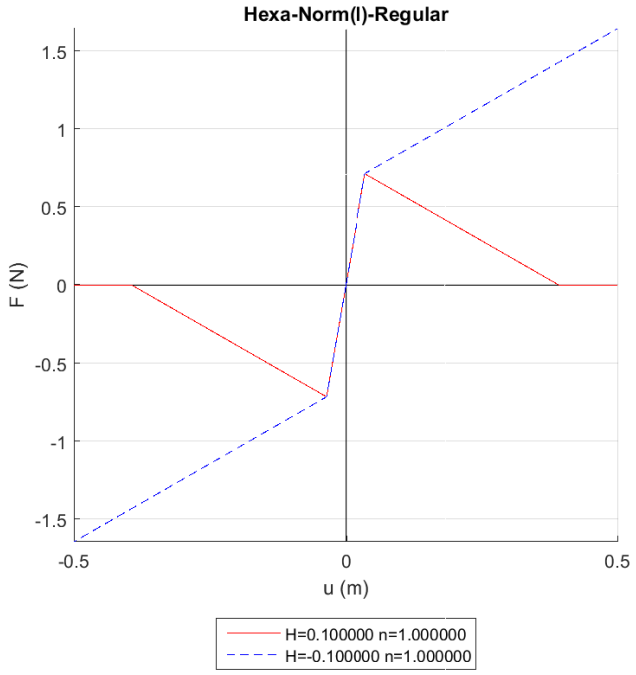

Figure 6.2.1.2.5 Force-displacement plot of Traction-Compression with Hardening-Softening

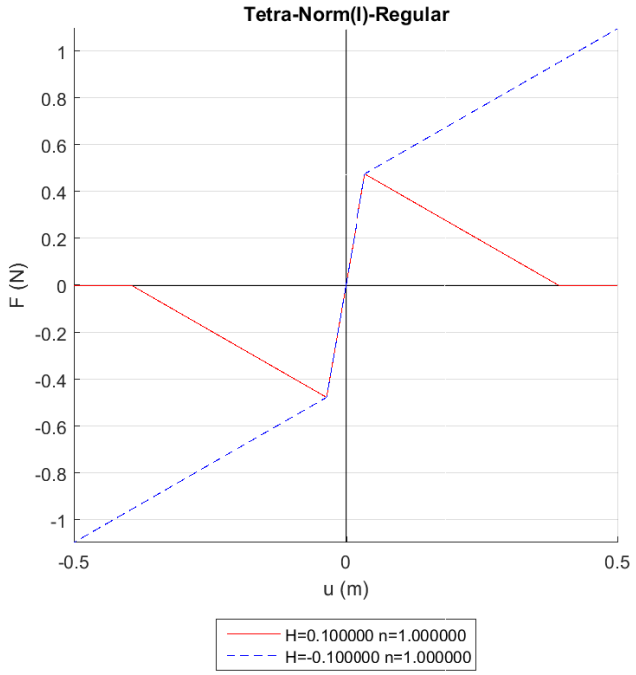

Figure 6.2.1.2.6 Force-displacement plot of Traction-Compression with Hardening-Softening

b) Norm 2

Softening:

Element	%	Increments	σ_y	H	G_f	σ_{sat}	n
CLL	0.01	500	1.43	-0.1	0	0	1
DKT+DR	0.01	500	1.43	-0.1	0	0	1
DKT	0.01	500	1.43	-0.1	0	0	1
Hexahedra	0.01	500	1.43	-0.1	0	0	1
Tetrahedra	0.01	500	1.43	-0.1	0	0	1

Table 9 Properties for a Traction-Compression with Softening

Hardening:

Element	%	Increments	σ_y	H	G_f	σ_{sat}	n
CLL	0.01	500	1.43	0.1	0	0	1
DKT+DR	0.01	500	1.43	0.1	0	0	1
DKT	0.01	500	1.43	0.1	0	0	1
Hexahedra	0.01	500	1.43	0.1	0	0	1
Tetrahedra	0.01	500	1.43	0.1	0	0	1

Table 10 Properties for a Traction-Compression with Hardening

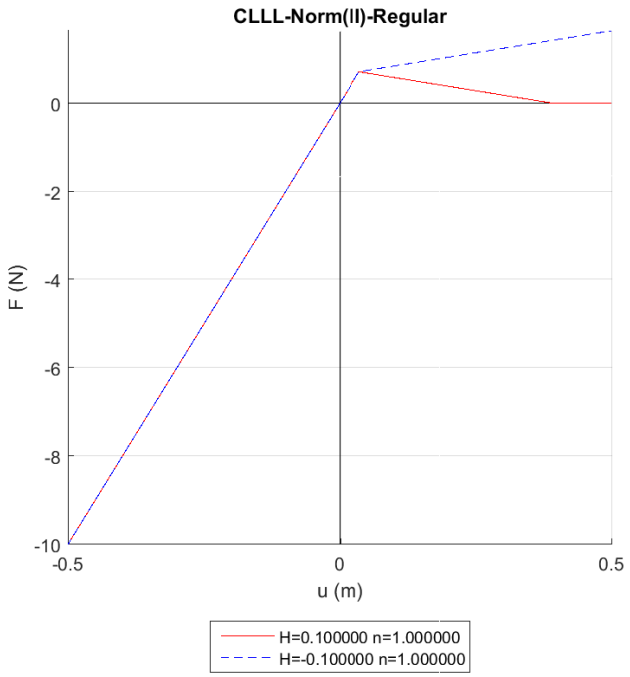

Figure 6.2.1.2.7 Force-displacement plot of Traction-Compression with Hardening-Softening

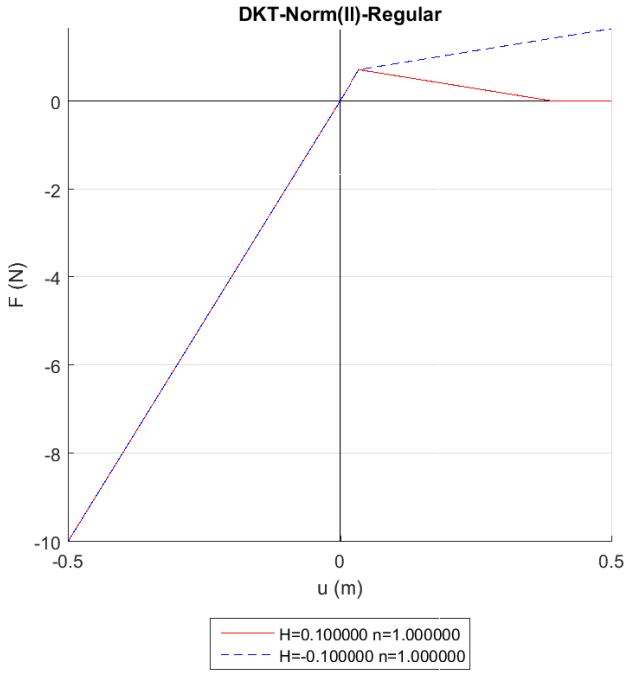

Figure 6.2.1.2.8 Force-displacement plot of Traction-Compression with Hardening-Softening

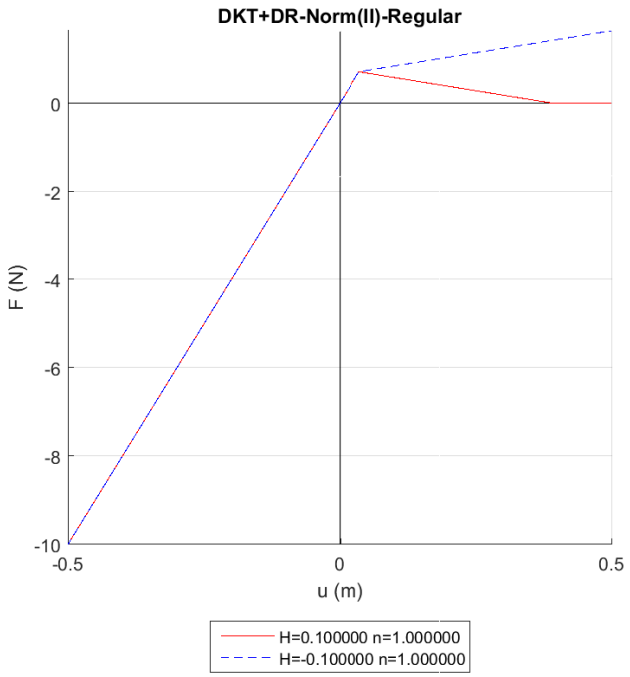

Figure 6.2.1.2.9 Force-displacement plot of Traction-Compression with Hardening-Softening

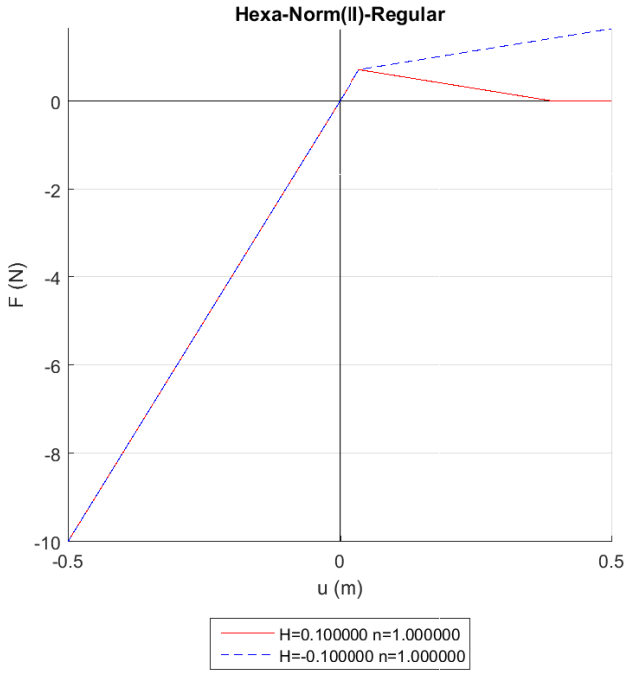

Figure 6.2.1.2.10 Force-displacement plot of Traction-Compression with Hardening-Softening

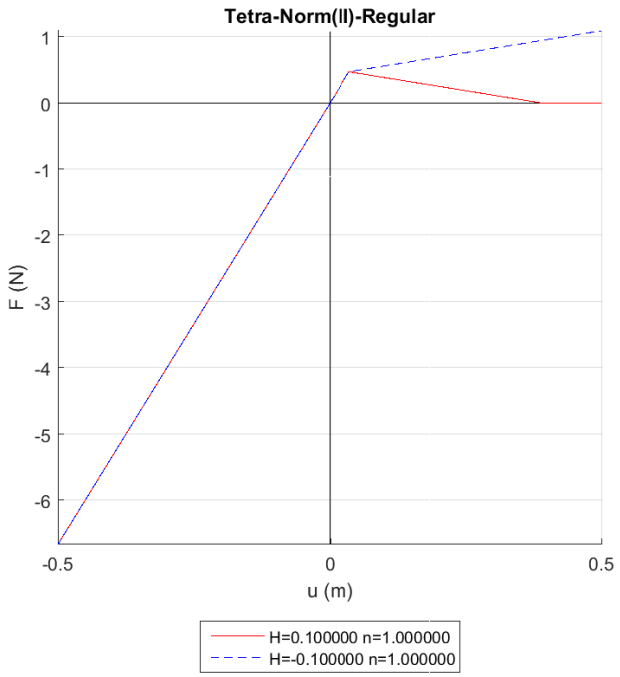

Figure 6.2.1.2.11 Force-displacement plot of Traction-Compression with Hardening-Softening

c) Norm 3

Softening:

Element	%	Increments	σ_y	H	G_f	σ_{sat}	n
CLL	0.01	500	1.43	-0.1	0	0	3
DKT+DR	0.01	500	1.43	-0.1	0	0	3
DKT	0.01	500	1.43	-0.1	0	0	3
Hexahedra	0.01	500	1.43	-0.1	0	0	3
Tetrahedra	0.01	500	1.43	-0.1	0	0	3

Table 11 Properties for a Traction-Compression with Softening

Hardening:

Element	%	Increments	σ_y	H	G_f	σ_{sat}	n
CLL	0.01	500	1.43	-0.1	0	0	3
DKT+DR	0.01	500	1.43	-0.1	0	0	3
DKT	0.01	500	1.43	-0.1	0	0	3
Hexahedra	0.01	500	1.43	-0.1	0	0	3
Tetrahedra	0.01	500	1.43	-0.1	0	0	3

Table 12 Properties for a Traction-Compression with Hardening

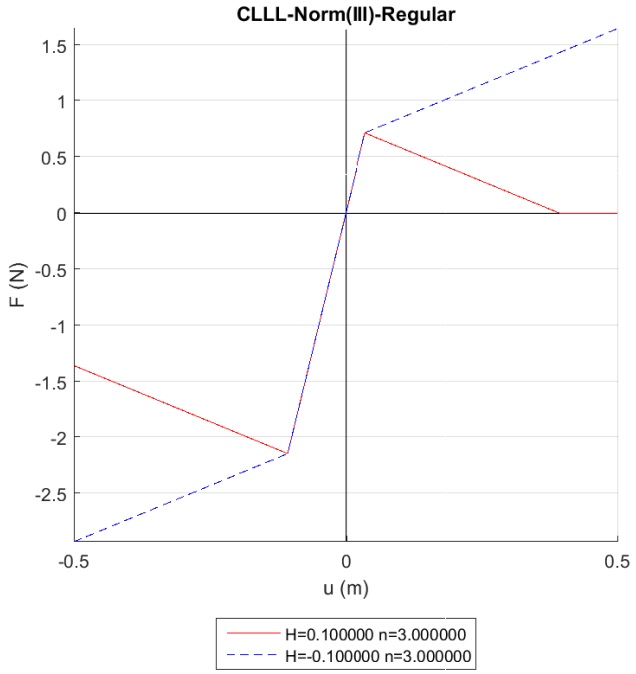

Figure 6.2.1.2.12 Force-displacement plot of Traction-Compression with Hardening-Softening

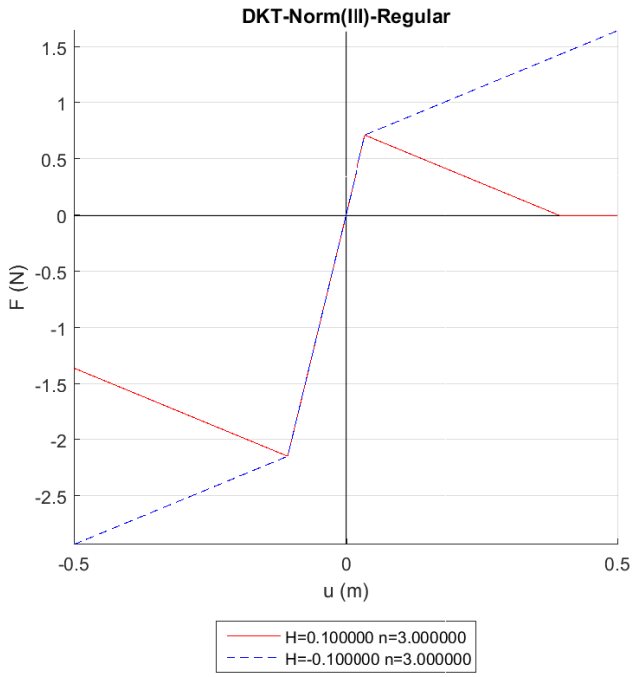

Figure 6.2.1.2.13 Force-displacement plot of Traction-Compression with Hardening-Softening

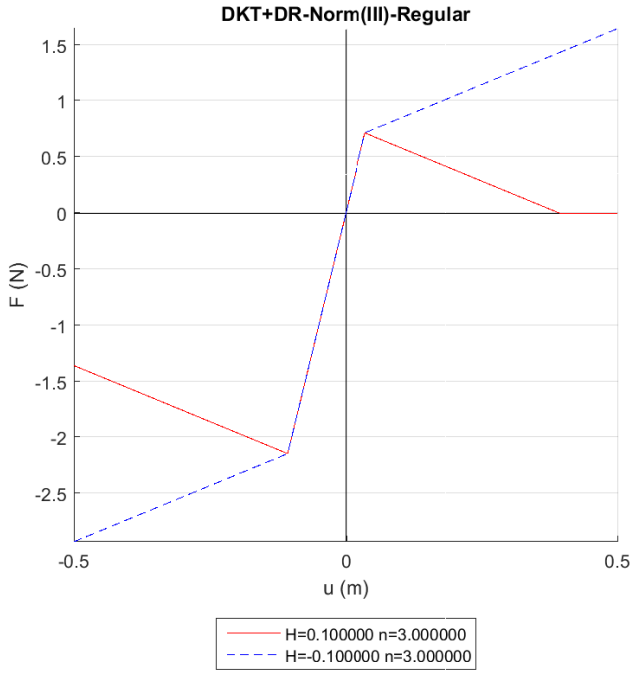

Figure 6.2.1.2.14 Force-displacement plot of Traction-Compression with Hardening-Softening

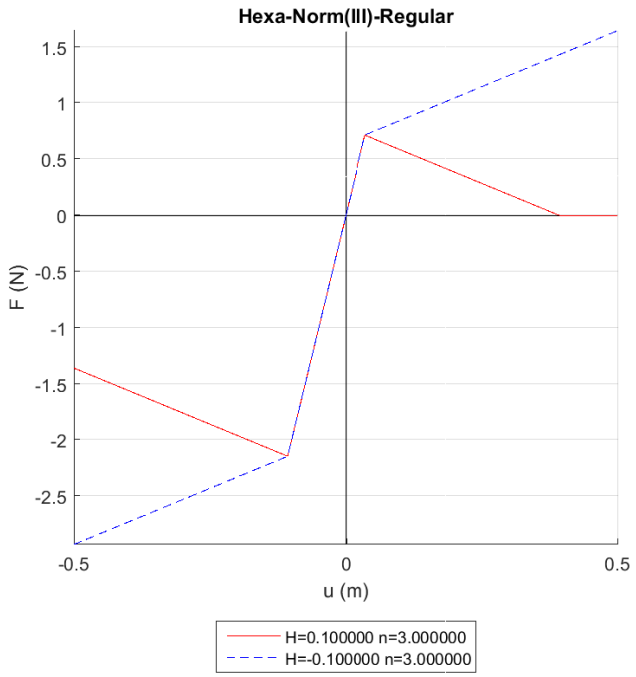

Figure 6.2.1.2.15 Force-displacement plot of Traction-Compression with Hardening-Softening

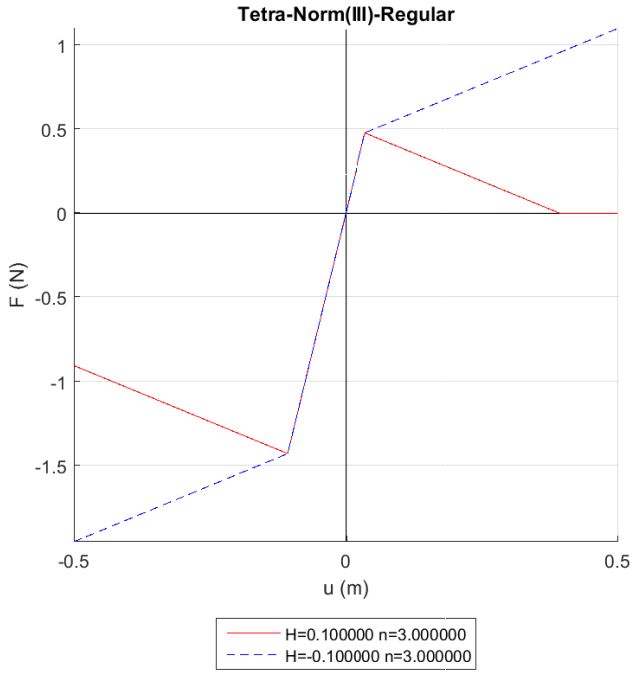

Figure 6.2.1.2. 15 Force-displacement plot of Traction-Compression with Hardening-Softening

Comments

Now the behaviour of the linear law is checked. As it can be seen, when the plasticity begins, the behaviour of the element is lineal, in elastic model, but with less stiffness. So, with less force, it will obtain more displacement because the element cannot longer hold more stress.

There are three different norms to verify, as in exponential. The norm one, as I say in theory, have a symmetric behaviour as it can be seen in the previous figures.

The norm two have different response in traction and in compression. The compression behaviour is lineal (the same for softening and hardening) and the traction lineal as in Norm 1

Finally, the norm three have a non-symmetrical behaviour but the traction and compression behaviour have a relationship between it, as we have seen in theory, in this case this relationship is 3.

Moreover, comparing the different response between hardening and softening. As it can be seen in all the plots, focusing on softening, it is concluded that all figures tend to 0. This is the expected behaviour. Once is set in 0, the force cannot continue going down because at that point, we have $d = 1$ and the theory says that damage cannot be greater than 1. Otherwise, hardening also tends to the expected value. If we want to check this value, we have to compare in the same field. It is important to convert the saturation stress into force field in order to compare it.

Also, is easy to know which value will have the damage variable. As I said in theory, it is obtained by solving a simple limit. The evolution of the damage also can be obtained but is not important to verify the behaviour. the damage evolution is going to be studied in the validation cases.

Between elements, there is no a suitable difference only in *Quadrilateral* where the energy facture is 20% less. Now we are studying only one element, is difficult to see differences but it is probably that if we do a finer mesh, all the elements tend to the same value of stress and strain.

Conclusions

Finally, comparing behaviour between lineal and exponential laws. The exponential behaviour is more realistic because is very difficult to obtain a material with lineal properties when it damage.

Both models have been created in order to represent the behaviour of different materials. Some materials will have a behaviour more similar to exponential and others to lineal, and it is difficult to find a material that can be exactly represented by one of these laws.

This is not a closed theory, anyone that could propose one law of representation, if it have mathematical consistence and it represents the behaviour of a material better than the others two, it is a good law.

6.2.2. Validation

In the same way as in the verification process, an experimental model is going to be studied in order to check the physical response for an isotropic damage model under a hydrostatic-normal to the surface domain-load.

The problem is a typical structural problem. We have an isotropic homogeneous shell with all the contours with totally restricted movement (all angles and all directions) with a surface normal pressure load. The constitutive model used is damage model.

In addition, the validation aims to show the importance of having some physical knowledge of the simulated structure. Different homogeneous constitutive models are going to be presented and studied. Making emphasis on know the performance of the model can be improved by means of a better choice of the constitutive model for certain zones depending on the range of internal stresses obtained. Thus, similar results will be obtained, but the impact of the computational cost in terms of time will be reduced significantly.

Description of the problem

As it has been explained before, it is a simple shell totally supported with a pressure load applied above them.

Geometrical characteristics

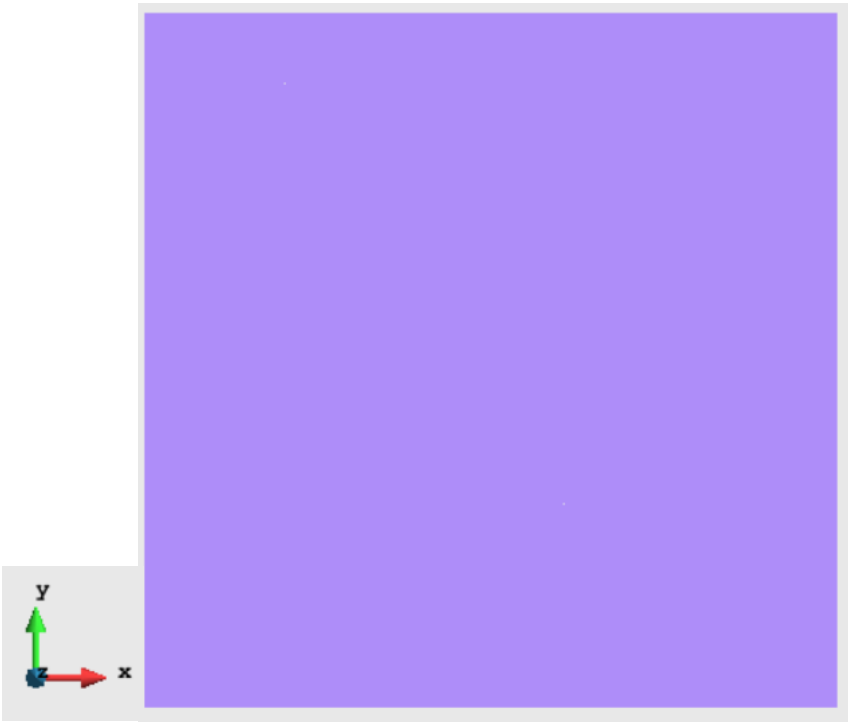

Figure 6.2.2.1 Schematic representation of the problem

- Surface: $1m^2$. (1mx1m)
- Thickness: 0.05m
- Layers: 10 (integration layers)

The geometry of this problem Is very simple in order to check the correct physical behaviour of our model.

Constrains

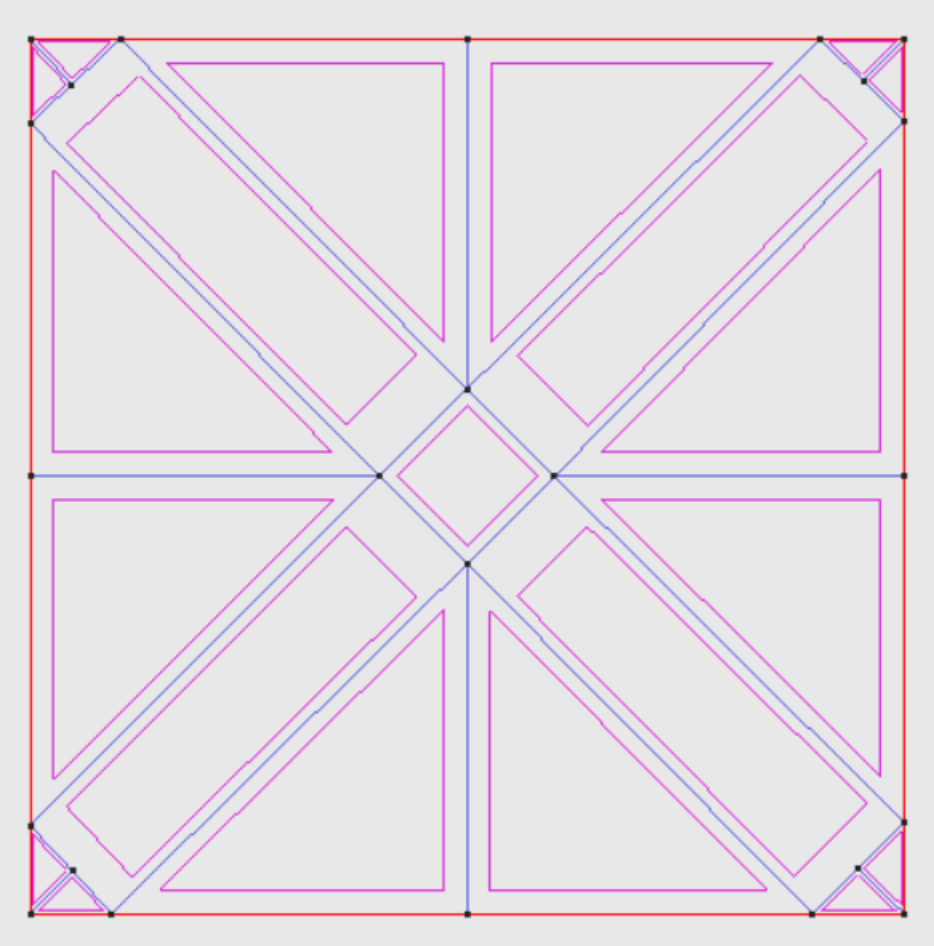

Figure 6.2.2.2 Schematic representation of the constrains

In this model only, displacement constrains are going to be applied, free rotation is set.

Degrees of freedom	Value
X	1
Y	1
Z	1
θ_x	0
θ_y	0
θ_z	0

Where:

- 1: Means that the movement is blocked.
- 0: Means that the movement is free.

NOTE: Then we will see why this division is applied.

Load

In this case, is a problem that the exact value is unknown of the force that produces the initial damage or the total fail damage of the structure. Because of this, different problems have to be solved in order to know, more or less, the value of the force. It is important to use a big mesh for this collaboration because the objective is not the exact value but the order of the magnitude of the force.

Because the non-linearity of the problem, incremental load analysis is used. This method is useful to get closer to non-linear curves of models. Consist in divide the curve in a number of divisions called increments (can be chosen by the user) and apply a percentage of the load (previously introduced) in each increment.

For example, the objective is to represent a model like the following green function:

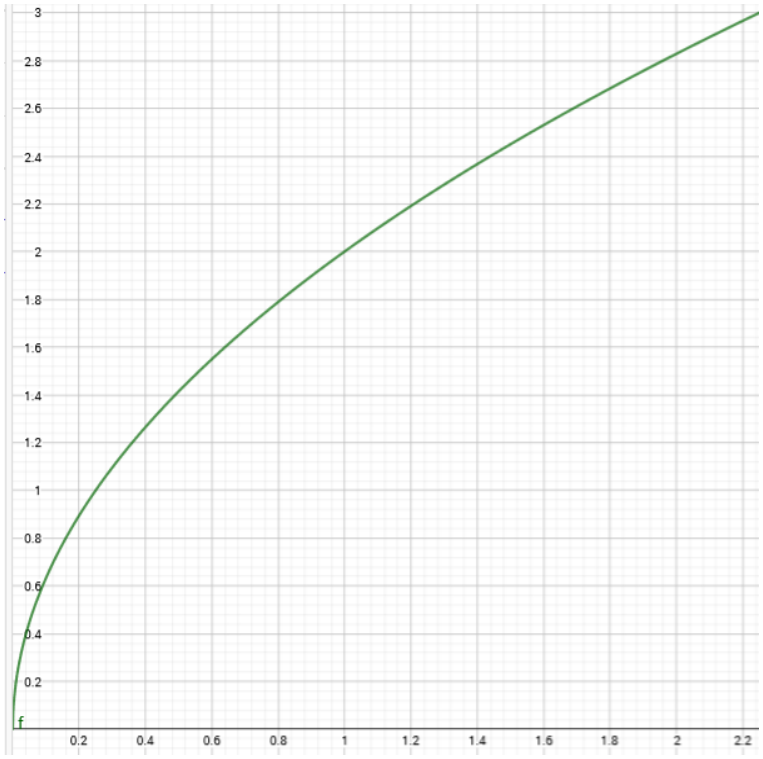

Dividing the curve in a number “x” of increments and apply the percentage wanted of the force:

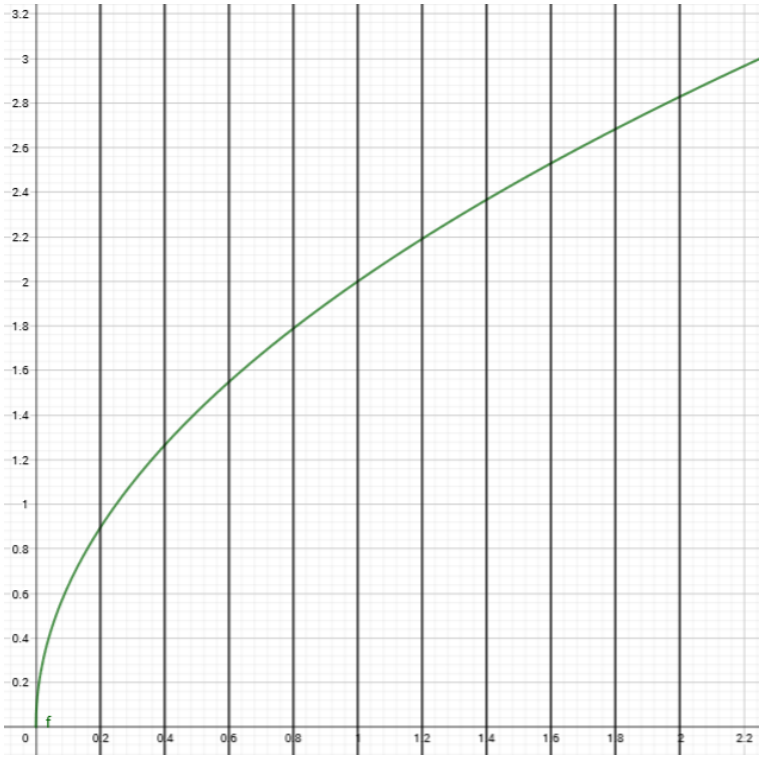

The objective is to approximate the curve with the tangent of each increment.

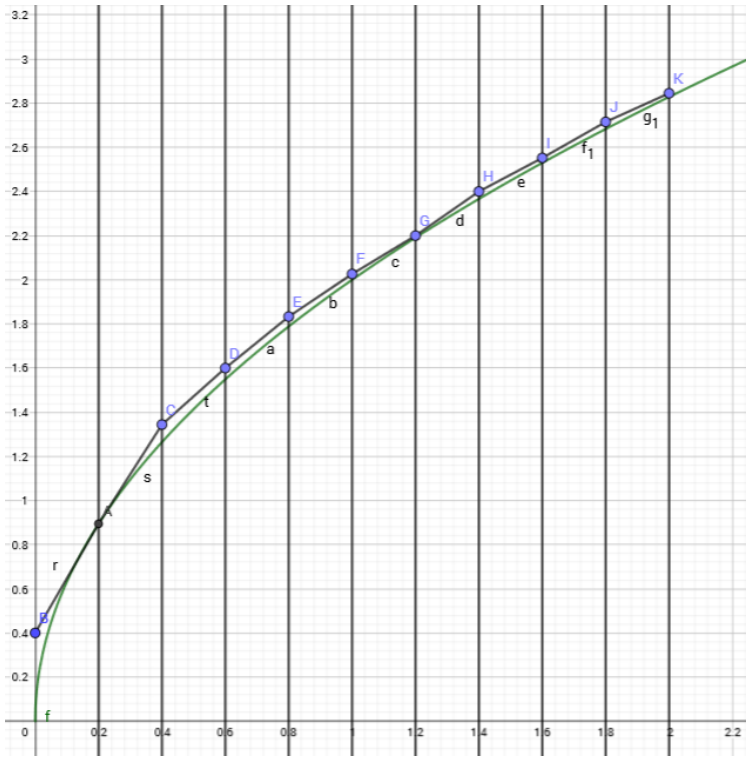

(Not a real case, only used to understand better the concept)

As it is said, in this validation we use this type of analysis because it provides smoother solutions when modifying the values of the increment and the percentage of the force applied. Reducing the amplitude of the increment, more points are obtained and in consequence the error will be smaller.

Only one load is applied in the centre of gravity in positive z direction. This load is uniformly distributed above all the shell's surface. We can see the graphical representation in the next figures:

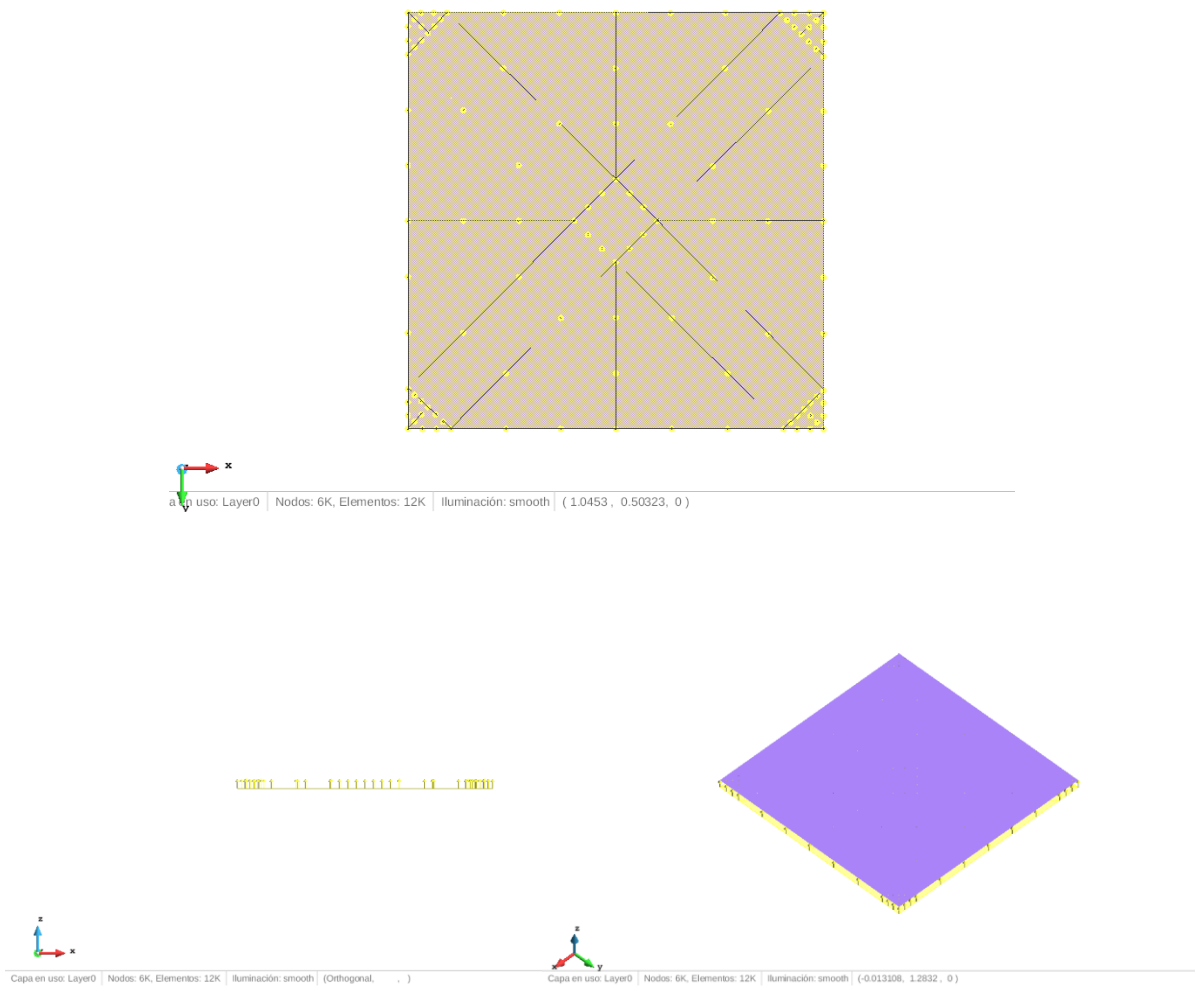

Figure 6.2.2.2 Schematic representation of the load applied

Material characteristics

In function of the type of the study we do, we are going to assign different material properties (*Elastic lineal, Damage)* in the different zones.

Elastic lineal

- Elastic modulus: $30000000000\ N/m^2$.
- Poisson coefficient: 0.3
- Yield limit: 1500N/m^2

Damage

- Exponential
- Softening
- Fracture energy $1 \cdot 10^{12}\ J$

Three different zones can be differentiated:

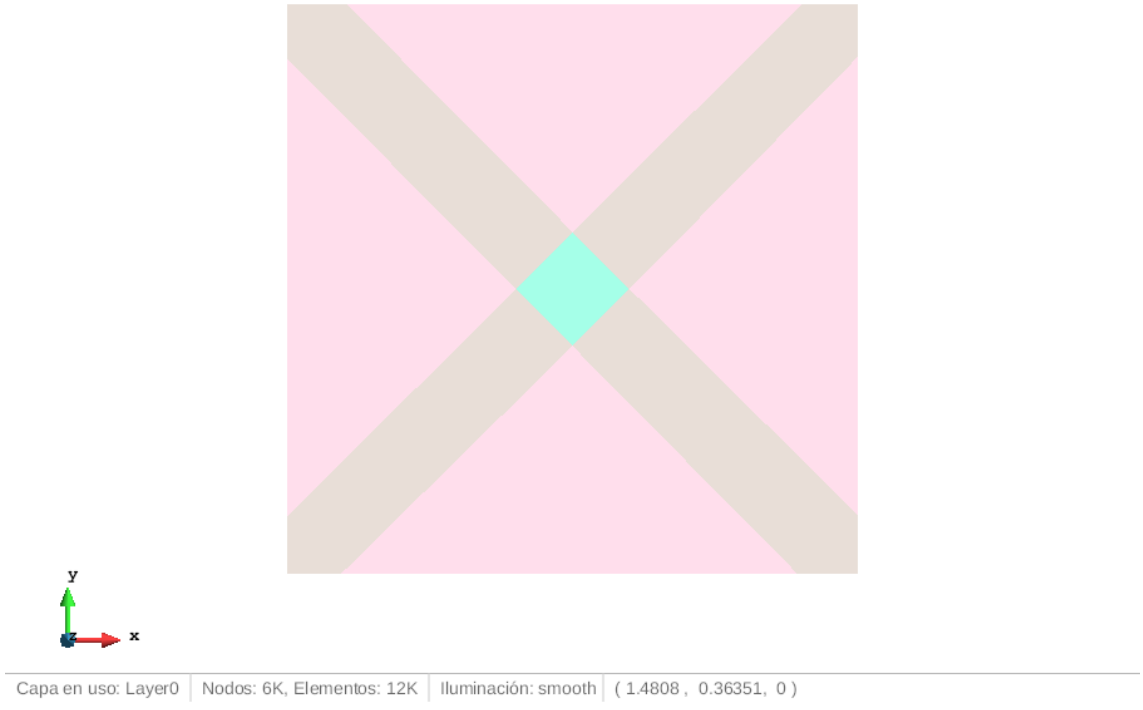

Figure 6.2.2.3 Schematic representation of the different zones of the shell

Zone 1: Represents the biggest part of the structure. This is the zone with less probability to suffer damage.

Zone 2: Represents the "X" area of our section (without *Zone 3*). This is a zone that is going to suffer more damage than Zone 1 because the geometrical problem we have. Remember that we have a shell totally constrained, so the boundaries don't have any displacement. If we have more length, because the distance from the centre to the corner is bigger than from the centre to the lateral, the displacement is going to be bigger too. Thus, when we have more displacement we also are going to obtain more damage. Also, we have to take into account that the Zone 2 and the Zone 3 are zones away from the boundaries. This zone will suffer more stress because the moments will be bigger than in Zone 1.

Zone 3: The centre zone. This is the zone with more stress because of the load and also because is the zone with more distance to the boundaries. Then the moment is going to be bigger than in other zone and in consequence the stress.

Mesh

The use of FEA software begins with a computer-aided design (CAD) model that represents the physical parts being simulated as well as knowledge of the material properties and the applied loads and constraints, as we have made. This information enables the prediction of real behaviour, often with very high levels of accuracy.

The precision that can be obtained from a model is directly related to the finite element mesh that is used. The finite element mesh is used to subdivide the model (drown in CAD) into smaller domains called *elements*, that are made from *nodes* over which a set of equations are solved. Also, the equation can be solved in gauss points, in fact, we use gauss points and not nodes to solve the equations. These equations approximately represent the governing equation of interest via a set of polynomial functions defined over each element. As these elements are made smaller and smaller, as the mesh is refined, the computed solution will approach the true solution, but the computational cost will be bigger.

For this problem an adaptative mesh is used. Our mesh is smaller in those points it is going to obtain more damage. So, we will have accuracy results in that region but without all the computational cost that would be refine all the mesh in the same way for all the model.

As it can be seen in [7] from the theory of rupture it is known which zones have more probability of damage

First of all, divide the geometry in order to do the mesh different in some regions.

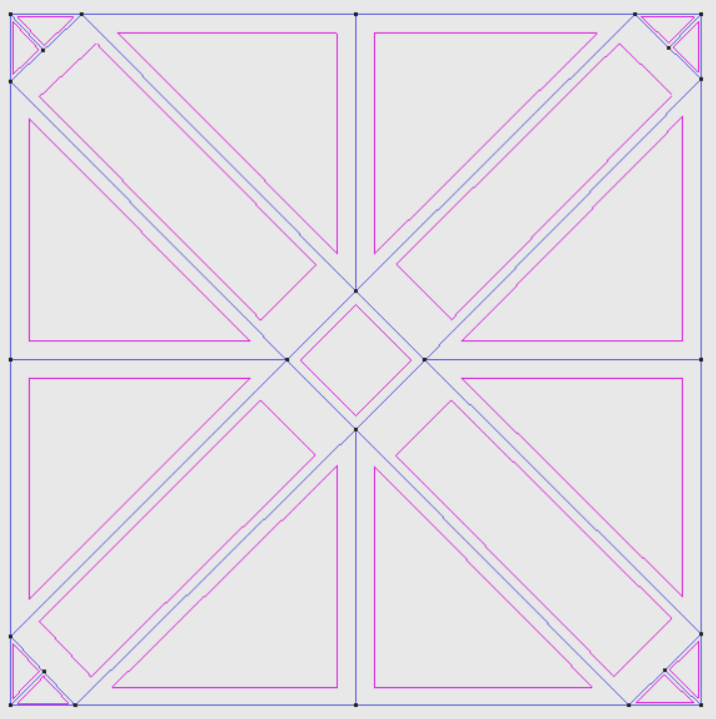

Figure 6.2.2.4 Schematic representation of the division

Now, we can do the mesh.

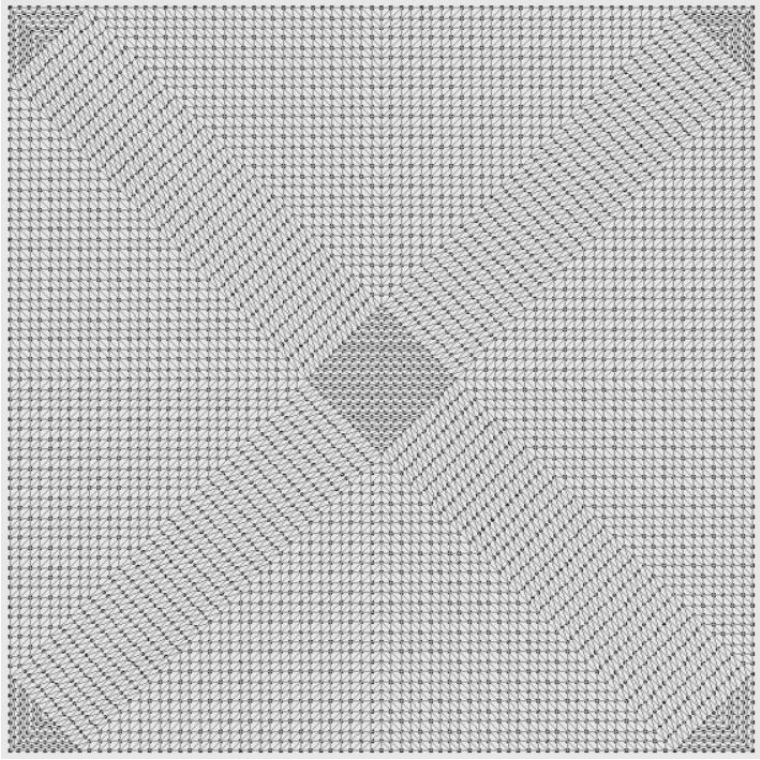

Figure 6.2.2.5 Adaptative Mesh applied to the problem

As it is explained before, we do this mesh because it is known, according to [7], that this "X" zone will have more displacement than the others. Thus, if it has more displacement also more damage

will be obtained (the material is isotropic and homogeneous). In fact, if we don't have an intuitive problem like this, first of all it is important to launch this case with all the zones with a damage model but with a big mesh. The objective is to find which zones are going to damage first in order to help the FEM element method to "localize" the damage zone.

Calibration

This process is useful because we can realize the magnitude and the limits of our problem. If we don't do this, for example we can launch a problem with a load applied that doesn't allow us to see the evolution of damage because it damages the structure very fast. Also, will appear localization problems, this happens when the method doesn't know where starts the damage in the structure. Then this work focusses a little bit more in localization problems and how they can be solved.

In this calibration process, is the first time we are going to see some results of the validation case. It is important to say that in the postprocess I fixed the limits of the damage variable (d) from 0 to 1. If I don't set the option of limit the value of damage, the postprocess shows us a damage with negative value in some point (in the results will appear in black because of the limits set). This is a consequence of use integration in gauss points. As it is said before, the FEM method is solved in each gauss point and then the postprocess shows the results in the nodes. The program has to interpolate the results in the nodes, and all the gauss points are inside the element so, the are some negative values.

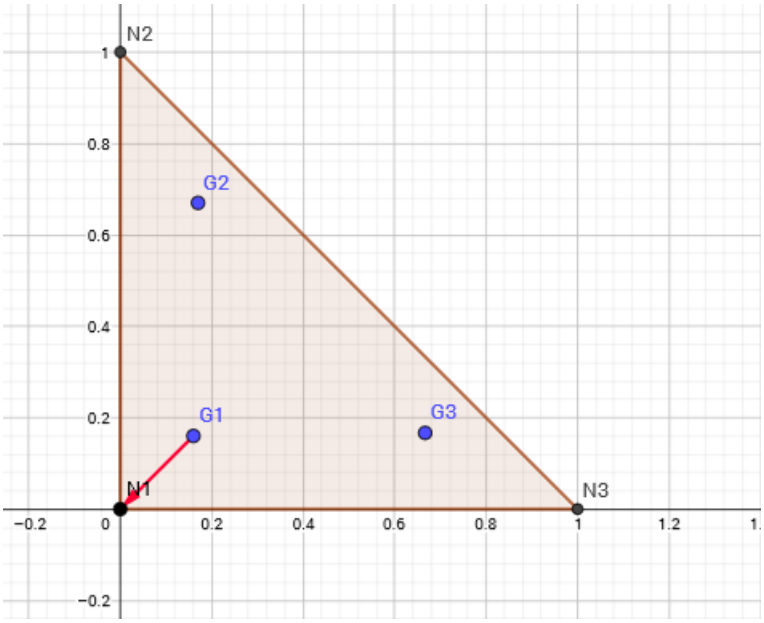

G1;G2;G3 represents the gauss point of a triangular element.

1. Calibration 1

Load (L)	1000 N
Percentatge (%)	$3 \cdot 10^{-3}$
Increments (n)	10
Final load applied$(\boldsymbol{L} \cdot \% \cdot \boldsymbol{n})$	30 N

In this first case, the structure have a total damage of the structure but with good process so the damage evolution can be obtained.

The last step we have without total damage Is 7, so the total load applied in this step is:

$$\boldsymbol{Fd = L \cdot \% \cdot n = 1000 \cdot 3e - 3 \cdot 7 = 21N}$$

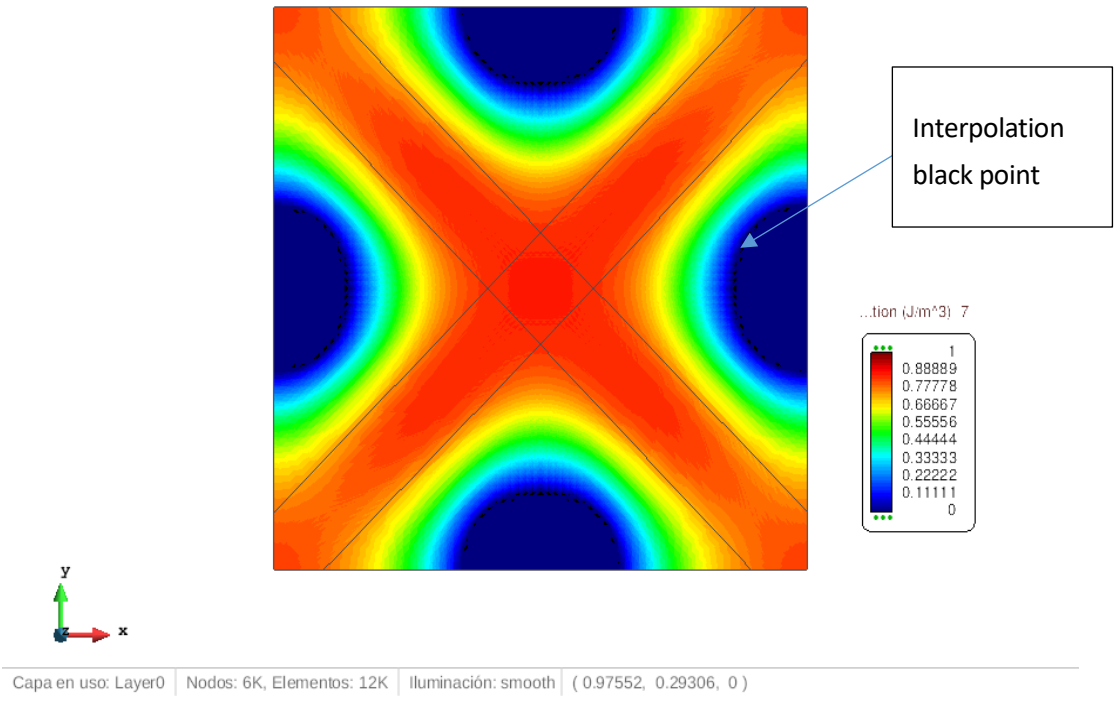

Figure 6.2.2.6 Damage variable (d) – Last step before damage

Then, the first step with total damage is 8. So, we obtain:

$$\boldsymbol{Fd = L \cdot \% \cdot n = 1000 \cdot 3e - 3 \cdot 8 = 24N}$$

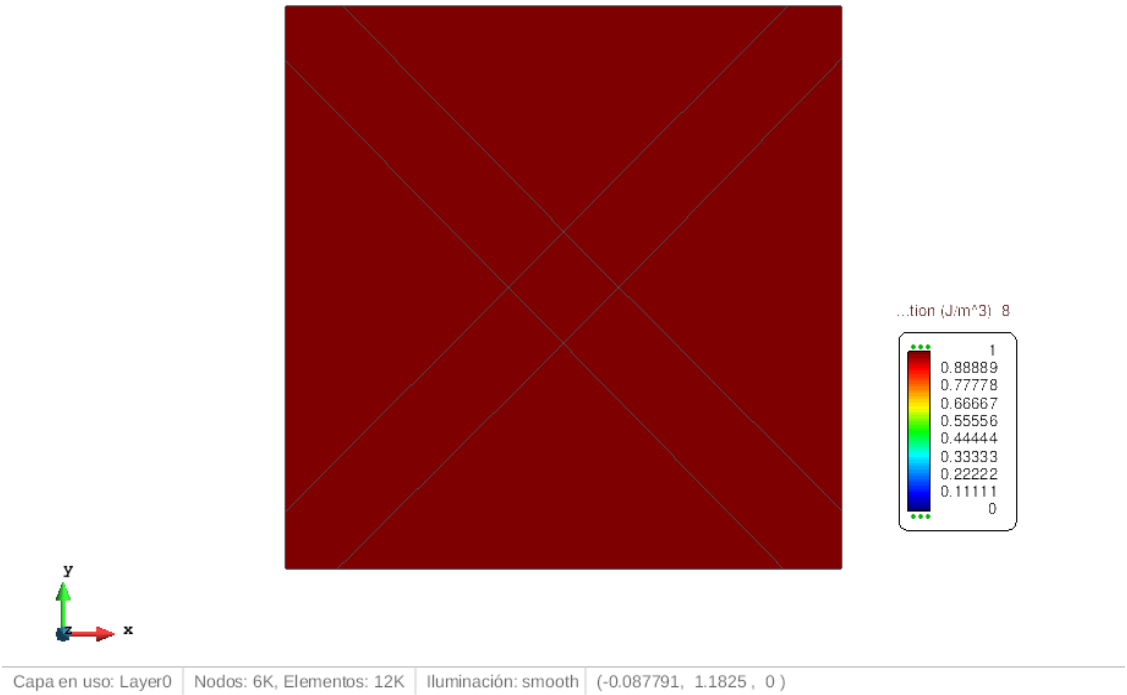

Figure 6.2.2.7 Damage variable (d) –Next step before damage

With this simple study, it is known for which range of value the structure is totally damaged (between 21N and 24N). And also, which are the zones with more probability of damage. We already know that because we have a geometrical problem, but when the structure is complex this can be very helpful in order to help the program solve the problem with a big mesh and faster.

2. Calibration 2

In this calibration the number of increments is going to be increased and the percentage of the load is going to be reduced taking into account that our damage happens when the force is between 21 and 24

Load (L)	1000 N
Percentatge (%)	$1.3 \cdot 10^{-4}$
Increments (n)	210
Final load applied$(\boldsymbol{L \cdot \% \cdot n})$	27,3 N

The last step we have without total damage Is 7, so the total load applied in this step is:

$$\boldsymbol{Fd = L \cdot \% \cdot n = 1000 \cdot 1.3 \cdot 10^{-4} \cdot 166 = 21,58N}$$

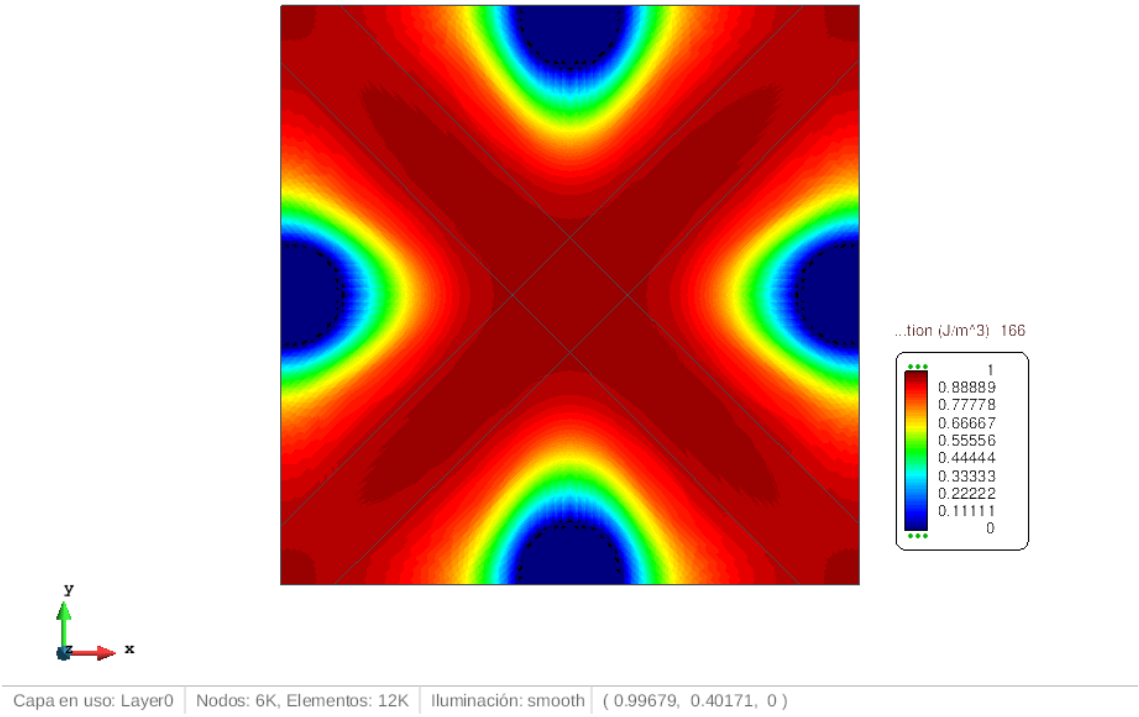

Figure 6.2.2.8 Damage variable (d) – Last step before damage

Then calculating the force applied in the next step, fully damaged, it is obtained:

$$\boldsymbol{Fd = L \cdot \% \cdot n = 1000 \cdot 1.3 \cdot 10^{-4} \cdot 167 = 21,71N}$$

With this calibration a lower range of damage force is obtained. Now it is known that the force that makes fully damage the structure is between: $[21{,}58; 21{,}71]$.

With this result, the next step is top prepare a validation with a low number of increments (less computational cost) and with the same precision because we know the values the structure starts damage, how it progresses and how it finalizes.

Also, the value of force where de structure starts to damage can be obtained. This is important for the validation cases when is only important the zone with more damage, or other zone because you have interest on it.

Validation cases

The values obtained from the calibration test, we can prepare a case with good evolution of damage and with less computational cost.

Load (L)	1000 N
Percentage (%)	$7.1833 \cdot 10^{-4}$
Increments (n)	33
Final load applied$(\boldsymbol{L} \cdot \% \cdot \boldsymbol{n})$	25,8 N

Different damage validations are going to be launched. All the problems will be the same, the only difference is the models we apply in the different zones of the materials. The objective is to demonstrate the importance of understanding the physics applied in a FEM program, so the same results and all the necessary information will be obtained faster and with less computational cost, so cheaper.

The first case to run is with a damage model applied in all the zones.

In the results we are going to analyze the displacement, the damage (d), the momentums and the stress in the bottom layer. It is important to say that the work study the layer with less damage, because if we apply a load in z positive direction, the up layer is going to suffer more than the bottom. But comparing the results in the same layer, the same conclusions can be obtained.

Model 1: All zones with damage model

Simulation type	Structural analysis: Shell
Dimensions	Three dimensional
Analysis type	Incremental load analysis
Geometry	Lineal geometry
Solver	PARDISO
N of elements	12064
Computational time	29 min

Displacement

The results are as we expect. The center and the diagonals are the zones with more displacement.

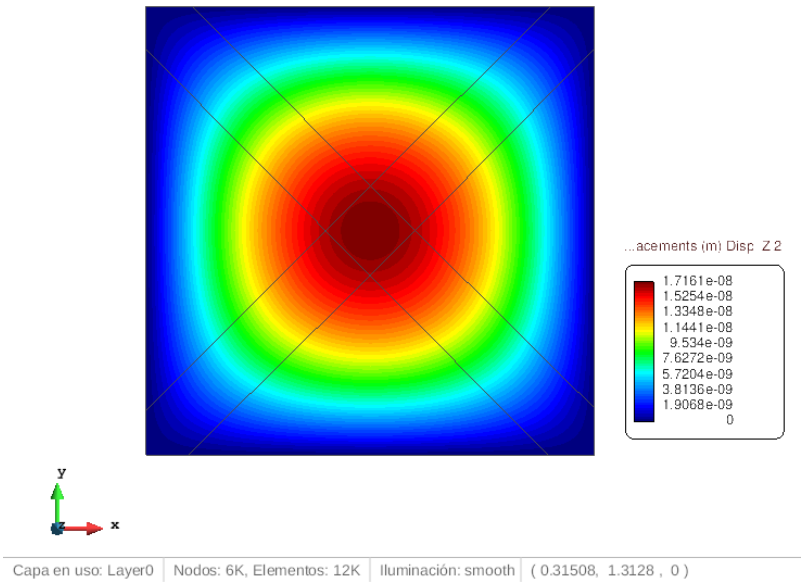

Figure 6.2.2.9 Displacement (z)

As it can be seen, the displacements are bigger at the center of the shell.

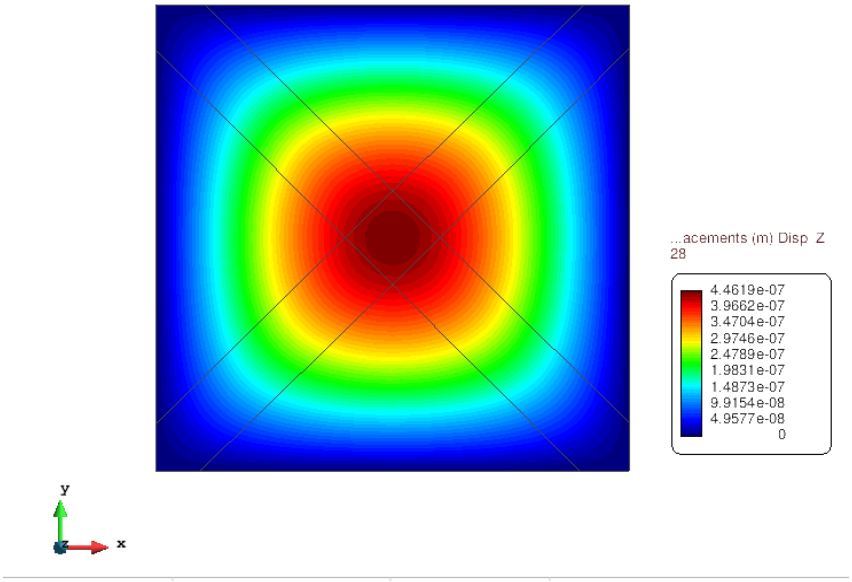

Figure 6.2.2.10 Displacement (z)

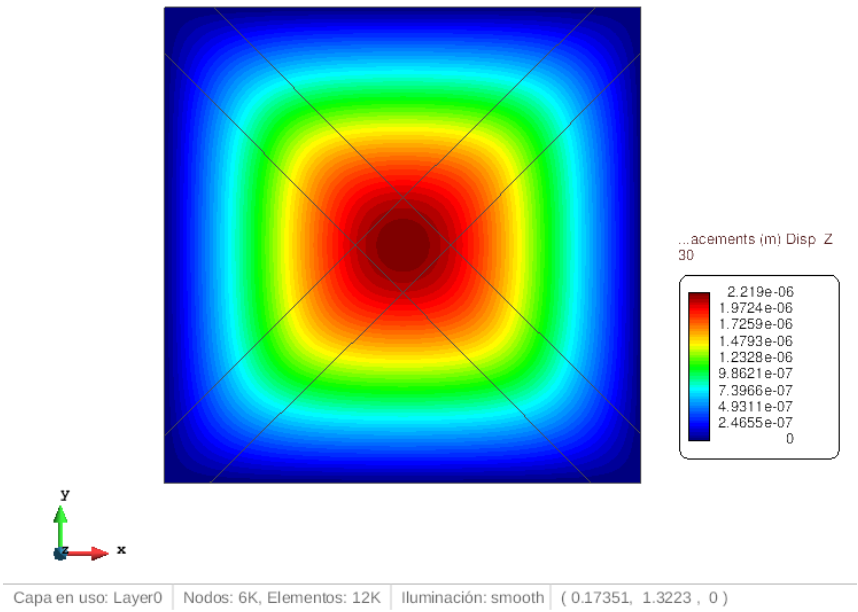

Figure 6.2.2.11 Displacement (z)

In order we get closer to the final iteration, the displacement field starts increasing faster in Zone 2 than in Zone 1. This is because the structure damage more in that zone.

In addition, the deform also can be plotted in order to understand more the results. It is important to say that the next plot is increased five times with the objective of understand clearer the result and the geometry process of our deformation.

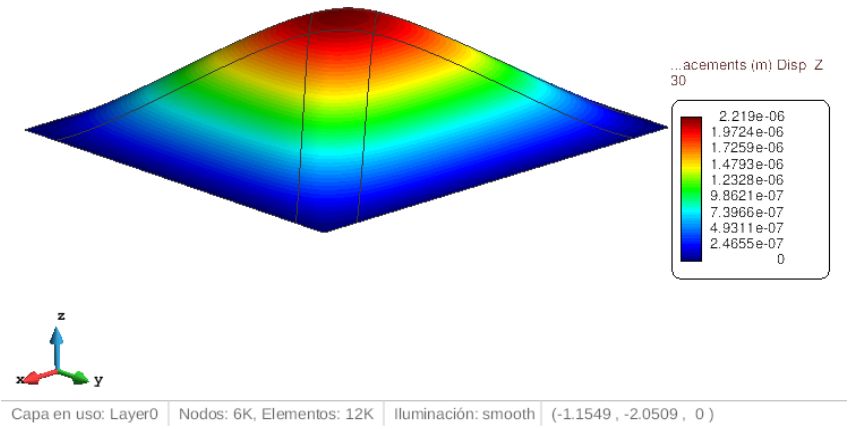

Figure 6.2.2.12 Displacement (z) and deformation

Damage

In order to understand why the damage localizes in some zones more than others, we are going to study the results with the moments, and later with the stresses. If you want to compare directly the stress results with the damage, you have to “transform” this principal stresses into an equivalent stress using the same criterion as damage yield’s surface (see damage theory).

Now, the evolution of the damage is going to be studied in order to check if it damage according to [7].

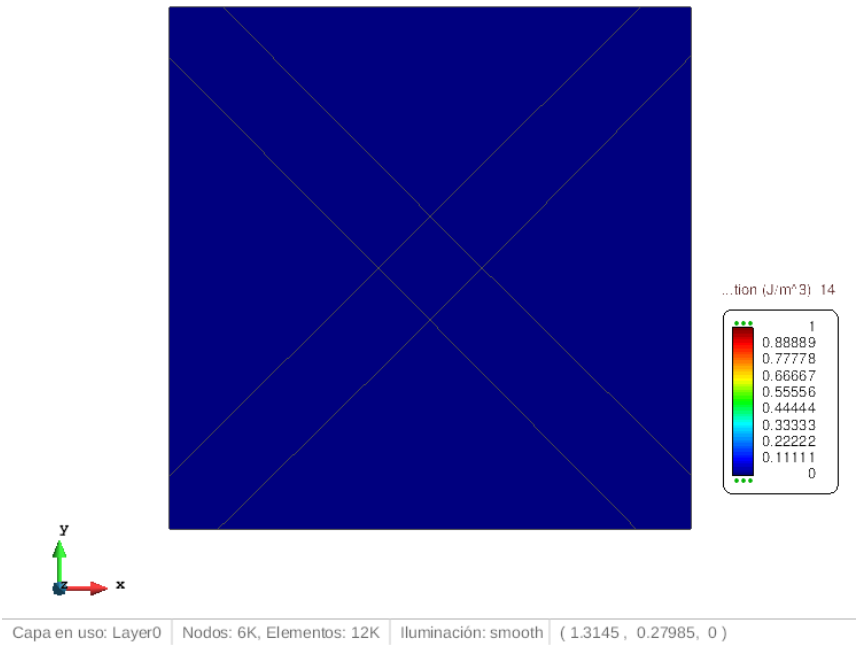

Figure 6.2.2.13 Damage variable (d)

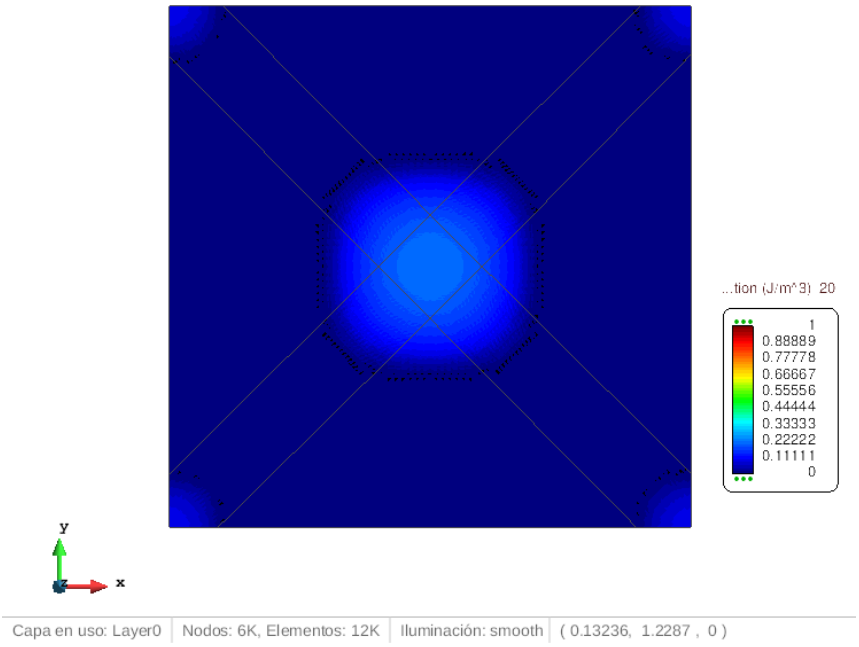

Figure 6.2.2.14 Damage variable (d)

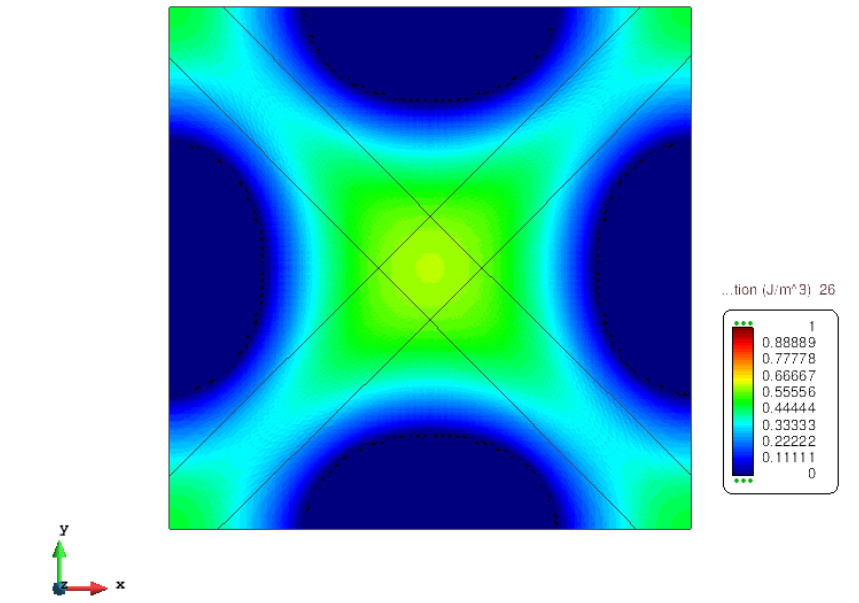

Figure 6.2.2.15 Damage variable (d)

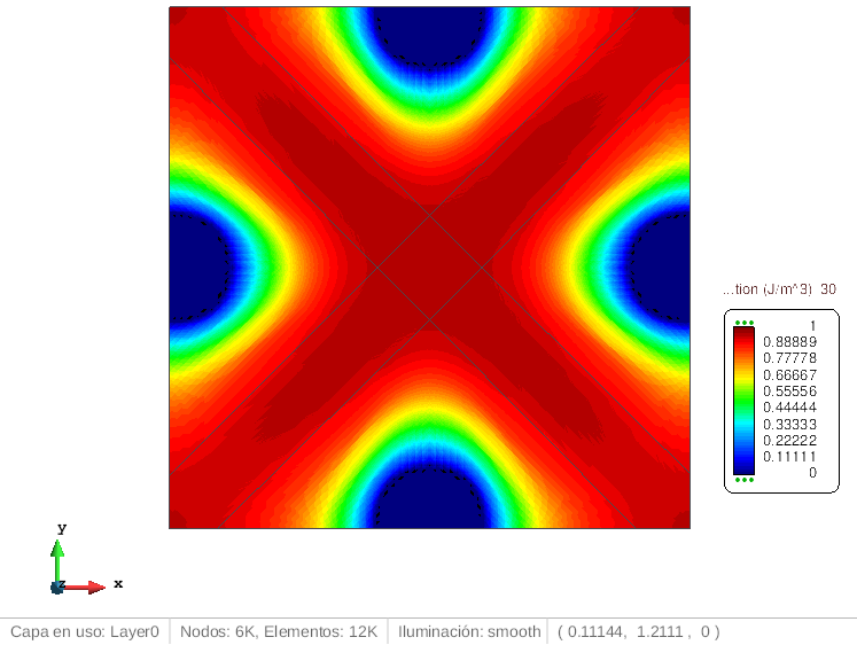

Figure 6.2.2.16 Damage variable (d)

As the failure modes of plates says, the damage is bigger in the cross section of the plate. This work is going to study other variable such moments and principal stress in order to understand why this plate fails in this zone earlier than in the others. You can clearly see that the zone 1 is the zone with less damage, even one increment before total damage, this zone still with no damage on it. Moreover, in the increment 20 we observe that the damage begins at the center but also at the corners of the structure. When we analyze momentums, we will realize why this happens.

Also, in this plot it can be seen the black points because of the interpolation of gauss points.

It is important to say that in the first plot the structure is not damaged yet because we still in the elastic zone of the defined material.

Momentum

In particular 3 Moments are going to be studied:

- M_x
- M_y
- M_{xy}

This moments are the responsible of create stress in the plate

Increment 14

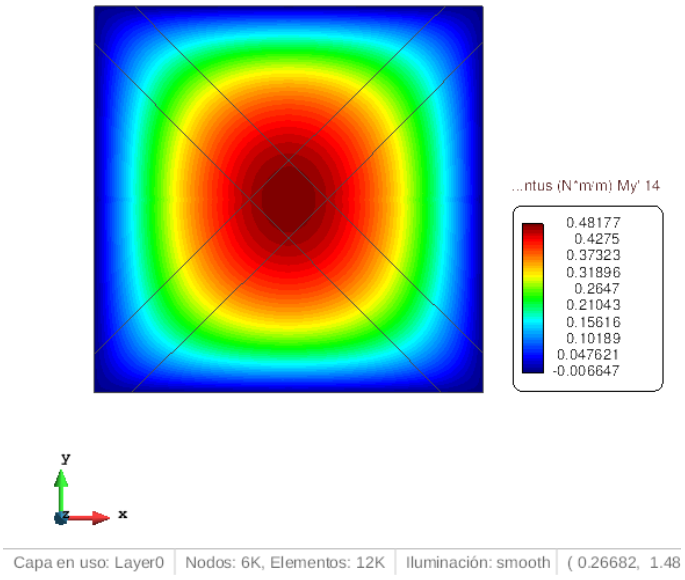

Figure 6.2.2.17 Momentum "Y"

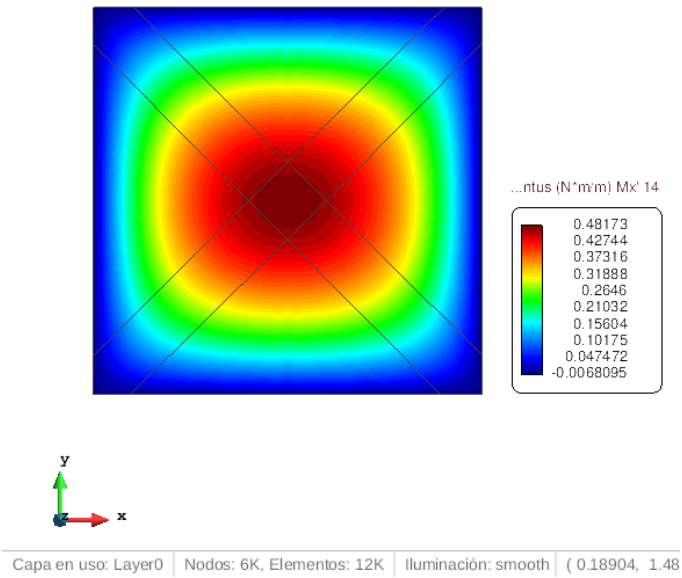

Figure 6.2.2.18 Momentum "X"

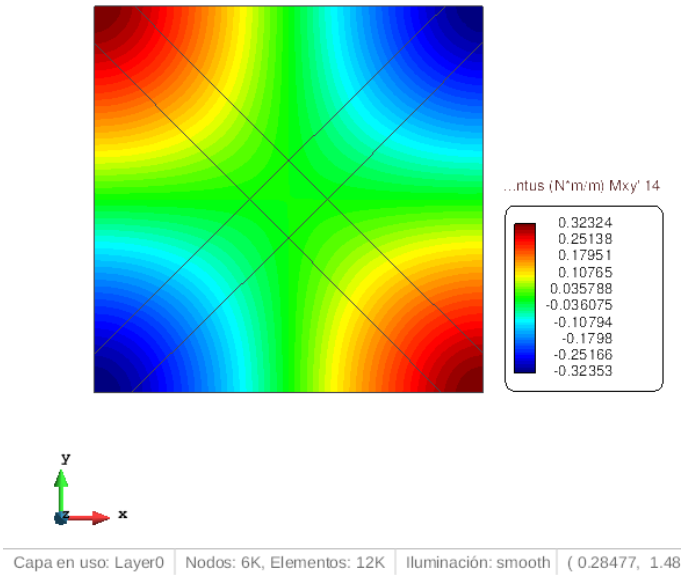

Figure 6.2.2.19 Momentum "XY"

Increment 30

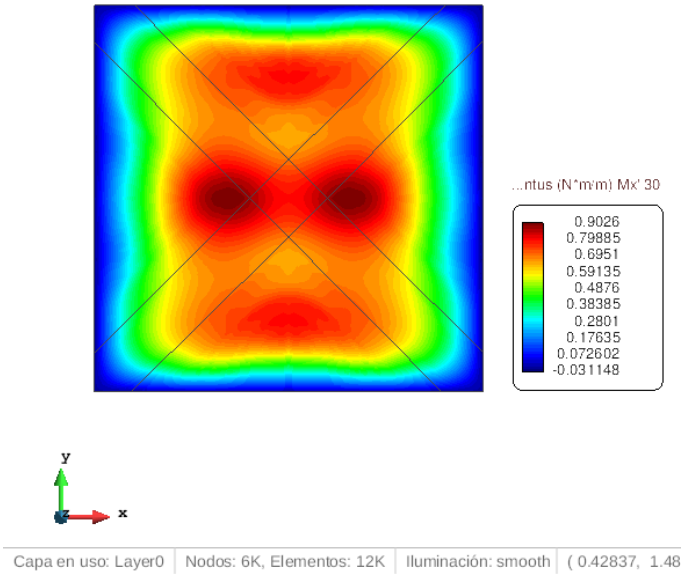

Figure 6.2.2.20 Momentum "X"

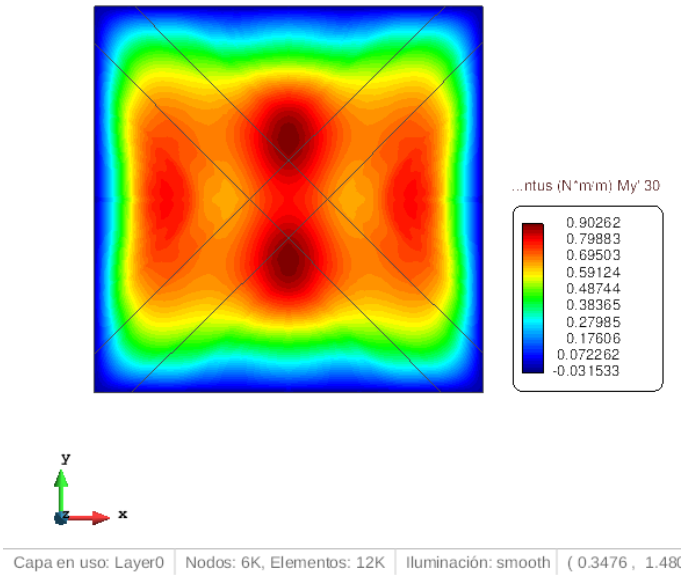

Figure 6.2.2.21 Momentum "Y"

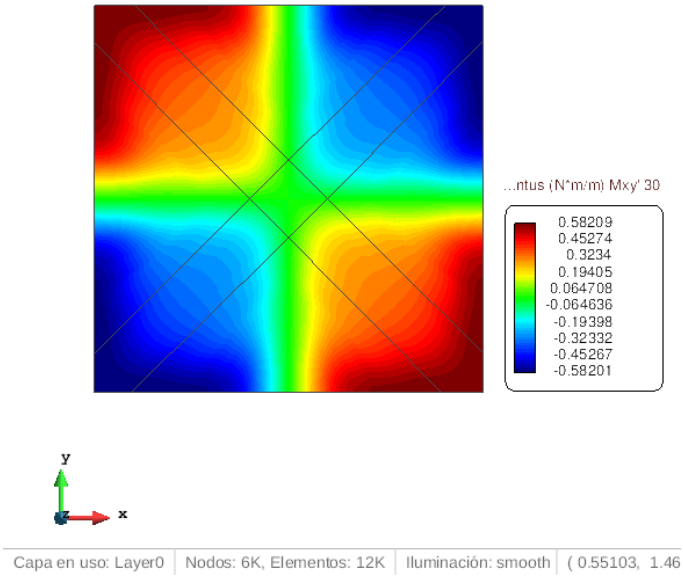

Figure 6.2.2.22 Momentum "XY"

As it can be seen, momentums are the responsible of the damage of the plate.

In the damage figures, we realized that the first zones to start damage where the corners and the center of the structure. Analyzing the plots, it can be observed that M_x and M_y cause the failure of the structure in the center while M_{xy} cause the failure at the corners and the cross section of the plate.

Comparing the damage results with the moments results, it is observed that in the way the momentums are increasing, also the damage increase and in the same zones that momentum do.

Otherwise, it can be observed that the stress results in the increment 14. They are directly related to momentums. We are going to study: $\sigma_x, \sigma_y, \tau_{xy}$

Stress

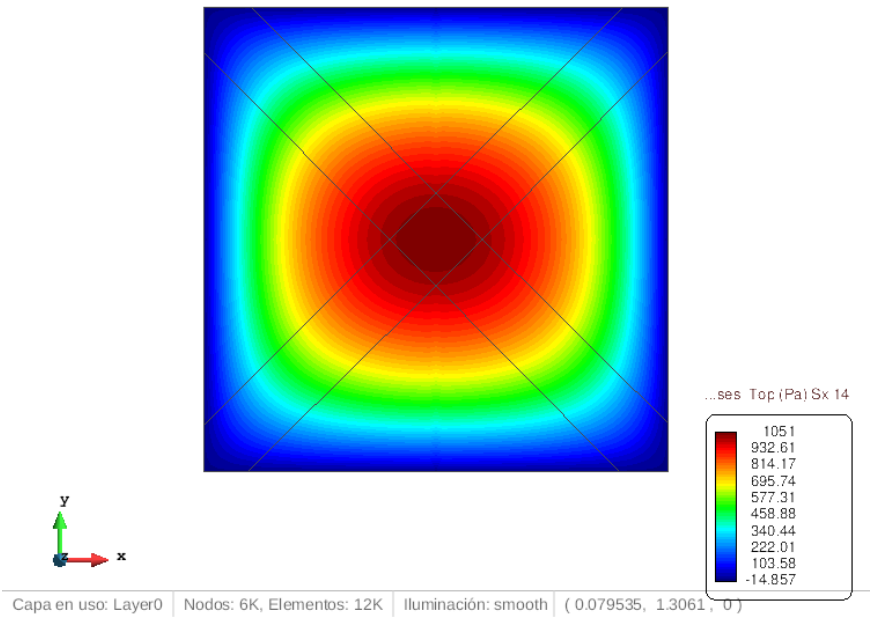

Figure 6.2.2.23 Stress "X"

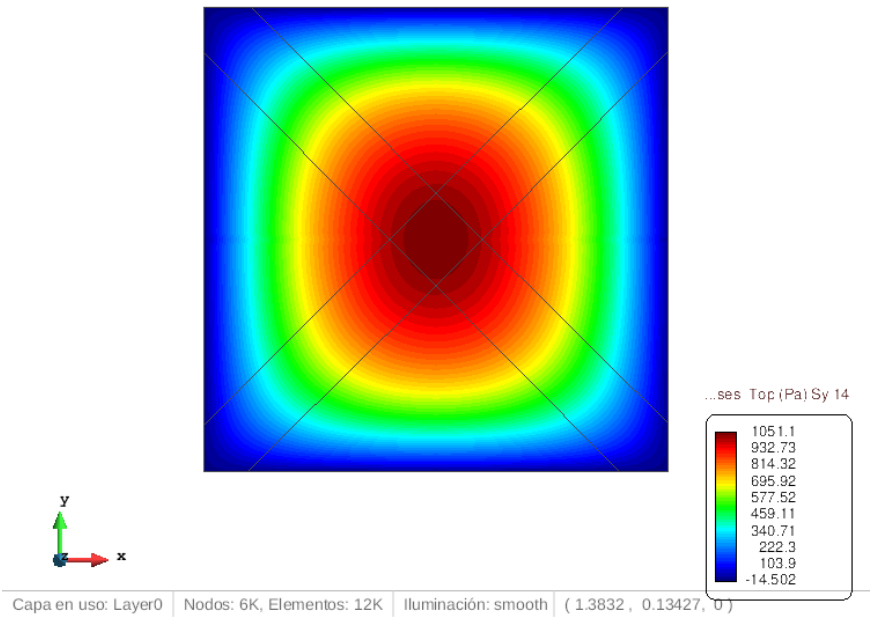

Figure 6.2.2.24 Stress "Y"

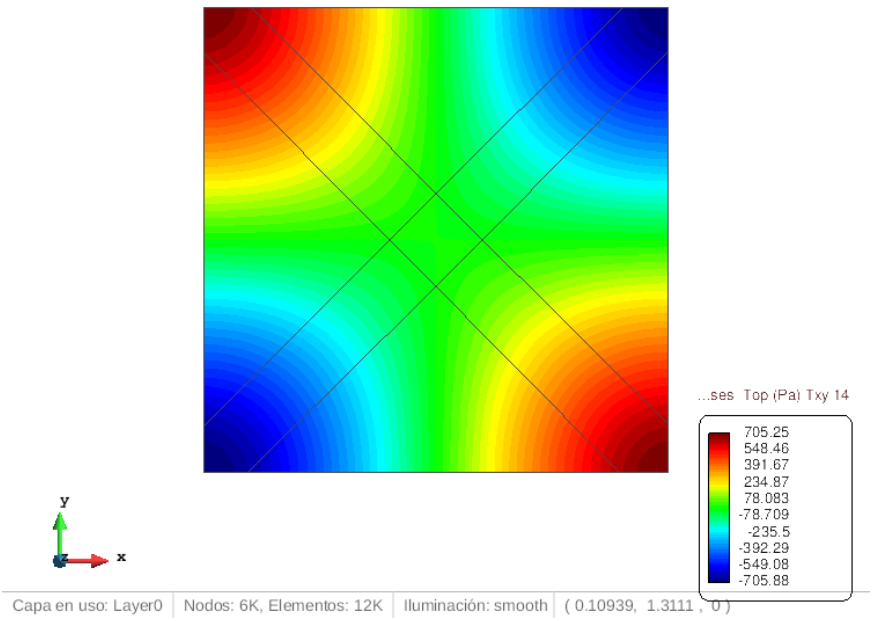

Figure 6.2.2.25 Stress "XY"

As it is said, they have direct relationship with momentums. But with these figures we can observe why the center damage is bigger than in the corners (see figure damage increment 20). As it can be seen, σ_x and σ_y are bigger than τ_{xy}. So thus, the damage also will be bigger.

Model 2: Zone 3 and Zone 2 with damage model. In Zone 1 we use a linear elastic model.

Simulation type	Structural analysis: Shell
Dimensions	Three dimensional
Analysis type	Incremental load analysis
Geometry	Lineal geometry
Solver	PARDISO
N of elements	12064
Computational time	26 min

The approach of using only damage model in the zones 2 and 3 can be done because in the calibration model it is seen that these two areas were the zones with more damage, with a big difference between these zones and zone 1. The results it is going to obtain have to be the same in the zone 2 and 3 because is the same problem. With this simplification, the simulation helps the FEM program to localize where the damage begins and which areas are important and also, we only focus in the zones we want to know the damage behavior of our structure.

As it can be seen in the previous table, we reduce the computational cost and computational time are reduced, this difference in a bigger problem can be important.

The last step before damage for this model is going to be plotted in order to check that the results, in zones, are the same as in the first model.

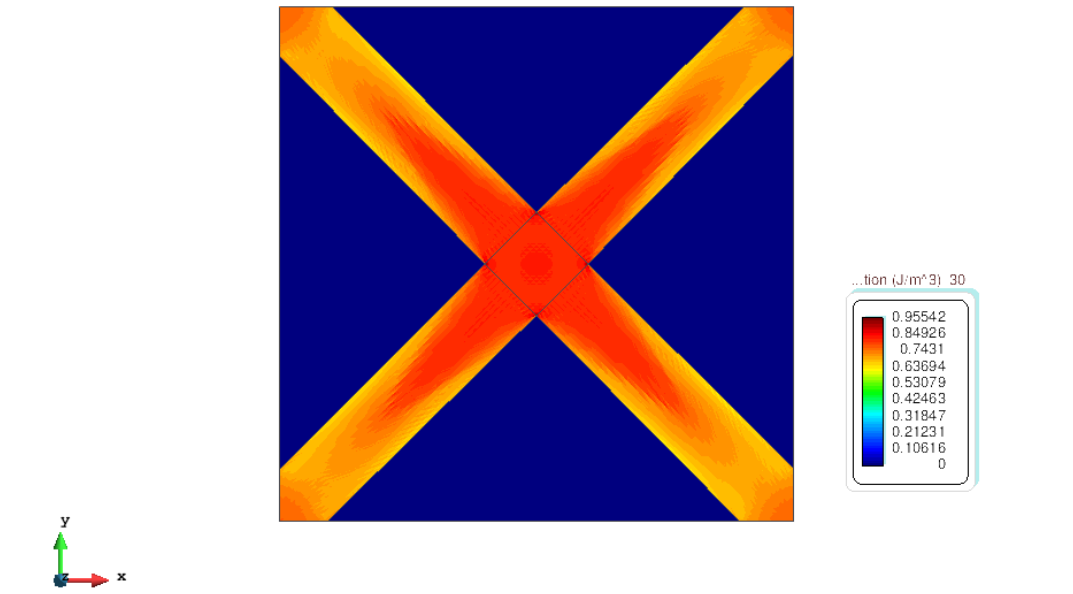

Figure 6.2.2.26 Damage variable (d)

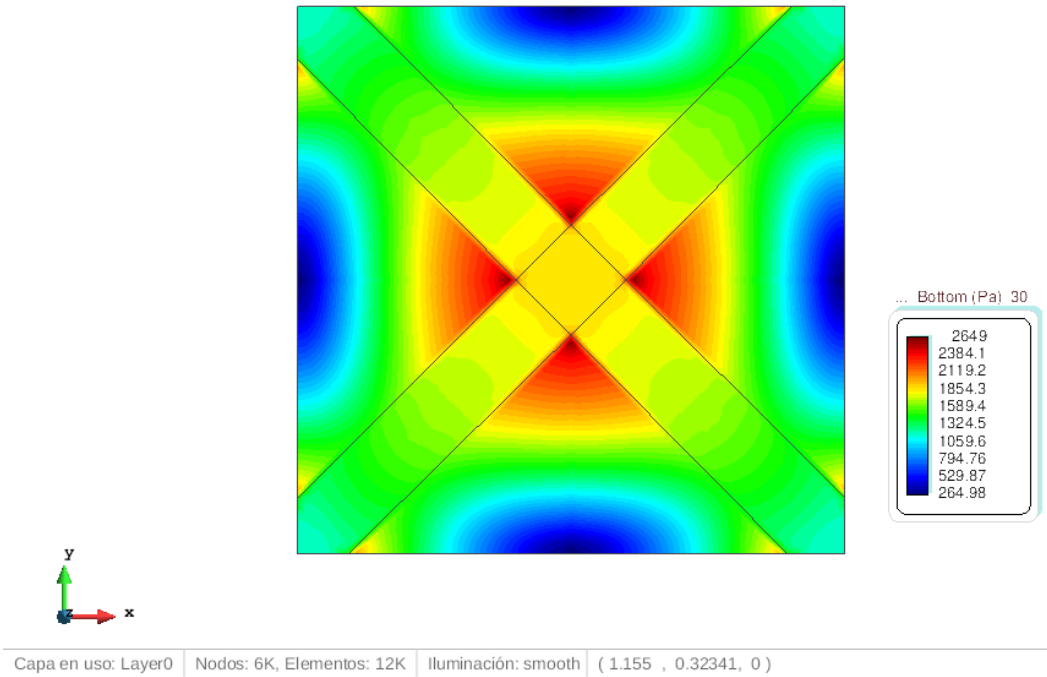

Figure 6.2.2.27 Stress bottom

It can be seen that in the first figure that the only zones with damage are zone 2 and 3 how we expected because zone 1 uses a linear model.

It can be observed that the difference between the models in the stress figure because the stress is clearly different between zones. This is because the zones use different constitutive models so, the stress behavior also will be different. This is not important because comparing this result of the non-linear zone with the results of the first validation in the same zone, there are the same. It happens the same in the damage plot.

Model 3: Zone 3 we are going to use damage model. In Zone 1 and Zone 2we use a linear elastic model.

Simulation type	Structural analysis: Shell
Dimensions	Three dimensional
Analysis type	Incremental load analysis
Geometry	Lineal geometry
Solver	PARDISO
N of elments	12064
Computational time	2.4 min

In this last computational model, we have done the approximation of set only the zone 3 with damage. Therefore, the computational cost and the computational time are smaller than the other cases.

This type of approximation can be useful when the objective is to know the maximum damage of the structure. It is not important to calculate the rest of the shell so; the cost will be less.

Load (L)	1000 N
Percentage (%)	$1.4 \cdot 10^{-3}$
Increments (n)	16
Final load applied$(\boldsymbol{L} \cdot \% \cdot \boldsymbol{n})$	22,4 N

For this validation, the number of increments is reduced and also the total load applied. There is not necessary to set too much increments because it is known that this zone of the structure will be the first zone to damage and also the first zone to failure. As the validation 2, this model has been made taking into account the calibration model, from there the values where the center starts to damage can be obtained.

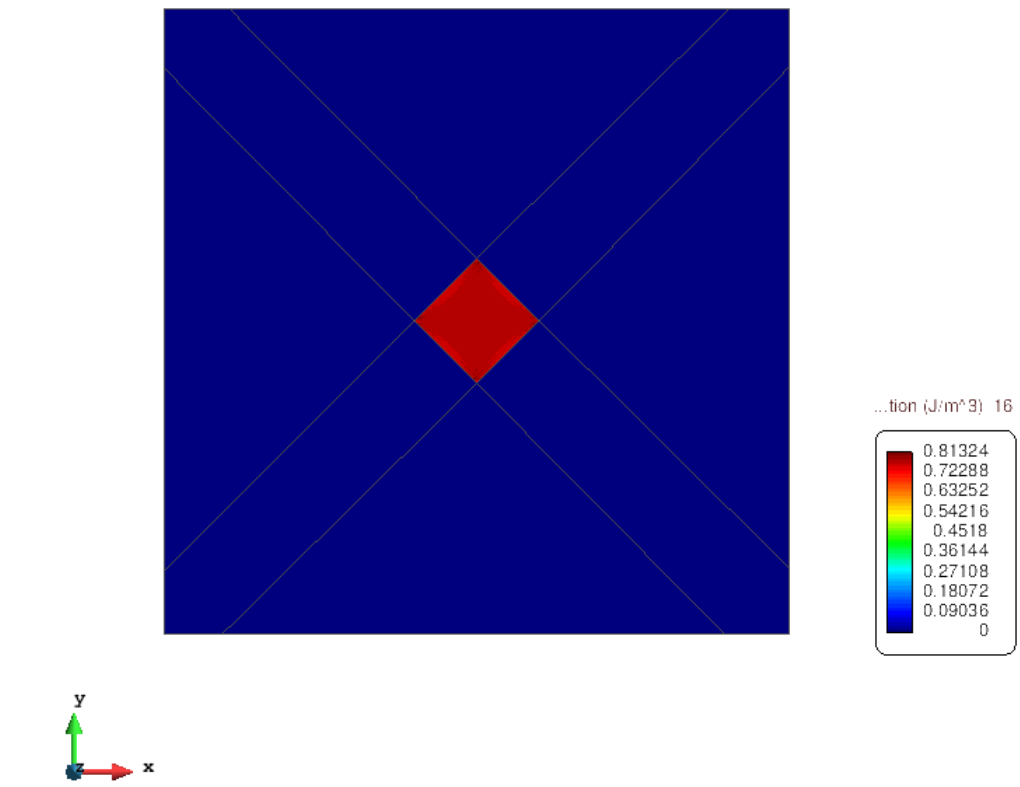

Figure 6.2.2.27 Damage variable

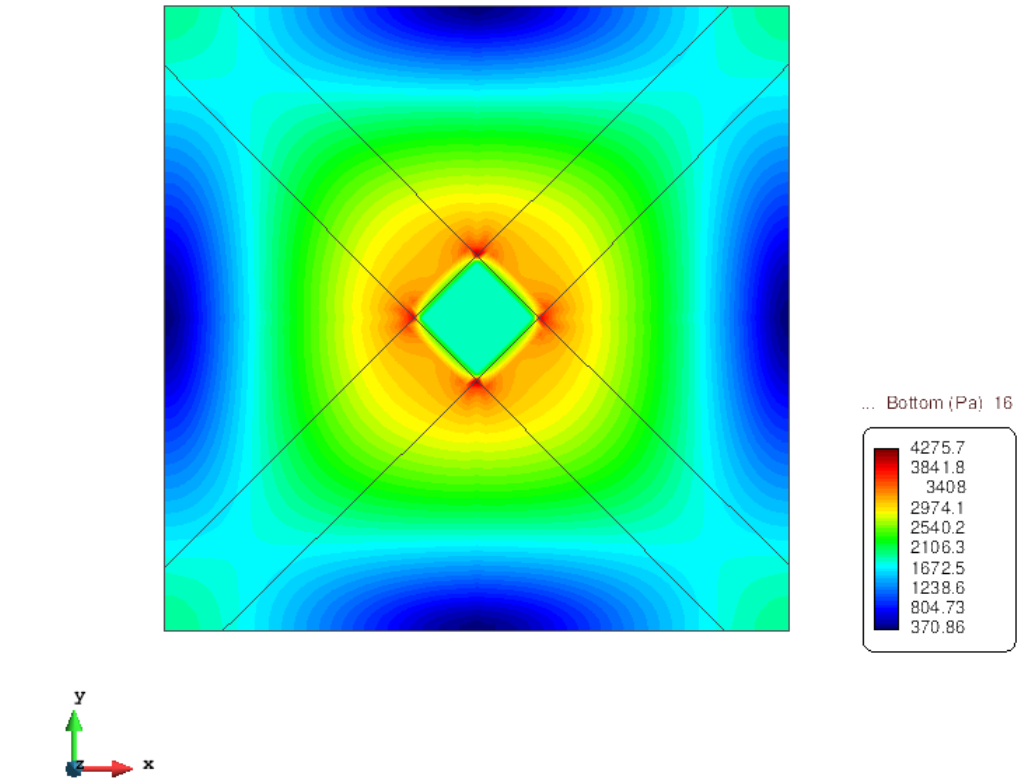

Figure 6.2.2.28 Stress bottom

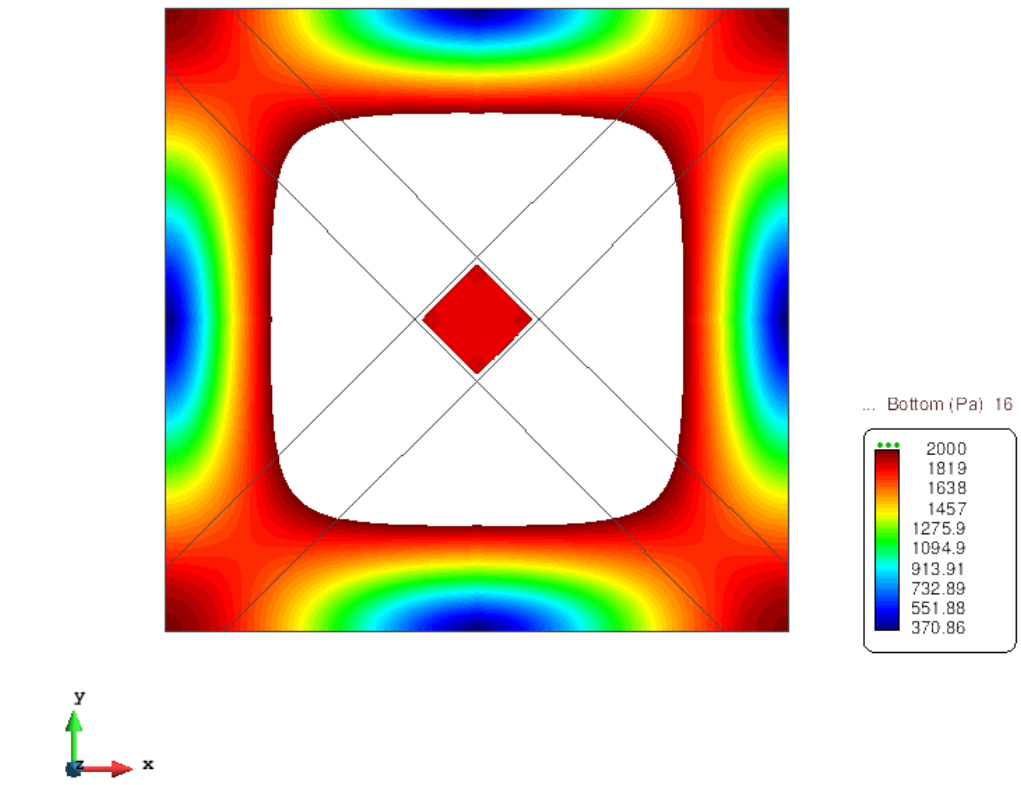

Figure 6.2.2.29 Stress bottom with limits

Conclusions validation models

As I said before, it is important to choose the validation model in function the objective wanted. For example, if the objective is to know the maximum damage of a structure due to a load and the zone this will happen is known, the 3 models can be used in order to obtain less computational cost.

However, it is important to take into account that model 1 can suffer problems because of the complexity of the constitutive model.

There are different points to comment:

1. Complexity of the model

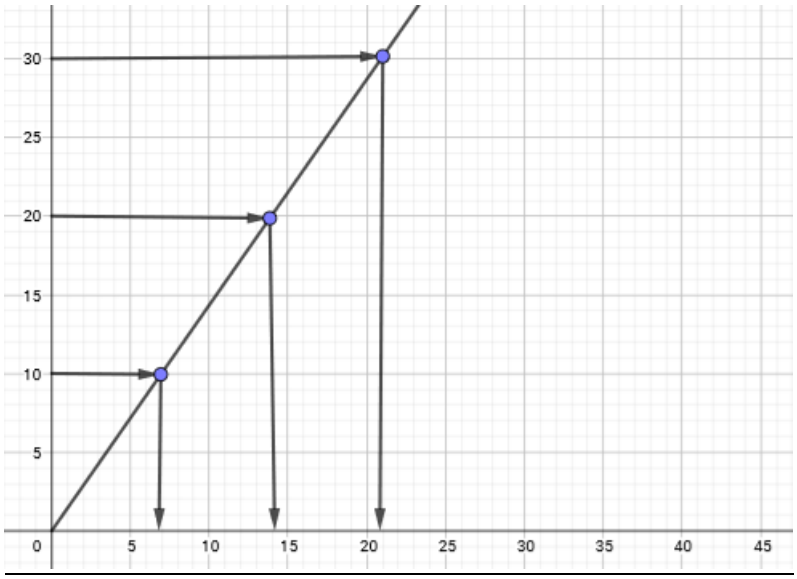

Working with a lineal model and applying a load a displacement response will be always obtained, but when working in a damage model, not all loads will have a displacement response, so is unable to obtain a solution. This is the reason why is important to apply lineal models to the zones that have been proved that will not damage because when one element with a damage model applied won't can obtain a solution, it will "send" it to an elastic element.

For example, as it is shown in previous figures, the first to loads will have response with the blue one not.

2. Pending change
   Problems in damage models will be created in the zone where changes from elasticity to plasticity take place. Sudden changes of pending are not good to numerical methods that works with derivates.
3. Last increments before damage
   When an advanced damage is affecting the stresses and the momentums begin to delocalize as a result of the damaged zones that cannot support the load. They search less damaged elements to accomplish the equations. Remember that when a structure is damaged, his stiffness is smaller.
4. Range of load
   In a damage study, if a bigger load than the resistance is applied to the material a total damage of the structure will be achieved before the total load is applied. Due to this, the convergence of the increments where all the elements of the structure are damaged will be bigger. In consequence, the same results will be obtained but with more time of computation and more computational cost. This is the reason why the first study is made.

6.3. Serial Parallel RoM cases

6.3.1. Verification

In order to validate de Rule of Mixtures and the Serial-Parallel Rule of Mixtures, we are going to compare the same tests to a Homogeneous material. Note that the tables are exactly the same as in damage verification.

Also, the geometries and characteristics of the problems are the same.

Also, comparing this verification for each element (CLL,DKT,Drill,Hexahedra,Tetrahedra) with the objective of checking the correct behaviour for all of them..

There are two important remarks to take into account before moving to the results:

- Note that the results of the Heterogeneous material are the same.
- There is a difference between the SP-RoM and the others. The SP-RoM lose convergence when a lineal law with softening is selected.

Exponential evolution law

Norm 1

Softening:

Element	%	Increments	σ_y	H	G_f	σ_{sat}	n
CLL	0.01	500	1.43	0	0.08	0	1
DKT+DR	0.01	500	1.43	0	0.1	0	1
DKT	0.01	500	1.43	0	0.1	0	1
Hexahedra	0.01	500	1.43	0	0.1	0	1
Tetrahedra	0.01	500	1.43	0	0.1	0	1

Table 1 Properties for Traction-Compression with Softening

Hardening:

Element	%	Increments	σ_y	H	G_f	σ_{sat}	n
CLL	0.01	500	1.43	0	0.08	2.86	1
DKT+DR	0.01	500	1.43	0	0.1	2.86	1
DKT	0.01	500	1.43	0	0.1	2.86	1
Hexahedra	0.01	500	1.43	0	0.1	2.86	1
Tetrahedra	0.01	500	1.43	0	0.1	2.86	1

Table 1 Properties for Traction-Compression with Hardening

Quadrilateral element

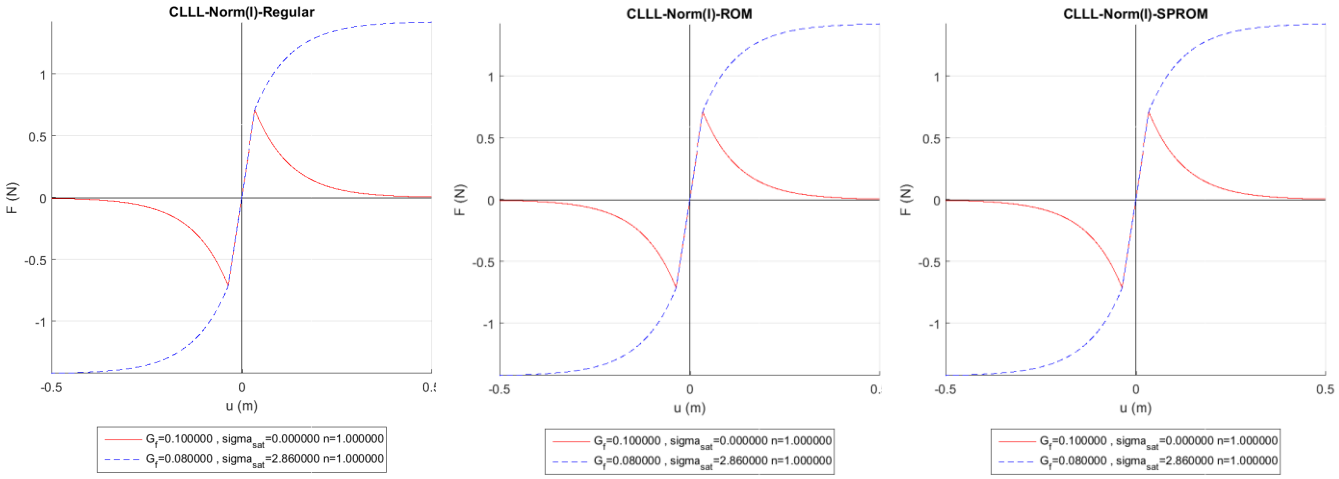

Figure 6.3.1.1 Force-displacement plot of a Traction-Compresion with Hardening-Softening

DKT element

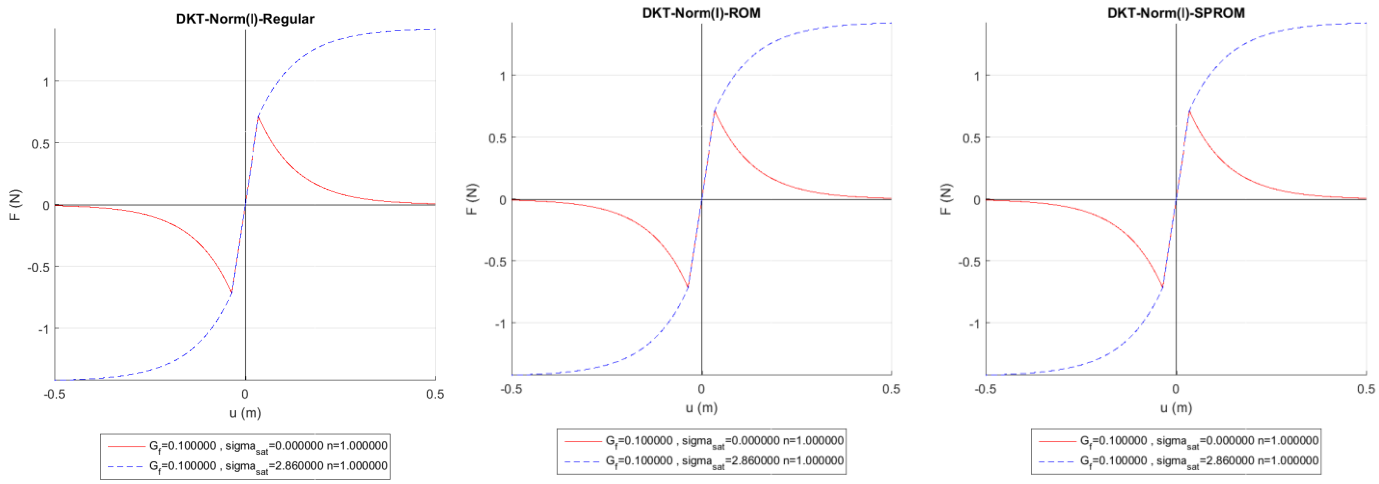

Figure 6.3.1.2 Force-displacement plot of a Traction-Compresion with Hardening-Softening

DKT+Drill Rotation element

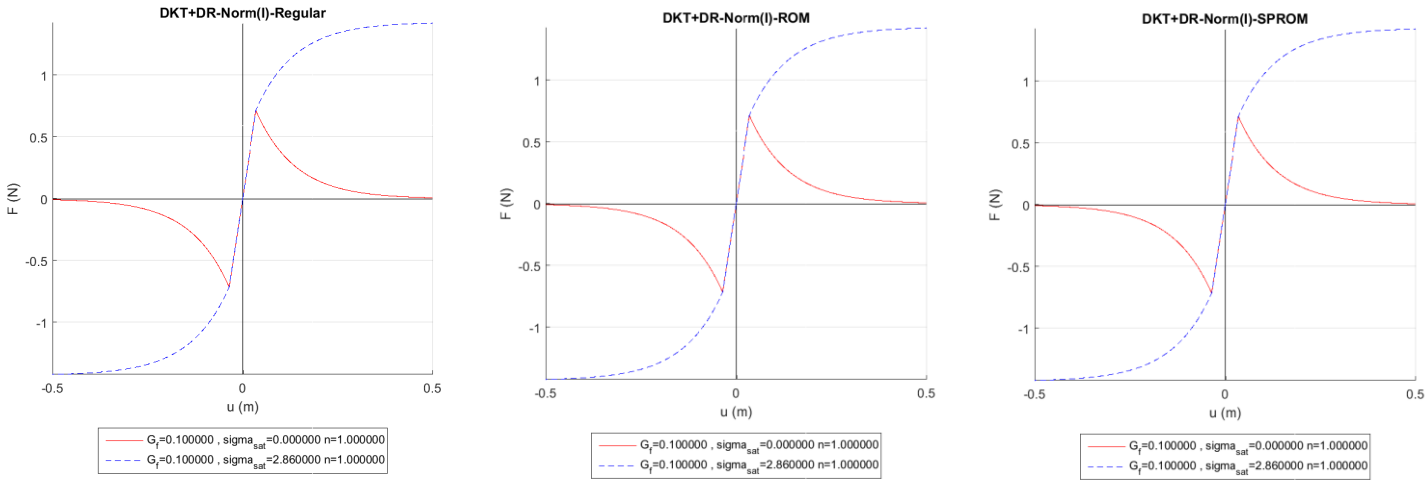

Figure 6.3.1.2 Force-displacement plot of a Traction-Compresion with Hardening-Softening

Hexahedral element

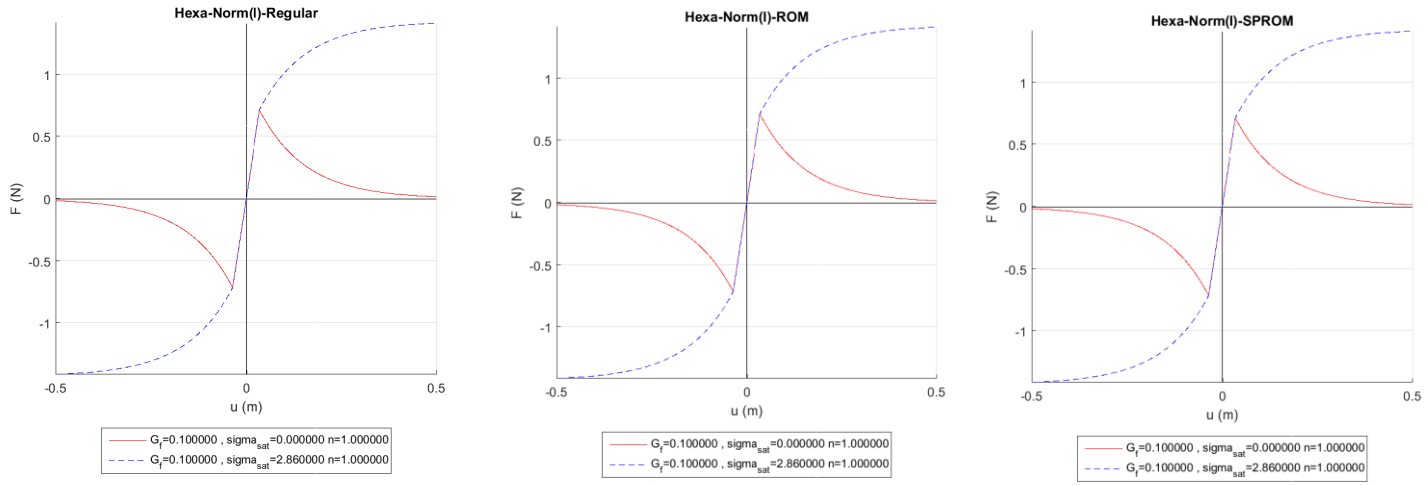

Figure 6.3.1.3 Force-displacement plot of a Traction-Compresion with Hardening-Softening

Tetrahedral element

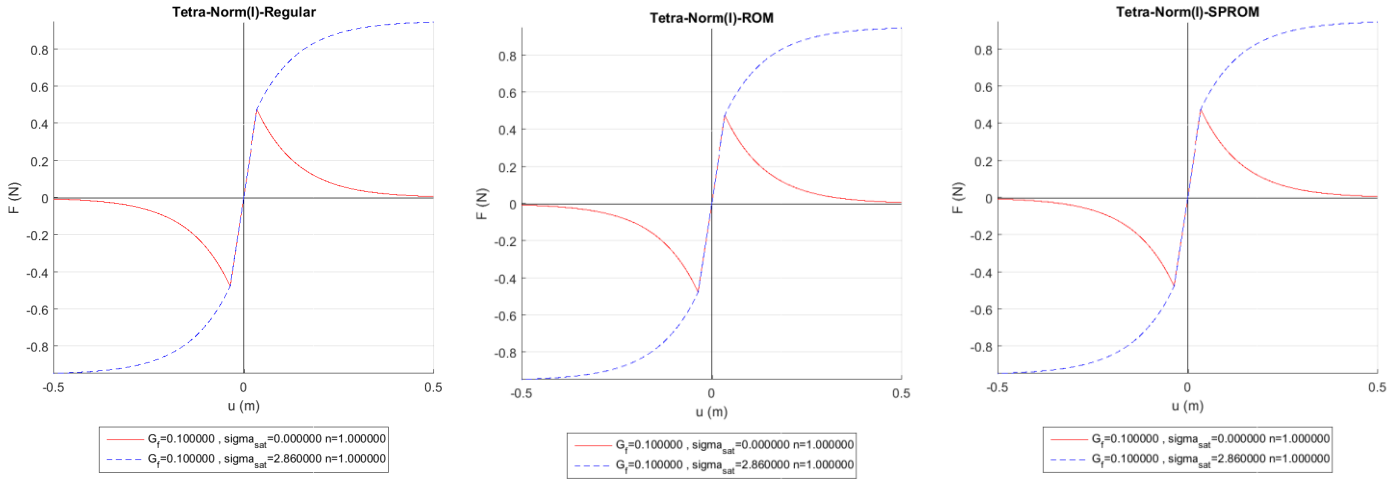

Figure 6.3.1.4 Force-displacement plot of a Traction-Compresion with Hardening-Softening

Norm 2

Softening:

Element	%	Increments	σ_y	H	G_f	σ_{sat}	n
CLL	0.01	500	1.43	0	0.08	0	1
DKT+DR	0.01	500	1.43	0	0.1	0	1
DKT	0.01	500	1.43	0	0.1	0	1
Hexahedra	0.01	500	1.43	0	0.1	0	1
Tetrahedra	0.01	500	1.43	0	0.1	0	1

Table 1 Properties for Traction-Compression with Softening

Hardening:

Element	%	Increments	σ_y	H	G_f	σ_{sat}	n
CLL	0.01	500	1.43	0	0.08	2.86	1
DKT+DR	0.01	500	1.43	0	0.1	2.86	1
DKT	0.01	500	1.43	0	0.1	2.86	1
Hexahedra	0.01	500	1.43	0	0.1	2.86	1
Tetrahedra	0.01	500	1.43	0	0.1	2.86	1

Table 1 Properties for Traction-Compression with Hardening

Quadrilateral element

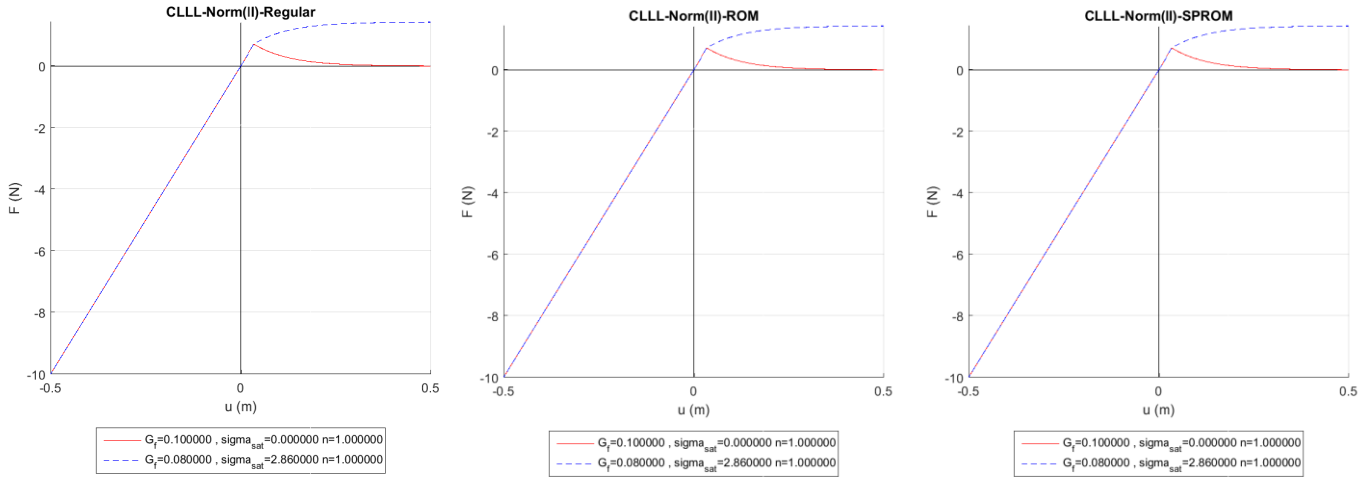

Figure 6.3.1.5 Force-displacement plot of a Traction-Compresion with Hardening-Softening

DKT element

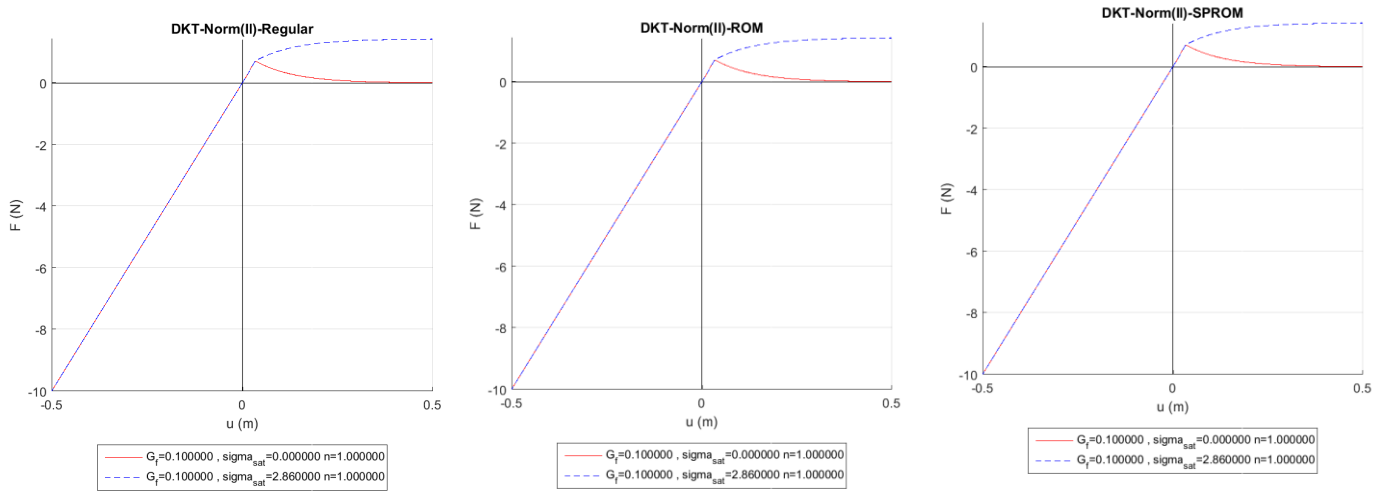

Figure 6.3.1.6 Force-displacement plot of a Traction-Compresion with Hardening-Softening

DKT + Drill Rotation element

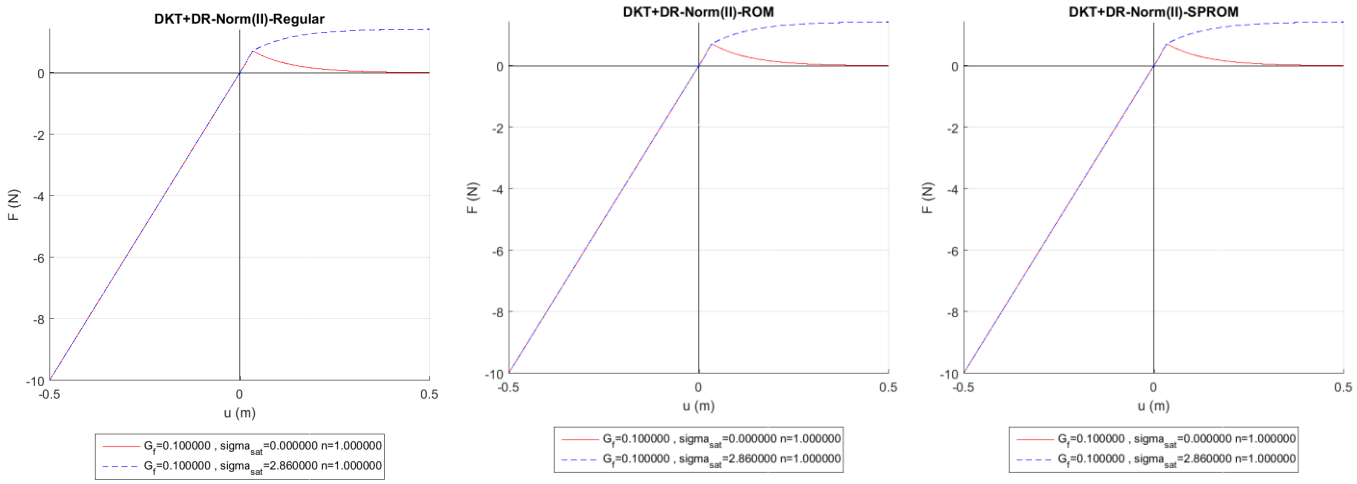

Figure 6.3.1.7 Force-displacement plot of a Traction-Compresion with Hardening-Softening

Hexahedral element

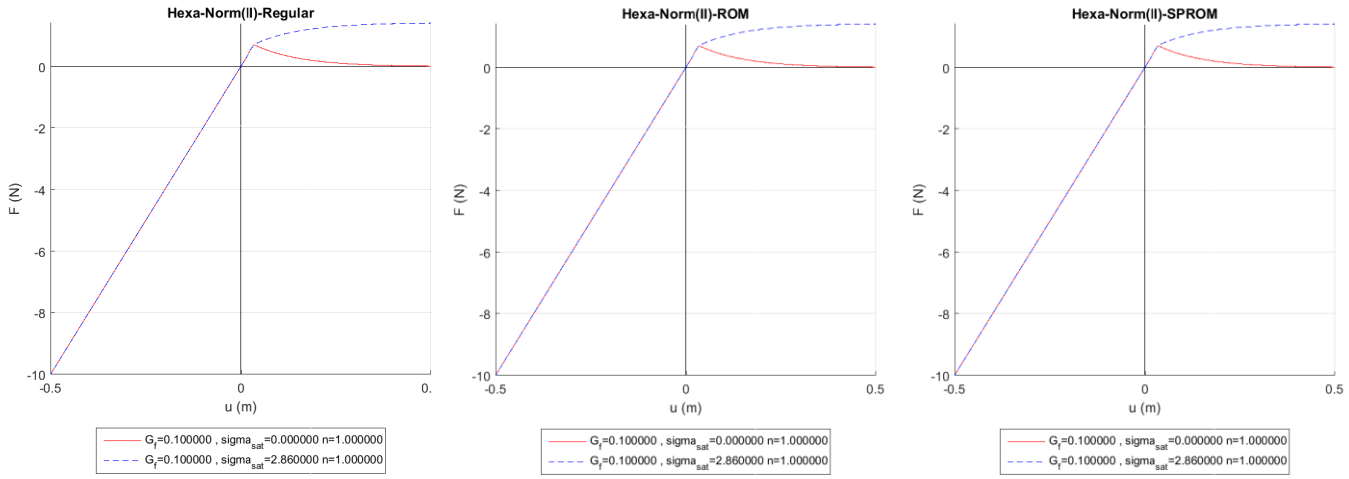

Figure 6.3.1.8 Force-displacement plot of a Traction-Compresion with Hardening-Softening

Tetrahedral element

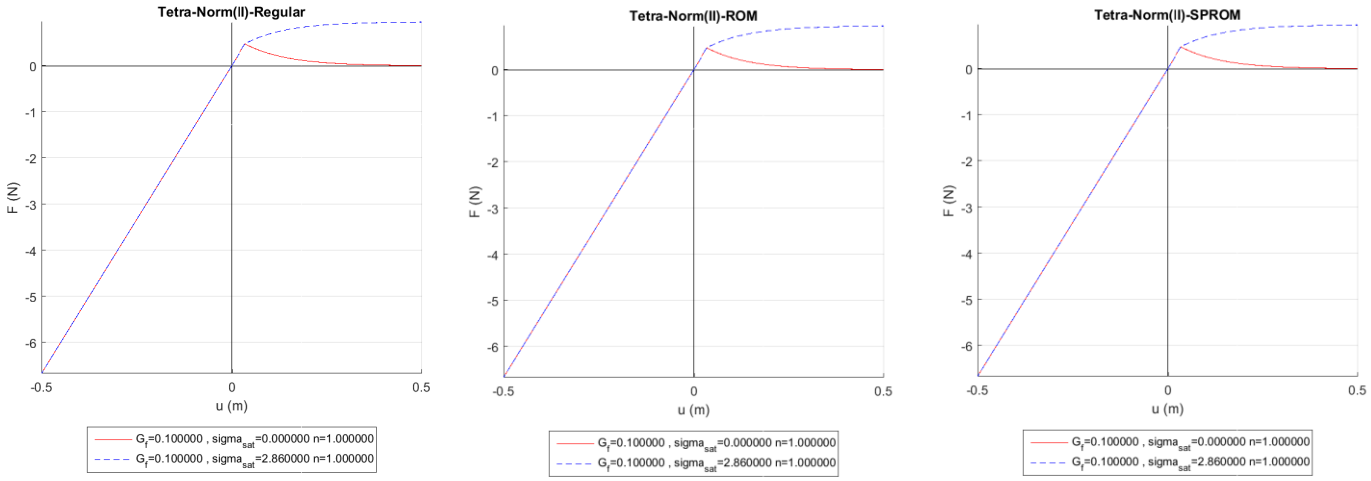

Figure 6.3.1.9 Force-displacement plot of a Traction-Compresion with Hardening-Softening

Norm 3

Softening:

Element	%	Increments	σ_y	H	G_f	σ_{sat}	n
CLL	0.01	500	1.43	0	0.08	0	3
DKT+DR	0.01	500	1.43	0	0.1	0	3
DKT	0.01	500	1.43	0	0.1	0	3
Hexahedra	0.01	500	1.43	0	0.1	0	3
Tetrahedra	0.01	500	1.43	0	0.1	0	3

Table 1 Properties for Traction-Compression with Softening

Hardening:

Element	%	Increments	σ_y	H	G_f	σ_{sat}	n
CLL	0.01	500	1.43	0	0.08	2.86	3
DKT+DR	0.01	500	1.43	0	0.1	2.86	3
DKT	0.01	500	1.43	0	0.1	2.86	3
Hexahedra	0.01	500	1.43	0	0.1	2.86	3
Tetrahedra	0.01	500	1.43	0	0.1	2.86	3

Table 1 Properties for Traction-Compression with Hardening

Quadrilateral element

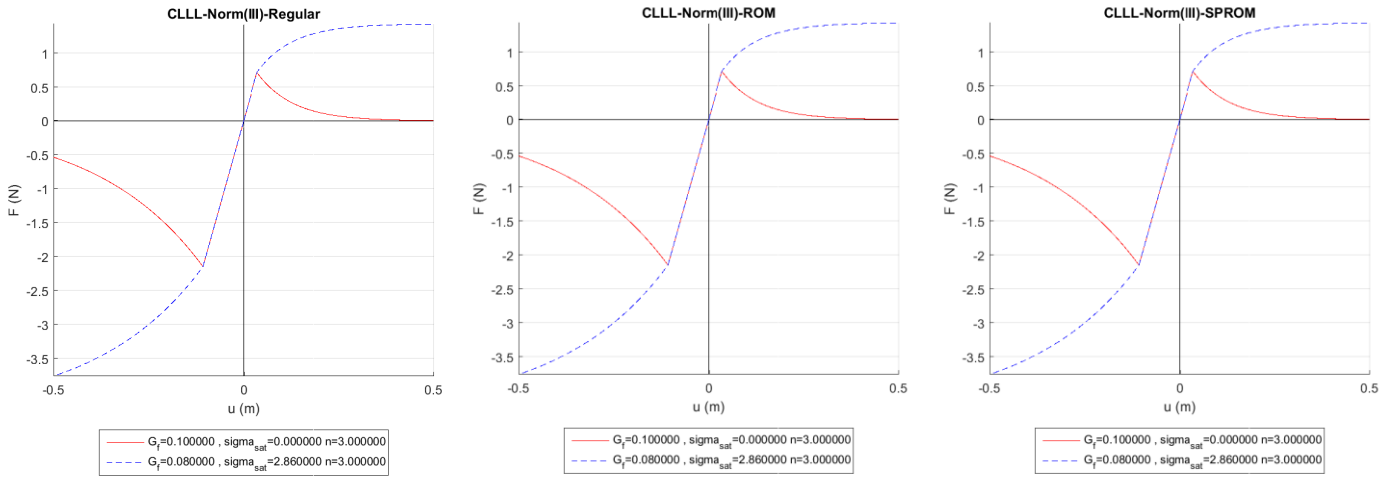

Figure 6.3.1.10 Force-displacement plot of a Traction-Compresion with Hardening-Softening

DKT element

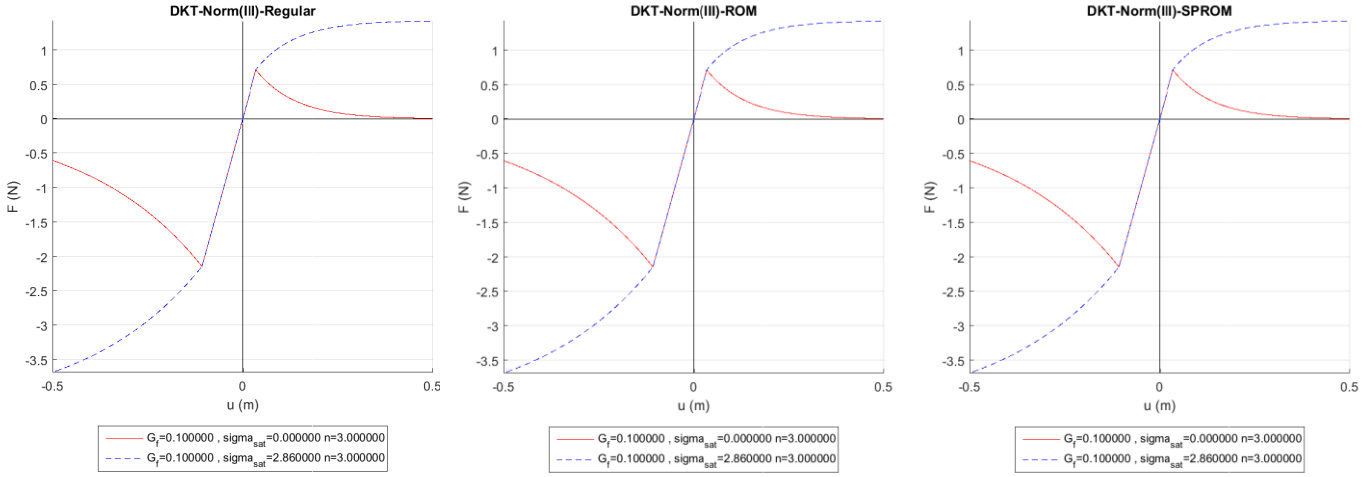

Figure 6.3.1.11 Force-displacement plot of a Traction-Compresion with Hardening-Softening

DKT+ Drill Rotation element

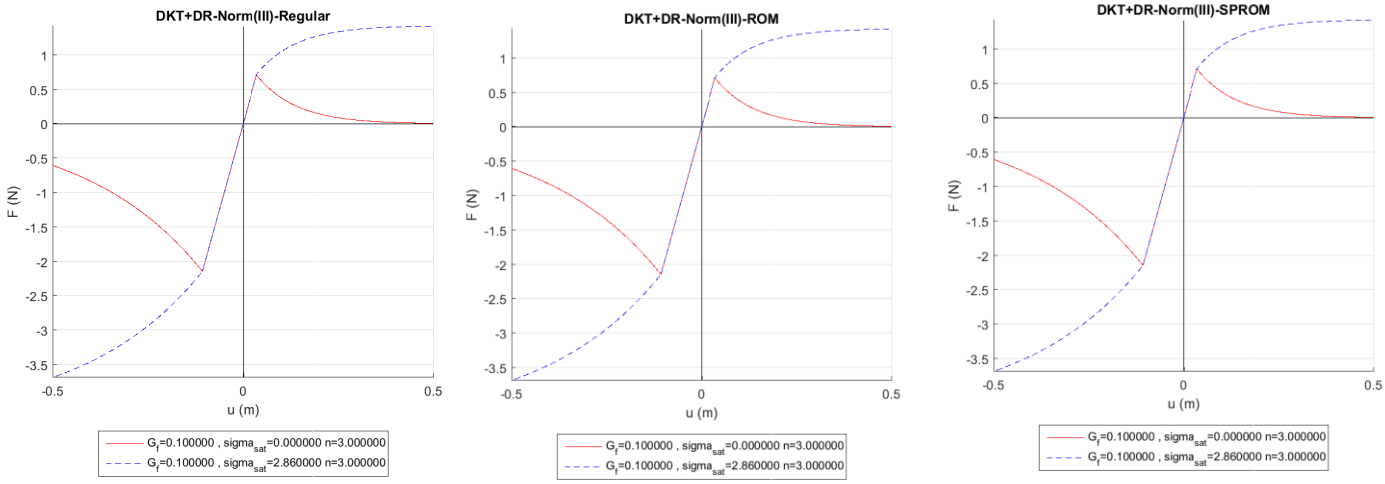

Figure 6.3.1.12 Force-displacement plot of a Traction-Compresion with Hardening-Softening

Hexahedral element

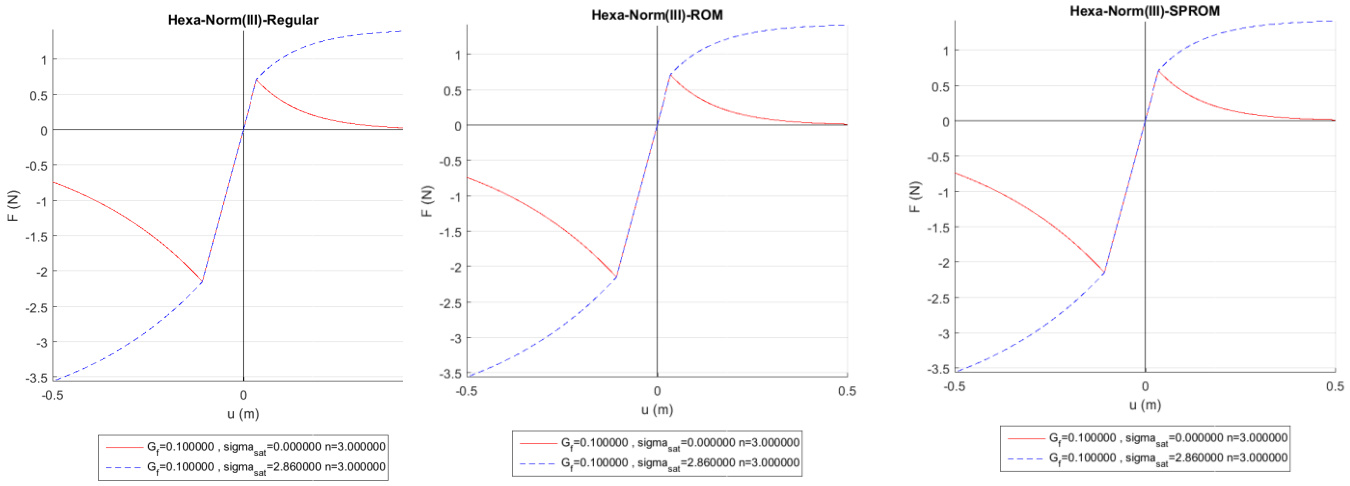

Figure 6.3.1.13 Force-displacement plot of a Traction-Compresion with Hardening-Softening

Tetrahedral element

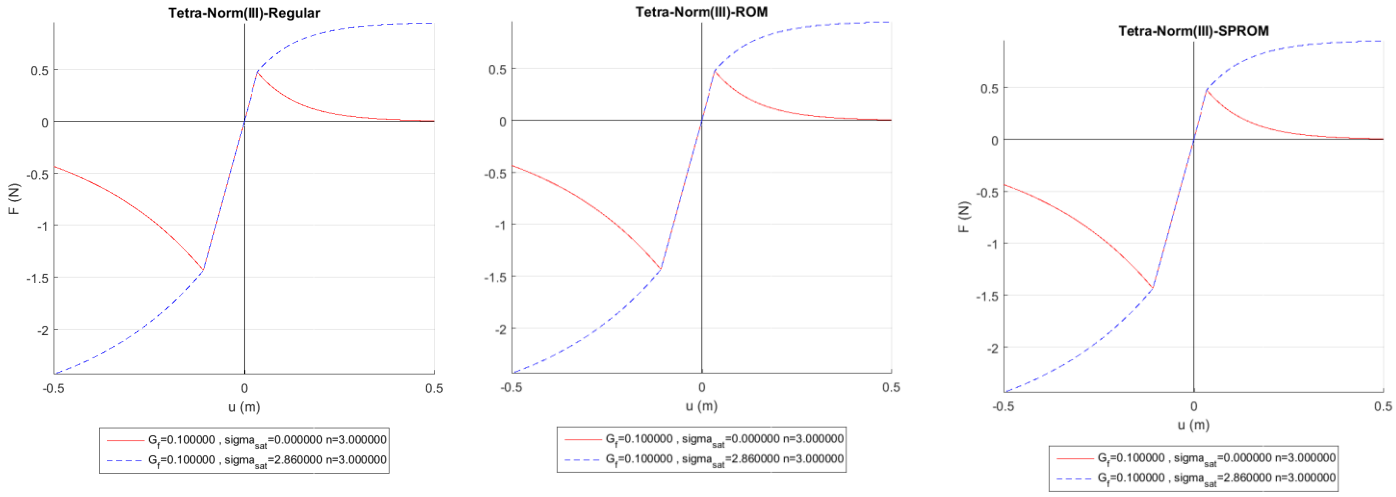

Figure 6.3.1.14 Force-displacement plot of a Traction-Compresion with Hardening-Softening

Lineal evolution law

Norm 1

Softening:

Element	%	Increments	σ_y	H	G_f	σ_{sat}	n
CLL	0.01	500	1.43	-0.1	0	0	1
DKT+DR	0.01	500	1.43	-0.1	0	0	1
DKT	0.01	500	1.43	-0.1	0	0	1
Hexahedra	0.01	500	1.43	-0.1	0	0	1
Tetrahedra	0.01	500	1.43	-0.1	0	0	1

Table 1 Properties for Traction-Compression with Softening

Hardening:

Element	%	Increments	σ_y	H	G_f	σ_{sat}	n
CLL	0.01	500	1.43	0.1	0	0	1
DKT+DR	0.01	500	1.43	0.1	0	0	1
DKT	0.01	500	1.43	0.1	0	0	1
Hexahedra	0.01	500	1.43	0.1	0	0	1
Tetrahedra	0.01	500	1.43	0.1	0	0	1

Table 1 Properties for Traction-Compression with Hardening

Quadrilateral element

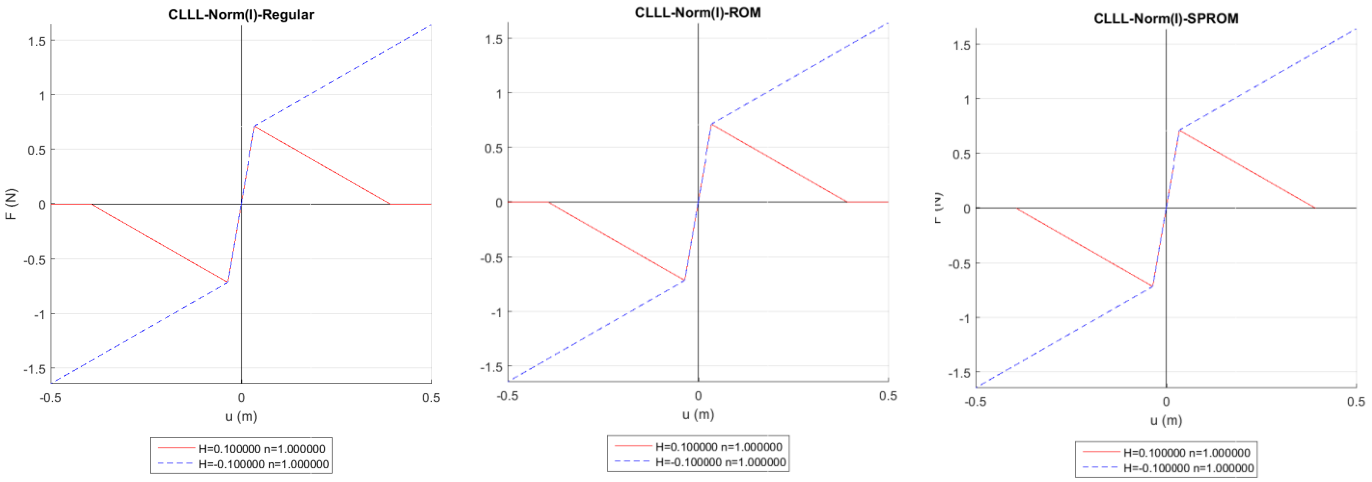

Figure 6.3.1.15 Force-displacement plot of a Traction-Compresion with Hardening-Softening

DKT element

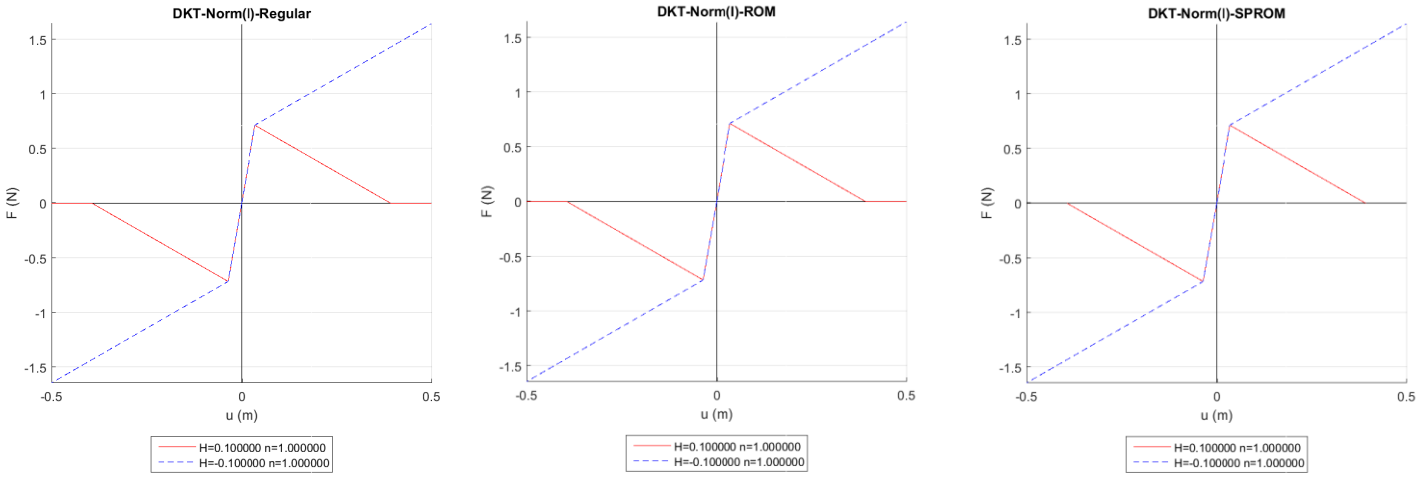

Figure 6.3.1.16 Force-displacement plot of a Traction-Compresion with Hardening-Softening

DKT+Drill Rotation element

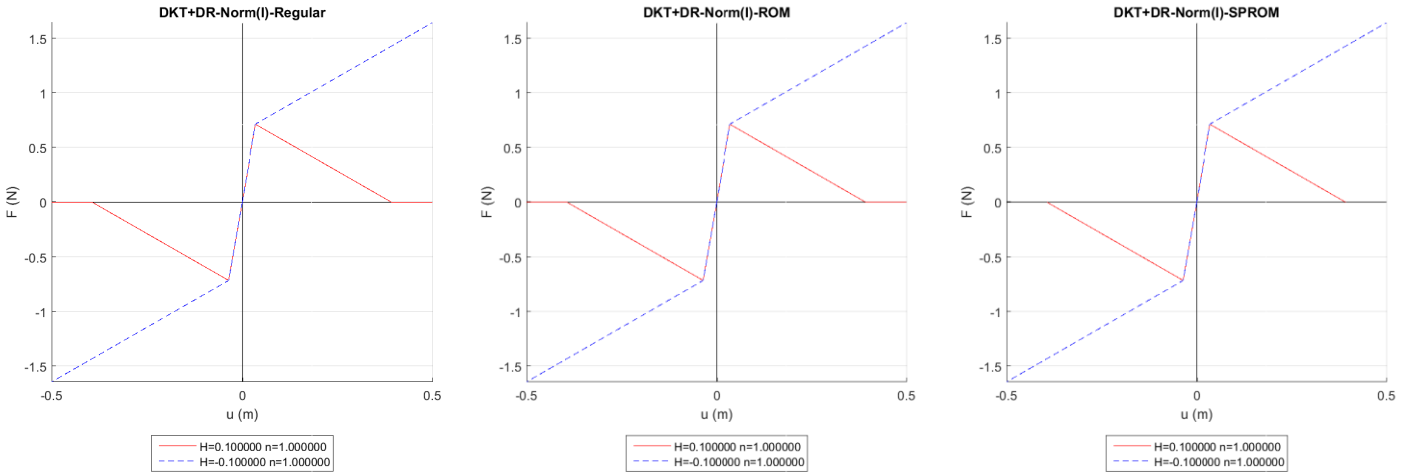

Figure 6.3.1.17 Force-displacement plot of a Traction-Compresion with Hardening-Softening

Hexahedral element

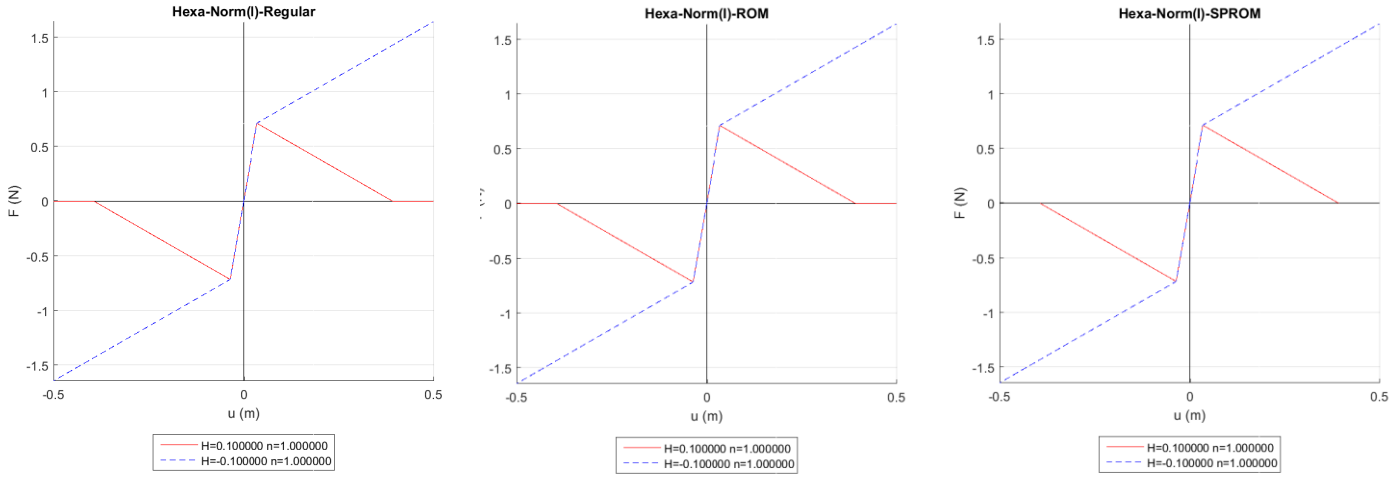

Figure 6.3.1.18 Force-displacement plot of a Traction-Compresion with Hardening-Softening

Tetrahedral element

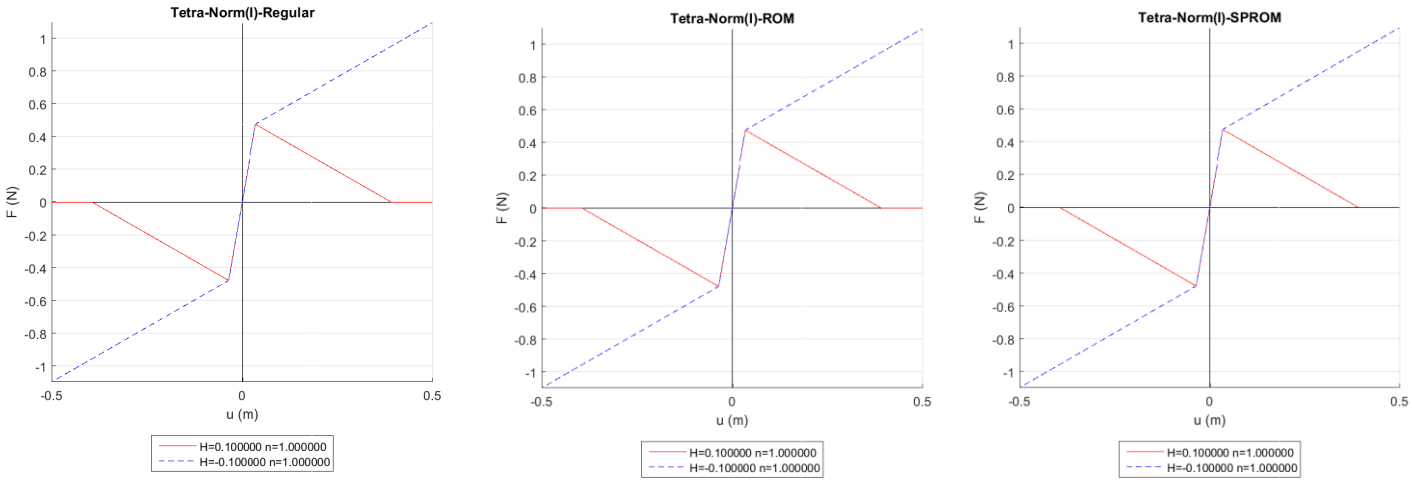

Figure 6.3.1.19 Force-displacement plot of a Traction-Compresion with Hardening-Softening

Norm 2

Softening:

Element	%	Increments	σ_y	H	G_f	σ_{sat}	n
CLL	0.01	500	1.43	-0.1	0	0	1
DKT+DR	0.01	500	1.43	-0.1	0	0	1
DKT	0.01	500	1.43	-0.1	0	0	1
Hexahedra	0.01	500	1.43	-0.1	0	0	1
Tetrahedra	0.01	500	1.43	-0.1	0	0	1

Table 1 Properties for Traction-Compression with Softening

Hardening:

Element	%	Increments	σ_y	H	G_f	σ_{sat}	n
CLL	0.01	500	1.43	0.1	0	0	1
DKT+DR	0.01	500	1.43	0.1	0	0	1
DKT	0.01	500	1.43	0.1	0	0	1
Hexahedra	0.01	500	1.43	0.1	0	0	1
Tetrahedra	0.01	500	1.43	0.1	0	0	1

Table 1 Properties for Traction-Compression with Hardening

Quadrilateral element

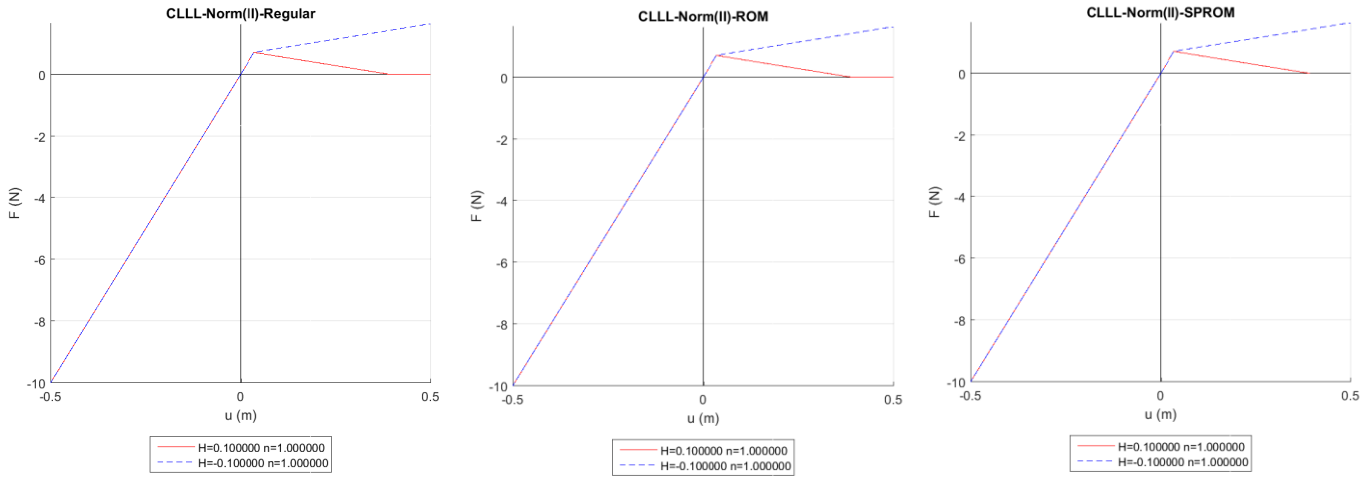

Figure 6.3.1.20 Force-displacement plot of a Traction-Compresion with Hardening-Softening

DKT element

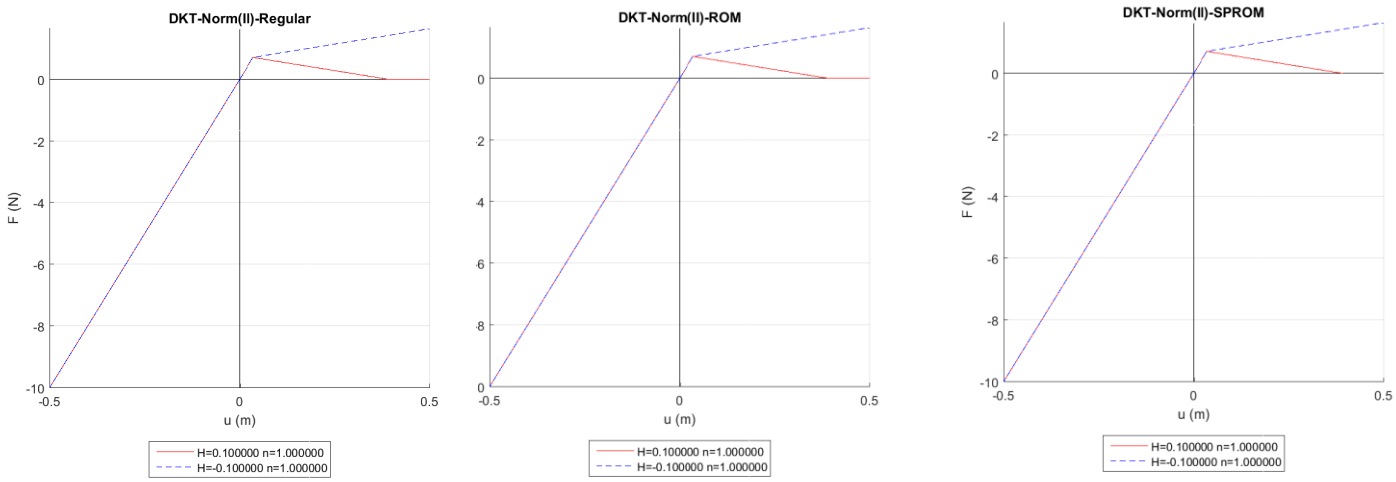

Figure 6.3.1.21 Force-displacement plot of a Traction-Compresion with Hardening-Softening

DKT+Drill Rotation element

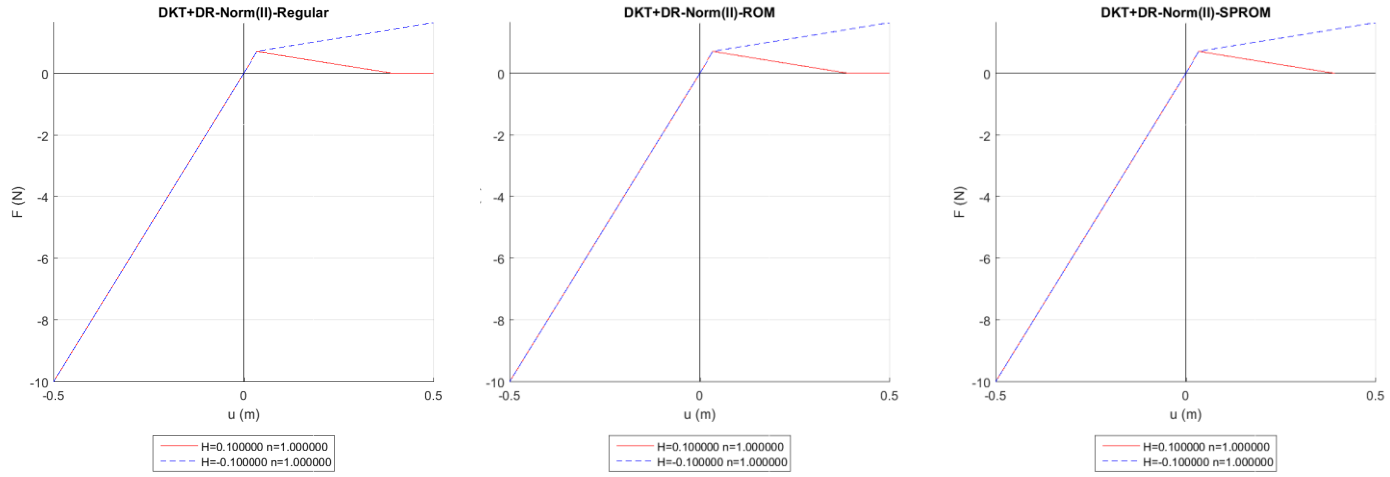

Figure 6.3.1.22 Force-displacement plot of a Traction-Compresion with Hardening-Softening

Hexahedral element

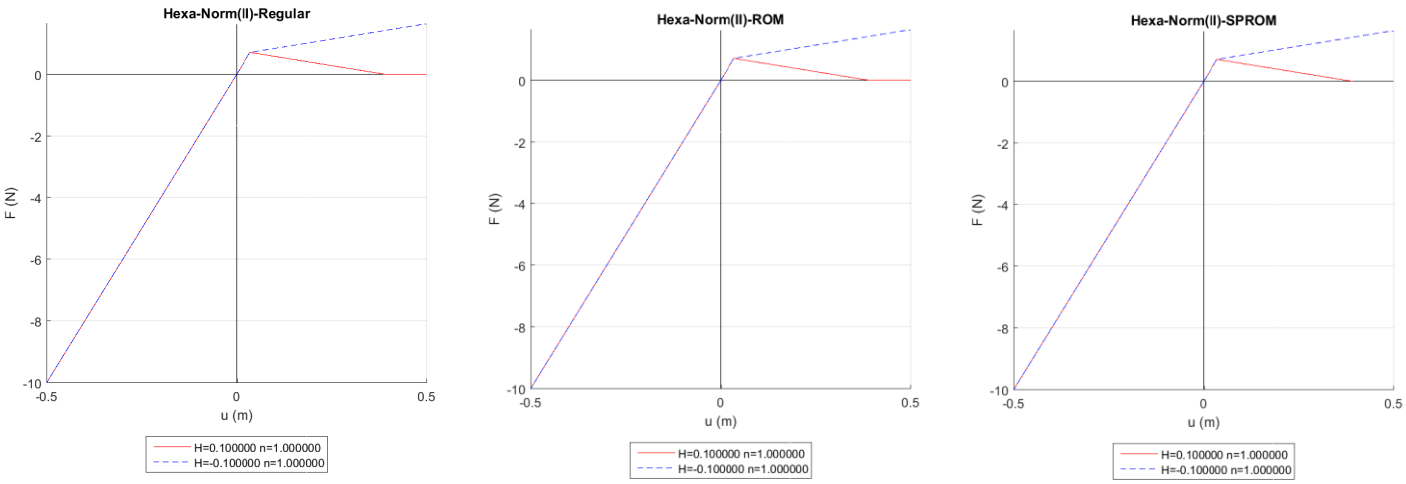

Figure 6.3.1.23 Force-displacement plot of a Traction-Compresion with Hardening-Softening

Tetrahedral element

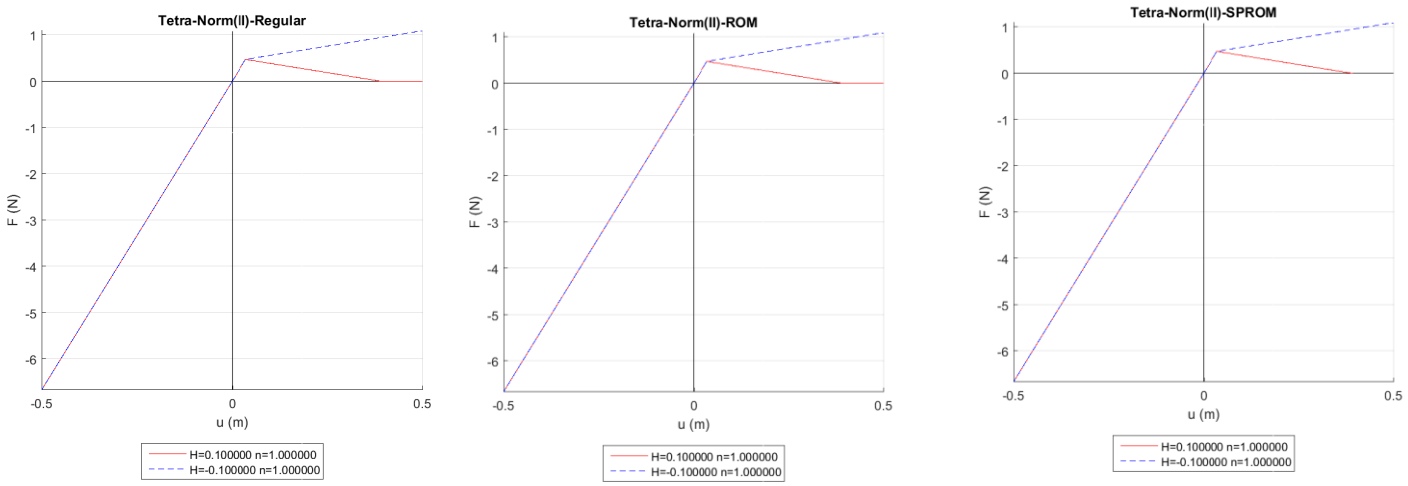

Figure 6.3.1.24 Force-displacement plot of a Traction-Compresion with Hardening-Softening

Norm 3

Softening:

Element	%	Increments	σ_y	H	G_f	σ_{sat}	n
CLL	0.01	500	1.43	-0.1	0	0	3
DKT+DR	0.01	500	1.43	-0.1	0	0	3
DKT	0.01	500	1.43	-0.1	0	0	3
Hexahedra	0.01	500	1.43	-0.1	0	0	3
Tetrahedra	0.01	500	1.43	-0.1	0	0	3

Table 1 Properties for Traction-Compression with Hardening

Hardening:

Element	%	Increments	σ_y	H	G_f	σ_{sat}	n
CLL	0.01	500	1.43	0.1	0	0	3
DKT+DR	0.01	500	1.43	0.1	0	0	3
DKT	0.01	500	1.43	0.1	0	0	3
Hexahedra	0.01	500	1.43	0.1	0	0	3
Tetrahedra	0.01	500	1.43	0.1	0	0	3

Table 1 Properties for Traction-Compression with Hardening

Quadrilateral element

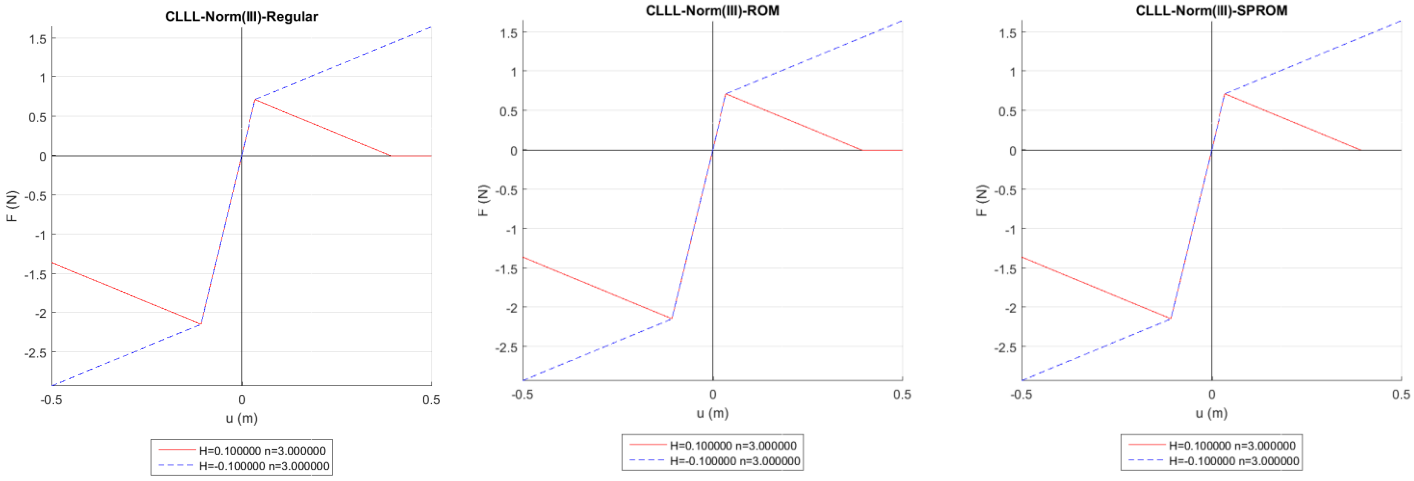

Figure 6.3.1.25 Force-displacement plot of a Traction-Compresion with Hardening-Softening

DKT element

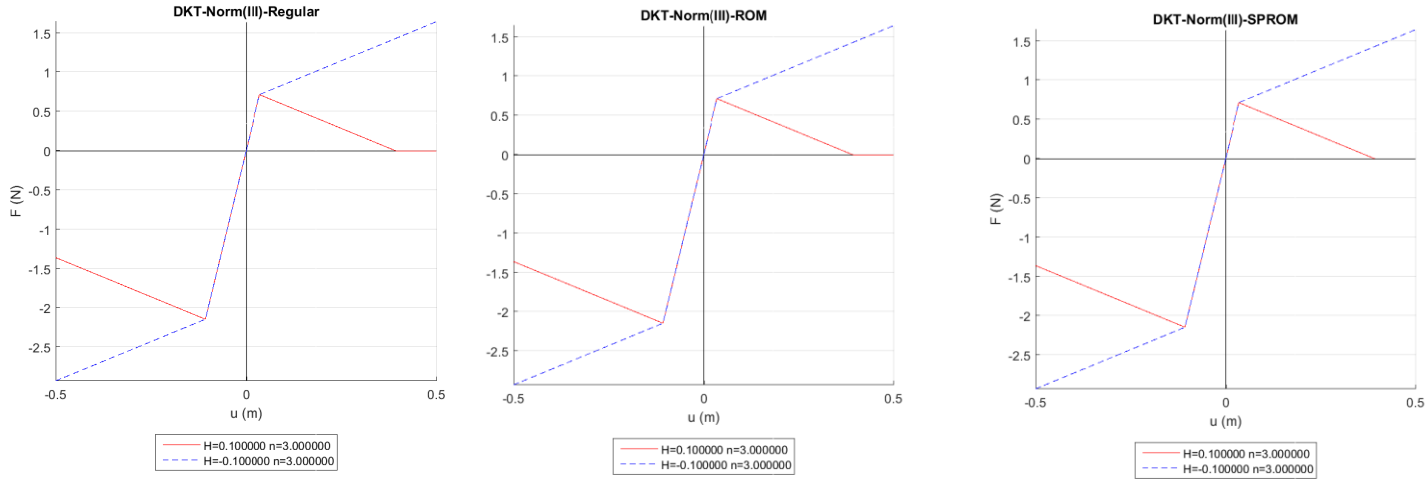

Figure 6.3.1.26 Force-displacement plot of a Traction-Compresion with Hardening-Softening

DKT+Drill Rotation element

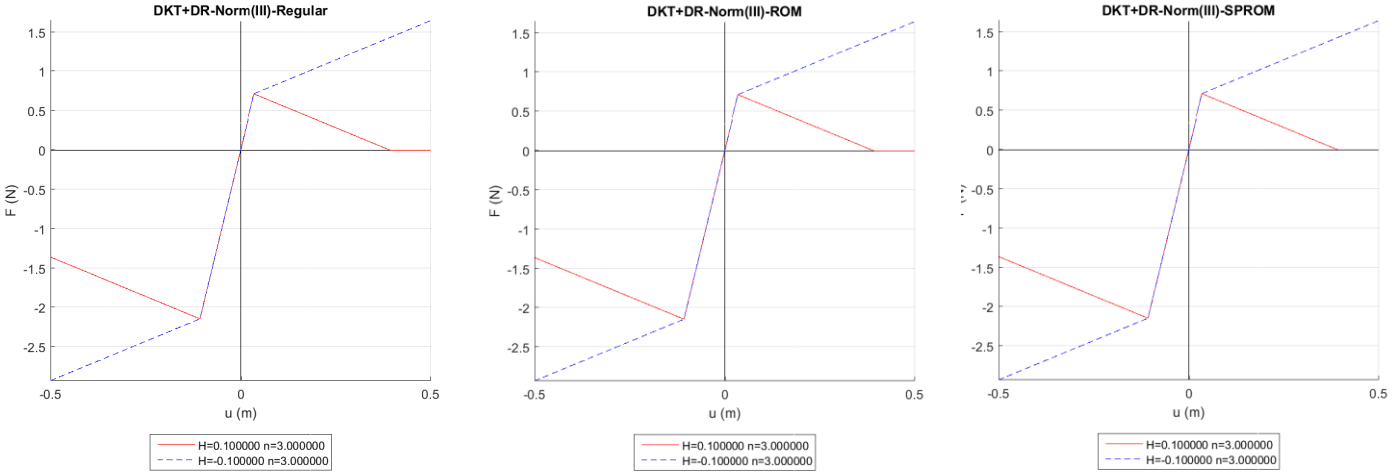

Figure 6.3.1.27 Force-displacement plot of a Traction-Compresion with Hardening-Softening

Hexahedral element

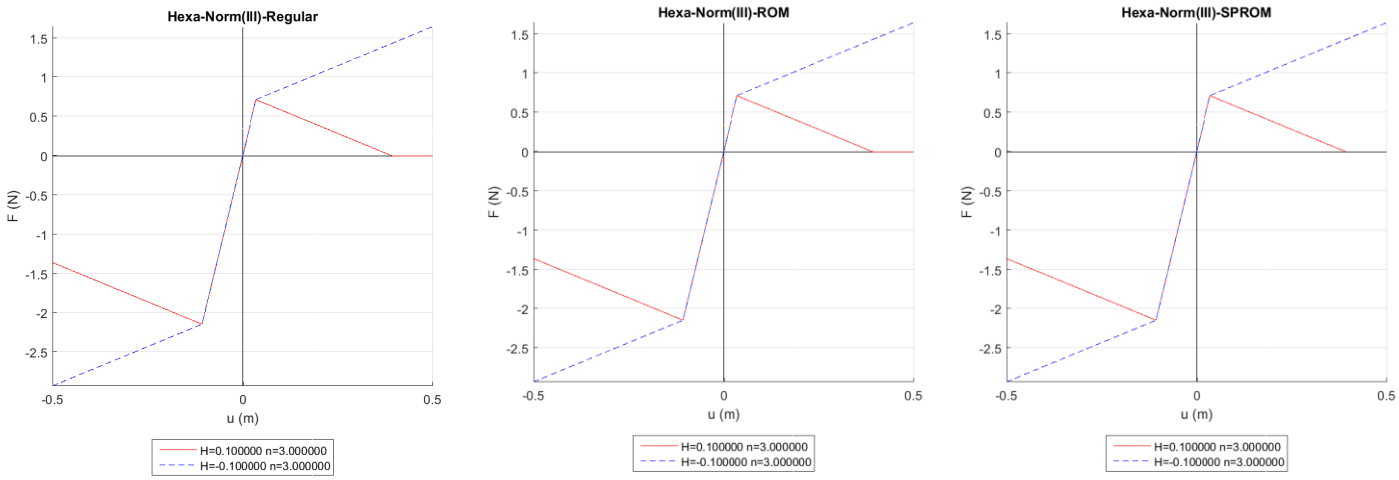

Figure 6.3.1.28 Force-displacement plot of a Traction-Compresion with Hardening-Softening

Tetrahedral element

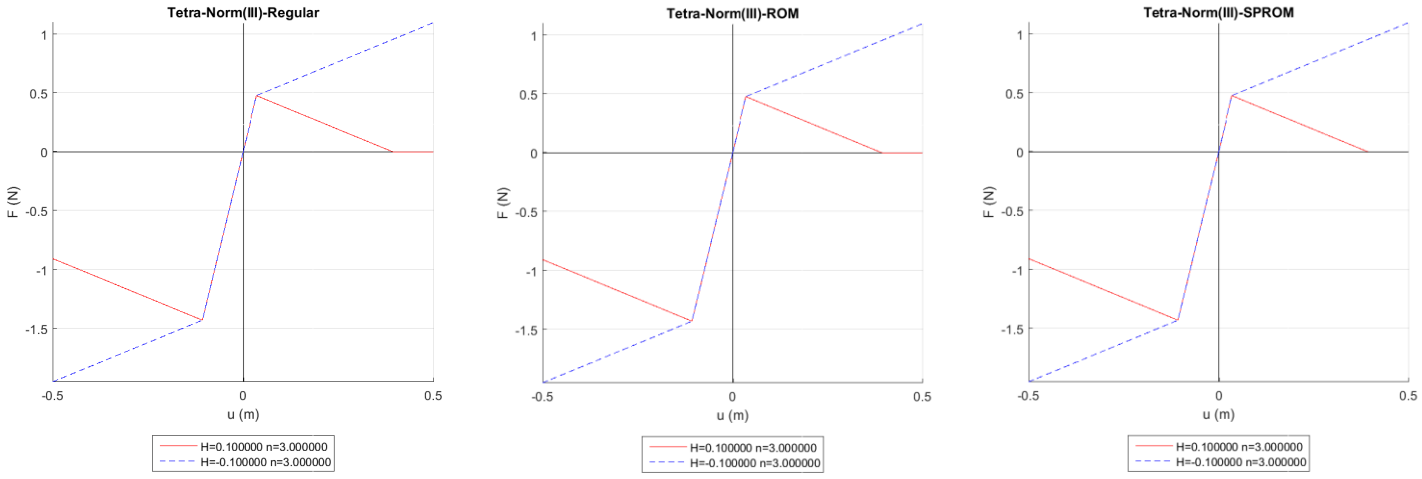

Figure 6.3.1.29 Force-displacement plot of a Traction-Compresion with Hardening-Softening

This work just already made different cases for SPROM and ROM to compare it with the used in damage verification. When the SPROM theory applied in a homogeneous material is used, the behavior must be the same, if it is well implemented in the software, as when we solve a homogeneous material with his constitutive model. Remember that the SPROM uses the constitutive relationship of each constituent separately and then applies the ROM i serial parallel conditions. In this case each part is the same material (fiber/matrix). So, the results have to be the same.

As it can be seen, these models are solved for all the different elements available in *Ramseries* to check the correct behavior with all of them.

Notice that all the plots have the same response in Regular (Damage), ROM (Rule of Mixtures + Damage) and SPROM (SPROM + Damage). This means that the SPROM is good implemented.

Although, there is an important difference between SPROM simulation and the others. When a linear evolution law with softening is set, the SPROM loss convergence respect the ROM and regular Damage. The SPROM is not able to succeed in the calculations for a completely damaged element $(d = 1)$. The reason is because the SPROM algorithm does an inversion of he local matrix and, as it is said in the theory, the constitutive tangent operator for a fully damaged element is 0 so, the algorithm cannot do the inversion of the matrix. Singular matrix is not invertible.

6.3.2. Validation

With the objective of validate the correct physical behaviour of the Serial Parallel Rule of Mixtures (SPROM) and also the Rule of Mixtures (ROM an experimental case will be reproduced. As you will see, there are different solutions for the same experimental case. It is well known that two experiments don't make two same solutions.

The process to obtain the experimental solution with the Serial Parallel Rule of Mixtures theory is the next:

1. First of all, obtain the experimental results of the studied case.

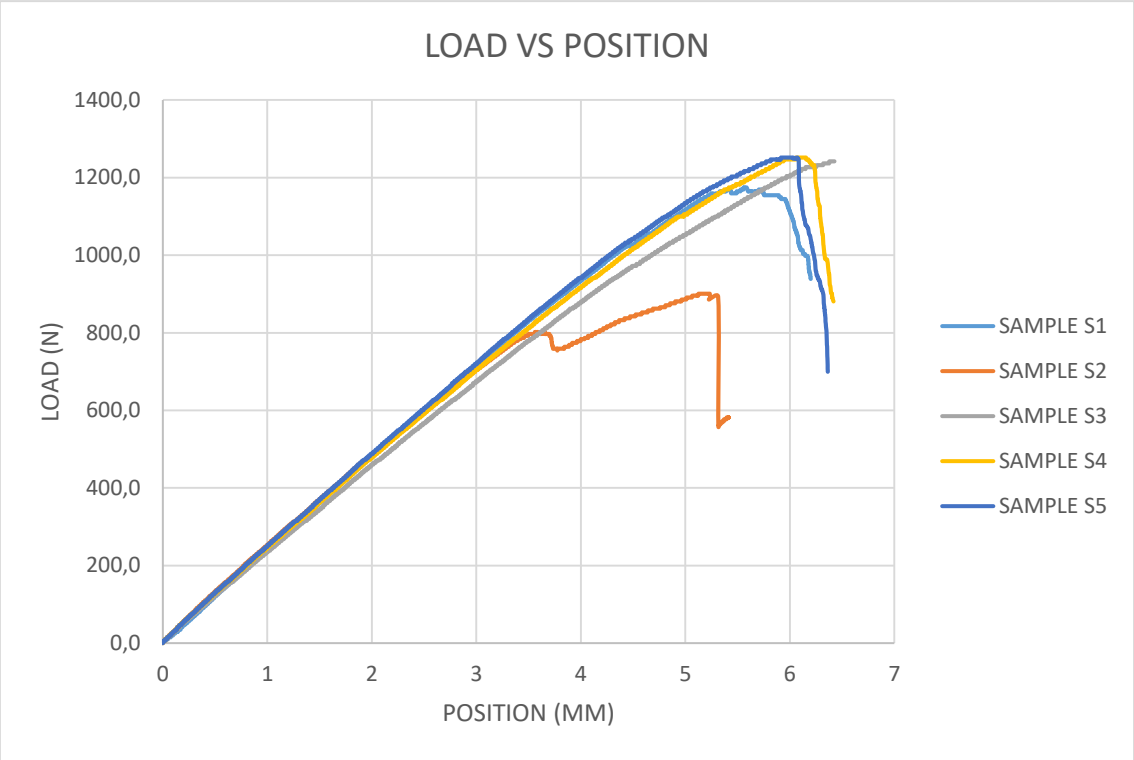

Figure 6.3.2.1 Force-displacement plot of a Traction composite material with Softening

From this result, It can be obtained have the value of the elastic limit, yield stress and fracture energy of the general composite. So, with a homogenisation made.

2. Then, a simulation is launched with the values of homogenisation. The results are not the same. In the next schematic figure, it can be showed:

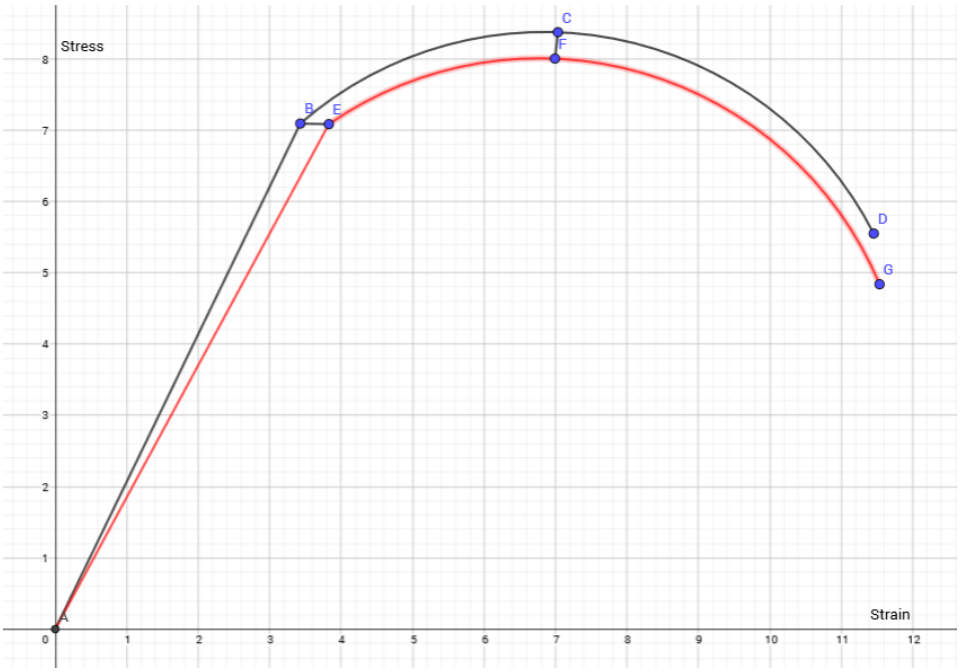

Figure 6.3.2.1 Schematic representation of the process

The red curve represents the simulated case with homogeneous values and the black one is the experimental curve obtained from the experimental case.

The objective of this second step is to reduce the surface between these two curves (without modifying the experimental one). This is made with an iterative Newton-Raphson algorithm that variates the values of the variables to obtain the minimum surface.

The first part to minimize is the elastic zone, the boundaries of this area are: A, B, E. And in this case the elastic limit is the only variable that have influence in this part.

Once we have the elastic limit, then we have to apply the same algorithm but now changing the yield limit, with the same objective, reduce the plasticity area. This area is the surface inside these points: B, E, C, F.

For last, the last variable to modify is the fracture energy.

Once these areas are reduced, we obtain new values for elastic limit, yield limit and fracture energy that represents better the behaviour of the experimental case.

3. Now, the objective is to check that these values obtained in the step 2 are similar when a Rule of Mixtures is applied.
   The Rule of Mixtures is applied with the values of the compounds obtained from the experimental solution.
   For example:

$$E_{RoM} = k_f \cdot E_{f,exp} + k_m \cdot E_{m,exp}$$

   Usually, experimental results are not a unique value. There are a range of values where, for example, the elastic limit can be. With this, the objective is to check if with the Rule of Mixtures can achieve, more or less, the same results as in step 2.

4. Finally, the Serial Parallel Rule of Mixtures theory is applied to obtain the simulation results and check if the behaviour is similar to the experimental case in step 1.

These are the solutions obtained with *Ramseries* with the SPROM implemented.

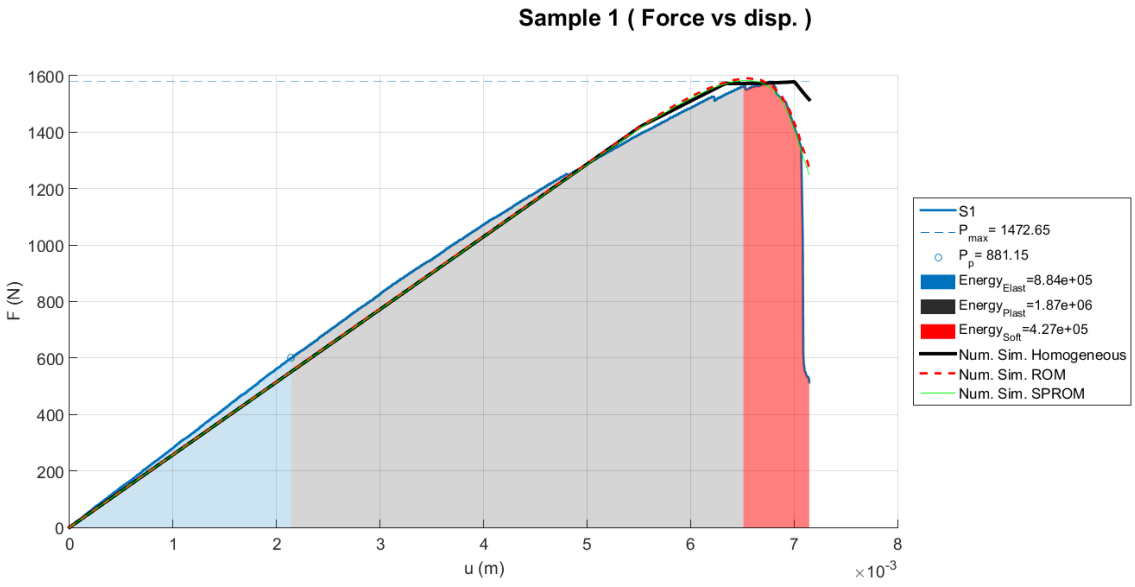

Figure 6.3.2.3 Force-displacement plot of a Traction composite material with Softening and the numerical solution

As it can be seen, the numerical solution is similar as the experimental solution. The final part is difficult to be simulated because the material is damaged so the SPROM algorithm has problems to

obtain a solution. As it can be observed, the numerical solution also has problems to reproduce correctly the behaviour when there are suddenly changes of the pendent. All finite element methods have problems when there are suddenly changes in the derivate.

Nevertheless, the numerical approximation is quite good and represents the behaviour of the experimental solution.

Conclusions

In this project, there are discussed different constitutive theories to use in shells with the objective of understanding the different possible methods to solve a structural shell problem. All this method can be easily implemented in a FEM software. In this work are explained the conditions we have to accomplish in order to choose which theory is better for our study.

Moreover, in the first part of the simulation, different studies are launched in order to know which elements are better in function the type of structure and boundaries condition we have. The conclusions are that it depends on the boundary conditions and the needed results. For example, from one problem, is better to obtain the displacement solutions with *DKT+DrillRotation element* and the stress field is better with *Lineal Quadrilateral.* So, if a study where the stress is needed is launched, is better with *Lineal Quadrilateral* to obtain less error.

Also, it is studied all the damage theory possibilities with the objective of knowing if *Ramseries* can reproduce the expected behaviour. The results say yes because all the response is obtained and checked correctly. Furthermore, this work also checked that the physical response is the expected with the theories studied in order to confirm that the theory is able to reproduce experimental cases. The results were the expected because the structure started to damage in the expected zones and with the evolution set.

To sum up I would like to focus on the importance of characterizing the behaviour of the materials before using it in bigger structures. These types of studies allow us to understand the behaviour of the material under different types of external interaction and to predict the response in order to obtain better solutions and with less computational cost. In this present work is made a characterization of a material in order to use it later in a European project called "*Fibership"*. As it can be seen in the results, the numerical solutions reproduce quite good the behaviour along all the curve but when it arrives at the end, when the structure is more damaged, the algorithm start to have problems to reproduce this behaviour. This is because SPROM algorithm uses an inverse matrix in the constitutive model so, when the structure tends to total damaged the tensor cannot be invertible and the algorithm cannot pass to the next step. One of the improvements for this algorithm is to implement a decomposition of the matrix we want to invert in order to make nonsingular.

References

[1] Bergan, P. G., & Felippa, C. A. (1985). A triangular membrane element with rotational degrees of freedom. *Computer Methods in Applied Mechanics and Engineering*, *50*(1), 25–69.

[2] Bonet, J., & Wood, R. D. (2008). *Nonlinear Continuum Mechanics for Finite Element Analysis*. *Communications in Numerical Methods in Engineering* (Vol. 24).

[3] Zhang, Y. X., & Kim, K. S. (2004). Two simple and efficient displacement-based quadrilateral elements for the analysis of composite laminated plates. *International Journal for Numerical Methods in Engineering*, *61*(11).

[4] Almeida, F. S., & Awruch, A. M. (2011). Corotational nonlinear dynamic analysis of laminated composite shells. *Finite Elements in Analysis and Design*, *47*(10), 1131–1145.

[5] Felippa, C. A. (2003). A study of optimal membrane triangles with drilling freedoms. *Computer Methods in Applied Mechanics and Engineering*, *192*(16–18), 2125–2168.

[6] Hughes, T. J. R. (2000). The Finite Element Method: Linear Static and Dynamic Finite Element Analysis. *Computer Methods in Applied Mechanics and Engineering*. httRastellini, F., Oller, S., Salomón, O., & Oñate, E. (2008). Composite materials non-linear modelling for long fibre-reinforced laminates. Continuum basis, computational aspects and validations. *Computers and Structures*, *86*(9), 879–896.

[7] Rudrapatna, N. S., Vaziri, R., & Olson, M. D. (1999). Deformation and failure of blast-loaded square plates. *International Journal of Impact Engineering*, *22*(4), 449–467.

[8] Wang, R. M., Zheng, S. R., & Zheng, Y. P. (2011). *Polymer matrix composites and technology*. *Polymer matrix composites and technology*.

[9] Oñate, E. (2009). *Structural Analysis with the Finite Element Method*. *Eugenio Oñate. Structural Analysis with the Finite Element Method.* Solids.

[10] Oñate, E. (2009). *Structural Analysis with the Finite Element Method*. *Eugenio Oñate. Structural Analysis with the Finite Element Method.* Shells and Plates

[11] Rastellini, F., Oller, S., Salomón, O., & Oñate, E. (2008). Composite materials non-linear modelling for long fibre-reinforced laminates. Continuum basis, computational aspects and validations. *Computers and Structures*, *86*(9), 879–896.

[12] Chaves. *Mecánica del medio continuo: Modelos constitutivos.* Editor: C.I.M.N.E ISBN 978-8496736689

[13] Martínez, X., Oller, S. (2008) Micro Mechanical Simulation of Composite Materials Using the Serial/parallel Mixing Theory . *UPC Escola Tècnica Superior d'Enginyers*

de camins, canals i ports. Departament de Resistència de Materials i estructures a l'Enginyeria.